ISSN 0021-9673

VOL. 635 NO. 2 APRIL 16, 1993

THIS ISSUE COMPLETES VOL. 635

JOURNAL OF CHROMATOGRAPHY

INCLUDING ELECTROPHORESIS AND OTHER SEPARATION METHODS

ELSEVIER

JOURNAL OF CHROMATOGRAPHY

INCLUDING ELECTROPHORESIS AND OTHER SEPARATION METHODS

Scope. The *Journal of Chromatography* publishes papers on all aspects of **chromatography, electrophoresis** and related methods. Contributions consist mainly of research papers dealing with chromatographic theory, instrumental developments and their applications. The section *Biomedical Applications*, which is under separate editorship, deals with the following aspects: developments in and applications of chromatographic and electrophoretic techniques related to clinical diagnosis or alterations during medical treatment; screening and profiling of body fluids or tissues related to the analysis of active substances and to metabolic disorders; drug level monitoring and pharmacokinetic studies; clinical toxicology; forensic medicine; veterinary medicine; occupational medicine; results from basic medical research with direct consequences in clinical practice. In *Symposium volumes*, which are under separate editorship, proceedings of symposia on chromatography, electrophoresis and related methods are published.

Submission of Papers. The preferred medium of submission is on disk with accompanying manuscript (see *Electronic manuscripts* in the Instructions to Authors, which can be obtained from the publisher, Elsevier Science Publishers B.V., P.O. Box 330, 1000 AH Amsterdam, Netherlands). Manuscripts (in English; *four* copies are required) should be submitted to: Editorial Office of *Journal of Chromatography*, P.O. Box 681, 1000 AR Amsterdam, Netherlands, Telefax (+31-20) 5862 304, or to: The Editor of *Journal of Chromatography*, *Biomedical Applications*, P.O. Box 681, 1000 AR Amsterdam, Netherlands. Review articles are invited or proposed in writing to the Editors who welcome suggestions for subjects. An outline of the proposed review should first be forwarded to the Editors for preliminary discussion prior to preparation. Submission of an article is understood to imply that the article is original and unpublished and is not being considered for publication elsewhere. For copyright regulations, see below.

Publication. The *Journal of Chromatography* (incl. *Biomedical Applications*) has 40 volumes in 1993. The subscription prices for 1993 are:

J. Chromatogr. (incl. *Cum. Indexes*, *Vols. 601–650*) + *Biomed. Appl.* (Vols. 612–651):
Dfl. 8520.00 plus Dfl. 1320.00 (p.p.h.) (total *ca.* US$ 5622.75)

J. Chromatogr. (incl. *Cum Indexes*, *Vols. 601–650*) only (Vols. 623–651):
Dfl. 7047.00 plus Dfl. 957.00 (p.p.h.) (total *ca.* US$ 4573.75)

Biomed. Appl. only (Vols. 612–622):
Dfl. 2783.00 plus Dfl. 363.00 (p.p.h.) (total *ca.* US$ 1797.75).

Subscription Orders. The Dutch guilder price is definitive. The US$ price is subject to exchange-rate fluctuations and is given as a guide. Subscriptions are accepted on a prepaid basis only, unless different terms have been previously agreed upon. Subscriptions orders can be entered only by calender year (Jan.–Dec.) and should be sent to Elsevier Science Publishers, Journal Department, P.O. Box 211, 1000 AE Amsterdam, Netherlands, Tel. (+31-20) 5803 642, Telefax (+31-20) 5803 598, or to your usual subscription agent. Postage and handling charges include surface delivery except to the following countries where air delivery via SAL (Surface Air Lift) mail is ensured: Argentina, Australia, Brazil, Canada, China, Hong Kong, India, Israel, Japan*, Malaysia, Mexico, New Zealand, Pakistan, Singapore, South Africa, South Korea, Taiwan, Thailand, USA. *For Japan air delivery (SAL) requires 25% additional charge of the normal postage and handling charge. For all other countries airmail rates are available upon request. Claims for missing issues must be made within six months of our publication (mailing) date, otherwise such claims cannot be honoured free of charge. Back volumes of the *Journal of Chromatography* (Vols. 1–611) are available at Dfl. 230.00 (plus postage). Customers in the USA and Canada wishing information on this and other Elsevier journals, please contact Journal Information Center, Elsevier Science Publishing Co. Inc., 655 Avenue of the Americas, New York, NY 10010, USA, Tel. (+1-212) 633 3750, Telefax (+1-212) 633 3764.

Abstracts/Contents Lists published in Analytical Abstracts, Biochemical Abstracts, Biological Abstracts, Chemical Abstracts, Chemical Titles, Chromatography Abstracts, Current Awareness in Biological Sciences (CABS), Current Contents/Life Sciences, Current Contents/Physical, Chemical & Earth Sciences, Deep-Sea Research/Part B: Oceanographic Literature Review, Excerpta Medica, Index Medicus, Mass Spectrometry Bulletin, PASCAL-CNRS, Referativnyi Zhurnal, Research Alert and Science Citation Index.

US Mailing Notice. *Journal of Chromatography* (ISSN 0021-9673) is published weekly (total 52 issues) by Elsevier Science Publishers (Sara Burgerhartstraat 25, P.O. Box 211, 1000 AE Amsterdam, Netherlands). Annual subscription price in the USA US$ 4573.75 (subject to change), including air speed delivery. Second class postage paid at Jamaica, NY 11431. **USA POSTMASTERS**: Send address changes to *Journal of Chromatography*, Publications Expediting, Inc., 200 Meacham Avenue, Elmont, NY 11003. Airfreight and mailing in the USA by Publications Expediting.

See inside back cover for Publication Schedule, Information for Authors and information on Advertisements.

0021-9673/93/$06.00

This issue is printed on acid-free paper.

Printed in the Netherlands

CONTENTS

(Abstracts/Contents Lists published in Analytical Abstracts, Biochemical Abstracts, Biological Abstracts, Chemical Abstracts, Chemical Titles, Chromatography Abstracts, Current Awareness in Biological Sciences (CABS), Current Contents/Life Sciences, Current Contents/Physical, Chemical & Earth Sciences, Deep-Sea Research/Part B: Oceanographic Literature Review, Excerpta Medica, Index Medicus, Mass Spectrometry Bulletin, PASCAL-CNRS, Referativnyi Zhurnal, Research Alert and Science Citation Index)

REGULAR PAPERS

Column Liquid Chromatography

Gas Chromatography

Planar Chromatography

(Continued overleaf)

Journal of Chromatography, 635 (1993) 177–186
Elsevier Science Publishers B.V., Amsterdam

CHROMSYMP. 2656

Effect of stationary phase solvation on shape selectivity in reversed-phase high-performance liquid chromatography☆

Steven R. Cole and John G. Dorsey*

Department of Chemistry, University of Cincinnati, Cincinnati, OH 45221-0172 (USA)

(First received June 14th, 1992; revised manuscript received December 1st, 1992)

ABSTRACT

The effect of stationary phase solvation on reversed-phase chromatographic shape selectivity has been investigated using *n*-hexanol as an additive to methanol–water mobile phases. A wide range of mobile phase compositions was evaluated to normalize for solvent strength selectivity differences. Monomeric C_{18} stationary phases of both high and low bonding density were synthesized and used to correlate selectivity changes caused by stationary phase ordering with those seen by the addition of *n*-hexanol. The temperature dependence of retention and selectivity was also investigated using Van 't Hoff plots, which provided insight into the nature of selectivity behavior for estrogens and polyaromatic hydrocarbons. The results showed that using *n*-hexanol as a mobile phase additive did not provide higher shape selectivity, suggesting that changes in the solvation of the stationary phase did not impart a significant change in the level of surface ordering or morphology. However, *n*-hexanol did impart solvent selectivity changes in the separation of estrogen diastereomers that could prove useful in future methods development schemes.

INTRODUCTION

Chromatographic selectivity, α, is generally defined as the interaction difference that two solutes experience between the mobile and stationary phases, such that

$$\ln \alpha = -\Delta(\Delta G/RT) \quad (1)$$

where ΔG is the Gibbs free energy of transfer between the mobile and stationary phase, R is the gas constant, and T is the absolute temperature. Because small increases in selectivity can lead to substantial increases in resolution, with concomitant decreases in analysis time, considerable effort has been expended to better understand the relevant interactions that govern selectivity in reversed-phase high-performance liquid chromatography (RP-HPLC) and the chromatographic conditions that can maximize selectivity.

In what proved to be great foresight, Bakalyar wrote in 1977 [1]: "It may well be that the standard column (for RP-HPLC) becomes a hydrocarbon bonded phase (analogous to the nitrogen gas mobile phase of gas chromatography) and that selectivity is adjusted by changing the mobile phase only (analogous to the column in GC)". Indeed, while changing the polarity of the stationary phase to optimize selectivity has been explored, selectivity is most often adjusted by changing either the mobile phase composition (solvent strength optimization) or the mobile phase organic modifier (solvent selectivity optimization). Extensive litera-

* Corresponding author.

☆ Presented at the *16th International Symposium on Column Liquid Chromatography, Baltimore, MD, June 14–19, 1992*. The majority of the papers presented at this symposium were published in *J. Chromatogr.*, Vols. 631 + 632 (1993).

0021-9673/93/$06.00

ture has been published for each of these three strategies [2–4].

The success of mobile phase or stationary phase optimization generally relies on the polar interactions of the solutes with the two phases. One class of compounds that does not show significant selectivity enhancement with changes in mobile phase or stationary phase polarity is that of shape isomers. Because they have identical structural composition, and differ only in geometric shape, shape isomers often have similar solubilities and thus similar retention properties, resulting in coelution. Sander and Wise [5–7] have studied shape isomer separations extensively using C_{18} stationary phases. Their results suggest that the separation of shape isomers is not enhanced by mobile phase optimization as compared to stationary phase effects. However, the greatest enhancement in shape selectivity occurs not from stationary phase polarity changes, but from the degree of stationary phase surface ordering [6,7]. The trends of this work show that shape selectivity is highest for polymerically bound (*i.e.*, trichlorosilanes with water in the reaction mixture) C_{18} stationary phases at low temperatures. By increasing the networking of the stationary phase by using polymeric bonding chemistry, and by increasing the stationary phase chain rigidity by decreasing the temperature, Sander and Wise propose that linear, planar solutes can partition more readily into the ordered surface than solutes that are bent, or non-planar, thus allowing a means of separation [6,8]. Similar results were reported by Sentell and Dorsey [9], who demonstrated that monomerically derivatized stationary phases of high bonding density provided higher shape selectivity than low bonding density columns. Again this increase in selectivity with bonding density was attributed to greater ordering of the stationary phase chains at high chain densities.

Martire and Boehm [10] proposed a stationary phase model that incorporated the idea of a "breathing" surface that could change its three-dimensional structure from a collapsed state in poor wetting solvents, to a more extended bristle-like structure in mobile phases of good wetting ability. The implications of this model are that the chromatographic properties of the system change not only as a function of mobile phase polarity, but that the mobile phase can change the nature of the stationary phase. A large number of scientists have reported evidence of mobile phase modifiers partitioning into stationary phases [11–13]. Although most non-polar modifiers are relatively strong eluents, it is not uncommon for solute retention to increase as a result of adding the modifier. This increase can be attributed to an increase in stationary phase volumes as the modifier becomes part of the stationary phase.

MacCrehan and Schonberger [14,15] showed that the addition of 10% *n*-butanol to methanol–water mobile phases reduced the retention of the shape isomers *cis*/*trans*-retinol and *cis*/*trans*-β-carotene dramatically, while maintaining separation selectivity. One proposed mechanism for this selectivity phenomenon was stationary phase solvation, in which *n*-butanol partitioned into the stationary phase to provide a more extended, ordered surface, thus improving the shape selectivity. However, this hypothesis was not investigated.

In an effort to improve shape selectivity for the wide range of stationary phases currently available, and to gain insight into the relationship between stationary phase solvation and shape selectivity, we have studied the systematic addition of *n*-alcohols to mobile phases to determine their effect on shape selectivity. The alcohols evaluated included *n*-propanol through *n*-octanol to determine which would provide the greatest solvation while maintaining system compatibility. Because of the great effect of solvent strength on selectivity, a wide range of mobile phase compositions was evaluated. Methanol was selected as the organic modifier to minimize the effect of solvent selectivity, as methanol is in the same solvent family as the *n*-alcohols and thus should provide more similar solution properties than other modifiers such as acetonitrile or tetrahydrofuran [16]. In order to evaluate the role of stationary phase ordering on selectivity, both high and low bonding density stationary phases were used such that selectivity changes caused by an increase in bonding density could be compared to those seen by adding the *n*-alcohol.

EXPERIMENTAL

Apparatus

All chromatographic data was collected on one of two HPLC systems comprised of a SP8800 ternary HPLC pump (Spectra-Physics, San Jose, CA, USA), a Rheodyne 7125 injector with a 20-μl loop (Rheodyne, Cotati, CA, USA) and either an Applied Biosystems 757 absorbance detector or an Applied Biosystems 1000S diode array detector (Applied Biosystems, Foster City, CA, USA). Constant temperature (±0.3°C) was maintained using a water or water–ethylene glycol bath pumped through both a pre-column and column glass jacket using a Model 9000 Isotemp Refrigerated Circulator Bath (Fisher Scientific, Springfield, NJ, USA). The detector output was recorded on an HP3394A integrator (Hewlett-Packard, Avondale, PA, USA). All experiments were conducted at 30°C unless otherwise specified, at controlled flow-rates of 1.0, 1.5 or 2.0 ml/min, which were calibrated regularly. The detection wavelength was adjusted to the absorbance maximum of each class of solutes studied.

Replicate injections of all solutes were made until the retention times were reproducible to within ±1% R.S.D. Solutes were dissolved in methanol and diluted with methanol–water with the exception of SRM 869 which was provided as an acetonitrile solution that was diluted with acetonitrile–water. Capacity factors were calculated using a t_0 value obtained from either the solvent disturbance at the beginning of the chromatogram, or by injecting water.

Columns

Stationary phase derivatization materials included dimethyloctadecylmonochlorosilane (Hüls America, Bristol, PA, USA), Novapak spherical silica, 5 μm diameter, 60-Å pores, and 120 m^2/g (a gift from Waters Chromatography Division, Millipore, Milford, MA, USA), N,N-dimethylaminopyridine (Nepera, Harriman, NY, USA), and dichloromethane (Fisher Scientific). Corroborative silica surface area analysis was provided gratis by Union Carbide, the results of which compared within 2% of the nominal values. The silica was derivatized according to the procedure outlined by Sentell *et al.* [17]. The only exception to this procedure was that the reaction was refluxed with stirring for 24 h rather than reacted under ultrasound. Two batches of silica were derivatized, one with a two-fold excess of silane (based on a 5 $\mu mol/m^2$ estimated surface silanol density) and one with an 80% charge of silane to produce phases of higher and lower bonding density. Samples were submitted for C, H and N analysis, and the bonding densities were calculated to be 3.3 and 2.5 $\mu mol/m^2$, respectively. The derivatized silicas were slurry packed into stainless-steel columns (25 cm and 15 cm length, respectively × 4.6 mm I.D.).

Reagents

Methanol and acetonitrile were of HPLC grade from Fisher Scientific, and were used without further purification. Water was distilled, followed by purification with a Barnstead Nanopure system to produce 17.8-MΩ or higher resistivity. The *n*-alkanols, *n*-propanol, *n*-butanol, *n*-pentanol, *n*-heptanol and *n*-octanol were of reagent grade and were obtained from Fisher Scientific. The *n*-hexanol (99%), estradiol-17α, estradiol-17β and equilin were obtained from Sigma Chemical (St. Louis, MO, USA). Napthacene was obtained from Eastman Kodak (Rochester, NY, USA), and benz[*a*]anthracene from K & K Laboratories (Plainview, NY, USA). Benzo[*c*]phenanthrene was purchased through the Alfred Bader Library of rare chemicals, Aldrich (Milwaukee, WI, USA). Benzo[*a*]pyrene (BaP), phenanthro[3,4-*c*]phenanthrene (PhPh), and 1,2:3,4:5,6:7,8-tetrabenzonaphthalene (TBN) were obtained as test mixture SRM 869 as a gift from Dr. Lane Sander, National Institute of Standards and Technology (Gaithersburg, MD, USA).

RESULTS AND DISCUSSION

The solutes in SRM 869 were separated on both the 2.5 and 3.3 $\mu mol/m^2$ columns using the recommended acetonitrile–water (85:15) mobile phase with UV detection at 254 nm [7]. The structures are shown in Fig. 1. The selectivity between TBN and BaP can be used as a measure

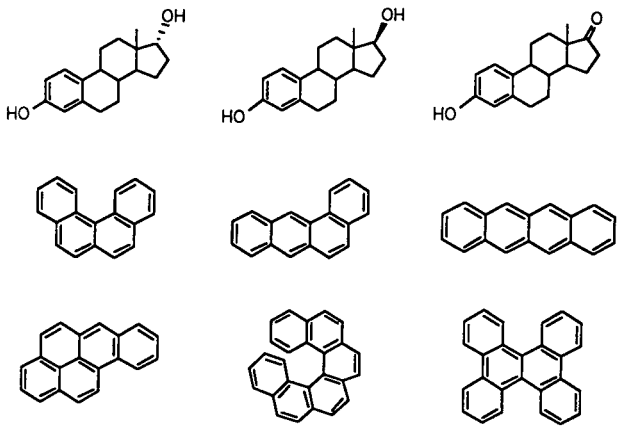

Fig. 1. Structures of the solutes used in these studies: top row: estradiol-17α, estradiol-17β, equilin; middle row: benzo(*c*)-phenanthrene (BcP), benz(*a*)anthracene (BaA), naphthacene (NAP); bottom row: benzo(*a*)pyrene (BaP), phenanthrophenanthrene (PhPh), tetrabenzonaphthalene (TBN).

of shape selectivity, with lower values of $\alpha_{TBN/BaP}$ indicating higher surface ordering and shape recognition. The $\alpha_{TBN/BaP}$ values for the 2.5 and 3.3 μmol/m^2 stationary phases were 1.74 and 1.65, respectively. These values are both near the border of "monomeric" ($\alpha_{TBN/BaP} > 1.7$) and "intermediate" ($\alpha_{TBN/BaP} < 1.7$ and >1.0) stationary phase behavior, with the higher bonding density showing more ordered behavior as predicted [7].

Initial screenings of *n*-alcohols ranging from *n*-propanol to *n*-octanol were conducted by adding 3% (v/v) of the alcohol to methanol–water mobile phases such that a final composition of methanol–*n*-alcohol–water (62:3:35) was achieved. A variety of solutes was screened using mobile phases with and without *n*-alcohol present. The result of these studies showed that a maximum in selectivity was achieved when using *n*-hexanol as the additive. Based on these studies, *n*-hexanol was selected for further study. It should be noted that all of the other *n*-alcohols, such as the *n*-butanol used by MacCrehan and Schonberger [14] showed significant chromatographic changes at the 3% (v/v) level. The optimum level of *n*-hexanol was somewhat governed by the solubility and viscosity of *n*-hexanol. At a level of 3% *n*-hexanol, the system back pressure was increased by approximately 10% and mobile phases of lower than about 45% methanol developed significant cloudiness due to the insolubility of *n*-hexanol. Given these properties, a maximum level of 5% *n*-hexanol in the methanol fraction was used. When the level of *n*-hexanol was decreased to 1% of the mobile phase volume, significantly lower selectivity changes were observed. Thus only higher percentages of *n*-hexanol were investigated.

In an effort to more closely compare chain ordering to the addition of *n*-hexanol, two classes of solutes were investigated. These included the estrogens equilin, estradiol-17α, and estradiol-17β, and the polyaromatic hydrocarbons (PAHs) benzo[*c*]phenanthrene, benz[*a*]-anthracene and naphthacene. The structures of these compounds are shown in Fig. 1. The three estrogens were previously studied by Olsson *et al.* [18], who showed that methanol–water mobile phases provided the best resolution of the three compounds. Equilin was used as a retention reference, and the compounds were separated on the 2.5 and 3.3 μmol/m^2 columns with detection at 280 nm. Baseline resolution of the α- and β-estradiols could only be achieved on the 3.3 μmol/m^2 column. Likewise the PAHs benzo[*c*]phenanthrene, benz[*a*]anthracene and naphthacene showed an increase in selectivity with an increase in stationary phase bonding density (the linear naphthacene showed an increase in separation from the angular benzo[*c*]-phenanthrene).

Mobile phases containing *n*-hexanol were prepared for the estrogen and PAH studies by dissolving 5% *n*-hexanol in methanol, and then using the *n*-hexanol–methanol mixture as the organic portion of the hydro–organic mobile phase. This made mobile phase preparation easy and accurate, and produced mobile phases that had a constant ratio of methanol to *n*-hexanol. Thus at a volume fraction of organic modifier, φ, of 0.5 (*i.e.*, 50% organic) the actual mobile phase composition was methanol–*n*-hexanol–water (47.5:2.5:50).

Under all conditions the selectivity of the α/β-estradiol pair was higher on the 3.3 μmol/m^2 column than on the 2.5 μmol/m^2 column. For a methanol–water (50:50) mobile phase at 30°C, the selectivity values for α/β were 1.22 and 1.02

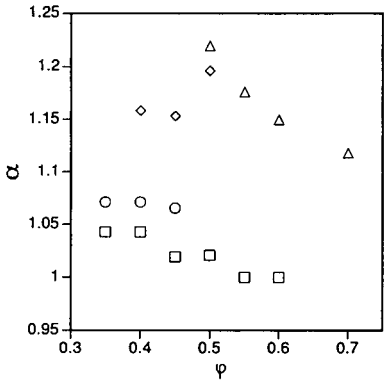

Fig. 2. Plot of the selectivity of estradiol-17α/estradiol-17β *versus* the volume fraction of methanol in the mobile phase for the 3.3 μmol/m^2 column (△) without and (◇) with, and the 2.5 μmol/m^2 column (□) without and (○) with 5% *n*-hexanol in the methanol fraction of the mobile phase.

for the 3.3 and 2.5 μmol/m^2 columns, respectively. Fig. 2 shows the effect of the volume fraction of methanol, φ, on the selectivity of the α/β pair for both the 3.3 and 2.5 μmol/m^2 columns with and without 5% *n*-hexanol in the mobile phase. It is apparent that the high bonding density column yields higher selectivity, and that as the mobile phase strength is increased the selectivity between the pair is decreased. When 5% *n*-hexanol is added to the methanol fraction of the mobile phase, retention is decreased dramatically [with k' (estradiol-17α) values of 15.3 and 2.77 on the 3.3 μmol/m^2 column at $\varphi = 0.5$ without and with *n*-hexanol, respectively]. Despite this difference in mobile phase strength, the selectivity for the α/β pair remains fairly constant with values of 1.22 and 1.20 without and with *n*-hexanol, respectively. However, the relationship between α and φ is entirely different for methanol–water systems and methanol–*n*-hexanol–water systems. While methanol–water mobile phases show a steady increase in selectivity as φ is decreased, the system that contains 5% *n*-hexanol in the methanol does not show a predictable pattern of selectivity. The most plausible reason for this incongruity in the selectivity *versus* φ plot is that while the strength of the mobile phase increases with increasing φ values, and thus should result in lower α values, the volume fraction of *n*-hexanol also increases. It is apparent that the *n*-hexanol is contributing to the selectivity of the system in a manner that is not found when just using methanol. Thus the increase in mobile phase strength is somewhat counterbalanced by the concomitant increase in *n*-hexanol concentration.

Because the estrogens contain polar hydroxyl functionalities, and because the shape difference between the estrogens was based on the position of the 17-hydroxyl moiety, further study was warranted. One concern was the effect of residual silanols on the separation selectivity. To ensure that the separation differences between the high and low bonding density columns were not caused by differences in the level of surface silanols, methanol–15 m*M* phosphate buffer (50:50) mobile phases were prepared with and without 0.2% triethylamine (TEA) at pH 3.0. The use of TEA to reduce the effects of residual silanols is well documented, and its effect should be most pronounced on the low bonding density column. Comparison of the selectivity of the α/β estradiol pair on the 2.5 μmol/m^2 column showed virtually no difference in selectivity upon the addition of 0.2% TEA. This provides clear evidence that the surface silanols are not a significant contributor to the separation.

While the estrogen separation improved by adding *n*-hexanol, it was not confirmed that the selectivity differences were caused by solvation or ordering of the stationary phase. This study was expanded to the PAHs benzo[*c*]phenanthrene (BcP), benz[*a*]anthracene (BaA) and naphthacene (NAP). The selectivity between BcP, the most angular solute of the three, and NAP, the most planar solute of the three, provided a measure of shape selectivity for different stationary phases. Using a methanol–water (80:20) mobile phase with the 2.5 and 3.3 μmol/m^2 columns yielded $\alpha_{NAP/BcP}$ values of 1.39 and 1.69, respectively. This increase in selectivity with bonding density is in agreement with previous work [9]. Fig. 3 shows a plot of the selectivity of the BaA/BcP and NAP/BcP pairs as a function of φ on the 2.5 μmol/m^2 column using mobile phases with and without 5% *n*-hexanol in the methanol fraction. The data for the methanol–water mobile phase show that the selectivity of the system is decreased in a regular manner with increasing methanol concentration.

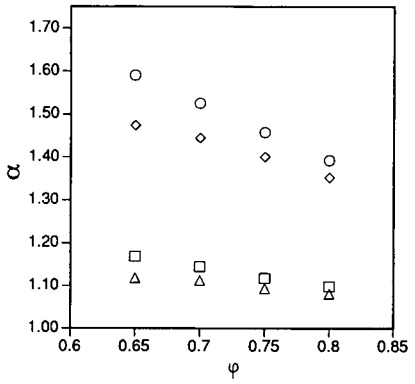

Fig. 3. Plot of the selectivity *versus* the volume fraction of methanol on the 2.5 μmol/m^2 column for the NAP/BcP pair (○) without and (◇) with, and the BaA/BcP pair (□) without and (△) with 5% *n*-hexanol in the methanol fraction of the mobile phase.

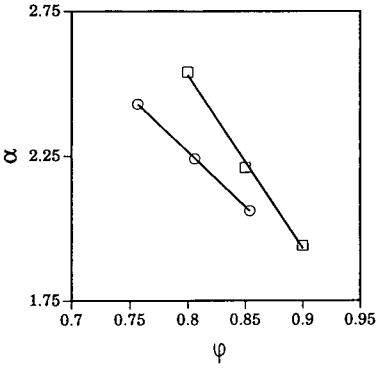

Fig. 4. Plot of the selectivity of the TBN/BaP pair *versus* the volume fraction of (□) methanol and (○) methanol with 5% *n*-hexanol on the 2.5 μmol/m^2 column.

The negative slope of the NAP/BcP pair is larger than that of the BaA/BcP pair, indicating that the mobile phase polarity is a significant contributor to the system selectivity. Similar trends are seen for the *n*-hexanol containing system in terms of the decrease in selectivity *versus* φ, and the steeper slope for the NAP/BcP pair relative to the BaA/BcP pair. The only substantial difference between the data is the magnitude of the selectivity values, which are consistently smaller for the *n*-hexanol containing mobile phase. This decrease was thought to occur because of the greater solvent strength of the *n*-hexanol containing mobile phase. In an effort to normalize for this solvent strength difference, the selectivity values obtained with both systems were compared at equivalent retention (*i.e.*, eluent strength). However, even at equivalent retention, no selectivity enhancement was observed by adding *n*-hexanol.

The test mix SRM 869 was also evaluated on both the 2.5 and 3.3 μmol/m^2 columns. Mobile phases with *n*-hexanol were prepared by adding 3% (v/v) *n*-hexanol directly to methanol–water mobile phases of fixed composition (*i.e.*, 80:3:20 methanol–*n*-hexanol–water). Fig. 4 is a plot of $\alpha_{TBN/BaP}$, the numerical indicator of shape selectivity, *versus* the volume fraction of organic, φ on the 2.5 μmol/m^2 column. As the volume fraction of organic is increased, the value of $\alpha_{TBN/BaP}$ is decreased. While a decrease in this term is typically associated with increased shape selectivity for a fixed mobile phase composition, these data indicate that the mobile phase strength can also produce changes in $\alpha_{TBN/BaP}$ that are not associated with shape selectivity. A thorough study of this phenomenon must include a normalization for this mobile phase strength effect. Examination of the $\alpha_{TBN/BaP}$ values for the mobile phase with 3% *n*-hexanol added show that the $\alpha_{TBN/BaP}$ values are consistently lower than the values obtained using methanol/water mobile phases at any composition. However, the 3% *n*-hexanol containing mobile phases are also stronger eluents than the corresponding methanol–water mobile phases of similar composition. Fig. 5 is a plot of $\alpha_{TBN/BaP}$ *versus* analysis

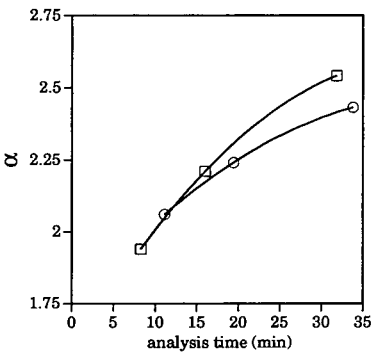

Fig. 5. Plot of the selectivity of the TBN/BaP pair *versus* analysis time for mobile phases using (□) methanol, and (○) methanol with 5% *n*-hexanol as the organic modifier on the 2.5 μmol/m^2 column.

time on the 2.5 μmol/m^2 column for mobile phases with and without 3% *n*-hexanol. While the selectivity appears to change slightly when *n*-hexanol is added to the mobile phase, the magnitude of this change is small when compared to the overall selectivity range observed and thus does not indicate that *n*-hexanol provided higher surface ordering.

While the addition of *n*-hexanol did not provide greater selectivity for the PAHs and SRM 869, improved separation of the estrogens was accomplished. To better understand the nature of these selectivity differences, a study of the temperature dependence of retention was conducted. Numerous scientists have examined the effect of temperature on chromatographic separations. The general findings are that as the temperature increases, retention decreases and chromatographic efficiency increases [19]. The increase in efficiency is most often attributed to a decrease in the mobile phase viscosity, which facilitates faster mass transfer of the solute in and out of the stationary phase. Of larger scope, the use of temperature as a system variable can provide information about the fundamental mobile phase and stationary phase properties that govern retention and selectivity.

The relationship often invoked to describe the temperature dependence of retention is known as the Van 't Hoff relationship and is expressed as

$$\ln k' = -\frac{\Delta H^0}{RT} + \frac{\Delta S^0}{R} + \ln \Phi \qquad (2)$$

where ΔH^0 and ΔS^0 represent the respective standard enthalpy and entropy of transfer of the solute from the mobile phase to the stationary phase, R is the gas constant, T is the absolute temperature in K, and Φ is the volume phase ratio of the stationary and mobile phase respectively [20]. Experimentally, retention data is collected over a wide temperature range and the data are plotted as $\ln k'$ *vs.* $1/T$. Eqn. 2 predicts a linear relationship between these two variables, with the slope of the line equal to $-\Delta H^0/R$, and the intercept equal to $\Delta S^0/R + \ln \Phi$. Thus the thermodynamic constants ΔH^0 and ΔS^0 can be determined if the value of Φ is known.

In addition to the thermodynamic information available from Van 't Hoff analysis, there have also been several reports of non-linear Van 't Hoff behavior [20–26]. These non-linear plots typically exhibit either a steady curve away from linearity, or distinct breaks from linearity at a particular temperature. The nature of these deviations has been debated. One theory suggests that as the temperature is varied high bonding density stationary phases undergo a phase transition from a more solid, ordered, state at low temperature to a more fluid, liquid-like state at high temperature [8,21]. Thus the stationary phase retention properties are not homogeneous throughout the temperature range, and deviations from linearity would be predicted. It has also been postulated that the mobile phase properties, such as heat capacity and hydrogen bonding, may not remain constant throughout the temperature range which could also lead to deviations from predictable retention behavior [25,26].

Whether linear or non-linear Van 't Hoff behavior is observed, and regardless of the cause of any deviation from linearity, Van 't Hoff analysis can provide a qualitative assessment of retention mechanism changes that occur throughout the temperature range investigated. A series of chromatograms was collected on both the 2.5 and 3.3 μmol/m^2 column over a temperature range of 0 to 70°C. This study included the solutes estradiol-17α and -β, which had previously shown improved separation when *n*-hexanol was added to the mobile phase, and the PAHs BcP, BaA and NAP which showed no shape selectivity enhancement upon the addition of *n*-hexanol. Mobile phases were prepared by mixing methanol or 5% *n*-hexanol in methanol with water to appropriate compositions. Because of the polarity differences between the solutes, 50% methanol or methanol with *n*-hexanol mobile phases were used for the estrogens, while 80% methanol or methanol with *n*-hexanol mobile phases were used for the PAHs. The chromatographic experiments were performed as above except at temperatures of 20°C or lower, which required flow-rates of 1.0, 0.75 or 0.5 ml/min to compensate for increased system backpressure.

The results of these studies were not defini-

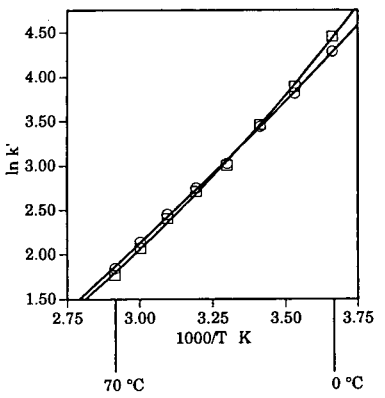

Fig. 6. Plot of ln k' of (○) estradiol-17α and (□) estradiol-17β *versus* $1/T$ for the 2.5 μmol/m^2 column using a methanol–water (50:50) mobile phase.

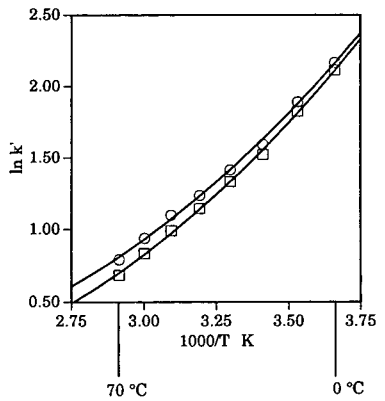

Fig. 7. Plot of ln k' of (○) estradiol-17α and (□) estradiol-17β *versus* $1/T$ for the 2.5 μmol/m^2 column using a methanol–*n*-hexanol–water (47.5:2.5:50) mobile phase.

tive, but gave insight into the nature of the selectivity effects seen. Figs. 6 and 7 show the Van 't Hoff plots of the estradiol isomers on the 2.5 μmol/m^2 column using methanol–water (50:50) and methanol–*n*-hexanol–water (47.5:2.5:50) mobile phases, respectively. The system that contained no *n*-hexanol shows a retention inversion of the α and β isomers at 30°C. This provided a clear explanation as to why the isomers were not separated at 30°C even under a wide range of mobile phase compositions, as illustrated by the selectivity values in Fig. 2. The addition of 2.5% *n*-hexanol to the system caused a shift in this retention inversion point to lower temperatures, allowing faster separation of the isomers in the room temperature regime.

The Van 't Hoff plot for the 3.3 μmol/m^2 column with methanol–water (50:50) mobile phase showed a retention inversion at 10°C, much lower than that of the 2.5 μmol/m^2 column. This inversion point is also shifted to lower temperature with the addition of *n*-hexanol, such that coelution does not occur over the entire temperature range investigated. The shift to lower temperature of the retention inversion point is observed both when *n*-hexanol is added, and when the bonding density is increased. If the *n*-hexanol is inducing greater ordering of the C_{18} chains to change the retention process, then this behavior should also be seen for the PAH solutes.

Figs. 8 and 9 show Van 't Hoff plots of the PAH data obtained on the 3.3 μmol/m^2 column using methanol–water (80:20) or methanol–*n*-hexanol–water (76:4:20) mobile phases. There are several trends worth noting. First, as the temperature is decreased, not only is retention increased, but the changes in the slope of the plot are solute dependent. The curves for NAP and BcP show distinct curvature toward higher and lower retention, respectively, as the temperature is decreased. The net result of this retention trend is that higher shape selectivity is seen at low temperatures, which is in agreement with previous work [8,24]. Similar results were observed for the 2.5 μmol/m^2 column, though at

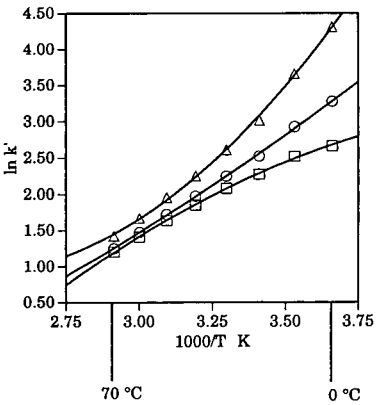

Fig. 8. Plot of ln k' of (△) NAP, (○) BaA, and (□) BcP for the 3.3 μmol/m^2 column using a methanol–water (80:20) mobile phase.

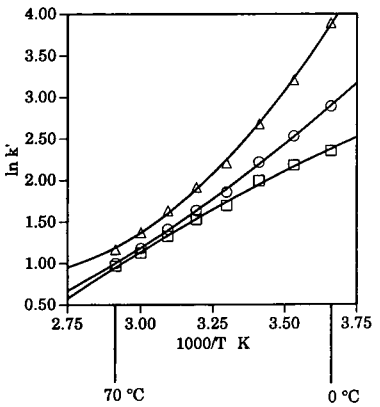

Fig. 9. Plot of ln k' of (△) NAP, (○) BaA, and (□) BcP for the 3.3 μmol/m^2 column using a methanol–n-hexanol–water (76:4:20) mobile phase.

any given temperature the selectivity was always highest for the 3.3 μmol/m^2 column. The temperature induced selectivity increase is consistent with greater chain ordering at low temperatures in that the linear NAP was progressively more retained while the angular BcP was progressively less retained as the temperature was decreased. If surface ordering were occurring at lower temperatures, as has been shown by Sander and Wise, one would expect that the linear, planar solutes such as NAP would partition more readily than bent or torqued solutes such as BcP [8].

When n-hexanol was added to the mobile phase, there was a decrease in retention as expected, but the basic shape of the plot remained the same as in the methanol–water mobile phase case. If increased ordering were induced by the addition of n-hexanol, the magnitude of the "breaks" from linearity in the Van 't Hoff plot for NAP and BcP should be more pronounced, and higher shape selectivity should be seen for the n-hexanol containing mobile phase.

Clearly if surface ordering is occurring from stationary phase solvation by n-hexanol, the effect is insignificant when compared to that of stationary phase bonding density and system temperature. A recent study by Montgomery *et al.* [27] examined the effect of water, methanol–water (80:20), and n-propanol–water (5:95) on the contact angle measurements and frequency-domain fluorescence anisotropy of a probe molecule on a C_{18} silica surface. The results showed that while the addition of alcohol to the system provided better interfacial wetting of the surface, "The results do not support the idea that a small amount of alcohol causes the C_{18} chains to become extended toward the surface normal" [27].

The enhanced separation of the estrogen pair is most likely a result of a solvent selectivity difference between methanol and the higher n-alcohols. While methanol is in the same solvent family as the higher alcohols, Snyder noted that for solvents that undergo strong self-hydrogen bonding, such as alcohols and amides, changes in selectivity between lower and higher homologues can be significant [16]. This type of interaction could well explain the selectivity differences seen in these experiments.

ACKNOWLEDGEMENTS

The authors are grateful for support of this work by NIH GM48561 and by AFOSR 91-0254.

REFERENCES

1 S.R. Bakalyar, R. McIlwrick and E. Roggendorf, *J. Chromatogr.*, 142 (1977) 353.
2 P.E. Antle, A.P. Goldberg and L.R. Snyder, *J. Chromatogr.*, 321 (1985) 1.
3 A.C.J.H. Droven, H.A.H. Billiet and L. de Galan, *J. Chromatogr.*, 352 (1986) 127.
4 L.R. Snyder, M.A. Quarry and J.L. Glajch, *Chromatographia*, 24 (1987) 33.
5 L.C. Sander and S.A. Wise, *J. Chromatogr.*, 316 (1984) 163.
6 L.C. Sander and S.A. Wise, *Crit. Rev. Anal. Chem.*, 18 (1987) 299.
7 L.C. Sander and S.A. Wise, *LC–GC*, 8 (1990) 378.
8 L.C. Sander and S.A. Wise, *Anal. Chem.*, 61 (1989) 1749.
9 K.B. Sentell and J.G. Dorsey, *J. Chromatogr.*, 461 (1989) 193.
10 D.E. Martire and R.E. Boehm, *J. Phys. Chem.*, 87 (1983) 1045.
11 R.P.W. Scott and C.F. Simpson, *Faraday Symp. Chem. Soc.*, 15 (1980) 69.
12 R.M. McCormick and B.L. Karger, *J. Chromatogr.*, 199 (1980) 259.
13 K. Wahlund and I. Beijersten, *Anal. Chem.*, 54 (1982) 128.
14 W.A. MacCrehan and E. Schonberger, *J. Chromatogr.*, 417 (1987) 65.

15 W.A. MacCrehan and E. Schonberger, *Clin. Chem.*, 33 (1987) 1585.
16 L.R. Snyder, *J. Chromatogr. Sci.*, 16 (1978) 223.
17 K.B. Sentell, K.W. Barnes and J.G. Dorsey, *J. Chromatogr.*, 455 (1988) 95.
18 M. Olsson, L.A. Sander and S.A. Wise, *J. Chromatogr.*, 537 (1991) 73.
19 J.R. Gant, J.W. Dolan and L.R. Snyder, *J. Chromatogr.*, 185 (1979) 153.
20 A. Tchapla, S. Heron, H. Colin and G. Guiochon, *Anal. Chem.*, 60 (1988) 1443.
21 D. Morel and J. Serpinet, *J. Chromatogr.*, 200 (1980) 95.
22 P. Claudy, J.-M. Letoffe, C. Gaget, D. Morel and J. Serpinet, *J. Chromatogr.*, 329 (1985) 331.
23 W.E. Hammers and P.B.A. Verschoor, *J. Chromatogr.*, 282 (1983) 41.
24 K.B. Sentell and A.N. Henderson, *Anal. Chim. Acta*, 246 (1991) 139.
25 L.A. Cole and J.G. Dorsey, *Anal. Chem.*, 64 (1992) 1317.
26 L.A. Cole, J.G. Dorsey and K.A. Dill, *Anal. Chem.*, 64 (1992) 1324.
27 M.E. Montgomery, M.A. Green and M.J. Wirth, *Anal. Chem.*, 64 (1992) 1170.

Journal of Chromatography, 635 (1993) 187–193
Elsevier Science Publishers B.V., Amsterdam

CHROMSYMP. 2654

Synthesis and characterization of highly stable polymer-coated aminosilica packing material for high-performance liquid chromatography☆

Hiroshi Kutsuna*, Yutaka Ohtsu and Michihiro Yamaguchi

Basic Research Laboratories, R & D Headquarters, Shiseido Co., Ltd., 1050 Nippa-cho, Kohoku-ku, Yokohama 223 (Japan)

(First received June 14th, 1992; revised manuscript received November 17th, 1992)

ABSTRACT

A synthetic procedure leading to an amino-bonded stationary phase for high-performance liquid chromatography was developed. The silica surface was first coated with a silicone polymer monolayer and an amino functionality was subsequently attached to the polymer layer. The polymer-coated amino-bonded phase showed improved stability and separation in the analysis of carbohydrates and nucleotides over conventional aminopropylsilylated silicas.

INTRODUCTION

Aminopropylsilylated silica is one of the most commonly used column packings for the analysis of carbohydrates [1], ionic compounds and other biologically important substances [2]. However, conventional aminopropylsilicas still have several problems. In general, aminopropylsilicas are chemically unstable and the lifetimes of packed columns are relatively short [3]. One of the reasons for the decrease in column efficiency is thought to be gradual dissolution of the primary amino phase in aqueous mobile phases [4]. Another complexity is that the three-dimensional structure of the aminopropyl phase formed on the silica surface varies depending on the reaction conditions owing to the multi-functionality of 3-aminopropyltriethoxysilane, the most commonly used silanizing reagent [5], which makes it difficult to obtain reproducible chromatographic separations.

Several efforts to prepare improved amino-bonded phases have been reported. Cationic polymers whose amino groups were cross-linked with diepoxides showed good reproducibility during continuous operation for several months [6,7].

The use of (3-aminopropyl)diisopropylethoxysilane, an alternative silanizing reagent, has been reported [8]. The two bulky isopropyl groups of the reagent were assumed to protect the silica surface against hydrolysis. Aminopropylsilica prepared by gas-phase silylation also gave improved results with regard to the peak shape of saccharides [9], although the durability of the column was still uncertain.

As mentioned above, the initial instability of silica-based aminopropyl-bonded stationary phases appears to be due to the gradual desorption of the respective silane, while further changes in the chromatographic properties during the operation seem to be caused by deactivation of the surface with impurities in the mobile phase. A simple and effective way to prevent

* Corresponding author.

☆ Presented at the *16th International Symposium on Column Liquid Chromatography, Balitmore, MD, June 14–19, 1992.* The majority of the papers presented at this symposium were published in *J. Chromatogr.*, Vols. 631 + 632 (1993).

0021-9673/93/$06.00

degradation caused by mobile phases is to use a protective column between the pump and the injection valve that is packed with the same sorbent. Such a protective column allowed the main column to be used for several months without any chromatographic change in a certain application [10].

In spite of these efforts, improvements in the chromatographic stability of primary amino-bonded phases still remains a major issue. So far, none of the commercially available amino-propylsilica columns seems to have reached an acceptable level in terms of its life span and separation efficiency.

A novel polymer-coating technique to form reactive polymethylsiloxane films on metal oxides by chemical vapour deposition of 1,3,5,7-tetramethylcyclotetrasiloxane (H4) was developed by Fukui *et al.* [11]. Ohtsu and co-workers [12,13] utilized this polymer coating technique to prepare a polymer-coated C_{18} silica packing. The polymer-coated C_{18} silica showed high chemical stability even in alkaline mobile phases [12] and separation characteristics similar to those of conventional octadecylsilylated silica (ODS) phases [14]. The polymer-coated C_{18} silica seems to have a more homogeneous surface than another type of polymer-coated silica phase on which the bulky C_{18}-modified silicone polymer was directly anchored [14,15]. Polymer-coated C_{18} packings, prepared from high-purity silica, also showed an excellent performance in the analysis of protonated amines and chelating compounds, which are normally considered difficult to analyse owing to their undesirable secondary interaction with the silica surface [16].

In this paper, an alternative way to develop a silica-based amino-bonded phase using the above-mentioned polymer coating technique is described. The synthetic procedure, the stability of the material and applications to various biologically important substances are discussed.

EXPERIMENTAL

Materials

High-purity silica (Shiseido, Tokyo, Japan) (particle size 5 μm, pore diameter 80 Å, specific surface area 400 m^2/g, metal impurities <5 ppm) was used as a starting material for the polymer-coated amino-bonded phase. 1,3,5,7-Tetramethylcyclotetrasiloxane (H4), the silicone monomer used for the polymer coating, was purchased from Toshiba Silicone (Tokyo, Japan). All the reagents and solvents used to synthesize the packing were of special grade from Nacalai Tesque (Kyoto, Japan), and were used as received. Carbohydrates, sugar alcohols, allantoin and fat-soluble vitamins used as standard compounds were obtained from Nacalai Tesque. Oligosaccharides were obtained from JASCO (Tokyo, Japan). Nucleotide monophosphates were purchased from Sigma (St. Louis, MO, USA). Acetonitrile used for the mobile phases was of HPLC grade from Nacalai Tesque. Potassium dihydrogenphosphate and phosphoric acid to adjust the pH of the mobile phase were of special grade from Nacalai Tesque. Water was purified with a Milli-Q system (Nihon Millipore Kogyo, Tokyo, Japan). A Nucleosil $5NH_2$ column (250 mm × 4.6 mm I.D.) was purchased from Macherey–Nagel (Düren, Germany) and was used for comparative studies as described later.

Synthesis of amino phase

The H4-coated silica was prepared according to the method of Fukui *et al.* [11]. The high-purity silica gel (100 g) was placed in contact with the vapour of H4 (40 g) at 100°C for 48 h under a nitrogen atmosphere. The H4 molecules were deposited on the silica surface and became polymerized. The measured thickness of the homogeneous polymer layer was *ca.* 7 Å, which corresponds to that of a monolayer. The silicone polymer formed still had a high proportion of reactive SiH groups (2.30 mmol/g), sufficient for the subsequent modification. Allyl glycidyl ether (AGE) (100 g) was reacted with the SiH groups of the polymer-coated silica (100 g) in refluxing 2-propanol (200 ml) for 5 h under a nitrogen atmosphere in the presence of hexachloroplatinic acid (50 mg). When the hydrosilylation reaction was complete, the solvent mixture was removed with a glass filter and the epoxysilica trapped on the filter was washed thoroughly with 2-propanol and methanol. The epoxysilica was dried *in*

vacuo for 5 h at 150°C to remove the residual AGE completely. Aqueous ammonia (100 g) or polyamines [$NH_2(CH_2CH_2NH)_nH$, ($n = 1$–5), 100 g] were added to the epoxysilica (100 g) and the mixture was heated in refluxing 2-propanol (200 ml) for 5 h under a nitrogen atmosphere. After the removal of the solvent, the aminosilica was washed with 2-propanol several times and then with methanol and water. The wet aminosilica was stirred in a mixture of formaldehyde (20 ml) and water (100 ml) for 30 min at room temperature, then droplets of 0.1% sodium carbonate solution were added to the slurry in order to adjust the pH to 9.0 and the slurry was stirred for an additional 30 min at room temperature. After filtering off the solvent, the cross-linked aminosilica was washed with water and methanol. The modified silica was dried *in vacuo* for 5 h at 120°C.

Characterization of polymer-coated aminosilica (NH_2-silica)

The modification density of the polymer-coated NH_2-silica was calculated from the nitrogen content measured by elemental analysis. The polymer-coated NH_2-silica (3.5 g) was dispersed in 30 ml of slurry solvent [cyclohexanol–methanol (40:60)] and the slurry was packed into a stainless-steel column (250 mm × 4.6 mm I.D.) with 80 ml of methanol and 80 ml of water at a constant pressure of 400 kgf/cm^2.

The durability of the polymer-coated NH_2-silica column was evaluated by comparing the decrease in the retention of maltose using a standard mobile phase [acetonitrile–water (75:25)] with that for the Nucleosil 5NH_2 column. Further, chemical stability of the polymer-coated NH_2 column was evaluated by checking the retention time and peak shape of carbohydrates, which were measured after two series of alternating 4-h flows (1.0 ml/min) of two different mobile phase conditions: (1) acetonitrile–water (75:25), pH 2, adjusted with phosphoric acid, and (2) acetonitrile–water (75:25), pH 11, adjusted with aqueous ammonia. This flow programme of the mobile phases is given in detail in Fig. 2.

In addition to the fundamental performance in the separation of mono- and disaccharides, oligosaccharides, sugar alcohols, allantoin and fat-soluble vitamins, the characteristics of the new amino-bonded phase as a weak anion exchanger was investigated by observing the retention behaviours of the five standard nucleotides at different pH values and buffer salt concentrations.

Equipment

The HPLC system consisted of a DGU-4A degasser, an LC-9A pump, a SIL-6B autoinjector, an SPD-6AV UV detector, an SCL-6B system controller and a C-R4AX data processor (all from Shimadzu, Kyoto, Japan).

RESULTS AND DISCUSSION

The density of AGE molecules (spacer molecules) attached to the polymer-coated silica by hydrosilylation was 0.7 mmol/g. Various compounds possessing primary and secondary amino groups could be attached to these spacer molecules (Table I). In a preliminary experiment, the epoxy groups of the spacer molecules were directly converted into primary amines by a simple reaction with aqueous ammonia. The density of primary amino groups formed in this reaction was 0.4 mmol/g. Although this product could be used as an amino-bonded stationary phase, the measured retention of maltose was not large enough for practical use (Table I). The retention of maltose increased when ammonia was replaced with larger polyamines [$NH_2(CH_2CH_2NH)_nH$ ($n = 1$–5)]. As shown in Table I, the retention of maltose increased as the degree of polymerization (n) increased. When pentaethylenehexamine ($n = 5$) was used, the modification density (sum of amino and imino groups) increased to 2.5 mmol/g and the retention of maltose became sufficient for further applications.

A column packed with the pentaethylenehexamine-modified silica, however, did not show a largely improved lifetime, which had been expected owing to the silicone polymer coating. A cross-linking procedure appeared to be one of the ways to improve the durability of the amino-bonded phase [6,7]. Three cross-linking reagents were tried for the pentaethylenehexamine-

TABLE I

POLYAMINE ADDITION AND RETENTION OF MALTOSE

Amine added[a]	C (%)	N (%)	Imino and amino groups (mmol/g)	$k'_{maltose}$ [b]
Aqueous ammonia	7.6	0.6	0.4	1.15
Ethylenediamine	8.2	1.8	1.3	2.32
Triethylenetetramine	10.4	2.4	1.7	4.61
Tetraethylenepentamine	12.2	3.1	2.2	5.43
Pentaethylenehexamine	12.8	3.5	2.5	6.22

[a] 0.72 mmol/g of epoxy group was added to the SiH moiety of silicone polymer film on the 80 Å pore silica gel (400 cm^2/g) prior to polyamine addition.

[b] Dead volume was determined by the retention volume of acetonitrile which was not considered to be retained in the NH_2 column.

modified phase; glycerol diglycidyl ether, epichlorohydrin and formaldehyde. As expected, all of these reagents lengthened the lifetime of the column considerably. With these three reagents, however, the retention of maltose decreased by 80%, 47% and 39%, respectively. This retention decrease seems to be attributable to the increase in surface hydrophobicity caused by the cross-linking procedure. Among the three reagents, formaldehyde seems to be the best cross-linking reagent, providing a high stability and maintaining retention characteristics similar to those of conventional aminopropylsilicas.

Fig. 1 shows the life span of the polymer-coated NH_2 phase cross-linked with formaldehyde and that of the conventional Nucleosil $5NH_2$ aminopropylsilylated silica column. The capacity factor (k') and theoretical plate number (N) of maltose on the polymer-coated NH_2 column remained almost constant during 150 h of continuous use. On the other hand, the k' of maltose on the Nucleosil $5NH_2$ column decreased to 70% of the initial value after 100 h and serious tailing of the peak was observed. Hence the polymer-coated NH_2 column has a much longer life span than that of the conventional column.

Fig. 2 shows the change in the chromatogram for sugar analysis with the polymer-coated NH_2 column under extreme conditions with the cyclic

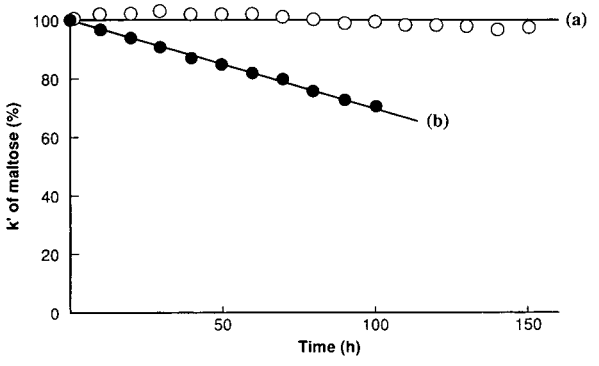

Fig. 1. Comparative degradation of silica-based NH_2 columns. Column: (a) polymer-coated NH_2; (b) Nucleosil $5NH_2$. Column dimensions, 250 × 4.6 mm I.D.; column temperature, 40°C; mobile phase, acetonitrile–water (75:25); flow-rate, 1.0 ml/min; detection, refractive index (RI); sample, maltose.

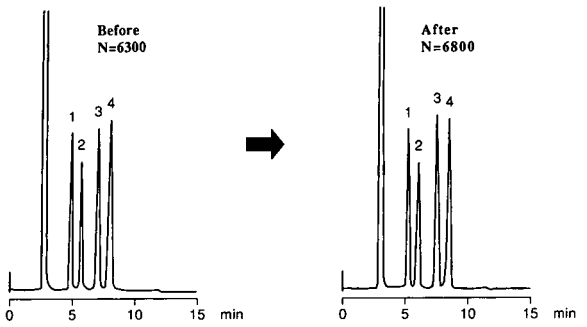

Fig. 2. Alteration of chromatogram of saccharides after cyclic test with acidic and basic mobile phases. Column, polymer-coated NH_2 (250 × 4.6 mm I.D.); temperature, 40°C. Mobile phase: acetonitrile–water (75:25), (1) pH 2 adjusted with H_3PO_4, (2) pH 11 adjusted with NH_3 solution and (3) pH not adjusted, with the following alternating cycle: (1) 4 h→(3) 1 h→(2) 4 h→(3) 1 h→(1) 4 h→(3) 1 h→(2) 4 h→(3) 6 h. Flow-rate, 1.0 ml/min; detection, RI. Sample: 1 = fructose; 2 = glucose; 3 = sucrose; 4 = maltose.

alternation of acidic (pH 2) and basic (pH 11) mobile phases. The peak shape and N value of maltose did not deteriorate significantly even after these extreme conditions. The hydrophobic silicone polymer film and cross-linked structure seem to prevent hydrolysis of the amino-bonded stationary phase.

The polymer-coated NH_2 column showed good performance in the analyses of mono-, di- (Fig. 3a) and oligosaccharides (Fig. 4), and sugar alcohols (Fig. 5). The overall retention of these

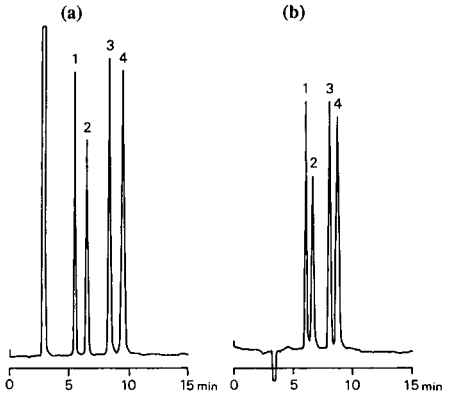

Fig. 3. Chromatograms of saccharides. Column: (a) polymer-coated NH_2; (b) Nucleosil 5 NH_2. Column dimensions, 250 × 4.6 mm I.D.; column temperature, 40°C; mobile phase, (a) acetonitrile–water (75:25) and (b) acetonitrile–water (70:30); flow-rate, 1.0 ml/min; detection, RI. Sample: 1 = fructose; 2 = glucose; 3 = sucrose; 4 = maltose.

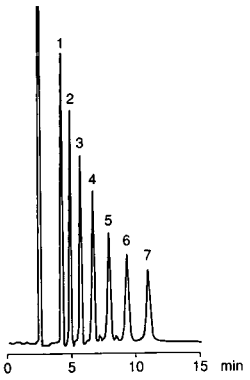

Fig. 4. Chromatogram of oligosaccharides. Column, polymer-coated NH_2 (250 × 4.6 mm I.D.); temperature, 40°C; mobile phase, acetonitrile–water (65:35); flow-rate, 1.0 ml/min; detection, RI. Sample: 1 = glucose; 2 = maltose; 3 = maltotriose; 4 = maltotetraose; 5 = maltopentaose; 6 = maltohexaose; 7 = maltoheptaose.

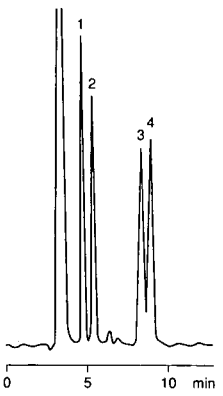

Fig. 5. Chromatogram of sugar alcohols. Column, polymer-coated NH_2 (250 × 4.6 mm I.D.), temperature, 40°C; mobile phase, acetonitrile–water (85:15); flow-rate, 1.0 ml/min; detection, RI. Sample: 1 = glycerine; 2 = pentaerythritol; 3 = D-sorbitol; 4 = mannitol.

standard analytes on the polymer-coated NH_2 column is slightly less than that on the conventional amino-bonded phase, probably owing to the increased hydrophobicity of the cross-linked polyamine. The overall retention of the standard analytes could be increased to the level for the conventional amino phase by increasing the acetonitrile content in the mobile phase by 5%. For instance, the retention of mono- and disaccharides on the polymer-coated NH_2 column with 75% acetonitrile in the mobile phase (Fig. 3a) was almost the same as that on the Nucleosil 5NH_2 column with 70% acetonitrile (Fig. 3b). Note that the polymer-coated NH_2 column gave a better separation of mono- and disaccharides than did the Nucleosil 5NH_2 column. It should be also noted that the large oligosaccharides ($M_r > 1000$) were separated with a relatively narrow peak width (Fig. 4), although these molecules were expected to be difficult to separate in this system having a small pore size (80 Å) and a bulky structure of the cross-linked polyamine.

Allantoin is one of the most common medicinal ingredients in cosmetics and eyewashes. Allantoin is normally determined using an amino-bonded phase, because it is not retained in an ODS column owing to its hydrophilic nature. Allantoin could be retained on the polymer-coated NH_2 column (Fig. 6). Nico-

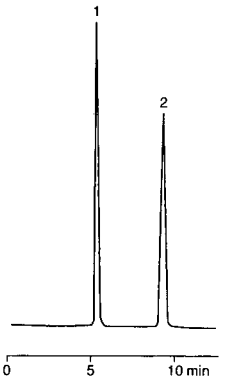

Fig. 6. Chromatogram of Allantoin. Column, polymer-coated NH_2 (250 × 4.6 mm I.D.); temperature, 40°C; mobile phase, 5 m*M* KH_2PO_4 (pH 2.0 adjusted with H_3PO_4) in acetonitrile–water (80:20); flow-rate, 1.0 ml/min; detection, UV (210 nm). Sample: 1 = allantoin; 2 = nicotinamide.

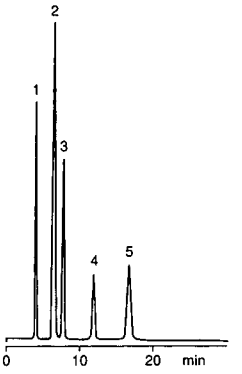

Fig. 8. Chromatogram of nucleotides. Column, polymer-coated NH_2 (250 × 4.6 mm I.D.); temperature, 40°C; mobile phase, 50 m*M* $(NH_4)_2HPO_4$ (pH 3.0 adjusted with H_3PO_4); flow-rate, 1.0 ml/min; detection, UV (260 nm). Sample: 1 = 5′-CMP; 2 = 5′-AMP; 3 = 5′-UMP; 4 = 5′-IMP; 5 = 5′-GMP.

tinamide seems to be a suitable internal standard for the determination of allantoin under the mobile phase conditions shown in Fig. 6.

Standard fat-soluble vitamins were separated with the polymer-coated NH_2 column using hexane as the mobile phase, as shown in Fig. 7. Vitamin A palmitate and vitamin E acetate were separated as sharp peaks. The use of non-polar solvents, such as hexane, is not possible with certain polymer-based amino phases having a swelling nature.

Further, the polymer-coated NH_2 column was applied to the separation of nucleotide mono-

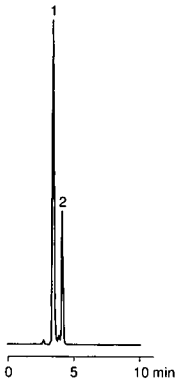

Fig. 7. Chromatogram of fat-soluble vitamins. Column: polymer-coated NH_2 (250 × 4.6 mm I.D.); temperature, 40°C; mobile phase, hexane; flow-rate, 1.0 ml/min; detection, UV (254 nm). Sample: 1 = vitamin A palmitate; 2 = vitamin E acetate.

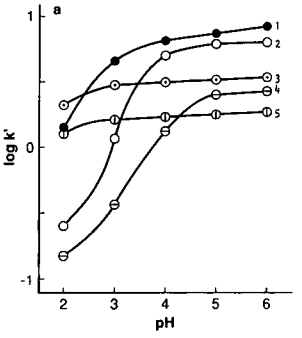

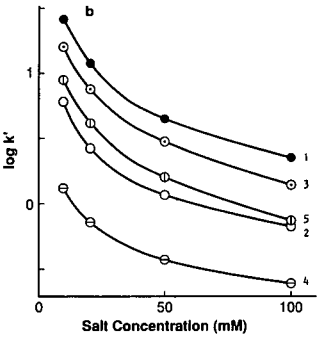

Fig. 9. Effects of (a) pH and (b) salt concentration on retention. Column, polymer-coated NH_2 (250 × 4.6 mm I.D.); temperature 40°C; flow-rate, 1.0 ml/min; detection, UV (260 nm). Mobile phase: (a) 50 m*M* $(NH_4)_2HPO_4$; (b) $(NH_4)_2HPO_4$ (pH 3.0). (1) = 5′-GMP; 2 = 5′-AMP; 3 = 5′-IMP; 4 = 5′-CMP; 5 = 5′-UMP.

phosphates (Fig. 8), for which a weak anion-exchange column has usually been used. The mobile phase was aqueous phosphate buffer. The retention of all the nucleotides decreased at lower pH (Fig. 9a) and with a higher salt concentration in the mobile phase (Fig. 9b). This type of retention behaviour of acidic solutes can be explained as an anion-exchange effect. The function as an anion exchanger of the polymer-coated amino-bonded phase seems to be due to the tertiary amine moiety of the cross-linked polyamine.

CONCLUSIONS

A polymer-coated NH_2 silica packing was developed by coating silica with a silicone polymer homogeneously and subsequent modification leading to a cross-linked polyamine phase. The polymer-coated NH_2 column showed a longer life span than that of a conventional silica-based NH_2 column owing to the existence of a protective silicone polymer film and a cross-linked polyamine. It is applicable not only to the analysis of saccharides, sugar alcohols, allantoin and fat-soluble vitamins, but also to the anion-exchange separation of nucleotides.

REFERENCES

1 R.E. Majors, *J. Chromatogr. Sci.*, 18 (1980) 488.
2 S.R. Abbott, *J. Chromatogr. Sci.*, 18 (1980) 540.
3 H. Engelhardt and D. Mathes, *J. Chromatogr.*, 142 (1977) 311.
4 F.M. Rabel, *J. Chromatogr. Sci.*, 18 (1980) 394.
5 E.T. Vandenberg, L. Bertilsson, B. Liedberg, K. Uvdal, R. Erlandsson, H. Elwing and I. Lundström, *J. Colloid Interface Sci.*, 147 (1991) 103.
6 D.M. Wonnacott and E.V. Patton, *J. Chromatogr.*, 389 (1987) 103.
7 E.V. Patton and D.M. Wonnacott, *J. Chromatogr.*, 389 (1987) 115.
8 J.J. Kirkland, J.L. Glajch and R.D. Farlee, *Anal. Chem.*, 61 (1989) 2.
9 P. Wikstrom, C.F. Mandenius and P.O. Larsson, *J. Chromatogr.*, 455 (1988) 105.
10 B. Porsch and J. Kratka, *J. Chromatogr.*, 543 (1991) 1.
11 H. Fukui, T. Ogawa, M. Nakano, M. Yamaguchi and Y. Kanda, *Controlled Interphases in Composite Materials*, Elsevier, New York, 1990, pp. 469–478.
12 Y. Ohtsu, H. Fukui, T. Kanda, K. Nakamura, M. Nakano, O. Nakata and Y. Fujiyama, *Chromatographia*, 24 (1987) 380.
13 Y. Ohtsu, O. Shirota, T. Ogawa, I. Tanaka, T. Ohta, O. Nakata and Y. Fujiyama, *Chromatographia*, 24 (1987) 351.
14 O. Shirota, Y. Ohtsu and O. Nakata, *J. Chromatogr. Sci.*, 28 (1990) 553.
15 Schomburg, *LC · GC*, 6 (1987) 1.
16 Y. Ohtsu, Y. Shiojima, T. Okumura, J. Koyama, K. Nakamura, O. Nakata, K. Kimata and N. Tanaka, *J. Chromatogr.*, 481 (1989) 147.

Journal of Chromatography, 635 (1993) 195–202
Elsevier Science Publishers B.V., Amsterdam

CHROM. 24 837

Robustness testing of an optimized reversed-phase high-performance liquid chromatographic system for the separation of six sulphonamides using the rules of error propagation

J. Wieling*

Pharma Bio-Research International BV, P.O. Box 200, NL-9470 AE Zuidlaren (Netherlands) and Chemometrics Research Group, University Centre for Pharmacy, University of Groningen, Antonius Deusinglaan 2, NL-9713 AW Groningen (Netherlands)

P.M.J. Coenegracht and D.A. Doornbos

Chemometrics Research Group, University Centre for Pharmacy, University of Groningen, Antonius Deusinglaan 2, NL-9713 AW Groningen (Netherlands)

J.H.G. Jonkman

Pharma Bio-Research International BV, P.O. Box 200, NL-9470 AE Zuidlaren (Netherlands)

(First received October 13th, 1992; revised manuscript received December 21st, 1992)

ABSTRACT

In a previous investigation, the composition of the mobile phase for the reversed-phase HPLC separation of twelve sulphonamides was optimized. The predicted chromatogram showed great similarity with a chromatogram measured under optimum conditions. For routine analysis, it is important to have robust analytical methods, *i.e.*, to have methods that are precise and accurate despite small variations in the measurement conditions. In the experiment described here, a number of routine chromatograms of six sulphonamides were recorded using the HPLC system with the optimum mobile phase to validate the robustness of the system under routine conditions. The variance of the capacity factor was calculated for each sulphonamide and the influence of this variance on the variance of the selectivity and the resolution of each pair of sulphonamides was studied. Considerable variability of the capacity factors was found. However, owing to the high correlation between the variances of the capacity factors of the compounds, relatively small variances of the selectivity $\alpha_{i,j}$ and of the resolution $R_{s_{i,j}}$ of pairs of compounds were found. It was concluded that, owing to the high correlation between the variances of the capacity factor, the chromatographic system was robust with respect to the selectivity and resolution of pairs of sulphonamides.

INTRODUCTION

At the present time, much emphasis is being placed on quality in the laboratory. Accurate and precise measurements are necessary for the consistent determination of the quality of products such as drugs or the quality of the environment. The quality of a product can only be guaranteed if the quality of the analysis is ascertained. Once the quality of laboratory management procedures (*e.g.*, logistics, such as informa-

* Corresponding author. Present address: Institute of Environmental Sciences TNO (IMW TNO), Department of Analytical Chemistry, P.O. Box 6011, 2600 JA Delft, Netherlands.

0021-9673/93/$06.00

tion flow) has been achieved and ascertained by good laboratory practice (GLP) rules or other compliance programmes, the quality of the chemical procedures may be improved, *e.g.*, the optimization of the robustness of methods or procedures.

Several definitions of quality have been given in the literature. The International Organization of Standardization (ISO) defines quality as "the totality of features and characteristics of a product, process or service that bear on its ability to satisfy stated or implied needs". A very explicit definition has been given by Taguchi and Wu [1]: the quality of a product is expressed by its loss to society. The parameter design procedure of Taguchi and Wu was developed to improve product performance and distinguishes between design variables (controllable variables) and noise variables (non-controllable factors). A particular experimental design is used, the goal of which is to select those settings of the design variables which give optimum results for the performance of a product. Moreover, those settings of the noise factors are selected which have minimal effects on the performance of the product.

Many papers have been published on the optimization of the composition of the mobile phase of reversed-phase high-performance liquid chromatography (RP-HPLC) [2–8]. The applied methods demonstrated good prediction of chromatographic behaviour. Robustness of chromatographic systems has also been described [9–11]. However, the publications concerned dealt with robustness with respect to variables other than the composition of the mobile phase; the influence of small deviations from the optimum settings of variables such as wavelength and flow-rate on the final analytical result was investigated. A similar investigation was performed by Hoogkamer *et al.* [12]. Gooding and Schmuck [13] concluded that through careful method development, the limits on the variability can be defined so that HPLC methods can have the ruggedness required for validation procedures in biotechnological and pharmaceutical situations. De Boer *et al.* [14,15] developed and introduced a robustness coefficient which they illustrated with an application in mixture design optimization strategies. Wieling *et al.* [16] developed a method to estimate the robustness of liquid–liquid extraction procedures of drugs from biological matrices prior to HPLC analysis.

The final aims of the investigation described in this paper were to detect any covariance structure in capacity factors in RP-HPLC and to use robustness parameters in RP-HPLC in future research. Some study of the significance of the implementation of the variance/covariance structure in HPLC separations was needed for this research.

As an example, the robustness of an optimized HPLC system with respect to separation power (expressed by the selectivity $\alpha_{i,j}$ and the resolution $R_{s_{i,j}}$ of peak pairs) under routine conditions was examined. The mobile phase composition that was selected after the optimization procedure [17] was examined with respect to inter-day reproducibility: during a period of 3 weeks the drift of the capacity factors and their influence on selectivity and resolution was investigated. The rules of the propagation of errors were used to determine the validity of the assumption of the presence of covariance between capacity factors.

Detailed discussions on error propagation in chromatography has been given by Ku [18] and Balke [19].

THEORY

The selectivity of a mobile phase for two compounds i and j is defined as the ratio of the capacity factors (k'_i and k'_j) of those compounds in that mobile phase:

$$\alpha_{ij} = k'_i / k'_j \tag{1}$$

After the recording of a series (n) of chromatograms, the means, $\bar{k}_i$ and $\bar{k}_j$, the variances of the capacity factors of compounds i and j, $S^2_{k_i}$ and $S^2_{k_j}$, and the covariance between the variances of k'_i and k'_j, $S^2_{k_i,k_j}$, are calculated as follows:

$$\bar{k}'_i = \frac{\sum_{p=1}^{n} k'_{i_p}}{n} \quad \text{and} \quad \bar{k}'_j = \frac{\sum_{p=1}^{n} k'_{j_p}}{n}$$

$$S^2_{k_i} = \frac{\sum_{p=1}^{n} (k'_{i_p} - \bar{k}'_i)^2}{n-1} \quad \text{and} \quad S^2_{k_j} = \frac{\sum_{p=1}^{n} (k'_{j_p} - \bar{k}'_j)^2}{n-1}$$

$$S^2_{k_i,k_j} = \frac{\sum_{p=1}^{n} (k'_{i_p} - \bar{k}'_i) \cdot (k'_{j_p} - \bar{k}'_j)}{n-1} \qquad (2)$$

Now, in HPLC systems that show significant variability, a positive or negative drift in capacity factors may arise, which may influence the value of $\alpha_{i,j}$. Under conditions where random variables contribute to the variance of the capacity factors of both compounds i and j and with the same direction and magnitude (*i.e.*, $S^2_{k_i}$ and $S^2_{k_j}$ are completely correlated), no change in $\alpha_{i,j}$ arises. This is demonstrated by the equation

$$S^2_{\alpha_{i,j}} = S^2_{k_i}\left(\frac{\partial \alpha_{i,j}}{\partial k'_i}\right)^2 + S^2_{k_j}\left(\frac{\partial \alpha_{i,j}}{\partial k'_j}\right)^2 + S^2_{k_i,k_j}\left(\frac{\partial \alpha_{i,j}}{\partial k'_i} \cdot \frac{\partial \alpha_{i,j}}{\partial k'_j}\right)$$

$$= \alpha^2_{i,j}\left[\left(\frac{S_{k_i}}{\bar{k}'_i}\right)^2 + \left(\frac{S_{k_j}}{\bar{k}'_j}\right)^2 - 2 \cdot \frac{S^2_{k_i,k_j}}{\bar{k}'_i \bar{k}'_j}\right] \qquad (3a)$$

in which the variance of the selectivity, $S^2_{\alpha_{i,j}}$, is expressed as a function of the partial derivatives of the selectivity $\alpha_{i,j}$ to the capacity factors of i and j and as a function of the (co)variances of the capacity factors of i and j.

The correlation coefficient r is a relationship between the covariance and the variances of k'_i and k'_j and expresses the correlation between these capacity factors:

$$r = S^2_{k_i,k_j} / S_{k_i} S_{k_j}$$

The larger the correlation, the more robust the separation of i and j is with respect to small variations of the conditions.

Similarly, these rules of error propagation are valid for the variance of the resolution as a function of the variance of the capacity factors. The resolution of two compounds i and j in an RP-HPLC system is expressed by the equation

$$R_{s_{i,j}} = \frac{\sqrt{N}}{2} \cdot \frac{k'_j - k'_i}{k'_j + k'_i + 2} \qquad (4)$$

where N is the plate number of the column.

Eqn. 5a gives the variance of the resolution of i and j as a function of $S^2_{k_i}$, $S^2_{k_j}$ and $S^2_{k_i,k_j}$:

$$S^2_{R_{s_{i,j}}} = S^2_{k_i}\left(\frac{\partial R_{s_{i,j}}}{\partial k'_i}\right)^2 + S^2_{k_j}\left(\frac{\partial R_{s_{i,j}}}{\partial k'_j}\right)^2 + S^2_{k_i,k_j}\left(\frac{\partial R_{s_{i,j}}}{\partial k'_i} \cdot \frac{\partial R_{s_{i,j}}}{\partial k'_j}\right)$$

$$= \frac{N}{4} \cdot \frac{S^2_{k_j}(2\bar{k}'_i + 2)^2 + S^2_{k_i}(2\bar{k}'_j + 2)^2 - 4S^2_{k_i,k_j}(\bar{k}'_i + 1)(\bar{k}'_j + 1)}{(\bar{k}'_i + \bar{k}'_j + 2)^4}$$

$$= R^2_{s_{i,j}} \cdot \frac{S^2_{k_j}(2\bar{k}'_i + 2) + S^2_{k_i}(2\bar{k}'_j + 2)^2 - 4S^2_{k_i,k_j}(\bar{k}'_i + 1)(\bar{k}'_j + 1)}{(\bar{k}'_j - \bar{k}'_i)^2} \qquad (5a)$$

Often, the covariance terms in the eqns. 3a and 5a are omitted, since it is accepted that there is no covariance between the experimental errors of the capacity factors of two compounds. Eqns. 3a and 5a are then simplified to yield the equations

$$S^2_{\alpha_{i,j}} = S^2_{k_i}\left(\frac{\partial \alpha_{i,j}}{\partial k'_i}\right)^2 + S^2_{k_j}\left(\frac{\partial \alpha_{i,j}}{\partial k'_j}\right)^2$$

$$= \alpha^2_{i,j}\left[\left(\frac{S_{k_i}}{\bar{k}'_i}\right)^2 + \left(\frac{S_{k_j}}{\bar{k}'_j}\right)^2\right] \qquad (3b)$$

$$S^2_{R_{s_{i,j}}} = S^2_{k_i}\left(\frac{\partial R_{s_{i,j}}}{\partial k'_i}\right)^2 + S^2_{k_j}\left(\frac{\partial R_{s_{i,j}}}{\partial k'_j}\right)^2$$

$$= R^2_{s_{i,j}} \cdot \frac{S^2_{k_j}(2\bar{k}'_i + 2) + S^2_{k_i}(2\bar{k}'_j + 2)^2}{(\bar{k}'_j - \bar{k}'_i)^2} \qquad (5b)$$

In eqns. 3b and 5b, the variance of the resolution and the variance of the selectivity are always negatively influenced (increase) by the variance of the capacity factors, whereas their extended forms (eqns. 3a and 5a) show that a positive correlation ($0 < r \leq 1$) positively influences (decreases) the variance of the selectivity and resolution. In fact, these variances are equal to zero when $r = 1$.

Here it is assumed that it is reasonable to expect a correlation between the variances of two capacity factors in the same experiment: random variables probably have more or less the same effect on i and j, especially in this instance, where a set of structurally related compounds

are used. In other words, the variances of the retentions of two compounds are more or less correlated. This leads to the hypothesis that, even if two compounds i and j have large variances, a separation may be good and robust if these variances of the retention of both compounds are highly correlated, that is, if random variables have identical effects on both compounds.

EXPERIMENTAL

Instruments and instrumental conditions

The assay was performed with an HPLC system consisting of a Spectra-Physics (San Jose, CA, USA) Model SP8700 solvent-delivery system used at a flow-rate of 1.0 ml min^{-1} and a Kratos (Ramsey, NJ, USA) Model 757 UV detector, wavelength 260 nm, range 0.005 a.u.f.s., rise time 1 s.

Injections of sulphonamide standard solutions into a Zymark (Hopkinton, MA, USA) Z 310 HPLC injection station, equipped with an electrically controlled Rheodyne valve and a 20-μl sample loop, were performed by a Zymate II robot system. The Zymark Z 310 analytical instrument interface was used to control the HPLC injection station. The analytical column was a 100 × 4.6 mm I.D. Microsphere 3-μm C_{18} cartridge system (Chrompack, Middelburg, Netherlands). Data analysis was performed by means of a Spectra-Physics Chromjet SP4400 computing integrator.

Chemicals and reagents

Six sulphonamides were supplied by Sigma (St. Louis, MO, USA): sulphisomidine (SOMI), sulphathiazole (THIA), sulphapyridine (PYRI), sulphamerazine (MERA), sulphamethoxypyridazine (MEPY) and sulphachloropyridazine (CLPY). Acetonitrile (ACN), tetrahydrofuran (THF) and methanol (MeOH) were supplied by Labscan (Dublin, Ireland) and were of HPLC grade. Acetic acid (100%) (HAc), triethylamine (TEA), phosphoric acid (85%) (H_3PO_4) and potassium dihydrogenphosphate (KH_2PO_4) were all of analytical-reagent grade and supplied by Merck (Darmstadt, Germany). Water was purified by using Milli-RO-15 and Milli-Q water purification systems (Millipore, Bedford, MA, USA). Unless stated otherwise, water of Milli-Q quality was used.

A phosphate buffer (pH 3.0; 0.05 M) was prepared by dissolving 6.80 g of KH_2PO_4 in 1000 ml of water. The pH was adjusted at 3.0 using concentrated phosphoric acid. To this buffer 4.15 ml of TEA and 10 ml of HAc were added. The mobile phase was prepared by mixing 1 ml of ACN, 5 ml of THF and 140 ml of MeOH and adding phosphate buffer (pH 3.0; 0.05 M) to 1000 ml. This mobile phase composition was the result of an optimization procedure using mixture designs and multicriteria decision making (MCDM) [17]. Before use, the mobile phase was filtered through a Millipore Type HVLP filter (0.45 μm) and degassed before use by ultrasonification for 15 min.

Stock solutions of sulphonamides were prepared by dissolving 100 mg of the compounds in 100 ml of MeOH to give concentrations of 1000.0 mg l^{-1}. These solutions were stored at 4°C. A test solution was prepared containing all six sulphonamides. The concentration of each sulphonamide was 500 μg l^{-1}. The solution was stored at 4°C.

System robustness testing under routine conditions

To test the robustness of the optimized HPLC system in routine analyses, the mixture of the six sulphonamides (SOMI, THIA, PYRI, MERA, MEPY and CLPY) was injected 33 times (eleven injections on three separate days). The 33 chromatograms obtained were used to calculate the mean and variance of the capacity factors and of the resolutions and selectivities for each combination of two sulphonamides.

RESULTS AND DISCUSSION

Fig. 1 gives a representative chromatogram after injection of the test solution. For a mixture of six sulphonamides the variances of the selectivity $\alpha_{i,j}$ and the resolution $R_{s_{i,j}}$ were calculated using eqns. 3a and b and 5a and b using the means and standard deviations determined after the 33 routine analyses (Table I). The ex-

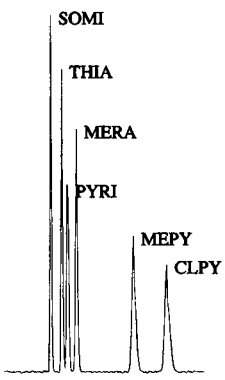

Fig. 1. Chromatogram after injection of the test solution of six sulphonamides.

perimental values of $\alpha_{i,j}$ and $R_{s_{i,j}}$ were determined using eqns. 1 and 4. From the 33 values obtained in this way, the means and the variances of $\alpha_{i,j}$ and $R_{s_{i,j}}$ were also calculated.

The data in Table I demonstrate a high and significant correlation between the experimental errors in the capacity factors. Estimation of the variability in the selectivity $\alpha_{i,j}$ and the resolution $R_{s_{i,j}}$ without the use of a covariance term would lead to overestimated values. This justifies the use of the covariance terms in eqns. 3a and 5a. Further evidence for the use of these terms is given in Tables II and III, where the values for $\alpha_{i,j}$ and $R_{s_{i,j}}$ are given with their standard deviations determined with three methods: (1) by calculating these data from the experimental values of the selectivity $\alpha_{i,j}$ and the resolution $R_{s_{i,j}}$, (2) by calculation by means of eqns. 3a and 5a and (3) by omitting the covariance terms (eqns. 3b and 5b). The tables demonstrate, with the experimentally obtained values for the variance of the selectivity $\alpha_{i,j}$ and the resolution $R_{s_{i,j}}$, that eqns. 3a and 5a are correct. Tables II and III are graphically displayed in Fig. 2. The selected HPLC system is robust with respect to the selectivity and resolution during a long period of analyses: the measured standard deviations of $\alpha_{i,j}$ and $R_{s_{i,j}}$ are equal to the values calculated by eqns. 3a and 5a, whereas the values calculated by eqns. 3b and 5b are much larger. The relative standard deviations (R.S.D.s) of the capacity factors are relatively large (4.9–6.5%, Table I), whereas the values of $\alpha_{i,j}$ and $R_{s_{i,j}}$, which are calculated from these figures, are relatively small; R.S.D.s are 0.5–1.9% for $\alpha_{i,j}$ and 0.5–7.8% for $R_{s_{i,j}}$.

Tables II and III also show the large difference between the standard deviations calculated with eqns. 3b and 5b as compared with the experimentally obtained values; for $\alpha_{i,j}$ these values are 4–16 times too high and for $R_{s_{i,j}}$ 2.5–21 times too high.

CONCLUSIONS

The assumption of the presence of covariance between capacity factors is valid for the separation of six sulphonamides in a mobile phase with constant pH. This conclusions may also be valid for mobile phase systems for the separation of

TABLE I

MEANS AND STANDARD DEVIATIONS OF THE CAPACITY FACTORS OF SIX SULPHONAMIDES AND THEIR CORRELATION COEFFICIENTS BETWEEN EXPERIMENTAL ERRORS USING THE OPTIMUM MOBILE PHASE COMPOSITION OVER A PERIOD OF 3 WEEKS ($n = 33$)

	SOMI	THIA	PYRI	MERA	MEPY	CLPY
Mean	1.5026	2.0970	2.4061	2.8825	5.9790	7.7730
S.D.	0.0799	0.1369	0.1294	0.1404	0.3253	0.4589
R.S.D. (%)	5.3	6.5	5.4	4.9	5.4	5.9
THIA	0.9774					
PYRI	0.9902	0.9952				
MERA	0.9918	0.9946	0.9990			
MEPY	0.9599	0.9956	0.9853	0.9849		
CLPY	0.9514	0.9934	0.9806	0.9800	0.9991	

TABLE II

VALUES OF THE SELECTIVITY $\alpha_{i,j}$ AND THE MEASURED AND CALCULATED STANDARD DEVIATIONS

	SOMI			THIA			PYRI			MERA			MEPY		
	$\alpha_{i,j}$	S.D.	R.S.D. (%)	$\alpha_{i,j}$	S.D.	R.S.D. (%)	$\alpha_{i,j}$	S.D.	R.S.D. (%)	$\alpha_{i,j}$	S.D.	R.S.D. (%)	$\alpha_{i,j}$	S.D.	R.S.D. (%)
THIA	1.395[a]														
		0.025[b]	1.8												
		0.024[c]	1.7												
		0.117[d]	8.4												
PYRI	1.601			1.148											
		0.012	0.7		0.015	1.3									
		0.012	0.7		0.015	1.3									
		0.121	7.6		0.097	8.4									
MERA	1.919			1.376			1.198								
		0.015	0.8		0.025	1.8		0.007	0.6						
		0.015	0.8		0.024	1.7		0.007	0.6						
		0.138	7.2		0.112	8.1		0.087	7.3						
MEPY	3.979			2.853			2.485			2.074					
		0.061	1.5		0.034	1.2		0.023	0.9		0.022	1.1			
		0.061	1.5		0.035	1.2		0.023	0.9		0.022	1.1			
		0.303	7.6		0.242	8.5		0.190	7.6		0.151	7.3			
CLPY	5.172			3.708			3.230			2.695			1.300		
		0.096	1.9		0.034	0.9		0.040	1.2		0.041	1.5		0.007	0.5
		0.095	1.8		0.035	0.9		0.040	1.2		0.040	1.5		0.007	0.5
		0.411	7.9		0.326	8.8		0.258	8.0		0.206	7.6		0.104	8.0

[a] Measured value of the selectivity $\alpha_{i,j}$.
[b] Measured standard deviation of the selectivity $\alpha_{i,j}$.
[c] Standard deviation of the selectivity $\alpha_{i,j}$ calculated with eqn. 3a (**with** correlation terms).
[d] Standard deviation of the selectivity $\alpha_{i,j}$ calculated with eqn. 3b (**without** correlation terms).

TABLE III

VALUES OF THE RESOLUTION $R_{s_{i,j}}$ AND THE MEASURED AND CALCULATED STANDARD DEVIATIONS

	SOMI			THIA			PYRI			MERA			MEPY		
	$R_{s_{i,j}}$	S.D.	R.S.D. (%)	$R_{s_{i,j}}$	S.D.	R.S.D. (%)	$R_{s_{i,j}}$	S.D.	R.S.D. (%)	$R_{s_{i,j}}$	S.D.	R.S.D. (%)	$R_{s_{i,j}}$	S.D.	R.S.D. (%)
THIA	4.204[a]														
		0.290[b]	6.9												
		0.287[c]	6.8												
		1.070[d]	25.5												
PYRI	6.064			1.891											
		0.151	2.5		0.148	7.8									
		0.151	2.5		0.147	7.8									
		0.962	15.9		1.154	61.0									
MERA	8.574			4.473			2.596								
		0.115	1.3		0.179	4.0		0.049	1.9						
		0.115	1.3		0.178	4.0		0.049	1.9						
		0.912	10.6		1.119	25.0		1.036	39.9						
MEPY	18.727			15.288			13.647			11.306					
		0.285	1.5		0.083	0.5		0.199	1.5		0.233	2.1			
		0.282	1.5		0.083	0.5		0.197	1.4		0.231	2.0			
		0.871	4.7		1.085	7.1		1.052	7.7		1.075	9.5			
CLPY	22.056			18.971			17.477			15.323			4.514		
		0.334	1.5		0.153	0.8		0.273	1.6		0.314	2.0		0.120	2.7
		0.329	1.5		0.150	0.8		0.269	1.5		0.310	2.0		0.119	2.6
		0.840	3.8		1.048	5.5		1.034	5.9		1.073	7.0		1.372	30.4

[a] Measured value of the resolution $R_{s_{i,j}}$.
[b] Measured standard deviation of the resolution $R_{s_{i,j}}$.
[c] Standard deviation of the resolution $R_{s_{i,j}}$ calculated with eqn. 5a (**with** correlation terms).
[d] Standard deviation of the resolution $R_{s_{i,j}}$ calculated with eqn. 5b (**without** correlation terms).

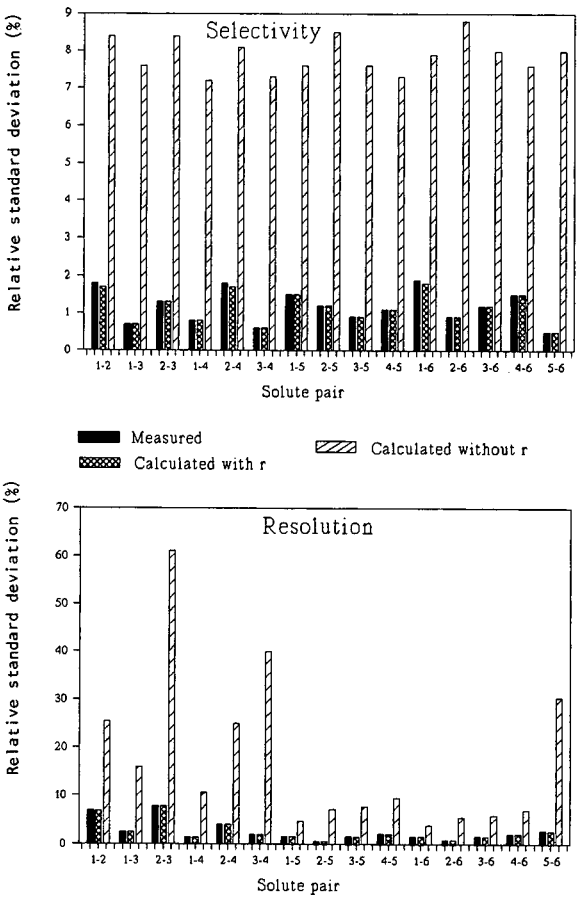

Fig. 2. Graphical comparison between the relative standard deviations of the selectivity and the resolution calculated with the experimental results and with eqns. 3a, 3b, 5a and 5b.

neutral compounds that use water instead of buffer systems. In systems that have small variability in buffer pH, *e.g.*, when pumps are used that combine two buffer systems into one mobile phase, the presence of covariance between capacity factors may be less clear, if the pK_a values of the compounds to be separated differ significantly. This may also be the case if pumps are used that combine several pure organic modifiers into one mobile phase; small changes in the polarity or the selectivity of the mobile phase due to small variations in the composition of the mobile phase may affect the change in the capacity factor of one solute differently to the change in the capacity factor of another solute.

The robustness of the separation power (expressed by the selectivity $\alpha_{i,j}$ and the resolution $R_{s_{i,j}}$ of peak pairs) with respect to variations in the capacity factors is very high under routine conditions. At the optimum mobile phase composition the precision of the selectivity and the resolution is much better than the precision of the capacity factors owing to the high correlation of the experimental errors of the capacity factors.

ACKNOWLEDGEMENT

The authors thank the Dutch Technology Foundation (Stichting voor de Technische Wetenschappen, STW) for its support of this project.

REFERENCES

1 G. Taguchi and Y. Wu, *Introduction to Off-Line Quality Control*, Central Japan Quality Control Association, Nagoya, 1980.
2 J.L. Glajch, J.J. Kirkland, K.M. Squire and J.M. Minor, *J. Chromatogr.*, 199 (1980) 57.
3 P.J. Schoenmakers, *J. Liq. Chromatogr.*, 10 (1987) 1865.
4 P.J. Schoenmakers, A.J.H.C. Drouen, H.A.H. Billiet and L. de Galan, *Chromatographia*, 15 (1982) 688.
5 J.W. Weyland, C.H.P. Bruins and D.A. Doornbos, *J. Chromatogr. Sci.*, 22 (1984) 31.
6 P.M.J. Coenegracht, A.K. Smilde, H.J. Metting and D.A. Doornbos, *J. Chromatogr.*, 485 (1989) 195.
7 R. Tijssen, H.A.H. Billiet and P. Schoenmakers, *J. Chromatogr.*, 122 (1976) 185–203.
8 J.W. Weyland, *Thesis*, State University Groningen, Groningen, 1986.
9 M. Mulholland and J. Waterhouse, *J. Chromatogr.*, 395 (1987) 539–551.
10 M. Mulholland and J. Waterhouse, *Chromatographia*, 25 (1988) 769–774.
11 M. Mulholland and J. Waterhouse, *Chem. Intell.*, 5 (1988) 263.
12 P.H. Hoogkamer and J.H.M. van den Berg, *LAB/ABC*, November (1989) 12–14.
13 K.M. Gooding and M.N. Schmuck, *BioTechniques*, 11 (1991) 232–234.
14 J.H. de Boer, A.K. Smilde and D.A. Doornbos, *Chem. Intell.*, 7 (1990) 223–236.
15 J.H. de Boer, A.K. Smilde and D.A. Doornbos, *Chem. Intell.*, 10 (1991) 325–336.
16 J. Wieling, P.M.J. Coenegracht, C.K. Mensink, J.H.G. Jonkman and D.A. Doornbos, *J. Chromatogr.*, 594 (1992) 45–64.
17 J. Wieling, J. Schepers, J. Hempenius, C.K. Mensink and J.H.G. Jonkman, *J. Chromatogr.*, 545 (1991) 101–114.
18 H.H. Ku, *J. Res. Natl. Bur. Stand., Sect. C*, 70 (1966) 263–273.
19 S.T. Balke, *Quantitative Column Liquid Chromatography, a Survey of Chemometric Methods*, Elsevier, Amsterdam, 1984, pp. 38–45.

Journal of Chromatography, 635 (1993) 203–209
Elsevier Science Publishers B.V., Amsterdam

CHROM. 24 874

Liquid chromatographic separation of radiopharmaceutical ligand enantiomers

J. Mark Green*, Rosemarie Jones, Richard D. Harrison, D. Scott Edwards and Joseph L. Glajch

DuPont Merck Pharmaceutical Company, 331 Treble Cove Road, North Billerica, MA 01862 (USA)

(First received October 29th, 1992; revised manuscript received January 12th, 1993)

ABSTRACT

A unique cyclodextrin-based chiral separation is presented for enantiomers which do not fit the commonly held selection criteria for chiral separations. The enantiomers of N,N'-1,2-ethylenediylbis(cysteine), diethyl ester are separated as the analogous rhenium(V)oxo complexes using a Cyclobond II column and a methanol–water mobile phase. The rigidity added to the molecule via the formation of the metal complex is sufficient to replace the normal requirement for an aromatic ring in the molecule for successful separation.

INTRODUCTION

There is great interest in determining the chiral purity of pharmaceuticals because of the profound pharmacological differences which may exist between optical isomers. An example of these differences are the enantiomers of penicillamine [1]. The *R* enantiomer of penicillamine is an antiarthrytic while the *S* enantiomer is highly toxic. It is this type of pharmacological difference which has led regulatory agencies and pharmaceutical manufacturers to reevaluate the strategy of developing racemic *versus* single-enantiomer drugs. In 1989, the US Food and Drugs Administration (FDA) approved 23 new drugs, 9 non-chiral, 6 racemic, and 8 single enantiomers. Justification for developing a racemic mixture rather than a pure isomer drug is now expected. The same concerns over the chiral purity of therapeutic drugs are valid for diagnostic drugs, where enantiomers may exhibit large differences in distribution. This is the case for radiopharmaceuticals such as Neurolite (DuPont Merck, North Billerica, MA, USA), the active ingredient of which is the topic of this paper.

Historically, optical rotation measurements have been used to determine optical purity. However optical rotation measurements do not always provide adequate sensitivity [2] and they are not well suited to mixtures which contain more than one optically active component. For these reasons a more specific method such as chiral chromatography is often preferred.

The determination of chiral purity has blossomed in recent years with the development of chromatographic techniques which can be used to separate the enantiomers of a wide variety of compounds. There are several general approaches to the separation of enantiomers using commercially available chiral bonded phases for high-performance liquid chromatography. The first to be introduced were the Pirkle columns [3] which used derivatized silica columns in a normal-phase mode. Separations were achieved for compounds which had at least three modes of interaction with the stationary phase — π–π interactions, hydrogen bonding, dipole interac-

* Corresponding author.

0021-9673/93/$06.00

tions, etc. Cyclodextrin columns were the first chiral phases intended for use in the reversed-phase mode [4]. These columns facilitate chiral separations through the formation of analyte–bonded phase inclusion complexes. A variety of modified cyclodextrin columns are now available for normal- and reversed-phase separations. A number of polymeric phases have also been used to achieve separation of enantiomers, among them the cellulosic [5], protein [6] and methacrylate [7] columns. A fourth type of chiral stationary phase are the ligand-exchange columns [8] which achieve enantiomeric separations via formation of metal–diastereomeric complexes.

Each of the four modes of chiral bonded phase chromatography requires specific functional group interactions in order to separate enantiomers. With the exception of ligand-exchange separations, some cellulosic columns (for example Chiralcel columns by Diacel), and recent reports using β- [9] and derivatized β-cyclodextrin columns [10], these techniques generally require that an aromatic ring be present in the molecule. This obviously restricts separations to those compounds containing such a group or those which may be derivatized. In the case of N,N′-1,2-ethylenediylbis(cysteine), diethyl ester, no ring is present, and the conditions required for derivatization close to the chiral center (high pH) are such that oxidation and racemization occur. Attempts at separating the enantiomers without derivatization were not successful. Attempts at separating the enantiomers by ligand exchange were likewise unsuccessful.

We first reported the separation of non-aromatic enantiomers using cyclodextrin columns in 1990 [11]. In this paper, we present a review of the development of a chiral separation for the enantiomers of N,N′-1,2-ethylenediylbis-(cysteine), diethyl ester (also referred to as ECD). N,N′-1,2-Ethylenediylbis-L-cysteine, diethyl ester, the single L,L-ECD enantiomer, is the active ingredient in Neurolite, a technetium based agent for single-photon emission computed tomography (SPECT) brain imaging. Upon radiolabelling of racemic ECD with technetium (or rhenium, as described here) there are four possible isomers; two enantiomers and two *meso* compounds. The separation of these enantiomers is unique in that it was accomplished for molecules which do not contain an aromatic ring. This successful separation suggests the need for an aromatic ring for selectivity in cyclodextrin based separations may in some cases be based on the rigidity it adds to the molecule rather than direct chemical interaction with a source of aromaticity.

EXPERIMENTAL

Reagents and chemicals

The L,L, D,D, and D,L isomers of N,N′-1,2-ethylenediylbis cysteine, diethyl ester were synthesized using modifications of the procedure by Blondeau *et al.* [12]. The structure of L,L-ECD · 2HCl is shown in Fig. 1. The conformations of the purified Re(O)ECD (hereafter referred to as ReECD) enantiomers were confirmed via X-ray crystallography [13]. The structures of the ReECD stereoisomers are shown in Fig. 2. Ammonium perrhenate (99+%) was obtained from Aldrich (Milwaukee, WI, USA). Sodium dithionite (Sodium hydrosulfite) was obtained from Mallinkrodt (Paris, KY, USA). Ultrapure water (Milli-Q, Millipore, Bedford, MA, USA) was used in preparation of the

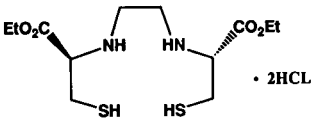

Fig. 1. Structure of L,L-ECD · 2HCl.

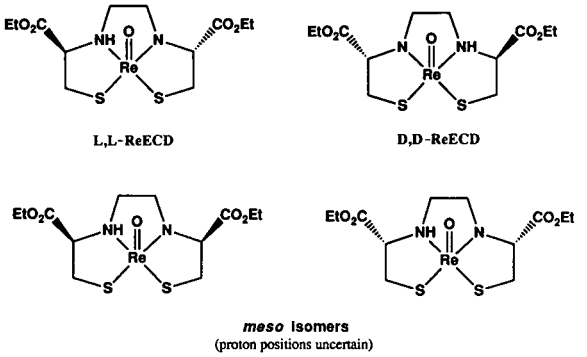

Fig. 2. Structures of stereoisomers of ReECD.

mobile phase. ACS-Grade sodium hydrogencarbonate, HPLC-grade methanol, and HPLC-grade chloroform were obtained from Fisher Scientific (Pittsburgh, PA, USA).

Chromatographic system

The HPLC consisted of a Hewlett-Packard 1090M system (Hewlett-Packard, Avondale, PA, USA), equipped with a diode array UV–Vis detector monitoring at a wavelength of 210 nm. The analytical columns, Cyclobond I, I 3,5-dimethylphenyl carbamate (DMP), II and III were obtained from ASTEC Scientific (Whippany, NJ, USA). The majority of the work was performed using 500 mm × 4.6 mm Cyclobond II (γ-cyclodextrin) columns. Mixtures of methanol and Milli-Q water were prepared weekly and degassed by purging with helium. The flow-rate was varied during this study, but unless otherwise noted was set at 0.2 ml/min.

Preparation of rhenium complexes

Low-oxygen water (LOW) was prepared by purging Milli-Q water with low-oxygen nitrogen (LON). Ammonium perrhenate (169 mg), ECD · 2HCl (25.0 mg), and sodium hydrogencarbonate (10.6 mg) were added to a 30-ml vial with a crimp-seal top (the reaction vial). A 10-ml volume of LOW was added to the reaction vial, the vial was sealed and the contents dissolved through sonication. The reaction vial solution was then purged with LON for approximately 15 min via a syringe needle through the septum of the crimp seal.

A sodium dithionite solution was prepared at a concentration of 44 mg/ml in LOW. Immediately after dissolution, 5.0 ml of the solution were added to the 30-ml reaction vial. The contents of the vial were then allowed to react for a minimum of 3 h.

After the 3-h reaction time, the reaction vial solution is dark yellow in color and contains a dark precipitate. The contents of the reaction vial were added to a separatory funnel and extracted three times with 5-ml aliquots of chloroform, each time collecting the chloroform layer. The 15-ml extract solution was then taken to dryness. At the time of analysis, the sample was reconstituted with 10.0 ml methanol. A portion of this sample was then diluted with Milli-Q water to match the mobile phase composition.

RESULTS AND DISCUSSION

It would appear that the separation of ECD enantiomers was unlikely by the currently available separation modes without derivatization, given the commonly held selection criteria. We did attempt the direct use of a Pirkle type column (covalent L-leucine, Regis), a β-cyclodextrin column (Cyclobond I, Astec), and ligand-exchange TLC plates (Chiralplate, Macherey–Nagel) and obtained no separation of the ECD enantiomers. Based on our knowledge of ReECD chemistry, it was felt that a separation of the enantiomers as metal complexes via formation of inclusion complexes with cyclodextrins was feasible. For successful separations using cyclodextrins it is necessary that the molecules contain a relatively rigid hydrophobic section that fits tightly into the cyclodextrin cavity. Interaction of analytes with the hydroxyls at the rim of the cyclodextrin cone serves to further orient the molecules within the cyclodextrin cavity. The Re complex of ECD is easily formed, is stable and is less susceptible to oxidation than free ECD. The rigidity added to ECD by forming the Re complex seemed a likely substitute for the presence of an aromatic ring. The Re oxo group also provides an additional point of interaction.

The preparation of ReECD, described earlier, is performed at room temperature to minimize possible racemization. Furthermore, the choice of a non-chiral derivatization precludes the problems inherent in chiral derivations used to produce diastereomers [2]. Typical yields from the reaction were approximately 60% (at 3 h) and the complex was stable for at least several weeks, even after dissolution in mobile phase.

Cyclodextrin columns are available in α, β and γ forms which have cones composed of 6, 7 and 8 glycopyranose units, respectively. Thus different cone diameters (approximately 7, 8 and 10 Å, respectively) are available for optimizing the fit between analyte and cyclodextrin. It is not necessary for the entire molecule to fit inside the cavity. A screening study was performed using a

sample of racemic ReECD and four different cyclodextrin bonded phase columns (α, β, γ and β-DMP), using a methanol water mobile phase. Successful chiral separations using the α-cyclodextrins have typically involved molecules which contain a single aromatic ring, and it was anticipated that ReECD (approximately $13 \times 8 \times 5$ Å) would be too large to enter the α-cyclodextrin structure. No separation of the enantiomers was achieved with the α-cyclodextrin, as the two enantiomers and one *meso* complex coeluted (Fig. 3). The retention of each isomer was determined using separate solutions of each enantiomer and a solution containing both meso isomers. The chromatography achieved with the β, derivatized β and γ phases (Fig. 3) shows at least a slight separation of the enantiomer peaks under the conditions of the screening experiments. These columns have been most successful in separating enantiomers containing two or more rings, and therefore molecules more similar in size to ReECD. Although the nature of the inclusion complex has not been determined, it is likely that ReECD is oriented with the thiolate groups pointed into the cyclodextrin cavity and that the ethyl ester and Re oxo groups interact with the external hydrogen bonding groups.

Optimization of the enantiomeric separation was continued using the γ-cyclodextrin column. For our purposes we were interested in detecting the presence of small amounts of D,D-ECD in the presence of L,L-ECD, the desired enantiomer. The column length was doubled to 50 cm to increase efficiency and counter the effects of injecting larger masses of sample onto the column. The most common mobile phases used

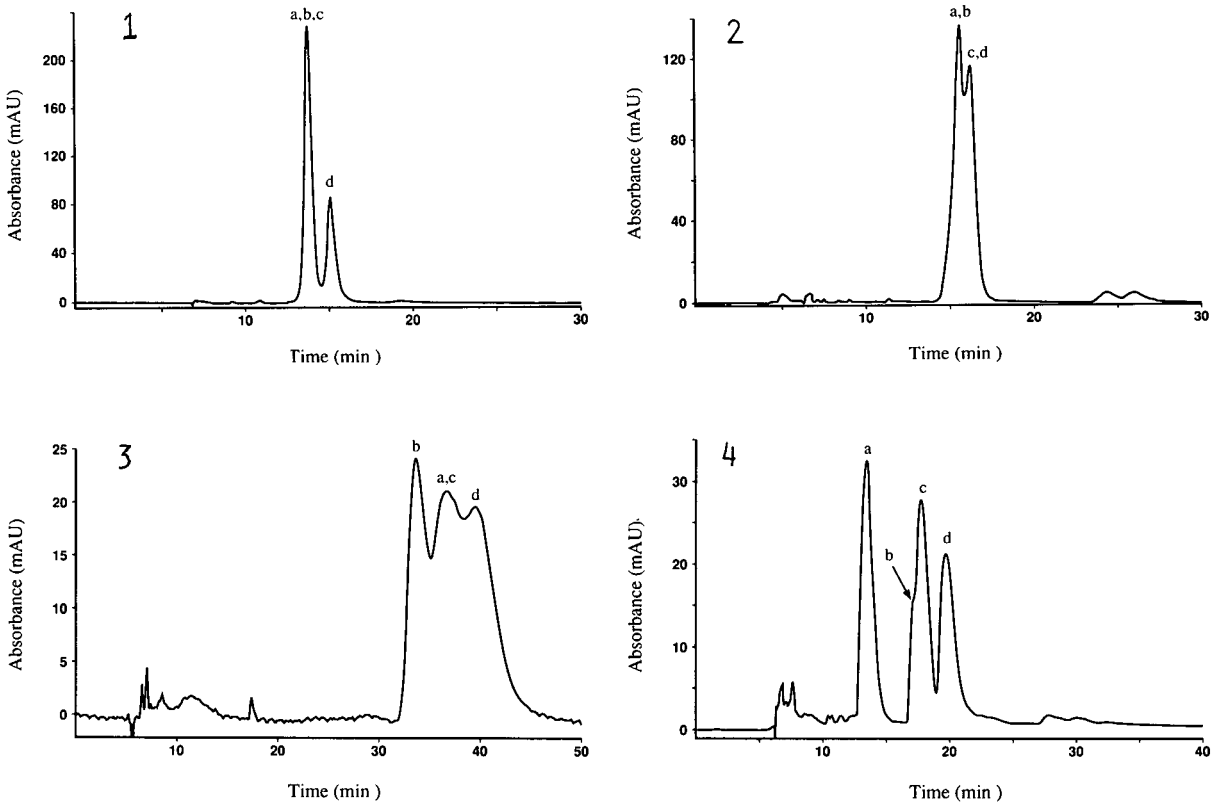

Fig. 3. Chromatograms of racemic ReECD using a (1) α-cyclodextrin column. [Cyclobond III, mobile phase methanol–water (25:75), flow-rate 0.5 ml/min], (2) β-cyclodextrin column [Cyclobond I, mobile phase methanol–water (20:80), flow-rate 0.5 ml/min], (3) derivatized β-cyclodextrin column [Cyclobond I DMP, mobile phase methanol–water (55:45), flow-rate 0.2 ml/min], and (4) γ-cyclodextrin column [Cyclobond II, mobile phase methanol–water (15:85), flow-rate 0.5 ml/min]. All columns were 25 cm × 4.6 mm. Peaks: a,d = *meso*-ReECD; b = D,D-ReECD; c = L,L-ReECD.

with cyclodextrin columns are mixtures of water and methanol or acetonitrile, a buffer, and an organic modifier such as triethylamine acetate (TEAA). These were evaluated using the γ-cyclodextrin column and it was determined that the modifier TEAA did not play a role in the separation and could be eliminated. Methanol, the lowest-strength solvent, was found to be sufficient to accomplish the separation. A plot of capacity factor *versus* percent methanol is shown in Fig. 4. This plot shows typical reversed-phase behavior —as the solvent strength increases the capacity factor decreases. This is in contrast to many cyclodextrin separations where at high organic mobile phase concentration increased retention occurs, presumably due to the increased strength of hydrogen bonding between the analyte and the cyclodextrin.

Reversed-phase separations using cyclodextrin columns often require lower flow-rates than commonly used in other types of reversed phase separations. We found that the best resolution was obtained using a 0.2 ml/min flow-rate. Also in contrast to typical reversed-phase separations where an increase in temperature quite often results in increased efficiency, the opposite effect is often seen for separations based on formation of inclusion complexes. The stability of cyclodextrin complexes are, in general, much greater at lower temperatures. In our case however we found only a small increase in resolution (1.02 *vs.* 1.10) by lowering the temperature from room temperature to 4°C. Greater benefits may be obtained using acetonitrile instead of methanol at lower temperatures since it exhibits less viscosity change as a function of temperature.

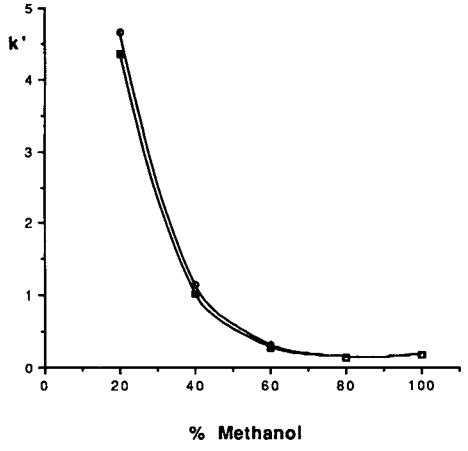

Fig. 4. Capacity factors for D,D-ReECD (■) and L,L-ReECD (○) as a function of % methanol in the mobile phase. Separation conditions, Cyclobond II column, 50 cm × 4.6 mm, flow-rate 0.2 ml/min.

As the separation conditions were optimized, we discovered that the sample capacity of the gamma column was quite low relative to typical reversed phase columns. The maximum sample mass injected before acceptable resolution was lost was approximately 3 μg. As a result of this mass limitation, the detection limit for the D,D enantiomer was determined to be 1%. Chromatograms showing a typical L,L-ECD sample (no D,D or *meso* isomers present) and a L,L-ECD sample spiked with 1% D,D-ECD are shown in Figs. 5 and 6. The optimized separation of a racemic mixture of ECD is shown in Fig. 7.

As part of our method ruggedness studies, we have evaluated this separation using five different Cyclobond II columns. These columns ranged from new, unused columns to columns on which hundreds of injections had been made. A plot of stereoisomer retention *versus* mobile phase methanol composition for a typical column is shown in Fig. 8. The chromatographic differences between the five columns is illustrated in Fig. 9, in which the L,L-ReECD retention for each column is plotted *versus* the mobile phase methanol composition. Adequate separation of the enantiomers and *meso* complexes were obtained with each column, but each column differed in the ratio of methanol and water required

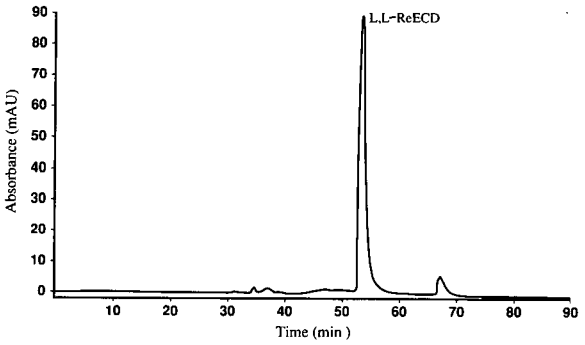

Fig. 5. Chromatogram of a typical L,L-ReECD sample. Column, Cyclobond II, 50 cm × 4.6 mm; mobile phase, methanol–water (50:50), flow-rate, 0.2 ml/min.

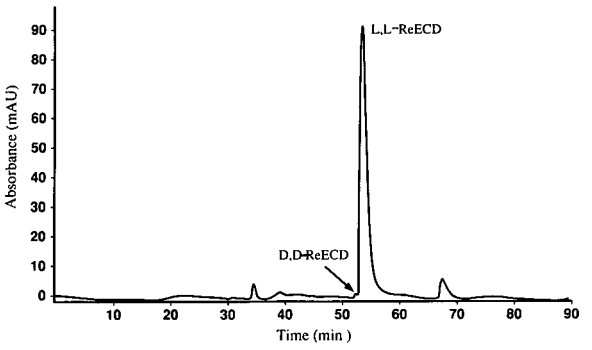

Fig. 6. Chromatogram showing detection of 1% D,D-ReECD in the presence of L,L-ReECD. Column, Cyclobond II, 50 cm × 4.6 mm; mobile phase, methanol–water (50:50), flow-rate, 0.2 ml/min.

for the separation. This is illustrated in Table I, where the % methanol required for a 65-min retention time for L,L-ReECD was calculated along with the retentions of the remaining three stereoisomers. Among the possible causes for these differences are column manufacturing variability (which may not be noticeable for the majority of separations performed with these columns), and changes in retentivity upon use due to accumulation of permanently retained sample components. In general we have found that a retention of between 60 and 70 min for the L,L-ReECD peak will result in adequate separation ($R_s \geq 1$) of the enantiomers.

This work has presented a new approach to the separation of non-aromatic enantiomers using cyclodextrin columns. The presence of a rigid non-aromatic ring can function in place of

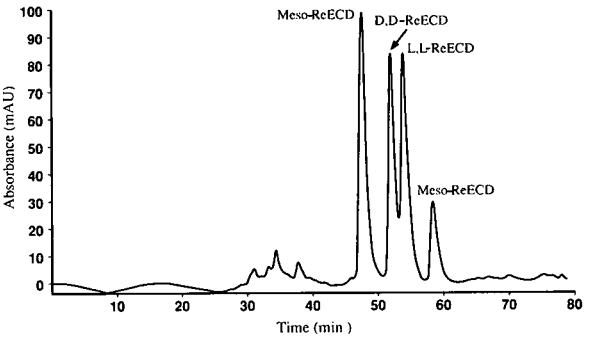

Fig. 7. Chromatogram of racemic ReECD using a γ-cyclodextrin column. Column, Cyclobond II, 50 cm × 4.6 mm; mobile phase, methanol:water (50:50), flow-rate, 0.2 ml/min.

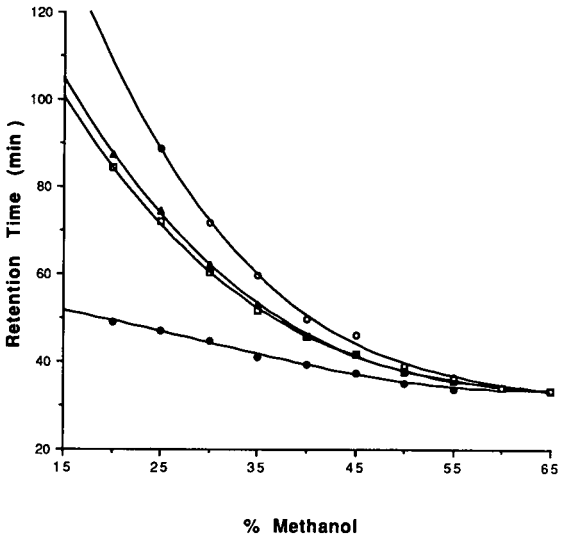

Fig. 8. Column ruggedness study showing retention changes as a function of mobile phase methanol concentration for a typical Cyclobond II column (50 cm × 4.6 mm). Symbols: ● = Re(*meso*ECD)1; □ = D,D-ReECD; ▲ = L,L-ReECD; ○ = Re(*meso*ECD)2.

an aromatic ring when additional chemical interaction is not required. The formation of metal complexes may be desirable and generally applicable to the separation of the enantiomers of technetium labelled radiopharmaceuticals and other metal ligand complexes. If the thiolate

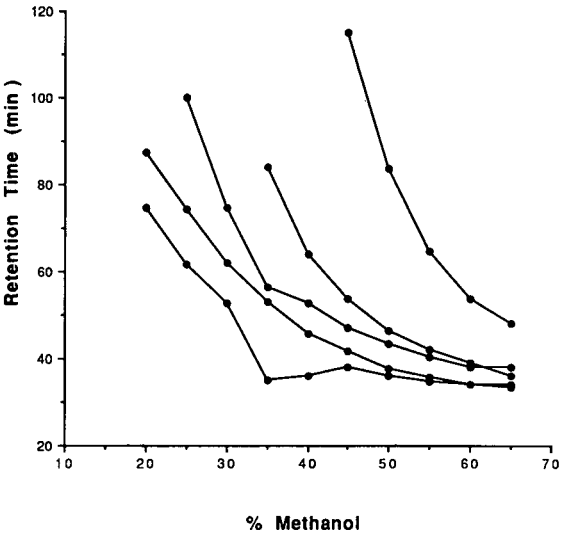

Fig. 9. Column ruggedness study showing L,L-ReECD retention changes as a function of mobile phase methanol concentration for five Cyclobond II columns (50 cm × 4.6 mm).

TABLE I

RETENTION TIMES FOR ReECD ISOMERS CALCULATED FROM FITTED CURVES (AS SHOWN IN FIG. 8) FOR EACH OF FIVE CYCLOBOND II COLUMNS

The % methanol is the percentage required to obtain a 65-min retention time for the L,L-ReECD peak.

Column no.	Retention time (min)				
	Meso 1	D,D-ReECD	L,L-ReECD	*Meso* 2	% MeOH
3818	51	63.5	65	70	23
4166	44	63.5	65	76	29
5460	59	62	65	71	55
5461	48	62	65	73	40
5462	49	62	65	73	33

groups are the key interaction with the interior of the cyclodextrin cavity, the separation of other cysteine related compounds may also be viable.

Additional studies are planned to evaluate the separation of ECD enantiomers by HPLC and capillary electrophoresis using cyclodextrin mobile phase additives. Recent studies have indicated that the use of cyclodextrins as mobile phase additives provides great flexibility in method development and yields efficiencies similar to that obtained with cyclodextrin bonded phase columns [14,15].

REFERENCES

1 M. Mack and H.E. Hauck, *Chromatographia*, 26 (1988) 197.
2 I.W. Wainer and T.J. Doyle, *LC Mag.*, 2 (1984) 88.
3 W.H. Pirkle, J.M. Finn, J.L. Schreiner and B.C. Hamper, *J. Am. Chem. Soc.*, 103 (1981) 3964.
4 D.W. Armstrong and W.J. DeMond, *J. Chromatogr. Sci.*, 22 (1984) 411.
5 I.W. Wainer and R.M. Stiffin, *J. Chromatogr.*, 411 (1987) 139.
6 S. Allenmark, *J. Liq. Chromatogr.*, 9 (1986) 425.
7 A. Ichida, *Am. Lab.*, 20 (1988) 100.
8 V.A. Davankov, A.A. Kurganov and T.M. Ponomarova, *J. Chromatogr.*, 452 (1988) 309.
9 J. Kutter and T. Class, *Chromatographia*, 33 (1992) 103.
10 S.C. Chang, L.R. Wang and D.W. Armstrong, *J. Liq. Chromatogr.*, 15 (1992) 1411.
11 J.M. Green, R. Jones, R.D. Harrison, D.S. Edwards and J.L. Glajch, presented at the *200th American Chemical Society National Meeting, Washington, DC, 1990.*
12 P. Blondeau, C. Berse and D. Gravel, *Can. J. Chem.*, 45 (1967) 49.
13 D. Edwards and T. Harris, DuPont Merck Pharmaceutical Company, in preparation.
14 K. Cabrera and G. Schwinn, *Am. Lab.*, 22 (1990) 22.
15 M. Gazdag, G. Szepesi and L. Huszar, *J. Chromatogr.*, 436 (1988) 31.

Journal of Chromatography, 635 (1993) 211–219
Elsevier Science Publishers B.V., Amsterdam

CHROM. 24 873

Reversed-phase liquid chromatographic measurement of the influence of a co-modifier functional group on the retention behavior of the β-cyclodextrin–pyrene complex

Noni Husain, Vincent C. Anigbogu[☆], Matthew R. Cohen[☆☆] and Isiah M. Warner*

Department of Chemistry, Louisiana State University, Baton Rouge, LA 70803 (USA)

(First received November 3rd, 1992; revised manuscript received January 12th, 1993)

ABSTRACT

Reversed-phase liquid chromatography was used to determine the stoichiometry and formation constants of the complex of β-cyclodextrin with pyrene in the presence of several secondary modifiers in a 59% (v/v) methanol in water mobile phase. All secondary modifiers contained a bulky and hydrophobic *tert.*-butyl moiety attached to functional groups of varying polarity and heteroatom composition. Although pyrene exhibits no interaction with β-cyclodextrin in a 59% (v/v) methanol in water solvent alone, the addition of a co-modifier resulted in dramatically short retention times. The stoichiometry of the β-cyclodextrin–pyrene was determined to be predominantly 2:1. Formation constants were estimated to be approximately 10^4 M^{-2}. Adding functionality and increasing chain length in co-modifiers resulted in a corresponding enhancement of formation constants and reduction of capacity factors. The effects of pH on the equilibrium and the applications of co-modifier effects in environmental analysis are discussed.

INTRODUCTION

Cyclodextrins (CDs) are cyclic oligosaccharides that form inclusion complexes with a variety of organic guest molecules [1,2]. The use of CDs as mobile phase modifiers in reversed-phase liquid chromatography has been widely documented [3–9]. The fixed cavity sizes of the cyclodextrins impart a high degree of selectivity upon the separation, since the elution time of a given analyte depends directly on the strength and stoichiometry of its complex with cyclodextrin [10,11].

The impact of polynuclear aromatic hydrocarbons (PAHs) on the environment has been well established [12–15]. As a result, significant effort has been focussed towards characterizing the behavior of such compounds in aqueous and non-aqueous media [16]. Complexation of PAHs with cyclodextrins has been widely studied using a variety of spectroscopic techniques, including absorbance and fluorescence [17–20]. Although these methods are highly sensitive and have relatively short analysis time, their use is limited to the determination of analytes that undergo a significant change in their spectroscopic properties upon inclusion in the CD cavity. Several studies have utilized reversed-phase HPLC as an alternative analytical technique to investigate the complexation of PAHs with cyclodextrins [21–

* Corresponding author.
☆ Present address: Department of Chemistry, Agnes Scott College, Decatur, GA 30030, USA.
☆☆ Present address: Department of Chemistry, Emory University, Atlanta, GA 30322, USA.

0021-9673/93/$06.00

24]. An example of a common PAH is pyrene, which has been shown to form a strong 2:1 (β-CD–pyrene) complex with β-CD [25]. Recently, Anigbogu *et al.* [26] investigated the retention behavior of β-CD:pyrene complexes in the presence of alcohol comodifiers using reversed-phase HPLC. The retention time of pyrene in a methanol–water solvent system was found to be relatively unchanged in the presence of increasing amounts of β-cyclodextrin. The addition of 1% *tert.*-butanol or cyclopentanol as a secondary modifier, however, caused a dramatic reduction in the capacity factor of pyrene. This effect has been attributed to the formation of a ternary β-CD–pyrene–alcohol complex. A later study of apparent formation constants determined that the alcohol strengthens the β-CD–pyrene complex [27].

The effect of an appropriate secondary modifier on the β-CD–PAH complex can have significant environmental applications in selective extractions of non-aqueous solutes in a complex mixture. This study is a comparison of several secondary modifiers in an effort to characterize these types of ternary complexes, which may improve upon existing methodologies in environmental analysis. The selection of modifiers was based upon the assumption that the bulky and hydrophobic *tert.*-butyl group in *tert.*-butanol is partially included in the β-CD cavity, with the hydroxyl group hydrogen bonding with the primary and secondary hydroxyl groups located on the periphery of the cyclodextrin. This orientation of the alcohol has previously been proposed by Muñoz de la Peña *et al.* [28] in their investigation of the β-CD–pyrene–*tert.*-butanol system in aqueous media. The nature and polarity of the functional group on the *tert.*-butyl may therefore have a significant effect upon the strength and extent of the hydrogen bonding occurring at the periphery of the cyclodextrin. The comodifiers used in this study contain the *tert.*-butyl (tBu) moiety attached to functional groups of varying polarity and heteroatom composition.

EXPERIMENTAL

Apparatus

The chromatographic apparatus used in this study has been described elsewhere [26].

Reagents

HPLC-grade methanol and water were purchased from B&J (Baxter, McGraw Park, IL, USA) and Fisher (Fair Lawn, NJ, USA), respectively. Pyrene (99+%) and the secondary organic modifiers, tBu-OH, tBu-acetate, tBu-formate, tBu-carbamate, tBu-carbazate, tBu-formate, tBu-acetate, N(tBu-carbonyl)glycine and N(tBu-hydroxy)carbamate were all purchased from Aldrich (Milwaukee, WI, USA) and were used as received. The β-CD used in this study was provided by American Maize Products (Hammond, IN, USA) and was recrystallized twice from deionized water before use. The potassium nitrite used for determining the void volume of the column was purchased from Mallinckrodt (Paris, KY, USA).

Procedure for the liquid chromatographic runs

The procedure for the chromatographic runs was similar to that previously described by Anigbogu *et al.* [26]. The mobile phase consisted of a mixture of 59% (v/v) methanol, 39% (v/v) water mixture, and 0.2 mol% (approximately 0.075 *M*) of secondary modifier.

RESULTS AND DISCUSSION

Effect of secondary organic modifier on the capacity factor of pyrene

Anigbogu *et al.* [26] recently reported the effects of the addition of *tert.*-butanol as a secondary modifier on the retention time of pyrene in the presence of β-CD in a water–methanol system. The capacity factor of pyrene was found to be remarkably reduced upon the addition of the alcohol. This was attributed to the formation of a ternary β-CD–pyrene–alcohol complex, which has been extensively investigated in aqueous media by researchers using fluorescence and proton NMR analyses [28]. The hydrophobicity of the *tert.*-butyl moiety of the

alcohol would make it more likely for it to be associated with the interior of the cyclodextrin cavity. Muñoz de la Peña *et al.* [28] suggested two possible configurations for the β-CD–pyrene–alcohol complex, both of which involve the hydrogen bonding interaction of the OH group of the alcohol with the hydroxyl groups lining the periphery of the cyclodextrin. As a result, changing the size and polarity of the functional group of the *tert.*-butyl modifier would cause a corresponding change in the formation of the ternary complex.

Table I provides a list of the modifiers used in this study. The purpose of selecting these particular *tert.*-butyl compounds was to systematically vary the polarity, chain size and heteroatom composition of the functional group in an effort to determine the influence of these variables on the retention of the β-CD–pyrene complex under reversed phase conditions. *tert.*-Butanol has been used as a reference to compare the extent of the effect of the various comodifiers on the retention time of pyrene.

Fig. 1a shows the effect of comodifiers I, II, III and IV on the capacity factor of the β-CD–pyrene complex. As expected, the addition of *tert.*-butanol (I) resulted in an overall decrease in the capacity factor of pyrene (Fig. 1a), which is in agreement with previous results [26]. It is interesting to note, however, that unlike the other secondary modifiers, *tert.*-butyl formate (II) and N(*tert.*-butoxycarbonyl)glycine (VIII) appear to significantly influence the capacity factor (k_0') of the uncomplexed pyrene (Fig. 1b). The factors that may have contributed to this

TABLE I

SECONDARY MODIFIERS

tert.-Butyl alcohol (I)	$(CH_3)_3C-O-H$
tert.-Butyl formate (II)	$(CH_3)_3C-O-CO-H$
tert.-Butyl acetate (III)	$(CH_3)_3C-O-CO-CH_3$
tert.-Butyl carbamate (IV)	$(CH_3)_3C-O-CO-NH_2$
tert.-Butyl carbazate (V)	$(CH_3)_3C-O-CO-NH-NH_2$
tert.-Butyl (N-hydroxy)-carbamate (VI)	$(CH_3)_3C-O-CO-NH-OH$
N(*tert.*-Butoxycarbonyl)-glycine (VII)	$(CH_3)_3C-O-CO-NH-CH_2-COOH$

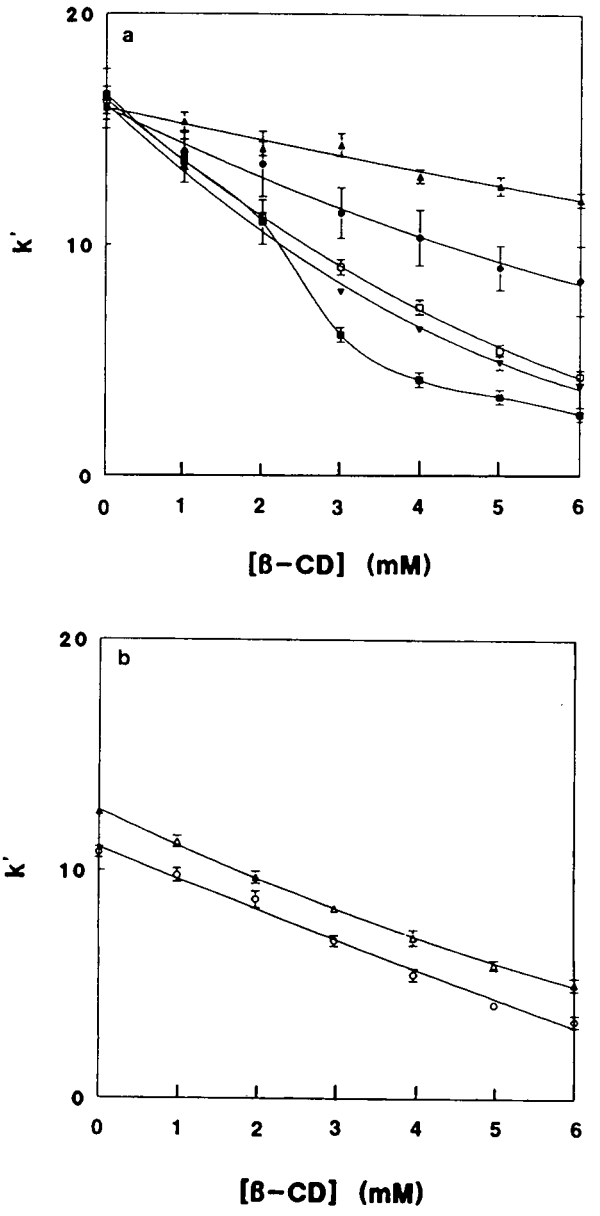

Fig. 1. Effect of β-CD concentration on the capacity factor of pyrene in the presence of different secondary modifiers. (a) ▲ = *tert.*-Butyl alcohol (I); ● = *tert.*-butyl acetate (III); □ = *tert.*-butyl carbazate (V); ▼ = *tert.*-butyl carbamate (IV); ■ = *tert.*-butyl N-(hydroxy)carbamate (VI). (b) △ = *tert.*-Butyl formate (II); ○ = N(*tert.*-butoxycarbonyl)glycine (VII).

apparent anomaly and the effects on the calculated K_f values are discussed later.

The effect of replacing the hydrogen in *tert.*-

butyl formate (II) with a methyl group may be seen in the *tert.*-butyl acetate (III) data in Fig. 1a. In this case, the co-modifier has no observable effect upon the retention time of free pyrene.

The retention times of the β-CD–pyrene complex, however, are significantly reduced in the presence of *tert.*-butyl acetate (III) compared to *tert.*-butyl alcohol (I). This suggests that the ester is involved in the formation of the inclusion complex in a way such that the pyrene molecule is further protected from interaction with the C_{18} mobile phase. This may be due to hydrogen bond formation between the carbonyl group of the co-modifier and the hydroxyl groups lining the periphery of the cyclodextrin.

Further evidence of the formation of hydrogen bonds can be seen when the methyl group on *tert.*-butyl acetate (III) is replaced by an amino group in *tert.*-butyl carbamate (IV). Fig. 1a shows that the addition of *tert.*-butyl carbamate as a secondary modifier to a methanol–water solvent results in a dramatic decrease in the capacity factors of the β-CD–pyrene complex. This suggests that the interaction of IV with the inclusion complex is stronger than that of III, which indicates that the amino group is either directly or indirectly involved in complex formation. Aqueous phase spectroscopic studies of the ternary β-CD–pyrene–amine species have revealed the formation of charge transfer complexes between the amine and pyrene, which would involve the nitrogen being in close proximity to the pyrene molecule [29,30]. Several of these investigations, however, assumed a 1:1 association ratio for the β-CD–pyrene complex. This stoichiometry would allow less water to be excluded from the cavity, causing it to be more polar, thereby making it more likely for the polar amino group to penetrate the cavity and interact with the pyrene. Recent studies in our laboratory have determined, however, that the stoichiometry between β-CD and pyrene is 2:1 (2 cyclodextrin molecules encapsulating 1 pyrene molecule) [25,28]. This configuration results in a larger amount of water being displaced from the cavity, making the cavity more hydrophobic. Taking into consideration the space and polarity restrictions of the cyclodextrin cavity, it seems more likely that the non-polar and bulky *tert.*-butyl group is included, with the carbonyl and amino groups protruding out into relatively aqueous microenvironment. The hydrogen bonding interactions are expected to be stronger for *tert.*-butyl carbamate (IV) compared to *tert.*-butyl acetate (III) due to the presence of the amino group in former, which may explain the enhanced reduction of pyrene retention times that occur upon its addition.

Fig. 1 also depicts the effect of changing both the chain size as well as the polarity of the functional group attached to the *tert.*-butyl moiety of the secondary modifier upon the retention times of the β-CD–pyrene complex. Addition of another amino group to *tert.*-butyl carbamate (IV) produces no significant change, as can be seen in the data obtained in the presence of *tert.*-butyl carbazate (V). When compared to *tert.*-butanol, however, the effect of *tert.*-butyl carbazate is very pronounced. Retention times of free pyrene undergo a significant decrease in the presence of N (*tert.*-butoxycarbonyl)glycine (VI), in which the second amino group of V is replaced by a hydroxyl group.

Determination of the stoichiometry of the β-CD–pyrene complex in the presence of secondary modifiers

Consider the reaction between pyrene (P) and β-CD

$$P + n(\beta\text{-CD})_m \rightleftharpoons [(\beta\text{-CD})_n\text{–}P]_m \quad (1)$$

where the subscript m denotes the concentration in the mobile phase. Armstrong *et al.* [4] determined the relationship between the capacity factor of the probe and equilibrium concentration of β-CD in a water–primary organic modifier mobile phase to be as follows:

$$1/k' = 1/k'_0 + K_f[\beta\text{-CD}]^n_m/k'_0 \quad (2)$$

where k' is the capacity factor of the probe; k'_0 is the capacity factor of the probe in the absence of β-CD; K_f is the formation constant for the β-CD–probe complex, and $[\beta\text{-CD}]_m$ is the equilibrium concentration of β-CD. Assuming a correct stoichiometry between β-CD and the guest, a plot of $1/k'$ *versus* $[\beta\text{-CD}]^n_m$ would be

linear with slope K_f/k'_0 and intercept $1/k'_0$. The equilibrium concentration of β-CD can be determined by the following equation

$$[\beta\text{-CD}]_m = [\beta\text{-CD}]/(1 + K_{m1}[M_1] + K_{m2}[M_2]) \quad (3)$$

where M_1 and M_2 are the primary (*e.g.* methanol) and secondary (*e.g. tert.*-butyl carbamate) modifiers, respectively, and K_{m1} and K_{m2} are the formation constants for β-CD–M_1 and β-CD–M_2 complexes, respectively. Assuming negligible interaction between the modifiers and β-CD, the initial concentration of β-CD equals its equilibrium concentration. Initial β-CD concentrations were used to determine stoichiometries and formation constants for the β-CD–pyrene complex in the presence of the various modifiers.

Fig. 2 shows a plot of $1/k'$ *vs.* [β-CD] for pyrene in a water–methanol system with 0.20 mol% tBu-carbamate. Assuming a 1:1 stoichiometry between β-CD and pyrene, a curvilinear fit is obtained. Assuming that two cyclodextrins associate with every pyrene molecule, *i.e.*, $n = 2$, the plot of $1/k'$ *vs.* $[\beta\text{-CD}]_m$ gives a linear fit, indicating that the stoichiometry between the species is predominantly 2:1 (β-CD–pyrene). Similar results were obtained when different comodifiers were used. The correlation coefficients for both 1:1 and 2:1 fits for all the comodifiers are reported in Table II. These values indicate that the predominant stoichiometry is 2:1 in the presence of all the secondary modifiers used in this study. This is consistent with previous studies of β-CD–pyrene complexes [25,27], which reported the formation of a 2:1 complex between β-CD and pyrene.

Determination of formation constants for the β-CD–pyrene complex in the presence of different secondary modifiers

The equilibrium constant of the β-CD–pyrene complex with various co-modifiers quantifies the strength and stability that may be conferred upon this inclusion complex due to the presence of the secondary component. This information can have significant impact upon method development procedures using cyclodextrins in pharmaceutical and analytical applications. Apparent formation constants for the β-CD–pyrene complex in the presence of the various co-modifiers were determined by utilizing eqn. 2. The slopes and intercepts of the linear plots obtained by assuming a 2:1 pyrene–β-CD stoi-

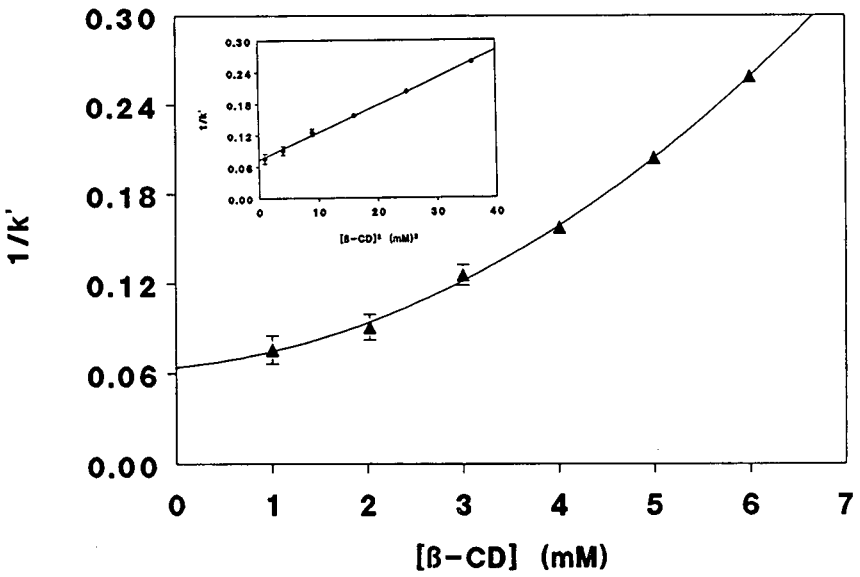

Fig. 2. Plot of $1/k'$ *vs.* $[\beta\text{-CD}]^n_m$ for pyrene in the presence of 0.075 *M tert.*-butyl carbamate assuming a (▲) 1:1 ($n = 1$) and (●) 2:1 ($n = 2$) (inset) β-CD–pyrene stoichiometry.

TABLE II

CORRELATION COEFFICIENT VALUES FOR THE PLOTS OF $1/k'$ *VS.* [β-CD] IN THE PRESENCE OF DIFFERENT SECONDARY MODIFIERS

Co-Modifier	1:1 Stoichiometry	2:1 Stoichiometry
tert.-Butyl alcohol (I)	0.973	0.991
tert.-Butyl formate (II)	0.989	0.998
tert.-Butyl acetate (III)	0.981	0.990
tert.-Butyl carbamate (IV)	0.984	0.998
tert.-Butyl carbazate (V)	0.976	0.998
N(*tert.*-Butyl hydroxy)carbamate (VI)	0.981	0.997
N(*tert.*-Butoxycarbonyl)glycine (VII)	0.971	0.997

chiometry were used to estimate the K_f values. Table III lists the apparent K_f values calculated for the β-CD–pyrene complex in the presence of the different co-modifiers used in this study.

Previous studies utilizing β-CD in a methanol–waster mobile phase have shown that pyrene and other polyaromatic hydrocarbons interact more with the C_{18} stationary phase and are not eluted off the column in significant quantities [31,32]. As a result, the association constant of the pyrene–β-CD complex under these conditions is negligible. Introducing a secondary modifier like *tert.*-butyl alcohol was found to enhance the interaction between the solute and the β-CD mobile phase, suggesting the formation of a ternary complex, and subsequently it became possible to estimate a value for the formation constant of the pyrene–β-CD complex. The value of the apparent formation constant in the presence of *tert.*-butyl alcohol at 59% methanol calculated here is along the same order of magnitude as that reported by Anigbogu *et al.* [27].

TABLE III

APPARENT FORMATION CONSTANTS FOR THE β-CD–PYRENE COMPLEX IN THE PRESENCE OF SEVERAL SECONDARY MODIFIERS

Co-modifier	K_f (M^{-2}) ($\times 10^4$)
tert.-Butyl alcohol (I)	1.3 ± 0.2
tert.-Butyl formate (II)	2.9 ± 0.2
tert.-Butyl acetate (III)	1.4 ± 0.4
tert.-Butyl carbamate (IV)	1.4 ± 0.1
tert.-Butyl carbazate (V)	1.5 ± 0.1
N(*tert.*-Butyl hydroxy)carbamate (VI)	1.6 ± 0.2
N(*tert.*-Butoxycarbonyl)glycine (VII)	1.7 ± 0.3

A general increasing trend in K_f is observed in Table III as the hydroxyl group in *tert.*-butyl alcohol is replaced by ester groups of varying size and polarity. Close examination shows that there is a direct correlation between the K_f values in Table III and the slopes of the k_0' *versus* [β-CD] plots (Fig. 1) for the majority of the co-modifiers except for the *tert.*-butyl formate and the N(*tert.*-butoxycarbonyl)glycine data. An explanation is given later.

The addition of *tert.*-butyl acetate (III) as a secondary modifier results in a slightly higher formation constant for the pyrene–β-CD complex. This value is comparable to that estimated in the presence of *tert.*-butyl carbamate (IV). In contrast to I, both III and IV have longer chains and contain carbonyl groups, which may contribute to the stability of the ternary complex by forming hydrogen bonds with the hydroxyl groups located on the periphery of the β-CD torus. From the value obtained for *tert.*-butyl carbazate (V), it can be seen that increasing the chain length by the addition of another amino group to *tert.*-butyl carbamate produces a more significant increase in the formation constant value. Interestingly, in this case, keeping the chain length comparable but substituting the second amino group in V for a hydroxyl group in N(*tert.*-butyl hydroxy)carbamate (VI) results in a corresponding increase in the formation constant. Elongating the chain as well as adding another carbonyl group in N(*tert.*-butoxycarbonyl)glycine (VII) further enhances the value of the binding constant for the pyrene–β-CD complex.

The anomalous behavior exhibited by *tert.*-

butyl formate (II) and N(*tert.*-butoxycarbonyl)glycine (VII) may be attributable to the acidity of these two modifiers. The addition of either of these compounds resulted in a drastic decrease in the pH of the mobile phase (Fig. 3) to values as low as 2.2. It was previously noted that, unlike the other co-modifiers, II and VII caused a significant decrease in the capacity factor k'_0 of the uncomplexed pyrene. The reasons for the marked decrease in retention time of uncomplexed pyrene in the presence of these co-modifiers are not exactly known. It should be noted, however, that the lower pH limit generally recommended for the operation of C_{18} columns is 3.5. Below this pH, the column could undergo undesirable changes including stripping of the stationary phase. However, the response of the column used here was successfully restored to normal after regeneration by washing with methanol and water. It then follows that the observed effects were due to changes in the retention characteristics of the column under acidic conditions.

The method of determination of formation constants (K_f) employed here [which involves the division of the slope by the intercept (eqn. 2)] assumes that the intercept is relatively constant while the slope varies with the experimental conditions. Fig. 1 confirms the changing slopes and the relatively unchanging intercept for the majority of the modifiers. Under these circumstances, there is a direct correlation between the slope and the calculated K_f value. In the case of co-modifiers II and VII, the lower intercept values compared to those for the other co-modifiers, resulted in higher K_f values which, in turn, do not correlate with the slope of the k'_0 *versus* [β-CD] plots. Consequently, the formation constant values calculated for *tert.*-butyl formate (II) and N(*tert.*-butoxycarbonyl)glycine (VII) cannot be compared to those estimated for the other modifiers. This observation suggests that the K_f values determined by the RPLC technique are only comparable when the solutes of interest exhibit similar k'_0 values, a point already alluded to by Anigbogu *et al.* [26].

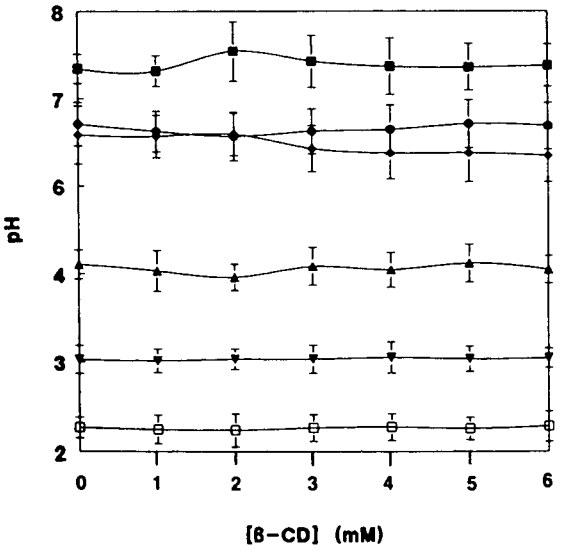

Fig. 3. Variation of pH with increasing β-CD concentration in the presence of several secondary modifiers. ◆ = *tert.*-Butyl alcohol (I); ▲ = *tert.*-butyl acetate (III); ■ = *tert.*-butyl carbazate (V); ● = *tert.*-butyl carbamate (IV); ▼ = N(*tert.*-butoxycarbonyl)glycine (VII); □ = *tert.*-butyl formate (II).

Although the nature of the forces contributing to the formation of cyclodextrin inclusion complexes is not fully understood, it is fair to assume that the driving force for the process is in a large part due to hydrophobic interactions, with some stability conferred upon the complex by hydrogen bond formation. In this particular case, several factors could influence the formation of the pyrene–β-CD complex. As expected, the presence of methanol as a primary organic modifier in the bulk aqueous solvent has been shown to adversely affect the formation constant of the complex [9]. This may be attributed to the competitive equilibrium which causes the pyrene to partition between the relatively hydrophobic bulk medium and the cyclodextrin cavity. In reversed-phase HPLC, the competition for pyrene is three-fold: between the cyclodextrin, the solvent and the stationary phase. Previous studies in our laboratory have revealed that in this case, pyrene is retained on the C_{18} column, suggesting that the formation constant for the pyrene–β-CD complex is negligible under these circumstances [26]. The addition of a small amount of secondary modifier was found to dramatically affect the retention behavior of pyrene, and formation constant values for its complex with β-CD at several methanol concen-

trations have been reported [27]. The enhancement of equilibrium constants due to the secondary modifier may be attributed to the formation of a more stable ternary complex. The stability of ternary cyclodextrin complexes may be a result of more polar water molecules being excluded from the cavity to accommodate the non-polar *tert.*-butyl group of the secondary modifier. Also, the formation of hydrogen bonds between the heteroatom containing functional groups of the co-modifier and the hydroxyl groups of the cyclodextrin may play a role in conferring stability upon the inclusion complex. This could be a plausible explanation for the enhancement of formation constants observed upon increasing functionality of *tert.*-butyl modifiers.

Effect of pH upon the retention characteristics of the β-CD–pyrene complex in the presence of secondary modifiers

Although ternary complex formation may be the primary reason for the low retention times observed, the addition of a secondary modifier may also change the pH of the bulk mobile phase, which may contribute to the affinity of pyrene for the solvent. Fig. 3 depicts the variation in pH with increasing amounts of β-CD for several of the modifiers. As expected, the differences in pH range from 3.0 to 7.5, depending upon the number of acid or amino groups present. Changing the pH of the methanol–water–β-CD bulk mobile phase in the absence of secondary modifiers did not significantly affect the retention of pyrene, which did not elute off the column. This indicates that the pH difference is not a major contributing factor to the retention characteristics observed in the presence of the co-modifiers. It is also interesting to note in Fig. 3 that varying the β-CD concentration does not affect the pH of the mobile phase for each co-modifier used, suggesting that the significant change in pyrene retention is due to some type of complex formation rather than pH effects.

Influence of secondary modifier concentration on the capacity factor of pyrene

Fig. 4 shows the effect of increasing modifier concentration on the capacity factor of pyrene

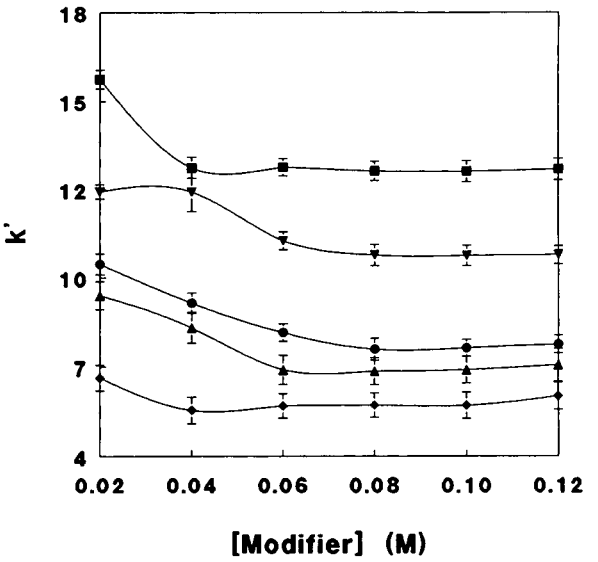

Fig. 4. Plot of capacity factor *vs.* secondary modifier concentration optimum co-modifier concentration. ■ = *tert.*-Butyl alcohol (I); ▼ = *tert.*-butyl acetate (III); ● = *tert.*-butyl carbazate (V); ▲ = *tert.*-butyl carbamate (IV); ◆ = N(*tert.*-butoxycarbonyl)glycine (VII).

for several of the compounds used in this study. It is evident that the greatest variation in retention characteristics occurs in the 0.01–0.06 *M* range for most of the modifiers. It may be inferred from this observation that at approximately 0.06 *M*, all the binding sites for the co-modifier on the inclusion complex are saturated. Thus, the addition of greater amounts of the secondary modifier are not used in ternary complex formation, and consequently do not affect the capacity factor.

CONCLUSIONS

The nature and polarity of the functional group attached to the *tert.*-butyl moiety of the secondary modifier appears to significantly affect the equilibrium of pyrene between the C_{18} stationary phase and the methanol–water–β-CD mobile phase. Since under these reversed-phase chromatographic conditions, CD inclusion complexes do not appear to form in the absence of a co-modifier, these compounds can play an important role in the cyclodextrin-aided extraction of environmentally significant PAHs from contaminated sites. In addition to facilitating remov-

al of PAHs, the use of secondary modifiers with added functionality may reduce analysis time, which would improve the practicality of employing cyclodextrins in industrial applications.

ACKNOWLEDGEMENTS

This research was supported by a grant from the National Science Foundation (CHE-9001412). The authors are grateful to G.A. Reed of the American Maize-Products Co. for providing the cyclodextrin used in this study.

REFERENCES

1 J. Szejtli, *Cyclodextrins and their Inclusion Complexes*, Akademiai Kiado, Budapest, 1982.
2 M. Vikmon, A. Stadler-Szoke, G. Hortobagyi, I. Kolbe and J. Szejtli, *Acta Pharm. Technol.*, 32 (1986) 29.
3 K.W. Street, Jr., *J. Liq. Chromatogr.*, 10 (1987) 655.
4 D.W. Armstrong, F. Nome, L.A. Spino and T.D. Golden, *J. Am. Chem. Soc.*, 108 (1986) 1418.
5 L.A. Spino and D.W. Armstrong, *Ordered Media in Chemical Separations* (*ACS Symposium Series*, No. 342), American Chemical Society, Washington, DC, 1987, pp. 235–246.
6 R.M. Mohseni and R.J. Hurtubise, *J. Chromatogr.*, 499 (1990) 395.
7 L.A. Blyshak, K.Y. Dodson, G. Patonay, I.M. Warner and W.E. May, *Anal. Chem.*, 61 (1989) 955.
8 H. Lamparczyk, P. Zarzycki, R.J. Ochocka and D. Sybilska, *Chromatographia*, 30 (1990) 91.
9 K. Fujimura, T. Ueda, M. Kitagawa, H. Takayanagi and T. Ando, *Anal. Chem.*, 58 (1986) 2668.
10 K. Uekama, F. Hirayama, K. Ikeda and K. Inaba, *J. Pharm. Sci.*, 66 (1977) 706.
11 W.L. Hinze and D.W. Armstrong, *Anal. Lett.*, 13 (1986) 1093.
12 G.M. Badger, *The Chemical Basis of Carcinogenic Activity*, Charles C. Thomas, Springfield, IL, 1962.
13 H.V. Gelboin and P. Ts'o (Editors), *Polycyclic Hydrocarbons and Cancer*, Academic Press, New York, 1978.
14 M.L. Lee, M.V. Novotny and K.D. Bartle, *Analytical Chemistry of Polycyclic Compounds*, Academic Press, New York, 1981.
15 M.C. Bowman, *Handbook of Carcinogens and Hazardous Substances*, Marcel Dekker, New York, 1982.
16 A. Nakajima, *Spectrochim. Acta*, 39A (1983) 913.
17 G. Nelson, G. Patonay and I.M. Warner, *J. Incl. Phenom.*, 6 (1988) 277.
18 S. Hashimoto and J.K. Thomas, *J. Am. Chem. Soc.*, 107 (1985) 4655.
19 S. Hamai, *J. Phys. Chem.*, 92 (1988) 6140.
20 G. Nelson and I.M. Warner, *J. Phys. Chem.*, 94 (1988) 576.
21 K. Uekama, F. Hirayama, S. Nasu, N. Matsou and T. Irie, *Chem. Pharm. Bull.*, 26 (1978) 3477.
22 Y. Nobuhara, S. Hirano and Y. Nakanishi, *J. Chromatogr.*, 258 (1983) 276.
23 J. Debowski, J. Jurczak and D. Sybilska, *J. Chromatogr.*, 282 (1983) 83.
24 M. Tanaka, T. Miki and T. Shono, *J. Chromatogr.*, 330 (1985) 253.
25 A. Muñoz de la Peña, T.T. Ndou, J.B. Zung and I.M. Warner, *J. Phys. Chem.*, 95 (1991) 3330.
26 V.C. Anigbogu, A. Muñoz de la Peña, T.T. Ndou and I.M. Warner, *J. Chromatogr.*, 594 (1992) 37.
27 V.C. Anigbogu, A. Muñoz de la Peña, T.T. Ndou and I.M. Warner, *Anal. Chem.*, 64 (1992) 484.
28 A. Muñoz de la Peña, T.T. Ndou, J.B. Zung, K.L. Greene, D.H. Live and I.M. Warner, *J. Am. Chem. Soc.*, 113 (1991) 1572.
29 K. Kano, I. Takenoshita and T. Ogawa, *Chem. Lett.*, (1980) 1035.
30 K. Kano, I. Takenoshita and T. Ogawa, *J. Phys. Chem.*, 86 (1982) 1833.
31 D.W. Amstrong and G.Y. Stine, *J. Am. Chem. Soc.*, 105 (1983) 2962.
32 T.K. Korpela and J.P. Himanen, *J. Chromatogr.*, 290 (1984) 351.

Journal of Chromatography, 635 (1993) 221–226
Elsevier Science Publishers B.V., Amsterdam

CHROM. 24 866

High-performance liquid chromatographic analysis of sulfonated aromatics using a β-cyclodextrin-bonded phase

D.R. Wilder*, G.W. Tindall, L.J. Cunningham and J.L. Little

Research Laboratories, Eastman Chemical Co., P.O. Box 1972, B-150, Kingsport, TN 37662 (USA)

(First received November 30th, 1992; revised manuscript received January 8th, 1993)

ABSTRACT

A cyclodextrin-bonded phase and methanol–aqueous ammonium acetate mobile phase were used in the liquid chromatographic analysis of a number of sulfonated aromatics. This separation system offered two advantages over the more conventional ion-pair approach to the liquid chromatographic analysis of these highly polar compounds. It achieved the resolution of positional isomers of sulfonated aromatics and allowed the use of thermospray liquid chromatography/mass spectrometry for the characterization of these compounds. Chromatographic selectivity for these solutes was found to be most significantly influenced by the ionic strength of the mobile phase mixture.

INTRODUCTION

Sulfonated aromatics are a group of polar, water-soluble compounds that are difficult to analyze by liquid chromatography. The conventional means for separating highly ionized compounds of this type is ion exchange or ion-pair chromatography [1]. These techniques will adequately perform separation by classes, *e.g.*, mono- from disulfonated substituted aromatics, but may not be able to resolve positional isomers of sulfonated aromatics.

Cyclodextrin-bonded phases have demonstrated an often remarkable selectivity in the liquid chromatographic separation of isomers [2–7]. In particular, β-cyclodextrin-bonded phases have proven to be especially useful for the resolution of positional isomers of a variety of disubstituted aromatics, including aromatic carboxylic acids [8–12]. The same sterically driven separation mechanism that resolves non-ionized disubstituted aromatics might also be expected to separate positional isomers of sulfonated aromatics.

This study reports the use of a conventional reversed-phase mobile phase system (a methanol–0.1 *M* ammonium acetate mixture) and a β-cyclodextrin column to accomplish the non ion-pair separation of sulfonated aromatics. This system possesses two advantages when compared to the ion-pair separation of this class of compounds. It achieves the separation of positional isomers of substituted sulfonated benzenes —a separation not obtained with the ion-pair, reversed-phase system. The second advantage arises from the use of the aqueous ammonium acetate buffer as a constituent of the mobile phase mixture. This mobile phase is the optimal choice for the use of mass spectrometric detection using the thermospray interface and so permits the on-line structural characterization of sample components.

* Corresponding author.

EXPERIMENTAL

Apparatus

The β-cyclodextrin column used in this work was a 250 mm × 4.6 mm Cyclobond I column from Advanced Separations Technologies. A Hewlett-Packard Model 1090 liquid chromatograph equipped with autoinjector and column oven was used for solvent delivery. All data were acquired using a column temperature of 35 ± 0.1°C. Sample injection size was 10 μl.

Two modes of detection were used. Monitoring of UV absorbance at 220 nm was the primary routine means of detection. This was accomplished using a Hewlett-Packard 1040 diode array detector. The ability to acquire the UV spectra of each of the components was utilized in arriving at the optimal wavelength, 220 nm, for the analysis. The peak purity function of the detector was also used to assure that no unresolved components were present. The acquisition and storage of individual spectra proved to be particularly useful in the verification of peak identity during the separation optimization portion of this work. Elution order changes made it imperative that some means of definitively identifying each component peak be employed. In addition, the UV spectra assisted in subsequent structural characterization of several unknown sample components. A Finnigan model 4600 mass spectrometer with a Vestec thermospray LC–MS interface constituted the second means of detection employed in this work. It was used to provide mass spectral data to help definitively identify unknown sample components. The interface was used in the discharge mode and positive ions were monitored to produce the mass chromatogram.

Chemicals and reagents

All sulfonated samples were produced at Eastman Chemicals. Reference samples of *ortho* and *para* sodium phenolsulfonate and 4,4′-dihydroxydiphenolsulfone were laboratory prepared and purified and characterized by NMR.

The methanol, ammonium acetate and acetic acid used to prepare mobile phase mixtures were obtained from J.T. Baker (Phillipsburg, NJ, USA) and were "HPLC" grade. Millipore (Milford, MA, USA) Milli-Q filtered, deionized water was used in the ammonium acetate and acetate buffer solutions.

RESULTS AND DISCUSSION

Sodium phenolsulfonates (SPSs) are useful industrial intermediates. A knowledge of the levels of the three positional isomers in reaction

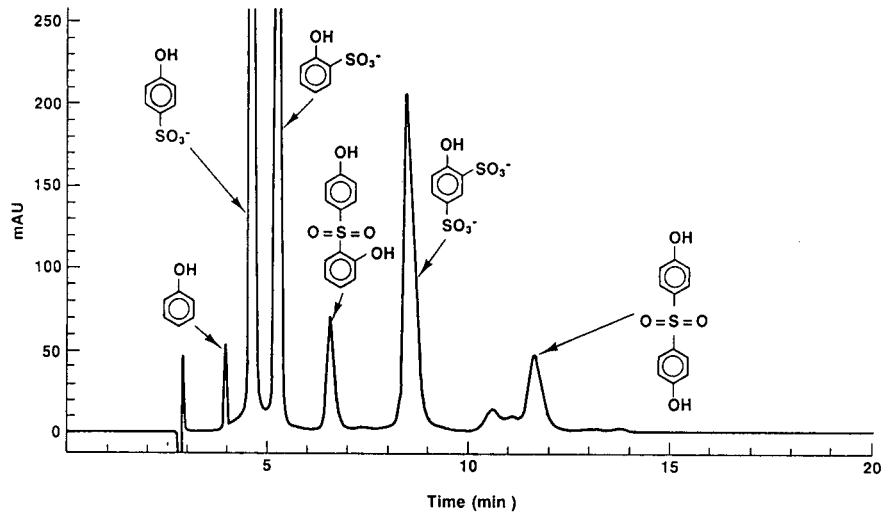

Fig. 1. Chromatogram of a reaction mixture sample of sodium phenolsulfonate. Conditions: column, 250 × 4.6 mm I.D. Cyclobond I; mobile phase, methanol–0.1 *M* aqueous ammonium acetate (43:57); temperature, 35°C; flow-rate, 1 ml/min; detection, UV at 220 nm.

samples of sodium phenol sulfonates, as well as the amount of disulfonated material and residual phenol, is important in optimizing the reaction to produce these materials. A liquid chromatographic method was developed to provide information for process control and product purity determinations. Fig. 1 presents the chromatogram of a typical crude reaction mixture sample containing SPSs and related impurities. It can be seen that the *para*- and *ortho*-SPS isomers are well resolved from each other and from phenol, disulfonated phenol (di-SPS), and two sulfone impurities. This chromatogram was obtained using a mobile phase mixture of methanol–0.1 *M* ammonium acetate in water (43:57) at a flow-rate of 1.0 ml/min. These conditions were optimal in terms of speed of analysis and resolution of components. Verification of known sample components as well as identification of unknown impurities in the reaction mixture sample was obtained using LC–MS with a thermospray interface. The choice of ammonium acetate as the buffer was partially dictated by the need for verification of peak identity by MS. A buffer system containing a volatile component, like ammonium acetate, is necessary for thermospray LC–MS. In the course of achieving this optimized separation, it was observed that the retention of three classes of components of interest —monosulfonated phenols, disulfonated phenol and the sulfones— were affected differently by changes in the ionic strength of the mobile phase mixture, percentage of methanol in the mobile phase and temperature.

Effect of buffer ionic strength

The most striking change in retention behavior was produced by changing the ionic strength of the mobile phase. Ionic strength was adjusted by the addition of ammonium acetate to the aqueous mobile phase component to provide concentrations from 0.005 to 0.300 *M*. The effect on retention time for three of the classes of compounds in this separation, *i.e.*, monosulfonated phenols, disulfonated phenols and sulfones, *vs.* concentration of ammonium acetate can be seen in Fig. 2. It may be seen from the plot that a decrease in concentration of ammonium acetate, and hence a decrease in the ionic strength of the

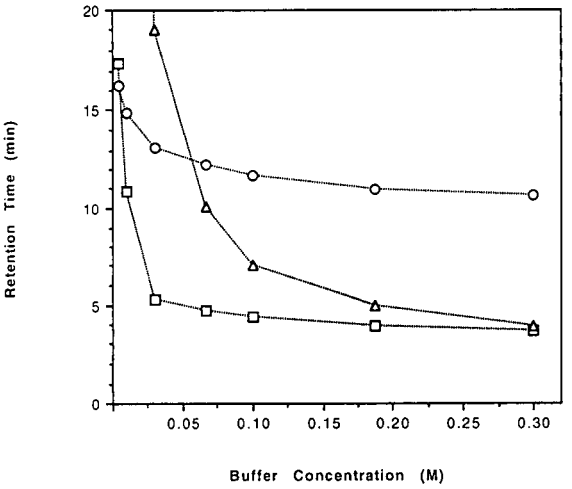

Fig. 2. Variation of retention time with change in ammonium acetate buffer concentration. Column, Cyclobond I; mobile phase, methanol–ammonium acetate buffer (43:57) at different concentrations; temperature, 35°C; flow-rate, 1 ml/min; detection, UV at 220 nm; □ = *para*-SPS; △ = 2,4-di-SPS; ○ = 4,4′-bis-diphenolsulfone.

mobile phase, produces an increase in retention time for each of the three solute classes. The increase is most pronounced for the ionizable solutes with the disulfonated phenol showing a greater effect than the monosubstituted phenol. At ammonium acetate concentrations below 0.02 *M*, the disulfonated phenol is essentially non-eluted. The monosulfonated phenols show a qualitatively similar behavior, but still may be eluted (although with a retention time of 17 min) at an ammonium acetate concentration of 0.005 *M*. The uncharged bis-sulfone displays a much smaller change in retention time with change in buffer concentration. Recent work by Beeson and Vigh [13] has shown that ionized carboxylic acids may be more strongly retained than the unionized acids on a β-cyclodextrin bonded phase. This is in agreement with our findings in this study.

Effect of methanol content

The plot of change in retention time with change in methanol cosolvent content at a fixed buffer concentration (0.1 *M*) is shown in Fig. 3. No attempt was made to keep the buffer ionic strength constant; that is, the addition of methanol was allowed to effectively dilute the

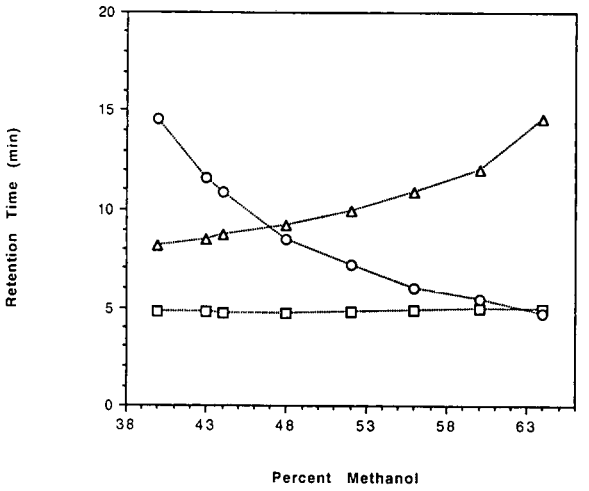

Fig. 3. Variation of retention time with change in percent methanol. Column, Cyclobond I; mobile phase, methanol at different concentrations–0.1 *M* ammonium acetate buffer; temperature, 35°C; flow-rate, 1 ml/min; detection, UV at 220 nm; □ = *p*-SPS; △ = 2,4-di-SPS; ○ = 4,4′-bis-diphenolsulfone.

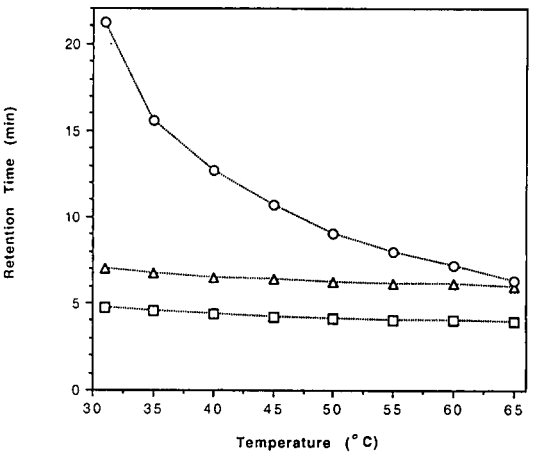

Fig. 4. Variation of retention time with change in temperature. Column, Cyclobond I; mobile phase, methanol–0.1 *M* ammonium acetate buffer (43:57); temperature, 31–65°C; flow-rate, 1 ml/min; detection, UV at 220 nm; □ = *p*-SPS; △ = 2,4-di-SPS; ○ = 4,4′-bis-diphenolsulfone.

aqueous ammonium acetate buffer concentration. It may be seen that the effect of methanol on retention time is less dramatic than that seen in Fig. 2 when buffer ionic strength was adjusted. An interesting trend is seen, however, in the different response obtained for the sulfone *vs.* sulfonic acid-containing solutes. The sulfone behaves as one would expect when an uncharged solute molecule is subjected to a "stronger" eluent, *i.e.*, one richer in methanol; its retention time decreases. The retention times for the sulfonated solutes increase and the increase is roughly consistent with the dilution of the ammonium acetate buffer (and hence dilution of ionic strength) by methanol.

Effect of temperature

The effect of temperature on retention was also investigated. Fig. 4 displays a plot of temperature *vs.* retention time of the three solute classes. The neutral sulfone undergoes the largest change in retention time, with the charged solute classes relatively less affected by temperature.

These data suggest that the neutral sulfone solute behaves according to accepted and well documented theory for the inclusion complexation of solutes in the cyclodextrin cavity. The equilibrium for this inclusion complexation is shifted, as expected, when the mobile phase environment is altered by the change in the methanol content and change in temperature. The retention mechanism for the sulfonated solutes, however, is less straightforward and appears to be dominated by a quantitatively stronger interaction, perhaps ion exchange. It has been documented that ions may be separated on a β-cyclodextrin bonded phase [14,15]. It is not clear from the data whether this effect works in concert with the conventional complexation mechanism or is an extraneous artifact produced by ion-exchange groups on the surface of the silica gel. The fact that we are able to separate positional isomers of the sulfonated phenol suggests at least some contribution to retention and resolution from the cyclodextrin moiety. The preparation of the bonded phase does not involve the use of potentially ionizable, *e.g.*, amine, functionalities that may act as fixed ion-exchange sites [16]. It is possible that a dynamic ion exchange mechanism may be involved. This might arise through inclusion of cationic constituents of the mobile phase —in the present case ammonium ion— in the cyclodextrin cavity, which then acts as a partially encapsulated ion-exchange site. We have not found literature

evidence for a strong ion-exchange effect internal to the cyclodextrin cavity —one in which a charged mobile phase ion (for example, ammonium) is trapped in the cyclodextrin cavity— but the results obtained in this work makes such an explanation attractive.

Effect of stronger electrolyte

To further explore the possibility of an ion-exchange retention mechanism for the sulfonic acid-containing solutes, the use of a stronger (in the context of ion exchange) mobile phase electrolyte was examined. Ammonium sulfate replaced ammonium acetate in the aqueous portion of the mobile phase solution. Theory indicates that sulfate should have more affinity for a hypothetical anion-exchange site than would acetate and so sulfate would be less easily displaced than acetate by sulfonate-containing solutes [17]. This would result in a reduction of retention time for the sulfonated solutes. Fig. 5 shows retention of the three classes of solutes as a function of ammonium sulfate concentration. The retention times for the solutes are diminished at a given electrolyte concentration compared to the ammonium acetate mobile phase. The difference is particularly well displayed for

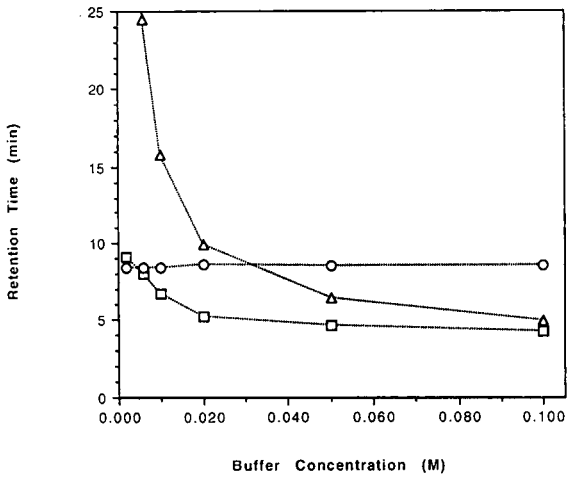

Fig. 5. Variation of retention time with change in ammonium sulfate buffer concentration. Column, Cyclobond I; mobile phase, methanol–ammonium sulfate buffer (43:57) at different concentrations; temperature, 35°C; flow-rate, 1 ml/min; detection, UV at 220 nm; □ = *p*-SPS; △ = 2,4-di-SPS; ○ = 4,4′-bis-diphenolsulfone.

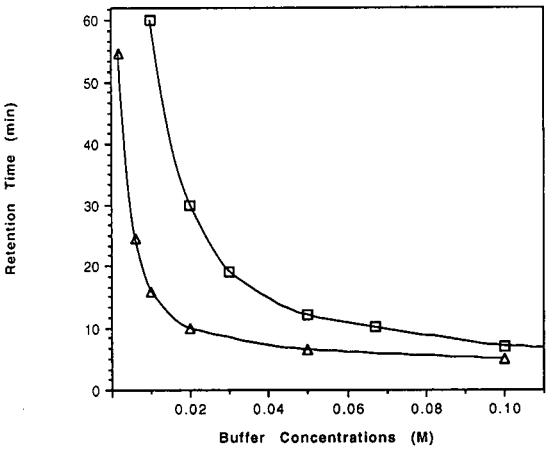

Fig. 6. Comparison of retention time for 2,4-disulfonated phenol in ammonium acetate *vs.* ammonium sulfate buffer. Column, Cyclobond I; mobile phase, methanol–buffer (43:57) at different concentrations; temperature, 35°C; flow-rate, 1 ml/min; detection, UV at 220 nm; □ = acetate; △ = sulfate.

the 2,4-disulfonated phenol solute in Fig. 6. As mentioned above, these data are consistent with an ion-exchange mechanism where the stronger sulfate anion should compete more favorably with the sulfonic acid-containing solutes for the anion-exchange sites.

Effect of different counter-ions

The effect of different counter-ions on retention was also investigated. All other conditions in this investigation were unchanged and were the same as that used to achieve the optimal separation, *i.e.*, 57% methanol, temperature, 35°C, flow-rate, 1 ml/min. Changing the cation from ammonium to sodium produced very little change in retention behavior. The substitution of potassium for ammonium, however, had a greater effect. No change in the retention of the neutral sulfones was seen, but the retention times of sulfonated solutes were reduced, with the effect on the disulfonated phenol being the greatest. Its retention time was reduced from 8.5 to 6.8 min.

CONCLUSIONS

This work has demonstrated the utility of a cyclodextrin-bonded phase for the separation of

highly ionized organic solutes. The aqueous ammonium acetate–methanol mobile phase system is particularly well suited to detection and characterization of analyte by thermospray LC–MS. Finally, a qualitative difference in the retention mechanism for neutral *vs.* ionizable solutes was observed. An analysis of the influence of ionic strength, percent methanol and temperature on solute retention suggests that an ion-exchange-like mechanism may be superimposed with inclusion complexation in the chromatographic retention of the sulfonated phenols.

ACKNOWLEDGEMENT

The authors wish to thank Professor D.W. Armstrong for helpful discussions.

REFERENCES

1 P.-O. Langstrom, *J. Chromatogr.*, 250 (1982) 43.
2 D.W. Armstrong and W. DeMond, *J. Chromatogr. Sci.*, 22 (1984) 411.
3 D.W. Armstrong, W. DeMond, A. Alak, W.L. Hinze, T.E. Riehl and K.H. Bui, *Anal. Chem.*, 57 (1985) 237.
4 K.G. Feitsina, J. Bosman, B.F.H. Drenth and R.A. de Zeeuw, *J. Chromatogr.*, 333 (1985) 59.
5 H.J. Issaq, M. Glennon, D.E. Weiss, G.N. Chmurny and J.E. Saavendra, *J. Liq. Chromatogr.*, 9 (1986) 2763.
6 C.D. Ridlon and H.J. Issaq, *J. Liq. Chromatogr.*, 9 (1986) 3377.
7 D.W. Armstrong, T.J. Ward, R.D. Armstrong and T.E. Beesley, *Science*, 232 (1986) 1132.
8 C.A. Chang, Q. Wu and D.W. Armstrong, *J. Chromatogr.*, 354 (1986) 454.
9 L. Bazant, M. Wurst and E. Smolková-Keulemansová, *J. Chromatogr.*, 445 (1988) 337.
10 K. Fujimura, M. Kitagawa, H. Takayanagi and T. Ando, *J. Chromatogr.*, 350 (1985) 371.
11 S. Li and W. Purdy, *J. Chromatogr.*, 543 (1991) 105.
12 S.L. Abidi, *J. Liq. Chromatogr.*, 12 (1989) 595.
13 M. Beeson and G. Vigh, *J. Chromatogr.*, 634 (1993) 197.
14 D.W. Armstrong, A. Alak, K. Bui, W. DeMond, T. Ward, T.E. Riehl and W.L. Hinze, *J. Incl. Phenomena*, 2 (1984) 533.
15 H. Issaq, *J. Liq. Chromatogr.*, 11 (1988) 2131.
16 D.W. Armstrong, personal communication.
17 H. Small, *Ion Chromatography*, Plenum Press, New York, 1989.

Journal of Chromatography, 635 (1993) 227–235
Elsevier Science Publishers B.V., Amsterdam

CHROM. 24 836

Simultaneous determination of ochratoxin A and zearalenone in maize by reversed-phase high-performance liquid chromatography with fluorescence detection and β-cyclodextrin as mobile phase additive

Volker Seidel, Edda Poglits, Karin Schiller and Wolfgang Lindner*

Institut für Pharmazeutische Chemie, Karl-Franzens-Universität Graz, Schubertstrasse 1, A-8010 Graz (Austria)

(First received December 1st, 1992; revised manuscript received December 22nd, 1992)

ABSTRACT

A reversed-phase high-performance liquid chromatographic method was developed for the simultaneous determination of the usually co-eluting peaks of ochratoxin A and zearalenone by fluorescence detection due to specific inclusion phenomena using β-cyclodextrin as a mobile phase additive. Additionally four different clean-up techniques were studied in order to optimize the recoveries of ochratoxin A and zearalenone in the range 0.5–1000 ppb (w/w) in maize, including liquid–solid extraction using Florisil, C_{18} and plain silica solid-phase extraction mini-columns and a base–acid liquid–liquid partitioning clean-up procedure.

INTRODUCTION

The infection of cereal grains with several species of fungal genera has been recognized as a potential threat to animal and human health. The contamination of animal feed with fungal secondary metabolites, the so-called mycotoxins, can cause serious reproductive problems and feeding difficulties, especially in pig-fattening stations and poultry farms. The effects of reduced litters, stillbirths, miscarriages [1], increased prenatal mortality, enteritis, diarrhoea, anorexia, kidney damages (known as mycotoxic porcine nephropathy) [2], cessation of milk production, hormonal disorders, sterility and numerous other anomalies in swine and cattle could directly be related to toxin content of the feed [1,3].

There is also a potential risk to human health by direct contamination of human food with toxigenic mould or indirect contamination by 'carry-over' of toxin residues in animal tissues [4], milk or meat [5,6] after feeding with contaminated feed, at the worst reported as Balkan endemic nephropathy [4,7].

Fungal infections of corn occur preharvest by field-growing *Fusarium* species and under storage conditions by *Aspergillus* and *Penicillium* species. The most frequently isolated field-growing fungi on Austrian corn are *Fusarium sacchari* var. *subglutinans* and *Fusarium graminearum* (Table I) [8], producing mycotoxins of the trichothecene family [especially deoxynivalenol (DON)], zearalenone (ZON) and the two diastereomers α- and β-zearalenol (ZOL) (Fig. 1), which have been suggested as precursors in biosynthetic pathway leading to ZON. α-Zearalenol possesses even 3–4 times more estrogenic activity than ZON, although it has been found only at low levels on Austrian maize. Ochratoxin A and B (Fig. 2) contamination, especially by *Penicillium verrucosum*, can appear when corn of high moisture content (23–40%) is stored at low temperatures [9], although such

* Corresponding author.

0021-9673/93/$06.00

TABLE I

FUSARIUM SPECIES AND MYCOTOXINS MOST FREQUENTLY FOUND ON AUSTRIAN CORN

Taken in part from ref. 8. *Fusarium* strains were isolated from 48 samples of oats, wheat and maize harvested in 1985–87 in different Austrian production areas and were tested for the production of mycotoxins on autoclaved moistened maize. The original grain samples were also analysed for *Fusarium* mycotoxins [8].

Fusarium species	Deoxynivalenol positive/total range (ppb)	Zearalenone positive/total range (ppb)	Zearalenol positive/total range (ppb)
F. graminearum	36/38 (25–310)	38/38 (5–1200)	9/38 (1–125)
F. culmorum	0/1	1/1 (25)	1/1 (2)
F. sambucinum	1/1 (25)	1/1 (5)	0/1
F. avenaceum	0/27	0/27	0/27
F. sacchari var. subglutinans	0/25	0/25	0/25
F. tricinctum	0/10	0/10	0/10
F. poae	0/22	0/22	0/22
F. verticillioides	0/4	0/4	0/4
F. oxysporum	0/3	0/3	0/3
F. equiseti	0/1	0/1	0/1

storage conditions are rare in Austrian maize cultivation regions, contrary to the situation in northern parts of Germany and the Scandinavian countries [10,11].

Many analytical methods for the determination of zearalenone and ochratoxin A have been developed, including thin-layer chromatography (TLC) [12–15], high-performance liquid chromatography (HPLC) [16–19], gas chromatography (GC) [20–24], enzyme immunoassay (EIA) [25] and enzyme-linked immunosorbent assay (ELISA) [26], but for highly sensitive and reliable detection there is still a need for further improvements to the existing methods.

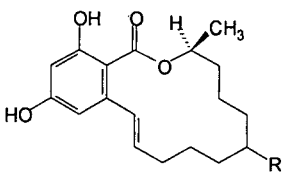

Fig. 1. Structures of zearalenone (ZON) (R = O), zearalanone (ZAON) (R = O), no double bond in position 1 and the two diastereomers α- and β-zearalenol (ZOL) (R = OH), which can be classified as 6-(10-hydroxy-6-oxo-*trans*-1-undecenyl)-β-resorcyclic acid lactones. IUPAC name: zearalenone = 3,4,5,6,9,10-hexahydro-14,16-dihydroxy-3-methyl-[*S*-(*E*)]-1*H*-2-benzoxacyclotetradecin-1,7(8*H*)-dione.

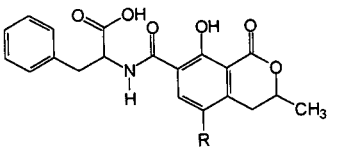

Fig. 2. Structures of ochratoxin A (R = Cl) and ochratoxin B (R = H), both closely related derivatives of isocoumarin linked to L-phenylalanine: (*R*)-N-[(5-chloro-3,4-dihydro-8-hydroxy-3-methyl-1-oxo-1*H*-2-benzopyran-7-yl)carbonyl]-L-phenylalanine.

As has been shown, HPLC can cover the requirements of a multi-toxin simultaneous screening method for the major toxins (DON, ochratoxin A, ZON) [27,28] better than all the others, but the trichothecenes possess only poor UV absorption (DON maximum at 220 nm) allowing determination in real samples only in the high ppb range) [29]. A higher sensitivity for DON can be gained by fluorescence detection after pre- or postcolumn derivatization procedures [30,31], but this complicates the overall analytical procedure, which might adversely influence its ruggedness, and therefore high-sensitivity trichothecenes analysis is performed these days by GC methods using electron-capture detection (ECD) [32–34] or MS detection [35,36].

The simultaneous determination of aflatoxin, ochratoxin A and ZON in feeds by HPLC with fluorescence detection was demonstrated by Howell and Taylor [37], incorporating selective

sample pretreatment procedures. For improvement of ochratoxin A recovery, Langseth *et al.* [38] described a modified HPLC method after purification of sample extracts using solid-phase extraction (SPE) columns. Ochratoxin A and ZON were eluted from the column in two fractions and finally chromatographed using an RP-HPLC system with separate injections.

In this paper, a method for simultaneous determination of zearalenone (ZON), zearalanone (ZAON), α- and β-zearalenol (ZOL), ochratoxin A (OA) and ochratoxin B (OB) in a single HPLC run with fluorescence detection is described. Two basic approaches are covered: chromatographic separation of mycotoxins in a single run and improvement of sample pretreatment procedures, including extraction and clean-up.

The separation of all toxins in a single run was achieved by forming inclusion complexes with β-cyclodextrin added to the mobile phase (Fig. 3), which renders possible a more accurate determination of the major toxins OA and ZON without interferences from related compounds (ZAON, ZOL, OB). In addition, four different clean-up procedures were developed and compared for optimization of the recovery of OA and ZON from maize in the range of 0.5–1000 ppb. Evaluation of the final assay for recovery and accuracy of the other related mycotoxins, which, however, are of minor importance in Austrian feeds [8], will be the subject of further investigations.

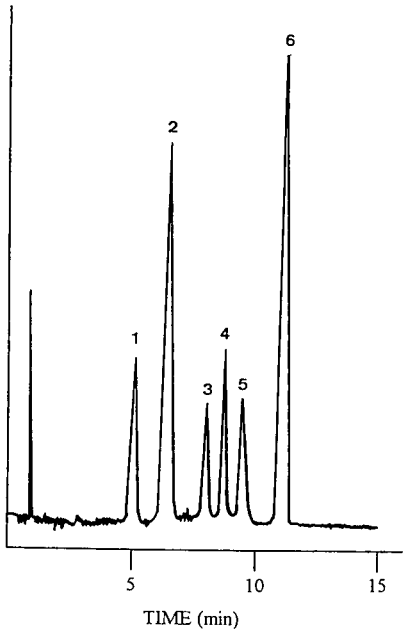

Fig. 3. HPLC of mycotoxin standard solution demonstrating the separation of 500 ng of β-zearalenol (1), 8 ng of ochratoxin B (2), 80 ng of α-zearalenol (3), 90 ng of zearalanone (4), 8 ng of zearalenone (5) and 4 ng of ochratoxin A (6) on a Merck LiChrospher 60, RP Select-B, 5 μm, 125 × 4 mm I.D. column. Mobile phase: methanol–water (45:55), pH 2.5 (12 m*M* phosphoric acid), containing 0.2 m*M* β-cyclodextrin. Fluorescence detection: $\lambda_{ex} = 315$ nm and $\lambda_{em} = 465$ nm.

EXPERIMENTAL

Instrumentation, chromatography

HPLC was performed using a Jasco 880-PU intelligent HPLC pump and a Jasco 820-FP intelligent spectrofluorimeter ($\lambda_{ex} = 315$ nm and $\lambda_{em} = 465$ nm). Separations were achieved on a Merck LiChroCART 125 × 4 mm I.D. column filled either with LiChrospher 60, RP-18 Select-B, 5 μm, or alternatively with LiChrospher 100, RP-18, 5 μm, or on a Shiseido Capcell PAK C_{18}, SG 120, 5 μm, 250 × 4.6 mm I.D. column. All columns were thermostated at 65°C in a water-bath. Samples were injected on to the column by a Rheodyne Model 7125 six-port valve equipped with 20-μl loop. Peak areas were calculated with a Merck–Hitachi D-2500 chromato-integrator. The mobile phase was methanol–phosphoric acid (5.95%, pH 1) (45:55) with addition of 0.1 m*M* β-cyclodextrin. The eluent was filtered and degassed before use and the flow-rate was set at 1.0 ml/min.

Standards and reagents

All solvents were of HPLC grade from Merck. C_{18} SPE columns (200 mg) and silica SPE columns (500 mg) were Bond Elut from Varian (Darmstadt, Germany). Florisil (0.15–0.25 mm, 60–100 mesh) was obtained from Serva (Heidelberg, Germany). Ochratoxin A, zearalenone, zearalanone, α-zearalenol, β-zearalenol and β-cyclodextrin (cycloheptaamylose, water content = 7.0 mol/mol) were purchased from Sigma (Deisenhofen, Germany). Ochratoxin B was obtained from R.A. Learmonth (Food Science

and Technology, Pretoria, South Africa). Methanolic standard solutions were stored at 5°C in a freezer.

Sample preparation

Maize samples were stored in a dry room at ambient temperature, conditions that did not allow any growth of toxigenic mould. An amount of at least 500 g of maize was finely ground in a grain mill prior to each sample clean-up and analysis.

Extraction and clean-up

A 5-g amount of maize was weighed into a 50-ml centrifuge tube and after adding 3.35 g (19 mmol) of ascorbic acid (pH 2.5–3.0, 0.6 *M*), was extracted with 30 ml of methanol–water (90:10) for 30 min with automatic shaking. After centrifugation (5 min, 3000 rpm) the process was repeated with another 20 ml for 15 min. The combined extracts were transferred into a 50-ml volumetric flask and diluted to volume with methanol–water (90:10).

Florisil. An aliquot of 5 ml of the methanolic extract was concentrated by rotary evaporation, dissolved in 2 ml of chloroform and transferred into a glass column (I.D. 9 mm; 5 ml) filled with 500 mg of Florisil [prerinsed with 2 ml of chloroform–methanol (70:30) and 4 ml of chloroform]. The mycotoxins were eluted with 20 ml of chloroform–acetic acid (90:10), and after evaporation to dryness by a gentle stream of nitrogen the residue was dissolved in 500 μl of mobile phase.

Silica. An aliquot of 5 ml of the methanolic extract was concentrated to dryness and the residue was dissolved in 2 ml of chloroform and transferred into a glass column (I.D. 9 mm; 5 ml) filled with 250 mg of silica gel 60 (0.040–0.063 mm), prerinsed with 2 ml of chloroform–methanol (70:30) followed by 4 ml of chloroform. The mycotoxins were eluted with 16 ml of chloroform–acetic acid (90:10) and, after evaporation to dryness, the residue was dissolved in 500 μl of mobile phase.

Alternatively, a commercially available SPE column was used. The column, after addition of 2 g of anhydrous Na_2SO_4 to the top, was connected to a vacuum manifold and preconditioned with 5 ml of chloroform–methanol–acetic acid (70:25:5) and 5 ml of dichloromethane. The residue was dissolved in 2 ml of dichloromethane and quantitatively transferred on to the column; according to protocol I the column was then washed with 2 ml of chloroform and the mycotoxins were eluted with 5 ml of chloroform–methanol–acetic acid (70:25:5).

Another washing and elution procedure (protocol II), reported by Langseth *et al.* [38], was also applied, whereby the SPE column was preconditioned with 5 ml of hexane and 5 ml of dichloromethane. After sample loading the column was washed with 10 ml of dichloromethane, 10 ml of hexane and 10 ml of toluene. Mycotoxins were eluted with 6 ml of toluene–acetic acid (9:1).

C_{18}. An aliquot of 5 ml of the extract was adjusted to *ca.* pH 7 (checked by pH paper strips) with 30% sodium hydroxide solution and concentrated by rotary evaporation. This should prevent any matrix interactions with the mycotoxins, especially observed under acidic conditions (for discussion, see later). The residue was dissolved in 2 ml of 5% acetic acid and transferred onto a C_{18} SPE column (prewashed with 4 ml of 5% acetic acid). The column was first washed with 200 μl of methanol–water–acetic acid solution (50:46:4) (pH 2.9) and the mycotoxins were eluted with 4.8 ml of methanol–water–acetic acid (80:15:5). The final extract was concentrated to dryness by a gentle stream of nitrogen and the residue was dissolved in 500 μl of mobile phase prior to HPLC injection.

pH-controlled liquid–liquid partition. A 30-g amount of finely ground sample was weighed into a 500-ml erlenmeyer flask and, after adding 20 ml of water and 5 g (28 mmol) of ascorbic acid (pH 3.2, 0.1 *M*), extracted by tumbling for 15 min with 250 ml of chloroform. A 100-ml volume of the organic extract was filtered into a centrifuge tube and centrifuged for 5 min at 3000 rpm. A 50-ml volume of the clear chloroform extract was transferred into a 250-ml separating funnel and, after adding 10 ml of aqueous saturated sodium chloride solution, treated with 50 ml of aqueous sodium hydroxide (2%). After complete phase separation, the lower (organic) phase was discarded. For analysis of mixed feed

an additional washing step with 50 ml of chloroform is recommended. The upper alkaline phase was mixed with 8.6 g of ascorbic acid and 6 ml of phosphoric acid (pH 1) to adjust the pH to *ca.* 2–2.5 and extracted twice with 50 ml of dichloromethane. The combined organic phases were dried over 2 g of sodium sulphate and the clear extract was concentrated to dryness. The residue was dissolved in 500 μl of mobile phase.

RESULTS AND DISCUSSION

Extraction

Chloroform–water (250:20) with 0.1 *M* ascorbic acid or methanol–water (90:10) with 0.6 *M* ascorbic acid turned out to be an effective extraction medium for zearalenone and ochratoxin [27,28,37,38], ensuring complete conversion of the possibly ionized ochratoxin A to the non-ionized form (estimated pK 3.5, similar to the pK values of phenylalanine-containing dipeptides). The use of ascorbic acid should protect the phenolic OH groups of the molecules from oxidation and interactions with the sample matrix, which might occur when using strong inorganic acids such as phosphoric acid alone. This was especially true for zearalenone; the recoveries fell below 50% after concentration of a phosphoric acid-acidified extract (no added ascorbate) prior to SPE clean-up. Acidification with acetic acid (no added ascorbate) was also successful in extracting all toxins without deterioration of zearalenone, but an additional neutralization step before solvent evaporation is recommended.

Clean-up

The recoveries of the toxins and the effectiveness of purification using a liquid–liquid and three different liquid–solid (Florisil, C_{18}, silica) clean-up techniques were studied. The use of silica SPE columns together with chloroform–acetic acid (90:10) elution required frequent exchange of the guard columns of the HPLC system, although showing no interferences from the maize matrix. The recovery was 85% at high ppb levels, but it dropped to 61% for ochratoxin A and 64% for zearalenone at low ppb levels. Also, the elution volume of 16 ml is rather high (Fig. 4A).

The use of a commercially available silica SPE column and elution with only 5 ml of chloroform–methanol–acetic acid (70:25:5) (protocol I) resulted in an increased ochratoxin A recovery of 75%.

"Clean" chromatograms and an increased lifetime of the guard columns were obtained by washing the silica SPE clean-up column with dichloromethane, hexane and toluene (protocol II) as reported by Langseth *et al.* [38]. However, the use of β-cyclodextrin as a mobile phase additive in HPLC analysis allowed the elution of both toxins in a single fraction of 6 ml of toluene–acetic acid (9:1) from the SPE column. The recoveries were 68% of zearalenone and 59% of ochratoxin A within a 1–50 ppb range. In addition, we would recommend using less Na_2SO_4, as a drastic loss of mycotoxins was observed owing to inclusion phenomena with moistened Na_2SO_4.

Single or combined purification techniques with Florisil and C_{18} SPE mini-columns were very successful in removing matrix interferences from maize samples, as also demonstrated for the GC–ECD determination of trichothecenes in maize [34]. Using chloroform–acetic acid (9:1) together with a Florisil SPE column the elution volume was high (20 ml; see Fig. 4B) and the toxin recoveries were still unsatisfactorily low in the low ppb range (ochratoxin A 49%; zearalenone 96%). Elution with 12 ml of chloroform–acetic acid–methanol (9:1:1) (Fig. 4C) gave recoveries of 66% for ochratoxin A and 87% for zearalenone.

A clean-up with a C_{18} SPE column allowed the removal of co-eluting interferents in the final HPLC system (Fig. 5) by successively washing the cartridge with 4 ml of 5% acetic acid and 200 μl of methanol–water–acetic acid (50:46:4). The final elution was performed with methanol–water–acetic acid (80:15:5) (Fig. 4D), yielding an 83% recovery for both toxins. Reproducibility tests of this SPE clean-up procedure indicated a relative standard deviation (R.S.D.) of 3.9% for ochratoxin A and 6.5% for zearalenone.

A pH-controlled base–acid liquid–liquid partitioning technique reported for zearalenone and

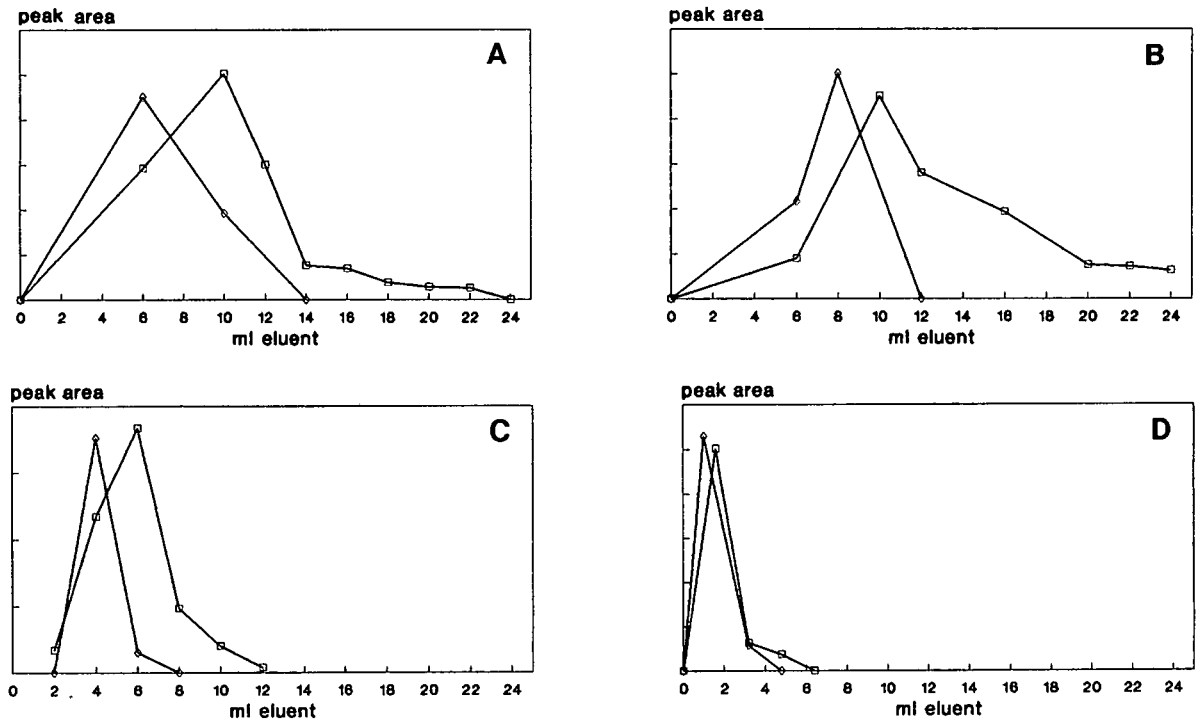

Fig. 4. Elution profiles of mycotoxins (□) ochratoxin A and (◇) zearalenone eluted with (A) chloroform–acetic acid (9:1) from a silica gel 60 SPE column; (B) ochratoxin A and zearalenone eluted with chloroform–acetic acid (9:1) from a Florisil SPE column; (C) chloroform–methanol–acetic acid (9:1:1) from a Florisil SPE column; (D) methanol–water–acetic acid (80:15:5) from a C_{18} SPE column.

zearalenol by Bagneris *et al.* [9] could easily be adapted to the additional ochratoxin A determination, giving recoveries of 43% and 88% for ochratoxin A and zearalenone, respectively. Sodium chloride was added to break emulsions that appeared with mixed feed extracts. Acceleration of phase separation was performed by washing warm tap water around the separating funnel. The resulting chromatograms showed fewer interferences than obtained in all the other purification techniques, but the procedure is labour intensive and hardly suitable for automation.

Precision data were evaluated for the pH-controlled liquid–liquid partitioning procedure in comparison with a clean-up with C_{18} SPE columns, revealing better repeatability of the SPE technique. The R.S.D. of independent test results from a single maize sample was 3.9% for ochratoxin A and 6.5% for zearalenone with C_{18} SPE clean-up; using the pH-controlled liquid–liquid partitioning purification technique for ochratoxin A and zearalenone R.S.D. values of 8.7% and 7.5%, respectively, were obtained.

Quantification was performed by external standard calibration owing to the good linearity and correlation of the results obtained from spiked maize samples in the range 0.5–1000 ppb. The correlation coefficients for ochratoxin A were 0.995 for C_{18} SPE clean-up and 0.989 for the liquid–liquid partitioning procedure.

Chromatographic separation

The formation of inclusion complexes between mycotoxins and β-cyclodextrin (a cyclic oligosaccharide, consisting of seven α-1,4-linked glucose units arranged in a torus [39]) molecules is mainly responsible for altering mycotoxin retention in the RP-HPLC system. The formation of an inclusion complex depends on the shape, size and geometrical properties of the solute, the diameter of the CD cavity (6.4 Å for β-CD) and other factors [39,40]. There have been some

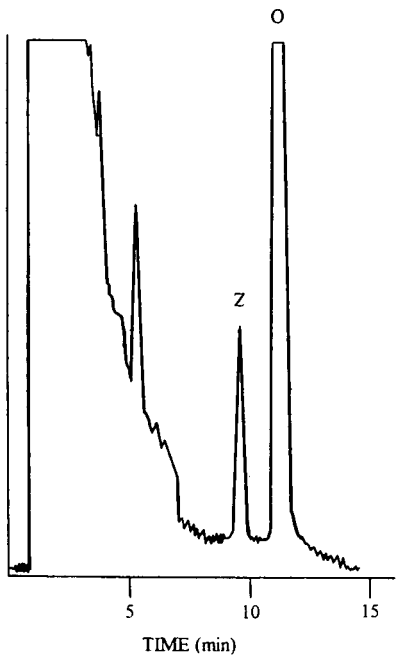

Fig. 5. HPLC of maize spiked with 20 ng/g each of zearalenone (Z) and ochratoxin A (O), after clean-up with C_{18} SPE columns, performed on a Merck LiChrospher 60, RP Select-B, 5 μm, 125 × 4 mm I.D. column. Mobile phase: methanol–water (45:55), pH 2.5 (12 m*M* phosphoric acid), containing 0.2 m*M* β-cyclodextrin. Fluorescence detection: $\lambda_{ex} = 315$ nm and $\lambda_{em} = 465$ nm.

reports relating stability constants of inclusion complexes to retention characteristics [41–44]. For optimization of the chromatographic toxin separation, some parameters (β-cyclodextrin concentration, column temperature and mobile phase composition) that might have an influence on the ability to form inclusion complexes and on the secondary equilibria in the RP-HPLC system with β-cyclodextrin (β-CD) were studied. Changing only the β-CD concentration between 0.1 and 5 m*M* revealed no significant effect on toxin resolution (Fig. 6). Between 0.2 and 1 m*M* β-CD, surprisingly a slight increase in retention was observed compared with higher β-CD concentrations owing to specific phenomena of adjustment of secondary equilibria on the surface of the column packing material. However, lower β-CD concentrations with careful setting of equilibria are recommended in order to keep the system back-pressure reasonable. Raising the column temperature to 65°C resulted

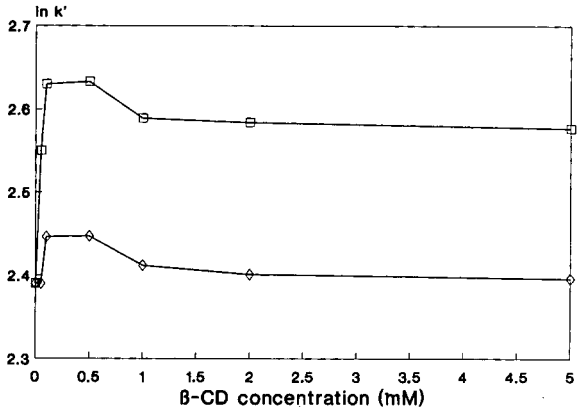

Fig. 6. Influence of β-cyclodextrin concentration on separation of (□) ochratoxin A and (◇) zearalenone. Analytical column: RP-8 Select-B, 5 μm, thermostated at 60°C in a water-bath. Mobile phase: methanol–water (45:55), pH = 2–3 (12 m*M* phosphoric acid), with β-cyclodextrin as mobile phase additive.

in a decrease in retention times (Fig. 7) but with no loss of resolution combined with an improvement in peak shape.

The methanol content of the mobile phase turned out to be a crucial parameter for toxin separation using β-CD as a mobile phase additive (Fig. 8). Above 50% methanol no separation of zearalenone and ochratoxin A could be achieved, which can be explained by competition of mycotoxins and methanol for the formation of an inclusion complex with β-CD [45]. Lowering

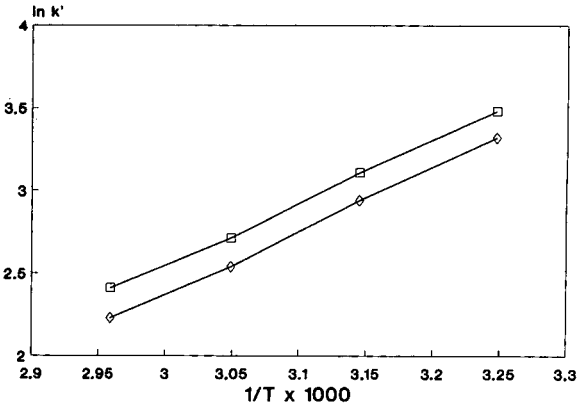

Fig. 7. Influence of column temperature on separation of (□) ochratoxin A and (◇) zearalenone using β-cyclodextrin as mobile phase additive. Analytical column: RP-8 Select-B, 5 μm. Mobile phase: methanol–water (45:55), pH = 2–3 (12 m*M* phosphoric acid).

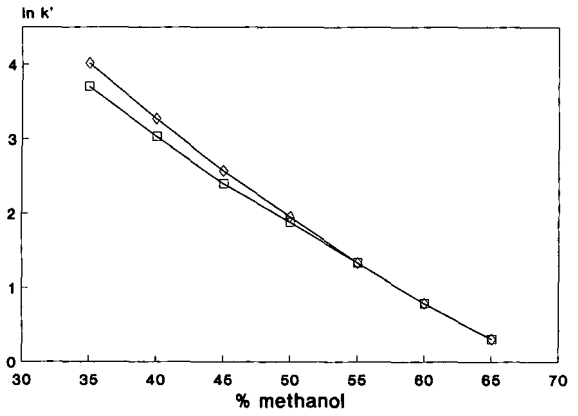

Fig. 8. Influence of methanol content of mobile phase on separation of (□) zearalenone and (◇) ochratoxin A using a constant amount of β-cyclodextrin as mobile phase additive. Analytical column: RP-8 Select-B, 5 μm, thermostated at 60°C in a water-bath. Mobile phase: methanol–water, pH = 2–3 (12 m*M* phosphoric acid).

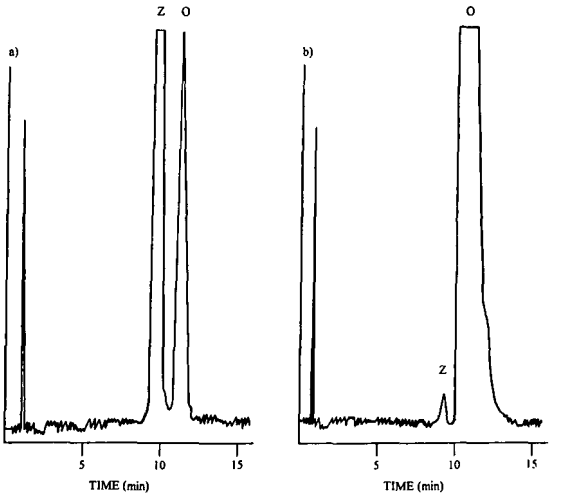

Fig. 9. HPLC of mycotoxin standard solution demonstrating the separation of (a) 100 ng absolute amount per 20 μl injection volume of zearalenone (Z) and 0.1 ng of ochratoxin A (O) and (b) 0.4 ng of zearalenone (Z) and 100 ng of ochratoxin A (O) on a Merck LiChrospher 60, RP Select-B, 5 μm, 125 × 4 mm I.D. column. Mobile phase: methanol–water (45:55), pH 2.5 (12 m*M* phosphoric acid), containing 0.2 m*M* β-cyclodextrin. Fluorescence detection: $\lambda_{ex} = 315$ nm and $\lambda_{em} = 465$ nm.

the methanol content was directly related to an increase in resolution. A Shiseido Capcell PAK C_{18} analytical column (polymer-coated RP material) gave similar results to conventional RP columns (LiChrospher 100, RP-18 or LiChrospher 60, RP-8 Select B).

A mobile phase composition of methanol–water (45:55) proved to be the best compromise of a good resolution of zearalenone and ochratoxin A and a short analysis time. The resulting separation factor (α) of 1.2 was sufficient for the simultaneous detection of zearalenone and ochratoxin A even when there was a large difference in concentration [Fig. 9: (a) 0.4 ng absolute amount per injection of zearalenone and 100 ng of ochratoxin; (b) 0.1 ng of ochratoxin and 100 ng of zearalenone]. This improvement gives rise to a marked increase in confidence in terms of determining especially zearalenone in addition to ochratoxin A, particularly because the fluorescence signal of zearalenone is 5–10 times lower than that of ochratoxin A.

In addition, a slight increase of 15% in the fluorescence sensitivity of ochratoxin A was observed with the use of β-cyclodextrin according to a higher UV absorption in the range 310–350 nm. Without β-CD in the mobile phase, all the RP-HPLC systems tested were not able to resolve these two mycotoxins and therefore all techniques rely totally on a perfect and selective preseparation of zearalenone and ochratoxin A in the course of sample clean-up and pretreatment prior to the final HPLC analysis. Even when the separation of both toxins seems to be possible, as reported for an Econosphere C_{18}, 5 μm, 150 × 4.6 mm I.D. analytical column (Alltech) [28], the use of β-CD as a mobile phase additive can improve the ruggedness of the RP-HPLC system, allowing also the use of all conventional RP-C_{18} analytical columns.

CONCLUSIONS

Using the above-described HPLC system and sample work-up procedure, we were able to reach detection limits of 400 pg absolute amount per 20-μl injection volume of zearalenone and 50 pg per 20 μl of ochratoxin A ($\lambda_{ex} = 315$ nm and $\lambda_{em} = 465$ nm), resulting in limits of determination of 5 ppb of zearalenone and 0.5 ppb of ochratoxin A in naturally contaminated maize. Mycotoxin detection could be improved by the use of a detector allowing time-programmed

setting of the excitation wavelength to the specific absorption maxima of 270 nm for zearalenone and 320 nm for ochratoxin A, giving a 20% increase in sensitivity for zearalenone and 10% for ochratoxin A (note: these values are strongly dependent on the physical properties of the light source in the fluorescence detector; therefore, diffferent values have been reported for different equipment [9,17,18,27,37,38]). An excitation wavelength of 315 nm was the best compromise for the highly sensitive and selective detection of zearalenone and ochratoxin A for the routine analysis of maize.

The method was successful in detecting zearalenone in several maize samples from southern parts of Austria in the range 28–660 ppb (mean = 274 ppb). Ochratoxin A and α-zearalenol were found at trace levels only. Ochratoxin B, zearalanone and β-zearalenol were not detected.

REFERENCES

1 C.J. Mirocha and C.M. Christensen in I.F.H. Purchase (Editor), *Mycotoxins*, Elsevier, New York, 1974, p. 141.
2 P. Krogh, *Acta Pathol. Microbiol. Scand., Sect. A, Suppl.*, 269 (1978) 1.
3 P. Krogh (Editor), *Mycotoxins in Food*, Academic Press, London, 1987, p. 97.
4 P. Krogh in A. Puchlev, V. Dinev, B. Milev and D. Doichinov (Editors), *Endemic Nephropathy*, 1974, p. 266.
5 H.P. Mortensen, B. Hald and A. Madsen, *Acta Agric. Scand.*, 33 (1983) 235.
6 F. Elling, B. Hald, C. Jacobsen and P. Krogh, *Acta Pathol. Microbiol. Scand., Sect. A*, 83 (1975) 739.
7 M. Pavlovic, R. Plestina and P. Krogh, *Acta Pathol. Microbiol. Scand., Sect. B*, 87 (1979) 243.
8 A. Adler, H. Lew and W. Edinger, *J. Landwirtsch. Forsch. Wien*, 41 (1990) 145.
9 R.W. Bagneris, J.A. Gaul and G.M. Ware, *J. Assoc. Off. Anal. Chem.*, 69 (1986) 894.
10 L. Rutquist, N.-E. Björklund, K. Hult, E. Hökby and B. Carlsson, *Appl. Environ. Microbiol.*, 36 (1978) 920.
11 P. Häggblom, *Appl. Environ. Microbiol.*, 43 (1982) 1205.
12 D.M. Wilson, W.H. Tabor and M.W. Trucksess, *J. Assoc. Off. Anal. Chem.*, 59 (1976) 125.
13 S. Swanson, R. Corley, D. White and W. Buck, *J. Assoc. Off. Anal. Chem.*, 67 (1984) 580.
14 B. Robert, M.E. Glancy and S.P.D. Patterson, *J. Assoc. Off. Anal. Chem.*, 64 (1981) 961.
15 G.B. Osborne, *J. Sci. Food Agric.*, 30 (1979) 1065.
16 G.M. Ware and C.W. Thorpe, *J. Assoc. Off. Anal. Chem.*, 61 (1978) 1058.
17 P. Lepom, *J. Chromatogr.*, 355 (1986) 335.
18 H. Cohen and M. Lapointe, *J. Assoc. Off. Anal. Chem.*, 69 (1986) 957.
19 M. Sharman, S. McDonald and J. Gilbert, *J. Chromatogr.*, 603 (1992) 285.
20 C.J. Mirocha, B. Schauerhammer and S.V. Pathre, *J. Assoc. Off. Anal. Chem.*, 57 (1974) 1104.
21 P. Scott, T. Panalaks, S. Kanhere and W. Milles, *J. Assoc. Off. Anal. Chem.*, 61 (1978) 593.
22 C.E. Kientz and A. Verweij, *J. Chromatogr.*, 355 (1986) 229.
23 Y. Jiao, W. Blaas, C. Rühl and R. Weber, *J. Chromatogr.*, 595 (1992) 364.
24 K. Schwadorf and H.-M. Müller, *J. Chromatogr.*, 595 (1992) 259.
25 E. Märtlbauer and G. Terplan, *Arch. Lebensmittelhyg.*, 39 (1988) 133.
26 O. Kawamura, S. Sato, H. Kajii, S. Nagayama, K. Ohtani, J. Chiba and Y. Ueno, *Toxicon*, 27 (1989) 887.
27 E. Josefson and T. Möller, *J. Assoc. Off. Anal. Chem.*, 62 (1979) 1165.
28 N. Chamkasem, W.Y. Cobb, G.W. Latimer, C. Salinas and B.A. Clement, *J. Assoc. Off. Anal. Chem.*, 72 (1989) 336.
29 C. Noonpugdee, *Chromatographia*, 23 (1987) 47.
30 A. Sano, S. Matsutani, M. Suzuki and S. Takitani, *J. Chromatogr.*, 410 (1987) 427.
31 M.A.J. Bayliss, R.B. Homer and M.J. Shepherd, *J. Chromatogr.*, 445 (1988) 393.
32 R.M. Black, R.J. Clarke and R.W. Read, *J. Chromatogr.*, 388 (1987) 365.
33 W. Langseth and P.-E. Clasen, *J. Chromatogr.*, 603 (1992) 290.
34 V. Seidel, B. Lang, S. Fraissler, C. Lang, K. Schiller, G. Filek and W. Lindner, *Chromatographia*, in press.
35 C.J. Mirocha, R.A. Pawlosky, K. Chatterjee, S. Watson and W. Hayes, *J. Assoc. Off. Anal. Chem.*, 66 (1983) 1485.
36 R.D. Plattner, M.N. Beremand and R. Powell, *Tetrahedron.*, 45 (1989) 2251.
37 M.V. Howell and P.W. Taylor, *J. Assoc. Off. Anal. Chem.*, 64 (1981) 1356.
38 W. Langseth, Y. Ellingsen, U. Nymoen and E.M. Økland, *J. Chromatogr.*, 478 (1989) 269.
39 J. Szejtli, *Cyclodextrins and Their Inclusion Complexes*, Akadémiai Kiadó, Budapest, 1982.
40 M.L. Bender and M. Komiyama, *Cyclodextrin Chemistry*, Springer, New York, 1978.
41 J. Zukowski, D. Sybilska and V. Jurczak, *Anal. Chem.*, 57 (1985) 2215.
42 K. Fujimura, T. Ueda, M. Kitagawa, H. Takayanagi and T. Ando, *Anal. Chem.*, 58 (1986) 2668.
43 B. Sebille, N. Thaud, J. Piquion and N. Behar, *J. Chromatogr.*, 409 (1987) 61.
44 R.M. Mohseni and R.J. Hurtubise, *J. Chromatogr.*, 499 (1990) 395.
45 Y. Matsui and K. Mochida, *Bull. Chem. Soc. Jpn.*, 52 (1979) 2808.

Journal of Chromatography, 635 (1993) 237–249
Elsevier Science Publishers B.V., Amsterdam

CHROM. 24 828

Purification of the cytochrome P-450 enzyme geraniol 10-hydroxylase from cell cultures of *Catharanthus roseus*

Annemarie H. Meijer*, Anthony De Waal[☆] and Robert Verpoorte

Biotechnology Delft Leiden, Project Group Plant Cell Biotechnology, Center for Bio-Pharmaceutical Sciences, Division of Pharmacognosy, Leiden University, Gorlaeus Laboratories, P.O. Box 9502, 2300 RA Leiden (Netherlands)

(First received September 18th, 1992; revised manuscript received December 23rd, 1992)

ABSTRACT

The cytochrome P-450 enzyme geraniol 10-hydroxylase (G10H) was purified from a suspension culture of *Catharanthus roseus*, grown on an alkaloid production medium. The cholate-solubilized G10H was purified in a four-step procedure, consisting of chromatography on DEAE-Sephacel, hydroxyapatite Ultrogel, ω-aminooctylagarose and TSK Phenyl-5PW. On DEAE-Sephacel a virtually complete separation of the cytochrome P-450 enzyme from NADPH:cytochrome P-450 (cytochrome *c*) reductase (EC 1.6.2.4) was achieved. The G10H activity of P-450-containing fractions was reconstituted by addition of the reductase and a lipid extract. Although a substantial loss of G10H activity occurred on solubilisation and the activity was much lower in the reconstituted system compared with solubilized preparations, the enzyme was remarkably stable during the later stages of its purification. An efficient separation of G10H from contaminating proteins was achieved by hydrophobic interaction chromatography on a high-performance TSK Phenyl-5PW column that was presaturated with non-ionic detergent. The G10H peak fractions from this column showed a single band on sodium dodecyl sulphate polyacrylamide gel electrophoresis with silver staining, corresponding to an M_r of 56 000. The purified enzyme catalyses the hydroxylation of both geraniol and nerol, and has a specific cytochrome P-450 content of 4.7 nmol/mg protein.

INTRODUCTION

The conversion of geraniol into its 10-hydroxy derivative, catalysed by the enzyme geraniol 10-hydroxylase (G10H, monoterpene hydroxylase), represents one of the initial steps in the biosynthesis of the monoterpenoid indole alkaloids in the plant family of the Apocynaceae. G10H was characterized as a membrane-bound cytochrome P-450 monooxygenase by Meehan and Coscia [1]. The hydroxylation of geraniol, or of its *cis* isomer nerol, was among the first cytochrome P-450-catalysed reactions discovered in higher plants. It has now been demonstrated that plant cytochrome P-450 enzymes are involved in a variety of biosynthetic pathways, *e.g.*, those leading to benzophenanthridine alkaloids [2], lignins and flavonoids, phytoalexins, cutins and suberins, phytohormones and steroids (for reviews, see refs. 3–6). In addition, the metabolism of exogenous compounds by plant cytochrome P-450 enzymes has been described (for reviews, see refs. 7 and 8). The substrate specificity of cytochrome P-450 enzymes and the regulation of their expression have been extensively studied in mammalian systems and in microorganisms, but the knowledge of plant P-450 enzymes is still limited. Only recently was the first cDNA sequence encoding a plant P-450 enzyme reported [9]. This concerned a ripening-related cDNA from avocado fruit (*Persea*

* Corresponding author. Present address: Institute of Molecular Plant Sciences, Leiden University, Clusius Laboratory, P.O. Box 9505, 2300 RA Leiden, Netherlands.
☆ Present address: Department of Molecular Biology, Netherlands Cancer Institute, Plesmanlaan 121, 1066 CX Amsterdam, Netherlands.

0021-9673/93/$06.00

americana). The polypeptide predicted from the nucleotide sequence shares some common features with animal P-450 proteins and probably the clone represents a P-450 enzyme that was purified to homogeneity from avocado mesocarp by O'Keefe and Leto [10]. Among the few other P-450 proteins that have been purified partially or to homogeneity from a plant source are *trans*-cinnamate 4-hydroxylase (EC 1.14.13.11) from *Helianthus tuberosis* [11], digitoxin 12β-hydroxylase from *Digitalis lanata* [12], a P-450 with unknown enzyme activity from *Tulipa gesneriana* [13] and 3,9-dihydroxypterocarpan 6a-hydroxylase (EC 1.14.13.28) from *Glycine max* [14]. The latter was purified to homogeneity and its separation from *trans*-cinnamate 4-hydroxylase provided the first real evidence for the existence of different types of P-450 proteins in a higher plant.

Madyastha *et al.* [15] described the isolation of G10H from seedlings of *Catharanthus roseus*. By ion-exchange chromatography the P-450 enzyme could be separated from NADPH:cytochrome P-450 (cytochrome *c*) reductase (EC 1.6.2.4), an enzyme that is essential for any cytochrome P-450-catalysed reaction, as it functions in the transfer of electrons from NADPH to the P-450 protein. The purification of the reductase to homogeneity and its characterization were described [16]. G10H activity could be reconstituted with the reductase, the partially purified cytochrome P-450 and a lipid fraction [15,17]. McFarlane *et al.* [18] proposed that a feedback inhibition at the level of G10H might be one of the regulatory mechanisms in alkaloid biosynthesis, as they observed that this enzyme is inhibited by catharanthine, an end-product of the pathway. G10H was also regarded as a potential site for regulatory control by Schiel *et al.* [19], who observed an increased G10H activity in cultures transferred to an alkaloid production medium and a close relation of G10H activity to the pattern of alkaloid accumulation. A detailed investigation of the expression of G10H and NADPH:cytochrome P-450 reductase on the protein and transcriptional level will help to gain a better insight into the regulation of alkaloid biosynthesis and will attribute to the knowledge of plant cytochrome P-450 systems in general. The purification of G10H is a first step in this direction. Here we describe the purification of this cytochrome P-450 enzyme from cell cultures of *Catharanthus roseus* by an efficient procedure consisting of four chromatographic steps.

EXPERIMENTAL

Materials

Geraniol (96%), nerol (95%) and citral (97%) were obtained from Fluka (Buchs, Switzerland). NaB^3H_4 (>100 Ci/mol) was from NEN Du Pont ('s-Hertogenbosch, Netherlands). [1-^{3}H]Farnesyl pyrophosphate (40 Ci/mol) and [4-^{3}H]squalene (10 Ci/mol) were gifts from Dr. D.R. Threlfall (University of Hull, UK). CHAPS {3-[(3-cholamidopropyl)dimethylammonio]propane-1-sulphonic acid}, CHAPSO {3-[(3-cholamidopropyl)dimethylammonio]-2-hydroxypropane-1-sulphonic acid}, polyvinylpyrrolidone (PVP) (insoluble form), leupeptin, cytochrome *c* (type III from horse heart) and ω-aminooctyl agarose were purchased from Sigma (St. Louis, MO, USA). Sodium cholate was from Merck (Darmstadt, Germany). Renex 690 was a gift from ICI Specialty Chemicals (Rotterdam, Netherlands). Glucose-6-phosphate dehydrogenase (lyophilized, from yeast) was obtained from Boehringer (Mannheim, Germany). Bovine serum albumin standard was obtained from Bio-Rad Labs. (Veenendaal, Netherlands). The TSK Phenyl-5PW column, DEAE-Sephacel, 2′,5′-ADP-Sepharose 4B and low-molecular-mass markers were purchased from Pharmacia LKB Biotechnology (Woerden, Netherlands), hydroxyapatite Ultrogel from IBF (Villeneuve la Garenne, France) and Extracti-gel D from Pierce (Rockford, IL, USA). Organic solvents were of analytical-reagent grade or distilled before use. All other chemicals were of the highest purity commercially available.

Synthesis of 10-hydroxygeraniol and 10-hydroxynerol

10-Hydroxygeraniol was synthesized essentially as described by Madyastha *et al.* [15] and Schiel *et al.* [19]. A 7.5-ml portion of geraniol was acetylated with 4.85 ml acetic anhydride

(95%) and 4.15 ml pyridine for 15 h at room temperature. After addition of water, geranyl acetate was extracted with ethyl acetate. The organic phase was washed with 1 *M* HCl and subsequently with 6.6% (w/v) $NaHCO_3$. After evaporation of the solvent under vacuum, geranyl acetate was subjected to SeO_2 oxidation to yield a mixture of 10-oxogeranyl acetate and 10-hydroxygeranyl acetate. The reaction was performed with 5.5 g of SeO_2 in 100 ml of boiling ethanol (96%) under reflux for 6 h. After evaporation of the solvent under vacuum, the product was applied to a silica gel 60 (Merck) column to remove selenium. The product was eluted with dichloromethane–methanol (8:2, v/v) and subjected to $LiAlH_4$ reduction to yield 10-hydroxygeraniol. The dried acetates were dissolved in 50 ml of sodium-dried diethyl ether and added dropwise with stirring to 2.5 g of $LiAlH_4$ in 100 ml of sodium-dried diethyl ether at 0°C and under reflux. After 45 min, excess of $LiAlH_4$ was removed by the dropwise addition of 25 ml of water. The reaction mixture was extracted with 10% (w/v) NH_4Cl and the aqueous phase was washed twice with diethyl ether. The combined ether phases were dried under vacuum and applied to a silica gel 60 column. After elution of unreduced acetates with chloroform–ethyl acetate (3:1, v/v), 10-hydroxygeraniol was eluted with methanol. 10-Hydroxynerol was synthesized from nerol by the same procedure.

The structures of 10-hydroxygeraniol and 10-hydroxynerol were confirmed by PMR spectroscopy [15] with tetramethylsilane as reference compound. 10-Hydroxygeraniol: δ (ppm) [C^2HCl_3], 1.670, 1.674 (3H, s, H-4; 3H, s, H-9), 2.10 (4H, m, H-5, H-6), 3.98 (2H, s, H-10), 4.14 (2H, d, *J* 6.9 Hz, H-1), 5.38 (2H, m, H-2, H-7). 10-Hydroxynerol: δ (ppm) [C^2HCl_3], 1.65 (3H, d, *J* 1.4 Hz, H-9), 1.75 (3H, d, *J* 1.2 Hz, H-4), 2.14 (4H, m, H-5, H-6), 3.98 (2H, s, H-10), 4.06 (2H, dd, *J* 7.3 and 0.7 Hz, H-1), 5.44 (2H, m, H-2, H-7).

Synthesis of labelled substrates

The synthesis of [1-^{3}H]geraniol and [1-^{3}H]-nerol was modified from Van Aller and Nes [20]. A 300-mg portion of citral [geranial–neral (65:35)] in 1 ml of ethanol was added slowly to 14.5 mg of NaB^3H_4 in 1 ml of ethanol on ice. After 30 min, the reaction mixture was diluted with diethyl ether and washed with 0.5 *M* HCl. The organic phase was concentrated under a stream of nitrogen and the products were purified by TLC on silica gel 60 F_{254}s (0.5 mm thickness, 20 × 20 cm, with a 4 cm concentration zone) (Merck). The plates were developed twice with hexane–ethyl acetate (4:1, v/v). By GC analysis less than 3% nerol was detected in the geraniol fractions and *vice versa*.

[1-^{3}H]Farnesol (40 Ci/mol) was obtained from [1-^{3}H]farnesyl pyrophoshate by hydrolysis with calf intestinal alkaline phosphatase.

[1-^{3}H]Geranyl pyrophosphate (0.5 Ci/mol) and [1-^{3}H]geranyl monophosphate (0.5 Ci/mol) were synthesized from [1-^{3}H]geraniol as described by Cornforth and Popják [21]. The products were purified by TLC on silica gel H (0.5 mm thickness, 20 × 20 cm) (Merck) with 2-propanol–ammonia solution–water (6:3:1, v/v/v).

Plant material

Cell suspension cultures were grown in the light at 25°C on gyratory shakers at 120 rpm. Cultures of *Catharanthus roseus* (L.) G. Don were subcultured every 7 days and *Tabernaemontana* cultures every 14 days by a fourfold dilution. *C. roseus* cultures were grown in LS medium [22] containing 3% sucrose, 2 mg/l 1-naphthaleneacetic acid and 0.2 mg/l kinetin. The alkaloid production medium was as described by Berlin *et al.* [23]. Cultures of *Tabernaemontana divaricata* (L.) R.Br. *ex* Roem. *et* Schult. and *Tabernaemontana pandacaqui* Poir. were grown in MS medium [24] containing 3% sucrose, 1 mg/l 2,4-dichlorophenoxyacetic acid and 1 mg/l kinetin.

Enzyme preparation

For purification of G10H, 7-day-old *C. roseus* cultures were diluted five-fold in 500 ml of alkaloid production medium and grown in 2-l erlenmeyer flasks for 5–6 days. The cells were harvested by filtration under suction, washed once with water and frozen in liquid nitrogen. Cells were kept at −80°C for storage. Liquid

nitrogen-frozen cells were homogenized in a Waring blender equipped with a stainless-steel beaker at maximum speed for 1 min, rapidly thawed in two parts of homogenization buffer containing 50 m*M* potassium phosphate (pH 7.6), 0.3 *M* sucrose, 1 m*M* EDTA, 1 m*M* dithiothreitol (DTT) and 5 μg/ml leupeptin, and additionally homogenized with an Ultra Turrax at medium speed for 2 min. Membranes sedimenting between 20 min at 1000 *g* and 60 min at 20 000 *g* were suspended in an approximately equal volume of 50 m*M* Tris–HCl buffer (pH 7.8) containing 20% (v/v) glycerol, 1 m*M* EDTA, 1 m*M* DTT and 5 μg/ml leupeptin.

In the screening experiment for G10H activity in different cell lines, 4 g of cell material were homogenized with 200 mg of PVP and two volumes of homogenization buffer without leupeptin by means of an Ultra Turrax at medium speed for 2 min at 0°C. A 1000–20 000 *g* pellet was isolated and suspended in 300 μl of 50 m*M* potassium phosphate buffer (pH 7.6) containing 1 m*M* EDTA and 1 m*M* DTT.

Solubilization and enzyme purification

The 1000–20 000 *g* membrane fraction (5–10 mg/ml of protein) was solubilized at 0°C by the dropwise addition of a 10% (w/v) sodium cholate solution to a final concentration of 1%. After 30 min of gentle stirring the suspension was centrifuged at 100 000 *g* for 90 min.

Solubilized protein isolated from 2.7 kg of cell material was applied on a DEAE-Sephacel column (34 × 2.6 cm I.D.), equilibrated in 50 m*M* Tris–HCl buffer (pH 7.8) containing 15% (v/v) glycerol, 0.1% (v/v) Renex 690 and 0.1 m*M* DTT. The column was washed with 400 ml of equilibration buffer and protein was eluted with a KCl gradient. The cytochrome P-450 was eluted with a linear gradient from 0 to 100 m*M* KCl in 1000 ml of equilibration buffer. The column was then washed with 400 ml of 100 m*M* KCl in equilibration buffer. Subsequently NADPH:cytochrome P-450 reductase was eluted with 600 ml of 300 m*M* KCl in equilibration buffer. The flow-rate was 0.5 ml/min and the fraction size was 10 ml.

G10H (cytochrome P-450)-containing fractions from DEAE-Sephacel were pooled, concentrated by ultrafiltration (Omega 30K membrane, Filtron) and applied to a hydroxyapatite Ultrogel column (24 × 1.6 cm I.D.) equilibrated in 10 m*M* potassium phosphate buffer (pH 7.7) containing 15% (v/v) glycerol, 0.2% (w/v) sodium cholate and 0.1 m*M* DTT. The column was washed with 50 ml of equilibration buffer. Elution was with a linear gradient from 10 to 500 m*M* potassium phosphate in 250 ml of equilibration buffer. The flow-rate was 0.25 ml/min and the fraction size was 7.5 ml.

The G10H pool from hydroxyapatite Ultrogel was concentrated by ultrafiltration (Omega 30K membrane, Filtron). Phosphate and cholate concentrations were reduced by repetitive dilution with aminooctyl equilibration buffer (see below), followed by concentration. The concentrate was applied to an ω-aminooctylagarose column (23 × 1.6 cm I.D.) equilibrated in 50 m*M* potassium phosphate buffer (pH 7.7) containing 15% (v/v) glycerol, 1 m*M* EDTA and 0.1 m*M* DTT. The column was washed with 100 ml of equilibration buffer. Elution was with a linear gradient from 0 to 0.2% (v/v) Renex 690 in 300 ml of equilibration buffer. The flow-rate was 0.25 ml/min and the fraction size was 7.5 ml.

The G10H pool from ω-aminooctylagarose was concentrated by ultrafiltration (Omega 30K membrane, Filtron) and applied to a TSK Phenyl-5PW HPLC column (7.5 × 0.75 cm I.D.). The column was equilibrated in 20 m*M* potassium phosphate buffer (pH 7.7) containing 15% (v/v) glycerol, 0.1% (v/v) Renex 690, 1 m*M* EDTA and 0.1 m*M* DTT until the absorbance at 280 nm (absorption of Renex 690) had reached a constant level. About 180 ml of equilibration buffer were required to saturate the column with detergent. After sample application the column was washed with 10 ml of equilibration buffer. Elution was with a linear gradient from 0.1 to 0.6% (v/v) Renex 690 in 35 ml of equilibration buffer. The flow-rate was 0.5 ml/min and the fraction size was 1 ml.

All chromatographic steps were performed at 4–7°C, except for the TSK Phenyl-5PW chromatography, which was performed at room temperature. The absorbance of the effluent was monitored at 280 and 405 nm. Purified enzyme preparations were stored at −80°C.

Determination of cytochrome P-450

Cytochrome P-450 concentrations ($\varepsilon = 91$ l mmol^{-1} cm^{-1} for absorbance at 450–490 nm) were determined from dithionite-reduced CO-difference spectra according to Omura and Sato [25].

Determination of G10H activity

The assay for G10H activity, based on the conversion of [1-^{3}H]geraniol into [1-^{3}H]-10-hydroxygeraniol, was modified from Madyastha *et al.* [15]. The incubation mixture (total volume 550 μl) contained 12.5 nmol of [1-^{3}H]geraniol (127 Ci/mol) in 10 μl of acetone, 1 I.U. of glucose-6-phosphate dehydrogenase, 2.5 μmol of glucose-6-phosphate, 0.5 μmol of NADP$^+$ and the enzyme preparation (10–50 μg of protein for 1000–20 000 *g* membrane fractions) in 50 m*M* potassium phosphate buffer (pH 7.6) containing 1 m*M* EDTA, 1 m*M* DTT, 10 μ*M* FAD and 10 μ*M* FMN. The geraniol concentration in the assay is approximately five times higher than the apparent K_m reported by Madyastha *et al.* [15]. The incubations were started by the addition of [1-^{3}H]geraniol, after a preincubation for 5 min at 30°C. After 60 min at 30°C, the mixture was extracted with 3 ml of ethyl acetate. The organic phase was dried under a stream of nitrogen, dissolved in 100 μl of acetone and a 10-μl aliquot was subjected to TLC (silica gel 60, 0.5 mm thickness, 20 × 20 cm). The plates were developed with toluene–ethyl acetate–acetone (6:4:1, v/v/v). Reference 10-hydroxygeraniol was rendered visible with anisaldehyde–acetic acid–methanol–sulphuric acid (1:20:170:10, v/v) spray reagent. The radioactivity in 10-hydroxygeraniol was determined by liquid scintillation spectrometry. Emulsifier-Safe scintillation fluid (Packard) was used.

The above-described assay for G10H activity was used during G10H purification and for all other experiments with the exception of the screening experiment for G10H activity in different cell suspension cultures. For this experiment a GC-based assay modified from Schiel *et al.* [19] was used. The incubation mixture (total volume 380 μl) contained 1.5 μmol of geraniol in 5 μl of ethanol, 0.5 μmol of NADPH and 75 μl of enzyme preparation (1000–20 000 *g* pellet, 5–10 mg/ml of protein), in 50 m*M* potassium phosphate buffer (pH 7.6) containing 1 m*M* EDTA and 1 m*M* DTT. After 30 min at 30°C the reaction was stopped with 75 μl of 2 *M* KOH. As an internal standard 1,10-decanediol (10 nmol in 20 μl of ethanol) was added and the mixture was extracted twice with 1 ml of ethyl acetate. The organic phase was dried under a stream of nitrogen and silylated with 50 μl of N-methyltrimethylsilyltrifluoroacetamide at room temperature for 15 min. The silylated samples were analysed by GC under the following conditions: 10 m × 0.22 mm I.D. WCOT CP-Sil 5cb fused-silica column, film thickness 0.13 μm (Chrompack); carrier gas, nitrogen at 100 kPa; splitting ratio 1:50; detector temperature, 290°C; injector temperature, 275°C; column temperature programme, 120°C for 3 min then increased from 120 to 195°C at 15°C/min and from 195 to 290°C at 30°C/min, then isothermal at 290°C for 10 min; detection, flame ionization.

Reconstitution of G10H activity

The G10H activity of P-450-containing fractions was reconstituted by addition of NADPH: cytochrome P-450 reductase and *C. roseus* lipids. The lipid fraction was extracted from 1000–20 000 *g* membrane fractions with chloroform-methanol (2:1, v/v) and dissolved in incubation buffer (see below) with a Branson microtip sonicator. To cytochrome P-450-containing fractions were added 360 pkat of reductase (from DEAE-Sephacel) and 10 μg of *C. roseus* lipids, in that order. Incubation buffer consisting of 50 m*M* potassium phosphate (pH 7.6), 1 m*M* EDTA, 1 m*M* DTT, 10 μ*M* FAD and 10 μ*M* FMN, was added to make a total volume of 200 μl. This mixture, followed by 300 μl of incubation buffer, was applied to a 250-μl column of Extracti-gel D detergent-removal gel. The eluate was collected and 50 μl of incubation buffer, containing 1 I.U. of glucose-6-phosphate dehydrogenase, 2.5 μmol of glucose-6-phosphate and 0.5 μmol of NADP$^+$ was added. After 5 min of preincubation at 30°C the reaction was started with [1-^{3}H]geraniol (12.5 nmol in 10 μl of acetone). After incubation for 60 min the

radioactivity in 10-hydroxygeraniol was determined as in the G10H assay described above.

Determination of NADPH:cytochrome c (P-450) reductase activity

The assay for NADPH:cytochrome *c* (P-450) reductase was modified from Madyastha *et al.* [15]. The incubation mixture (total volume 1.0 ml) consisted of 20 μl of enzyme solution and 50 nmol of cytochrome *c* (type III, from horse heart), 0.15 μmol of NADPH, 0.5 μmol of KCN, 5 nmol of flavin mononucleotide and 5 nmol of flavin–adenine dinucleotide (FAD) in buffer containing 0.5 *M* Tris–HCl buffer (pH 7.5). The reactions were started by the addition of enzyme and the reduction of cytochrome *c* was monitored for 3–4 min at 550 nm ($\varepsilon = 21$ l $mmol^{-1}$ cm^{-1}) and at 20°C.

Determination of trans*-cinnamate 4-hydroxylase activity*

trans-Cinnamate 4-hydroxylase activity was assayed by an HPLC method according to Dr. M. Petersen (University of Düsseldorf, Germany; personal communication). The incubation mixture (total volume 500 μl) consisted of 0.5 μmol of *trans*-cinnamate in 20 μl of 50% ethanol, 0.5 μmol of NADPH and the enzyme preparation (50–200 μg of protein for 1000–20 000 *g* membrane fractions) in 0.1 *M* Tris–HCl buffer (pH 7.5) containing 20 m*M* DTT. After incubation for 30 min at 30°C, the reaction was stopped by the addition of 100 μl of 6 *M* HCl and the mixture was extracted twice with 1 ml of ethyl acetate. The organic phase was dried under a stream of nitrogen and the residue was dissolved in 150 μl of methanol–water (50:50, v/v), containing 100 μl of H_3PO_4 (85%) per litre. HPLC was carried out at room temperature on a 250 × 4.6 mm I.D. Hypersil ODS column (particle size 5 μm) at a flow-rate of 1.5 ml/min. The analytical column was used in combination with a 20 mm × 2 mm I.D. precolumn (Upchurch) hand-packed with Perisorb RP-8 (Merck) with a particle size of 30–40 μm. The mobile phase consisted of methanol–water containing 100 μl of H_3PO_4 (85%) per litre and elution was with a linear gradient from 40 to 60% (v/v) methanol in 10 min, followed by 60% methanol for 3 min. The injection volume was 20 μl and detection was at 309 nm.

trans-Cinnamate 4-hydroxylase activity was reconstituted in an analogous manner to the method described for G10H. Incubation times up to 4 h were used in reconstitution experiments.

Gel electrophoresis, isoelectric focusing and N-terminal protein sequence analysis

Gel electrophoresis and isoelectric focusing were performed with a PhastSystem (Pharmacia LKB Biotechnology). Sodium dodecyl sulphate–polyacrylamide gel electrophoresis (SDS-PAGE) was carried out in PhastGel gradient medium 10–15 or PhastGel homogeneous medium 12.5. Protein staining was done according to the instructions for the PhastGel silver kit. Isoelectric focusing was with PhastGel IEF 3–9. N-Terminal sequence analysis by Edman degradation of protein electroblotted onto a polyvinylidene fluoride membrane was performed by Eurosequence (Groningen, Netherlands).

Alkaloid analysis

A 50-mg portion of freeze-dried cell material, 50 μl of internal standard (1.0 g/l dihydroquinine), 1 ml of buffer (pH 10) consisting of 62.5 m*M* glycine, 62.5 m*M* NaCl and 0.0375 *M* NaOH, 57.5 μl of 1 *M* NaOH and 5 ml of CH_2Cl_2 were mixed thoroughly for 1 min on a vortex apparatus. After centrifugation, the organic phase was evaporated under vacuum. The residue was dissolved in 0.5 ml of eluent consisting of 50 m*M* sodium phosphate (pH 3.9)–acetonitrile–2-methoxyethanol (80:15:5, v/v/v) and 100 μl were injected on to a 300 mm × 3.9 mm I.D. μBondapak Phenyl (Waters, Milford, MA, USA) column [26]. The flow-rate was 2 ml/min and a Waters 990 photodiode-array detector was used.

Protein determination

Protein was determined according to Peterson [27] with bovine serum albumin as a standard.

RESULTS AND DISCUSSION

G10H activity in Catharanthus roseus *and* Tabernaemontana *species*

To select a suitable source for G10H purification we determined G10H activity levels in cell suspension cultures of *Catharanthus roseus*, *Tabernaemontana divaricata* and *Tabernaemontana pandacaqui*, three members of the Apocynaceae family that produce related terpenoid indole alkaloids. During this screening experiment we also studied the relationship between the activity of G10H and the accumulation of terpenoid indole alkaloids. G10H activity was measured in a membrane fraction sedimenting between 1000 and 20 000 *g*. In addition to organelles such as mitochondria and plastids, this pellet contains provacuolar membranes, in which, according to Madyastha *et al.* [28], the G10H from *C. roseus* is localized. In agreement with their results, we found that the bulk of G10H activity in *C. roseus* was present in this fraction. Only about 15% of the total activity was detected in a 100 000 *g* microsomal fraction. The same distribution pattern was found for G10H from *T. divaricata*. Both in *C. roseus* and in *T. divaricata* we could also demonstrate the activity of the cytochrome P-450 enzyme *trans*-cinnamate 4-hydroxylase in the 1000–20 000 *g* pellet. In *C. roseus trans*-cinnamate 4-hydroxylase, like G10H, appeared to occur predominantly in this fraction, whereas only about 25% was found to be associated with microsomes.

G10H activity was monitored during growth of several suspension cultures. In a cell line of *C. roseus* that accumulates tryptamine, but no terpenoid indole alkaloids, G10H activity could not be detected. The enzyme, however, became induced when the culture was transferred to an alkaloid production medium. The terpenoid indole alkaloid ajmalicine appeared just after G10H activity had reached a maximum (Fig. 1). An increase in the activity of this enzyme in a *C. roseus* cell line on production medium was also observed by Schiel *et al.* [19].

In a cell line of *T. divaricata* maximum G10H activity was present during the first week of growth. The enzyme activity could no longer be detected when the stationary phase was reached.

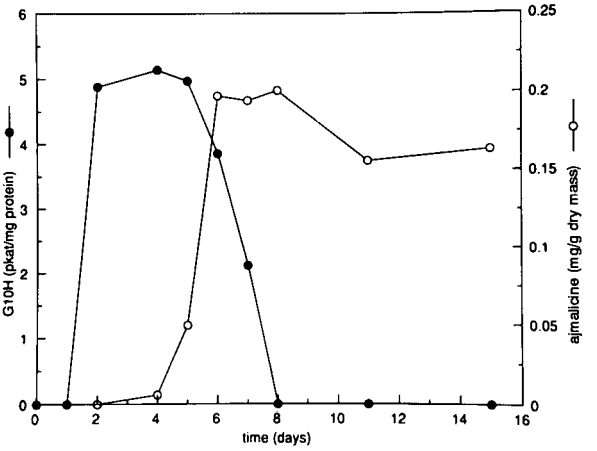

Fig. 1. G10H activity and ajmalicine accumulation in cell cultures of *Catharanthus roseus* on alkaloid production medium. Erlenmeyer flasks (250 ml) containing 50 ml of medium were inoculated with 5 g of cell material, filtered over a sterile glass filter. At each time point one flask was harvested. Cell material was homogenized in two volumes of 50 m*M* potassium phosphate buffer (pH 7.6), containing 0.3 *M* sucrose, 1 m*M* EDTA, 1 m*M* DTT and polyvinylpyrrolidone (50 mg/g cell material). G10H was measured in a 1000–20 000 *g* membrane fraction.

This cell line produced a variety of terpenoid indole alkaloids, with vallesamine and O-acetylvallesamine as major and voaphylline, tubotaiwine, apparicine and several acylindole alkaloids as minor components. Maximum levels were reached after the peak in G10H activity (Fig. 2).

During the growth of a cell suspension culture of *T. pandacaqui* no G10H activity could be detected. This cell line produced no terpenoid indole alkaloids. Only tryptamine (0.03–0.1 mg/g dry mass) and large amounts of a tryptamine derivative, probably 5-hydroxytryptamine, were present (at approximately ten times the level of tryptamine). G10H activity in this cell line was also found to be absent when in a later stage enzyme extractions were performed in the presence of leupeptin, a protease inhibitor which increased substantially the recovery of G10H from *C. roseus* cells.

Parallel to the experiments described here, cell line characterizations were performed, in which the activities of tryptophan decarboxylase and strictosidine synthase were measured during

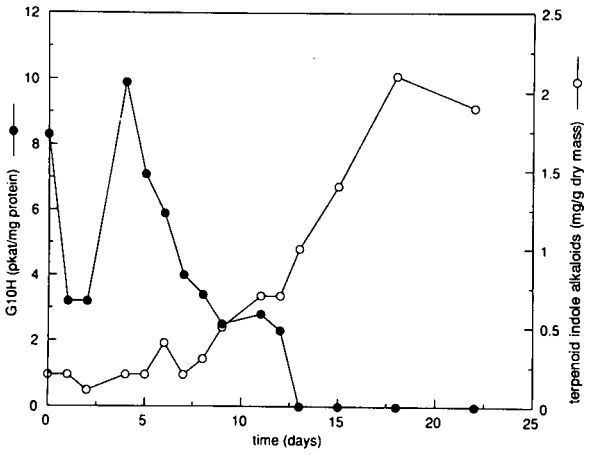

Fig. 2. G10H activity and alkaloid accumulation during growth of cell cultures of *Tabernaemontana divaricata*. The cultures reached stationary phase at day 11. Experimental details as in Fig. 1.

growth [29]. It appeared that the *C. roseus* line on growth medium and the *T. pandacaqui* line, in both of which G10H and terpenoid indole alkaloids were not detected, did possess tryptophan decarboxylase and strictosidine synthase activity. The absence of indole alkaloids in these cell lines seems therefore to be correlated with a shortage of terpenoid precursors. The fact that G10H activity could not be detected supports the arguments of McFarlane *et al.* [18] and Schiel *et al.* [19] to regard this enzyme as a potential site for control in the pathway for secologanin biosynthesis. However, other unknown regulatory enzyme activities in the secologanin pathway may also represent bottlenecks in alkaloid production.

The presence of induced levels of G10H activity in *C. roseus* suspensions rapidly after transfer to alkaloid production medium was found to be reproducible, and this cell material was considered the best source for G10H purification. Madyastha *et al.* [15] had reported partially purified G10H to be highly labile. After selection of the *C. roseus* cell material for G10H purification, we therefore tried to optimize the extraction procedure for this enzyme source in order to obtain a membrane preparation with high G10H specific activity as starting material. In the above-described screening experiments for G10H activity, enzyme extractions were performed in the presence of PVP (insoluble form) to bind phenolics and in the presence of the protease inhibitor EDTA. The addition of PVP (insoluble or soluble form), however, appeared not to be benificial. Several protease inhibitors were tested. With leupeptin (5 μg/ml), a fivefold increase in G10H activity was observed. Phenylmethylsulphonyl fluoride was not effective and benzamidine improved the recovery of G10H slightly. Leupeptin, however, was more effective alone than in combination with the other protease inhibitors. For purification of G10H, the *C. roseus* cell material was homogenized in the presence of only EDTA and leupeptin. In this way membrane preparations were obtained with a ten-fold higher G10H specific activity than the membrane fractions isolated by Madyastha *et al.* [15] from *C. roseus* seedlings.

Solubilization

The ionic detergent sodium cholate is often used for solubilization of cytochrome P-450 systems, since it causes little conversion of cytochrome P-450 to the catalytically inactive cytochrome P-420. Moreover, in contrast to most non-ionic detergents, cholate is only slightly inhibitory to the enzyme activity, even at the high concentrations necessary for solubilization [30]. Solubilization of cytochrome P-450 with the zwitterionic detergent CHAPS has also been successful [31]. We tested cholate, CHAPS, and CHAPSO for solubilization of G10H in the concentration range 0.2–1.2% and at a protein concentration of 5 mg/ml. In all instances most of the activity remained unsolubilized at concentrations below the critical micellar concentration (0.5% for CHAPS and CHAPSO, 0.6% for cholate). The solubilized activity was maximum when concentrations above the critical micellar concentration were used, but under those conditions the total of unsolubilized and solubilized activity was always less than 10% of the original activity. Enzyme solubilized with CHAPS or CHAPSO had to be passed through detergent-removal gel (Extracti-gel D) to measure G10H activity. This treatment had no effect on cholate-solubilized enzyme. Sonication with a microtip sonifier prior to cholate solubilization did not improve the yield of solubilized activity at any of

the detergent concentrations tested. In cholate-solubilized preparations the activity of *trans*-cinnamate 4-hydroxylase was also more than 90% lower than in the membrane fraction. With all the detergents tested about 100% of the NADPH:cytochrome *c* reductase activity could be solubilized. The loss of monooxygenase activity on solubilization can be explained by an inactivation or denaturation of the enzyme or by a less efficient interaction between the cytochrome P-450 and the reductase, possibly owing to their distribution over different micelles.

Separation of G10H from NADPH:cytochrome P-450 reductase and reconstitution of G10H activity

The cholate-solubilized protein was subjected to DEAE-Sephacel chromatography and eluted with a KCl gradient. Although the use of cholate has advantages for solubilization, cytochrome P-450 can be separated more completely from NADPH:cytochrome P-450 (cytochrome *c*) reductase in the presence of a non-ionic detergent [30]. Therefore, ion-exchange chromatography was performed in the presence of 0.1% Renex 690, a non-ionic detergent of the polyoxyethylene nonylphenol type, which is non-denaturing with respect to cytochrome P-450 [30]. A good separation of the two proteins was achieved. The cytochrome P-450 eluted between 25 and 35 m*M* KCl and the reductase could be eluted after a stepwise increase in the KCl concentration from 100 to 300 m*M*. No NADPH:cytochrome *c* reductase activity was associated with the P-450 peak. The reductase fractions contained only traces of cytochrome P-450.

After the separation of the P-450 component and the reductase, G10H activity can only be measured in a reconstituted system, in which the protein components are integrated into liposomes. Reconstitution of G10H activity could be achieved by the addition of partially purified reductase (DEAE-Sephacel fraction) and a crude extract of *C. roseus* lipids to the P-450-containing fraction. To avoid the sensitivity of the G10H assay becoming limiting during subsequent purification steps, it was essential to optimize the conditions of the reconstitution method. We found that the efficiency of reconstitution could be improved when the mixture of cytochrome P-450, reductase and lipid was passed through a small column of Extracti-gel D for detergent removal. When the Extracti-gel D step was omitted, more than 80% reduced G10H activities were observed. A similar decrease in activity was found on addition of 0.1% Renex 690 to the reconstituted system after the Extracti-gel treatment. The dependence of G10H activity on the concentrations of cytochrome P-450 and reductase was investigated. Omitting either of the protein components resulted in a complete loss of G10H activity. To allow us to determine the recovery of G10H activity during purification, a saturating reductase concentration was used in the reconstitution assay, which made G10H activity linearly dependent on the concentration of (geraniol-specific) cytochrome P-450. The reconstituted system was optimized with respect to lipid composition and concentration. Reconstitution with a crude extract of *C. roseus* lipids (10–250 μg) stimulated G10H activity. The highest (two-fold) increase was with 10 μg, and this amount was chosen for the routine procedure. A stimulation (1.5–2-fold) could also be effected with 10 μg of purified phospholipids [dilauroylphosphatidylcholine or a mixture of phosphatidylcholine and phosphatidylinositol (9:1)], but these were inhibitory at higher concentrations.

The highest G10H activity achieved in the reconstituted system was always less than 10% of the activity of the solubilized membrane fraction. A low G10H activity after reconstitution was also reported by Madyastha *et al.* [15]. Similar results were obtained with reconstitution of digitoxin 12β-hydroxylase [12] and *trans*-cinnamate 4-hydroxylase [32], but 3,9-dihydroxypterocarpan 6a-hydroxylase [14] could be reconstituted with a much higher yield of activity. Madyastha *et al.* [15] assumed that the low activity after reconstitution was probably due to the highly labile nature of cytochrome P-450. In contradiction to this, we found that the recovery of G10H activity was remarkably high during all subsequent chromatographic steps in our purification procedure. Moreover, we did not observe conversion of cytochrome P-450 to the P-420 form during these steps. Loss or denaturation of

protein may partly explain the initial decrease in activity. However, we consider it more likely that this is mainly caused by other effects, such as an incomplete removal of inhibitory detergent and a less efficient interaction between reductase and P-450 in the reconstituted system. Such differences in the efficiency of catalysis of the hydroxylation complicate the interpretation of the purification scheme (Table I). We believe that DEAE-Sephacel forms an efficient purification step, because there was virtually complete separation of P-450 and reductase, and the total P-450 was enriched seven-fold. A less efficient catalysis in the reconstituted system may explain the decrease in specific G10H activity.

Purification of G10H

The G10H pool from DEAE-Sephacel was subjected to hydroxyapatite Ultrogel chromatography. G10H and cytochrome P-450 eluted in a broad peak between 150 and 450 m*M* potassium phosphate, with the highest amounts at 250 m*M*. A three-fold increase in the specific activity of G10H was achieved. On this column the non-ionic detergent Renex 690 was exchanged for cholate, because Renex interferes with the binding of G10H to ω-aminooctyl agarose, which was planned as the next purification step, as aminooctyl has been described as an efficient ligand for the iron(III) form of cytochrome P-450 [33]. The G10H pool from the hydroxyapatite column was applied to an ω-aminooctylagarose column and G10H was eluted with a gradient from 0–0.2% Renex 690.

The G10H pool from ω-aminooctylagarose was further purified by hydrophobic interaction chromatography on a high-performance TSK Phenyl-5PW column. Protein purification by hydrophobic interaction chromatography usually involves binding of protein to the matrix under high-salt conditions and elution with a decreasing salt gradient. To elute strongly bound proteins, addition of a (poly)alcohol or detergent may be necessary. G10H, however, appeared to have such a high hydrophobicity that it could even be bound in the presence of detergent. Before the application of protein, the TSK Phenyl-5PW column was washed with buffer, containing 0.1% of the non-ionic detergent Renex 690, until the absorbance of the effluent at 280 nm reached a constant level. This presaturation of the column with detergent made the TSK Phenyl-5PW chromatography a very efficient purification step, as it prevented most of the protein in the sample from binding, while G10H was still retained on the column. G10H could be eluted by further increasing the detergent concentration with a linear gradient of Renex 690 from 0.1 to 0.6% (Fig. 3a). Four of the peak fractions showed an electrophoretically homogeneous protein with an M_r of 56 000 on SDS-PAGE with silver staining (Fig. 3b). The p*I* of this protein was 8.3. In earlier fractions of the peak a second band with a slightly lower molecular mass was present, and the later fractions contained minor impurities.

TABLE I

PURIFICATION OF THE CYTOCHROME P-450 ENZYME G10H FROM *CATHARANTHUS ROSEUS*

The table is based on purification from 2.7 kg (fresh mass) of *C. roseus* cell material, harvested 5–6 days after transfer of suspension cultures to alkaloid production medium.

Purification step	Protein (mg)	Cytochrome P-450 (nmol)	Specific cytochrome P-450 content (nmol/mg)	G10H activity (pkat)	Specific activity (pkat/mg)	Purification (-fold)	Recovery (%)
20 000 *g* Membrane fraction	1891.2	483.5	0.26	154 668.6	81.8	1.00	100.00
Cholate solubilization	600.6	61.1	0.10	5978.0	10.0	0.12	3.87
DEAE-Sephacel	55.1	38.8	0.70	358.1	6.5	0.08	0.23
Hydroxyapatite Ultrogel	15.7	34.5	2.20	303.6	19.3	0.24	0.20
ω-Aminooctylagarose	6.1	17.8	2.92	308.6	50.6	0.62	0.20
TSK Phenyl-5PW	0.36	1.7	4.72	187.0	519.4	6.35	0.12

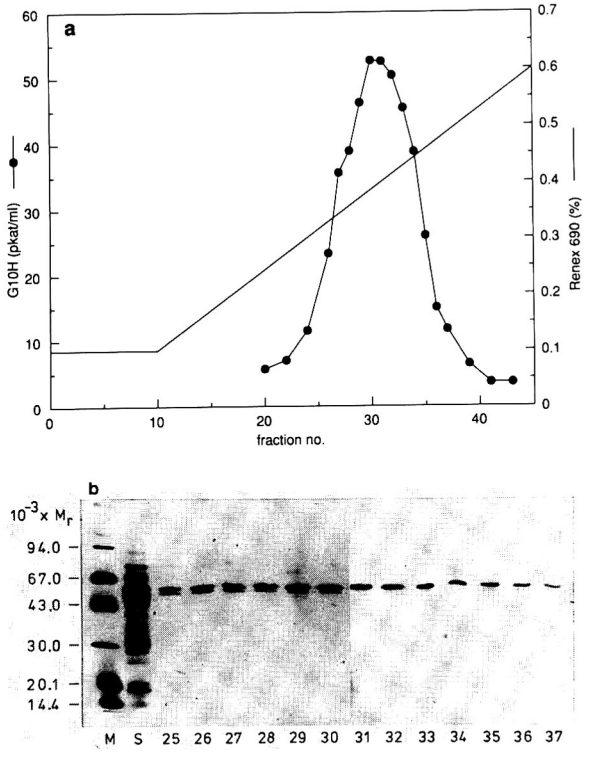

Fig. 3. TSK Phenyl-5PW chromatography of G10H. (a) Elution profile from TSK Phenyl-5PW. The column was equilibrated in 20 m*M* potassium phosphate buffer (pH 7.7) containing 15% (v/v) glycerol, 0.1% (v/v) Renex 690, 1 m*M* EDTA and 0.1 m*M* DTT. Elution was with 10 ml of equilibration buffer, followed by a linear gradient from 0.1 to 0.6% (v/v) Renex 690 in 35 ml of equilibration buffer. The fraction size was 1 ml. (b) SDS-PAGE of fractions from TSK Phenyl-5PW. SDS-PAGE was performed with a PhastSystem in PhastGel homogeneous medium 12.5. Detection was with silver staining. M = low-molecular-mass markers; S = sample applied on TSK Phenyl-5PW; 25–37 = fractions from TSK Phenyl-5PW [elution profile in (a)]; fractions 31–34 were pooled.

The four homogeneous fractions were pooled. The purification scheme is given in Table I. N-Terminal sequence analysis indicated that the M_r 56 000 protein band consisted of a single polypeptide. A partial amino acid sequence of sixteen residues starting with methionine was obtained. The sequence consisted of hydrophobic residues, which is in agreement with a function as membrane insertion signal peptide.

In the crude G10H membrane preparation at least one other cytochrome P-450 species is present, *trans*-cinnamate 4-hydroxylase. In the G10H pool from DEAE-Sephacel *trans*-cinnamate 4-hydroxylase activity could be measured after reconstitution with NADPH:cytochrome P-450 reductase and lipid by the same method as used for G10H. Analogous with G10H activity, a low *trans*-cinnamate 4-hydroxylase activity was realised in the reconstituted system. On hydroxyapatite Ultrogel and ω-aminooctylagarose, *trans*-cinnamate 4-hydroxylase co-purified with G10H, with high recovery. The G10H pool from TSK Phenyl-5PW, however, was free of *trans*-cinnamate 4-hydroxylase activity. We verified that the high concentrations of Renex 690 present in TSK Phenyl-5PW fractions do not interfere with reconstitution of *trans*-cinnamate 4-hydroxylase activity. Possibly this enzyme is bound more tightly to TSK Phenyl-5PW than G10H, as the activity was also not detected in the other fractions, eluting between 0.1 and 0.6% of the Renex 690 gradient, or in the unbound fraction.

The specific activity of the purified G10H for geraniol was 519 pkat/mg, measured in the reconstituted system. The purified enzyme also accepted nerol, the *cis* isomer of geraniol, as a substrate. Conversion of the structurally related C_{15} and C_{30} terpenoids farnesol and squalene under the standard assay procedures was not observed. Licht *et al.* [34] reported that no hydroxylation of the pyrophosphates of geraniol or nerol was observed with G10H from both *C. roseus* or animal membrane preparations. We tested geraniol monophosphate and geraniol pyrophosphate as substrates for crude G10H and observed no hydroxylation of these compounds.

The purified G10H had a specific P-450 content of 4.7 nmol/mg protein, which was much higher than that for the homogeneous 3,9-dihydropterocarpan 6a-hydroxylase from *Glycine max* (0.64 nmol/mg protein) [14], but lower than that for purified cytochrome P-450 from *Tulipa gesneriana* (6.7 nmol/mg protein) [13] and *Persea americana* (17.5 nmol/mg protein) [10]. Specific contents reported for highly purified cytochrome P-450 isoforms from animal sources vary between *ca.* 4 and 18 nmol/mg protein [35]. The specific content can show slight variations between individual purifications, owing to differences in the loss of haeme. A CO-difference

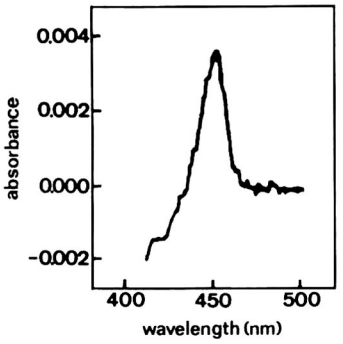

Fig. 4. CO-difference spectrum of purified G10H. A sample of the pooled G10H-containing fractions from TSK Phenyl-5PW was diluted to 8.2 μg/ml in 20 m*M* potassium phosphate buffer (pH 7.7) containing 15% (v/v) glycerol and a difference spectrum (dithionite-reduced *versus* dithionite-reduced, CO-saturated) was measured.

spectrum of the purified enzyme preparation is shown in Fig. 4.

The described purification procedure was reproducible. In terms of enzyme activity the recovery was low, but probably this was due to incomplete removal of inhibitory detergents or a less efficient interaction between NADPH:cytochrome P-450 reductase and cytochrome P-450 in the reconstituted system. Despite the low yield of enzyme activity, the amounts of purified G10H protein obtained from *C. roseus* cultures grown on alkaloid production medium were relatively high for a membrane-bound plant enzyme. The purification of cytochrome P-450-dependent G10H is the first step towards cloning of the corresponding gene, which will permit further studies concerning the regulation of this enzyme.

CONCLUSIONS

The membrane-bound cytochrome P-450 enzyme geraniol 10-hydroxylase (G10H) was purified from *Catharanthus roseus* cell cultures by an efficient procedure consisting of four chromatographic steps. The purified enzyme had an M_r of 56 000, a specific cytochrome P-450 content of 4.7 nmol/mg and catalysed the hydroxylation of both geraniol and nerol. The N-terminal amino acid residues of the purified protein were hydrophobic and may serve as a membrane anchor. As cytochrome P-450 enzymes in plants are present at low levels, an important step in G10H purification was the selection of cell cultures from which membrane preparations with a high G10H specific activity could be obtained. *C. roseus* cells grown on alkaloid production medium were identified as a suitable enzyme source. After cholate solubilization an almost complete separation of cytochrome P-450 and NADPH:cytochrome P-450 reductase was achieved by ion-exchange chromatography on DEAE-Sephacel. Reconstitution of G10H activity by the addition of the reductase and a *C. roseus* lipid extract was found to occur most efficient when Extracti-gel D was used to remove detergent. Further purification of G10H was achieved by chromatography on hydroxyapatite Ultrogel, ω-aminooctylagarose and TSK Phenyl-5PW. The hydrophobic nature of the enzyme allowed the application of hydrophobic interaction chromatography in a highly efficient manner. Presaturation of TSK Phenyl-5PW matrix with non-ionic detergent created conditions that prevented most of the contaminating proteins in the sample from binding, while G10H was still retained on the column. Subsequent elution of G10H by further increasing the detergent concentration resulted in an electrophoretically homogeneous protein preparation. Application of this method may be useful for the purification of other membrane-bound enzymes.

ACKNOWLEDGEMENTS

The authors thank Mr. A.G.M. Goosen and Mr. K. Weisz for expert technical assistance, Dr. G. Lodder for advice and assistance with the synthesis of labelled substrates, Dr. M. Petersen for making available the *trans*-cinnamate 4-hydroxylase assay and Dr. J.H.C. Hoge for critically reading the manuscript.

REFERENCES

1 T.D. Meehan and C.J. Coscia, *Biochem. Biophys. Res. Commun.*, 53 (1973) 1043.
2 T. Tanahashi and M.H. Zenk, *Phytochemistry*, 29 (1990) 1113.

3 R.P. Donaldson and D.G. Luster, *Plant Physiol.*, 96 (1991) 669.
4 G. Hendry, *New Phytol.*, 102 (1986) 239.
5 K. Higashi, *GANN Monogr. Cancer Res.*, 30 (1985) 49.
6 C.A. West, in D.D. Davies (Editor), *Biochemistry of Plants*, Vol. 2, Academic Press, New York, 1980, p. 317.
7 K. Higashi, *Mutat. Res.*, 197 (1988) 273.
8 D.P. O'Keefe, J.A. Romesser and K.J. Leto, *Recent Adv. Phytochem.*, 21 (1987) 151.
9 K.R. Bozak, H. Yu, R. Sirevåg and R.E. Christoffersen, *Proc. Natl. Acad. Sci. U.S.A.*, 87 (1990) 3904.
10 D.P. O'Keefe and K.J. Leto, *Plant Physiol.*, 89 (1989) 1141.
11 B. Gabriac, D. Werck-Reichhart, H. Teutsch and F. Durst, *Arch. Biochem. Biophys.*, 288 (1991) 302.
12 M. Petersen and H.U. Seitz, *Biochem. J.*, 252 (1988) 537.
13 K. Higashi, K. Ikeuchi, M. Obara, Y. Karasaki, H. Hirano, S. Gotoh and Y. Koga, *Agric. Biol. Chem.*, 49 (1985) 2399.
14 G. Kochs and H. Grisebach, *Arch. Biochem. Biophys.*, 273 (1989) 543.
15 K.M. Madyastha, T.D. Meehan and C.J. Coscia, *Biochemistry*, 15 (1976) 1097.
16 K.M. Madyastha and C.J. Coscia, *J. Biol. Chem.*, 254 (1979) 2419.
17 A.H. Meijer, E.J.M. Pennings, A. de Waal and R. Verpoorte, in H.J. Nijkamp, L.H.W. Van der Plas and J. Van Aartrijk (Editors), *Progress in Plant Cellular and Molecular Biology*, Kluwer, Dordrecht, 1990, p. 769.
18 J. McFarlane, K.M. Madyastha and C.J. Coscia, *Biochem. Biophys. Res. Commun.*, 66 (1975) 1263.
19 O. Schiel, L. Witte and J. Berlin, *Z. Naturforsch., Teil C*, 42 (1987) 1075.
20 R.T. Van Aller and W.R. Nes, *Phytochemistry*, 7 (1968) 85.
21 R.H. Cornforth and G. Popják, *Methods Enzymol.*, 15 (1969) 359.
22 E.M. Linsmaier and F. Skoog, *Physiol. Plant.*, 18 (1965) 100.
23 J. Berlin, E. Forche, V. Wray, J. Hammer and W. Hösel, *Z. Naturforsch., Teil C*, 38 (1983) 346.
24 T. Murashige and F. Skoog, *Physiol. Plant.*, 15 (1962) 473.
25 T. Omura and R. Sato, *J. Biol. Chem.*, 239 (1964) 2370.
26 R. Van der Heijden, P.J. Lamping, P.P. Out, R. Wijnsma and R. Verpoorte, *J. Chromatogr.*, 396 (1987) 287.
27 G.L. Peterson, *Anal. Biochem.*, 83 (1977) 346.
28 K.M. Madyastha, J.E. Ridgway, J.G. Dwyer and C.J. Coscia, *J. Cell. Biol.*, 72 (1977) 302.
29 L.H. Stevens, J. Schripsema, E.J.M. Pennings, A. de Waal and R. Verpoorte, *Planta Med.*, 55 (1989) 660.
30 A.Y.H. Lu and W. Levin, *Biochim. Biophys. Acta*, 344 (1974) 205.
31 L.M. Hjelmeland, D.W. Nebert and J.C. Osborne, Jr., *Anal. Biochem.*, 130 (1983) 72.
32 I. Benveniste, B. Gabriac and F. Durst, *Biochem. J.*, 235 (1986) 365.
33 C.R.E. Jefcoate, J.L. Gaylor and R.L. Calabrese, *Biochemistry*, 8 (1969) 3455.
34 H.J. Licht, K.M. Madyastha, C.J. Coscia and R.J. Krueger, in M.J. Coon, A.H. Conney and R.W. Estabrook (Editors), *Microsomes, Drug Oxidations, and Chemical Carcinogenesis*, Academic Press, New York, 1980, p. 211.
35 G.-R. Jänig and D. Pfeil, in K. Ruckpaul and H. Rein (Editors), *Cytochrome P-450 —Structural and Functional Relationships; Biochemical and Biophysical Aspects of Mixed Function Oxidases*, Akademie-Verlag, Berlin, 1983, p. 58.

Journal of Chromatography, 635 (1993) 251–256
Elsevier Science Publishers B.V., Amsterdam

CHROM. 24 809

Separation and detection of tissue CoASH and long-chain acyl-CoA by reversed-phase high-performance liquid chromatography after precolumn derivatization with monobromobimane

Abraham Demoz* and Bjørn Netteland

Department of Clinical Biology, Division of Biochemistry, Haukeland Hospital, University of Bergen, 5021 Bergen (Norway)

Asbjørn Svardal and Mohamad A. Mansoor

Department of Clinical Biology, Division of Pharmacology and Toxicology, University of Bergen, 5021 Bergen (Norway)

Rolf Kristian Berge

Department of Clinical Biology, Division of Biochemistry, Haukeland Hospital, University of Bergen, 5021 Bergen (Norway)

(First received September 2nd, 1992; revised manuscript received December 4th, 1992)

ABSTRACT

A method for the determination of tissue levels of free coenzyme A (CoASH) and long-chain acyl-CoA was developed using reversed-phase high-performance liquid chromatography and fluorescence detection. CoASH in acid-soluble and processed acid-insoluble liver homogenates was derivatized with the fluorescent agent monobromobimane, which selectively binds sulphydryl groups. The optimum requirements for sample preparation and conditions for derivatization with monobromobimane are discussed. The separation of the CoA–bimane adducts was achieved with a 3-μm Hypersil ODS C_{18} column (150 × 4.6 mm I.D.) using gradient elution with tetrabutylammonium hydroxide, acetic acid, phosphoric acid and acetonitrile. The detection limit was lower than 3 pmol. The method is more specific and more sensitive than the existing HPLC method with UV spectrophotometric detection. Furthermore, the method permits the detection and determination of other tissue thiols such as cysteine, cysteinylglycine and glutathione simultaneously.

INTRODUCTION

Tissue levels of acyl-coenzyme A (acyl-CoA) and particularly the ratios of long-chain acyl-CoA to free CoASH are known to act as intercellular regulators in several steps of intermediary metabolism [1–3]. For example, the levels of long-chain acyl-CoA and free CoASH in rat livers have been shown to increase after starvation and repeated administration of peroxisome proliferator compounds such as clofibrate and tiadenol [4–9]. A similar phenomenon was observed in our laboratory with peroxisome proliferating hypolipidaemic sulphur-substituted fatty acid analogues [10]. Furthermore, excess long-chain acyl-CoA levels in tissue have been implicated as potentially harmful amphiphiles with possible adverse effects on cellular metabolism through interaction with membrane structures [11]. It is of importance, therefore, to have

* Corresponding author.

0021-9673/93/$06.00

reliable, sensitive, specific and reproducible means to determine these compounds.

The separation and detection of tissue levels of free CoA and long-chain acyl-CoA by high-performance liquid chromatography (HPLC) with UV spectrophotometryic detection, developed originally by Ingebretsen and Farstad [12] and subsequently modified by Berge *et al.* [13,14], is frequently used. The present paper describes a major modification of this procedure in terms of the reagent used to hydrolyse the thio–ester bond and the HPLC conditions for separation and detection of tissue levels of both free CoA and long-chain acyl-CoA. The principle of the detection of the CoASHs in this method is based on derivatization of the free sulphydryl groups with the fluorescent agent monobromobimane [15]. The method is superior in terms of sensitivity and specificity over the existing method. Moreover, other cellular protein-bound thiols such as glutathione, cysteine and cysteinylglycine can be determined in one run from the tissue precipitates.

EXPERIMENTAL

Materials

N-Ethylmalemide, N-ethylmorpholine, dithioerythritol (DTE), cysteine, cysteinylglycine, glutathione, sodium tetrahydroborate ($NaBH_4$) and coenzyme A (CoASH) were obtained from Sigma (St. Louis, MO, USA). 5-sulphosalicylic acid dihydrate, dimethyl sulphoxide (DMSO), hydrogen bromide (HBr), perchloric acid, acetic acid, phosphoric acid and methanol from Merck (Darmstadt, Germany), monobromobimane (mBrB) from Calbiochem, Behring Diagnostics (La Jolla, CA, USA), tetrabutylammonium hydroxide from Janssen Chimica (Beerse, Belgium) and Hypersil ODS (3 μm) from Shandon (Runcorn, UK). Columns for reversed-phase HPLC (150 × 4.6 mm I.D.) were packed with 3-μm Hypersil ODS at 9000 p.s.i. (1 p.s.i. = 6894.76 pa) using a Shandon column packer.

A mixed standard solution was prepared by dissolving 40 μM cysteine, 10 μM cysteinylglycine, 320 μM glutathione and 80 μM CoASH in a 5% solution of sulphosalicylic acid containing 50 μM DTE.

Principles of determination of long-chain acyl-CoA

The method was essentially developed first by using palmitoyl-CoA as a prototype of long-chain acyl-CoA. The thio–ester bond of palmitoyl-CoA was cleaved after incubation with sodium tetrahydroborate. Optimum assay conditions were developed by using different concentrations of sodium tetrahydroborate, incubation temperatures and incubation times. Subsequently, the free sulphydryl group of the CoA moiety was derivatized with mBrB as described below. In acid precipitates of tissue, the method can also cleave the protein-bound thiols and hence can also be used to determine them simultaneously.

Tissue preparation for determination of long-chain acyl-CoA

Livers from male Wistar rats obtained from Møllegaard Breeding Laboratory (Ejby, Denmark) were used when they were *ca.* 4 weeks old, weighing 170–180 g. The animals were killed under light halothane anaesthesia and the livers from individual rats were homogenized immediately in ice-cold 5% sulphosalicylic acid in 50 μM DTE to obtain 10% (w/v) liver homogenates. Aliquots of 500 μl of tissue homogenates were centrifuged at 600 *g* for 10 min. The resultant supernatants were used to measure the acid-soluble CoASH, while the tissue precipitates were washed twice with 5% sulphosalicylic acid and once with distilled water and processed further.

The tissue precipitates were incubated with 25 μl of octanol (to prevent foaming) and 250 μl of either 1.4 or 2.0 M $NaBH_4$ for 30 min at 37°C in a water-bath. After incubation the samples were left on ice for 10 min and then 250 μl of 5% sulphosalicylic acid were added to neutralise the excess of $NaBH_4$. Subsequently, the samples were centrifuged at 600 *g* for 10 min and the supernatants were used to determine the hydrolysed CoASH and other thiols.

Precolumn derivatization

The principle of the derivatization of free sulphydryl groups with mBrB described below was a further development of a previously pub-

lished method for the determination of various thiols in red blood cells [15] and plasma [16]. To 60 μl of either pretreated palmitoyl-CoA, untreated CoASH or tissue homogenates prepared as described above were added 30 μl of 20% sulphosalicylic acid, 130 μl of 140 m*M* HBr in 65% DMSO, 50 μl of 1.0 M N-ethylmorpholine and 10 μl of 20 m*M* mBrB in 100% acetonitrile in that order. After 10 min of incubation at ambient temperature in the dark, 20 μl of 10% perchloric acid were added to stop further reaction.

Chromatography

Volumes of 10 μl of derivatized samples were injected into a 150 × 4.6 mm I.D. column packed with 3-μm particles of Hypersil ODS (C_{18}), equipped with a guard column packed with Pelliguard LC-18. Elution solvent A consisted of 10 mmol of tetrabutylammonium phosphate, 2.5 ml of glacial acetic acid and 0.675 ml of orthophosphoric acid diluted to 1 l with distilled water and adjusted to pH 3.4 with 2.0 *M* NaOH, solvent B was 200 ml of acetonitrile, 10 mmol of tetrabutylammonium phosphate, 2.5 ml of glacial acetic acid and 0.675 ml of orthophosphoric acid diluted with to 1 l distilled water and the pH adjusted to 3.25 with 2.0 *M* NaOH and solvent C was acetonitrile–water (75:25). Elution was carried out at ambient temperature at a flow-rate of 1.5 ml/min. The profile of the elution with a mixture of solvents A and B was as follows: 0–13 min, 4–22% B; 13.1–23 min, isocratic, 40% B; 23.1–30 min, 40–60% B; and 30.1–41.5 min, isocratic, 95% B. After each run the column was washed for 5 min with solvent C to remove late-eluting fluorescent material.

Instrumentation

A Spectra-Physics SP 8800 solvent-delivery system coupled to a Gilson 232-401 automatic sample processor was used. The detector was a Shimadzu RF 535 spectrofluorimeter equipped with concave diffraction grating excitation and emission monochromators operating at an excitation wavelength of 400 nm (13 nm bandpass) and an emission wavelength of 475 nm (15 nm bandpass). The sensitivity of the detector was enhanced about three-fold with a Hamamatsu R 982:08 photomultiplier. The integrator was a Spectra-Physics Chromjet SP 4400.

RESULTS AND DISCUSSION

Fig. 1A shows a typical HPLC trace of a standard mixture containing CoASH, cysteine, cysteinylglycine and glutathione that had been treated with $NaBH_4$ before derivatization with mBrB. With the gradient system adopted, a baseline separation of the CoA–bimane adduct

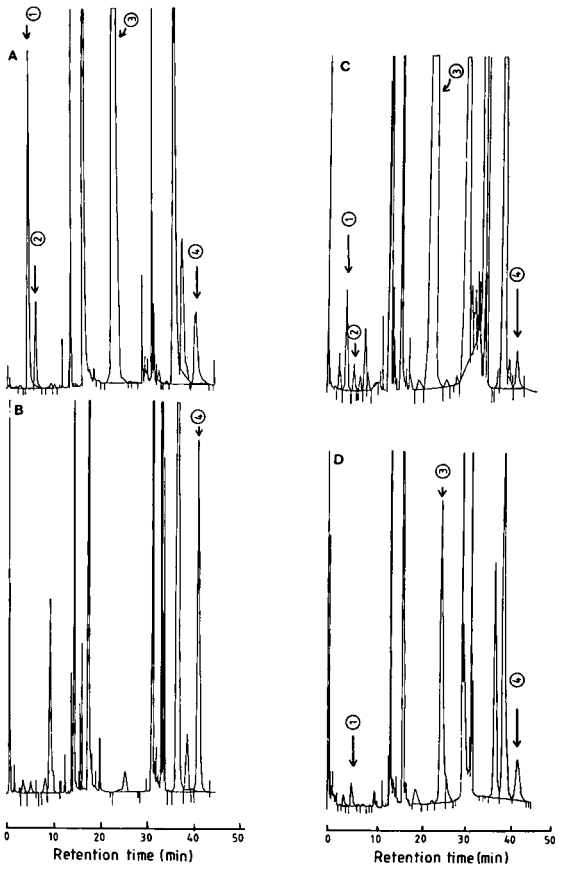

Fig. 1. Chromatograms obtained from monobromobimane-derivatized samples of (A) standard solution containing 80 μM CoASH, 40 μM cysteine, 10 μM cysteinylglycine and 320 μM glutathione dissolved in a 5% solution of sulphosalicylic acid containing 50 μM DTE; (B) standard solution of palmitoyl-CoA (150 μM) treated with 2.0 *M* $NaBH_4$; (C) acid-soluble liver extract obtained from 10% liver homogenates in 5% sulphosalicylic acid containing 50 μM DTE; and (D) acid-insoluble liver precipitates incubated with 2.0 *M* $NaBH_4$. Peaks: 1 = cysteine; 2 = cysteinylglycine; 3 = glutathione; 4 = CoASH.

and the other thiol–bimane adducts from the reagent peaks was achieved. The retention times for the bimane derivative of CoASH was 40–41 min and for those of cysteine, cysteinylglycine and glutathione 7.0, 8.0 and 29 min, respectively. In a subsequent experiment in which a standard sample of palmitoyl-CoA was treated with $NaBH_4$, a CoA–bimane adduct with a retention time of 40–41 min was also observed (Fig. 1B).

The method was further developed to determine CoASH and long-chain acyl-CoA in biological samples. A CoA–bimane adduct with a similar retention time was also observed in chromatograms from both acid-soluble (Fig. 1C) and acid-insoluble (Fig. 1D) liver extracts treated in the same way as the palmitoyl-CoA standards. Thus, this method can be used without any modification for the determination of CoASH (in the acid-soluble extract) and long-chain acyl-CoA (in the acid-insoluble extract) in tissues. The detection limit for both free CoASH and long-chain acyl-CoA was about 3 pmol per injection with a signal-to-noise ratio of 3.

In another experiment, we investigated whether any materials co-eluted with the CoA–bimane adduct. A liver extract was spiked with a standard solution containing both CoASH and palmitoyl-CoA, treated with $NaBH_4$ before derivatization. The standards co-eluted exactly with the peaks from the tissue extracts (data not shown).

Calibration graphs obtained with different concentrations of pure CoASH and palmitoyl-CoA are shown in Fig. 2A and B, respectively. The correlation coefficent (r) between the areas of peaks measured at 475 nm and the concentrations of CoASH and palmitoyl-CoA used was 0.988. It is worth noting, however, that the addition of 50 μl of DTE was neccessary in order to obtain a linear calibration graph, especially at lower concentrations. Furthermore, as shown in Fig. 2A, the yield of the CoA–bimane adduct was higher following treatment of the standard CoASH solution with $NaBH_4$ than without. This may be explained by the fact that $NaBH_4$ acts as a reductant, thereby minimizing the possible oxidative degradation of the CoASH molecule during processing.

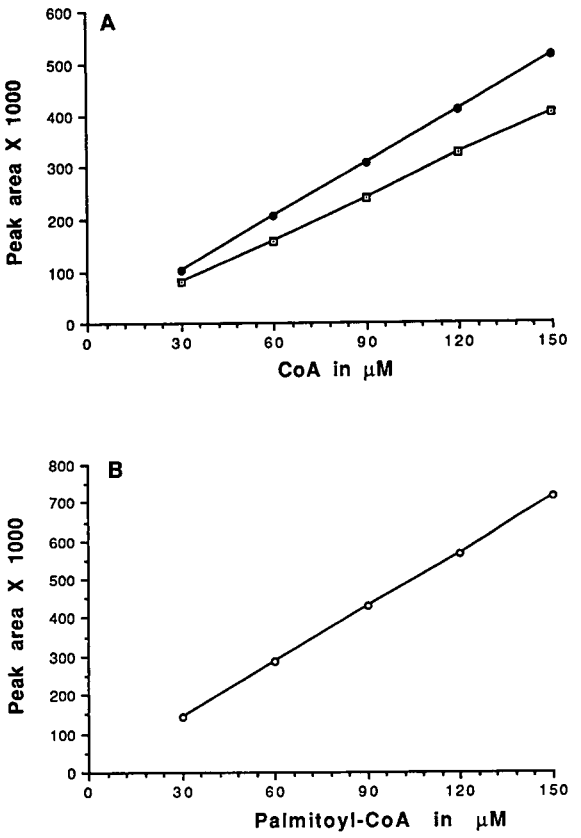

Fig. 2. Calibration graphs obtained from different concentrations of (A) free CoASH dissolved in 5% sulphosalicylic acid containing 50 μM DTE, (●) treated with $NaBH_4$ and (□) untreated, and (B) palmitoyl-CoA after incubation with 2.0 M $NaBH_4$ at 37°C for 30 min.

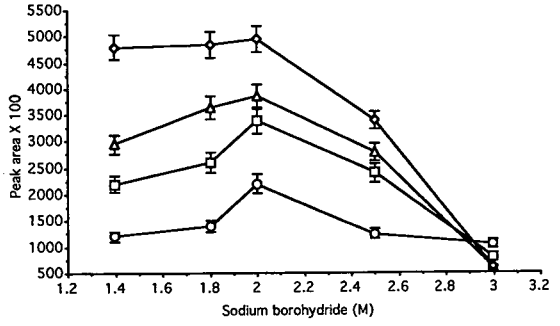

Fig. 3. Yield of CoA–bimane adduct from a solution of 150 μM palmitoyl-CoA incubated with 1.4, 1.8, 2.0, 2.5 and 3.0 M $NaBH_4$. Incubation time at 37°C: ○ = 5; □ = 10; △ = 20; ◇ = 30 min. The values represent means ± standard deviations for four rat livers.

The optimum concentration of $NaBH_4$ required to cleave completely the thio–ester bond between the CoA and acyl moiety was studied by determining the yield of the CoA–bimane adduct obtained after incubating palmitoyl-CoA in different concentrations of $NaBH_4$ for different times (Fig. 3). The results indicated that $NaBH_4$ at a concentration of 2.0 *M* and incubation for 30 min were the optimum assay conditions. At concentration below 2.0 *M* the recovery of the CoASH from the long-chain acyl-CoA was low, mainly owing to incomplete bond cleavage. Similarly, a low recovery was obtained at concentrations higher than 2.0 *M*, mainly owing to the interference of the $NaBH_4$ with either the formation or the stability of the CoA–bimane adduct.

As shown in Fig. 4, a parallel experiment in which palmitoyl-CoA was incubated with 2.0 *M* $NaBH_4$ at different temperatures for various times showed a maximum yield of the adducts at 37°C with incubation for 30 min. Higher temperatures increased the effervescence of $NaBH_4$ and were therefore impractical and the yield at lower temperatures was erratic and low. Table I shows the recoveries obtained for free CoASH and palmitoyl CoA after incubation with 1.4 or 2.0 *M* $NaBH_4$ at 37° for 30 min, confirming the above findings.

The determination of long-chain acyl-CoA in 10% liver homogenates prepared in 5% sulphosalicylic acid containing 50 μM DTE is shown in Table II. In agreement with the experiment mentioned above, higher yields were obtained with tissue incubated with 2.0 *M* than with 1.4 *M* $NaBH_4$. Furthermore, larger amounts of free CoASH and long-chain acyl-CoA were obtained from liver homogenates with the present method than with the older UV method.

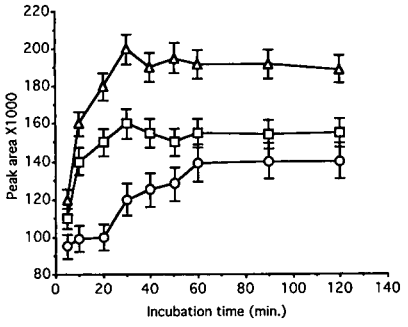

Fig. 4. Yield of CoA–bimane adducts from a 150 μM solution of palmitoyl-CoA in 5% sulphosalicylic acid containing 50 μM DTE at different incubation temperatures and times. ○ = 20°C; □ = 30°C; △ = 37°C.

TABLE I

RECOVERIES OF FREE CoASH AND PALMITOYL-CoA FOLLOWING TREATMENT WITH (A) 1.4 *M* OR (B) 2.0 *M* $NaBH_4$ AT 37°C FOR 30 min

Type of compound	Treatment	Calculated concentration (m*M*)	Recovery (%)[a]	
			25°C	37°C
Free CoASH	A	1.0	98	98
	B	1.0	98	98
Palmitoyl-CoA	A	1.0	68	85
	B	1.0	87	95

[a] Mean ($n = 6$).

TABLE II

LEVELS OF ACID-SOLUBLE CoASH AND ACID-INSOLUBLE LONG-CHAIN ACYL-CoA in LIVERS OBTAINED AFTER INCUBATION WITH (A) 1.4 *M* OR (B) 2.0 *M* $NaBH_4$ AT 37°C FOR 30 min, AND (C) LEVELS OBTAINED WITH THE PREVIOUS UV METHOD [13]

Type of compound	Concentration (nmol/g)[a]		
	A	B	C
Acid-soluble CoASH	156.7 ± 10.2	159.2 ± 14.2	107 ± 23
Long-chain acyl-CoA	81.7 ± 6.5	98.8 ± 9.0	88 ± 10.2

[a] Means ± standard deviations ($n = 4$).

To test the reproducibility of method, we prepared three aliquots of a liver tissue homogenate as described above and derivatized the samples on three different days. The variations in the levels of both acid-soluble CoASH and acid-insoluble CoA between the samples were found to be less than 10% (data not shown).

In conclusion, the present method is more sensitive and more specific than the previous UV method for the detection and determination of tissue levels of CoASH. In addition, it can be used to measure protein- and non-protein bound

thiols such as cysteine, cysteinylglycine and gluthatione in biological specimens simultaneously.

ACKNOWLEDGEMENTS

This work was supported by research grants from Norsk Hydro, Pronova and the Norwegian Council for Scientific and Industrial Research.

REFERENCES

1 B.E. Corkey and J.T. Deeney, in K. Tanaka and P.M. Coates (Editors), *Progress in Clinical and Biological Research, Fatty Acid Oxidation: Clinical, Biochemical, and Molecular Aspects*, Alan R. Liss, New York, 1990, pp. 217–232.
2 J.A. Ontko, *J. Biol. Chem*, 247 (1972) 1788.
3 J.F. Oram, S.L. Bennetch and J.R. Neely, *J. Biol. Chem.*, 248 (1973) 5299.
4 A Orellana, P.C. Hidalgo, M.N. Morales, D.Mezzana and M. Bronfman, *Eur. J. Biochem.*, 190 (1990) 57.
5 R.K. Berge, L.H. Hosøy, A. Aarsland, O.M. Bakke and M. Farstad, *Appl. Pharmacol.*, 73 (1984) 35.
6 M.R. Ball, K.A. Gumaa and P. McLean, *Biochem. Biophys. Res Commun.*, 87 (1979) 489.
7 J. Bhuiyan, K. Bartlett, H. Sherrat and L. Aguis, *Biochem. J.*, 253 (1988) 337.
8 J. Caldwell, *Biochem. Soc. Trans.*, 12 (1984) 9.
9 A Nilsson, M.S. Thomassen and E.N. Christiansen, *Lipids*, 19 (1984) 187.
10 A. Asiedu, A. Aarsland, J. Skorve, A. Svardal and R.K. Berge, *Biochim. Biophys. Acta*, 1004 (1990) 211.
11 P. Brecher, *Mol. Cell. Biochem.*, 57 (1983) 3.
12 O.C. Ingebretsen and M. Farstad, *J. Chromatogr.*, 202 (1980) 439.
13 R.K. Berge, A. Aarsland, O.M. Bakke and M. Farstad, *Int. J. Biochem.*, 15 (1983) 191.
14 R.K. Berge, H. Osmundsen, A. Aarsland and M. Farstad, *Int. J. Biochem.*, 15 (1983) 205.
15 R.C. Fahey, G.L. Newton, R. Dorian and E.N. Kosower, *Anal. Biochem.*, 111 (1981) 357.
16 P.M. Ueland and H. Refsum, *J. Lab. Clin. Med.*, 114 (1989) 473.

Journal of Chromatography, 635 (1993) 257–263
Elsevier Science Publishers B.V., Amsterdam

CHROM. 24 868

Separation of some metals as their anionic oxalate complexes by reversed-phase ion-interaction chromatography

Pavel Janoš

Research Institute of Inorganic Chemistry, Teplická 86, 400 60 Ústí nad Labem (Czech Republic)

(First received March 31st, 1992; revised manuscript received January 8th, 1993)

ABSTRACT

The separation of some metal cations in the form of their oxalate complexes was investigated in a reversed-phase system with tetrabutylammonium cation (TBA^+) as an ion-interaction agent. The analyte retention is governed by the ion-interaction mechanism and is predominantly affect by the oxalate concentration and by the other eluting anion (perchlorate) concentration and also by the TBA^+ concentration. Further, the analyte retention and separation can be influenced by the mobile phase pH and by the addition of an organic modifier to the mobile phase. The dependences of the analyte capacity factors on the above-mentioned mobile phase parameters have a similar character, which were observed in common anion separations by ion-interaction chromatography.

INTRODUCTION

At present, high-performance liquid chromatographic (HPLC) methods have a major role in metal determinations [1]. Metal cations are usually separated on special low-capacity cation exchangers by ion-exchange chromatography (IEC) [2–4]. The separation may also occur on non-polar stationary phases with the addition of the ionogenic, ion-interaction agents to the mobile phase [5] (reversed-phase ion-interaction chromatography, RP-IIC).

Some metals may be separated and determined in the form of anionic complexes by either IEC or RP-IIC. For example, platinum group metals and other noble metals have been determined in the form of the cyano or chloro complexes [6,7] and transition and heavy metals have been separated in the form of anionic complexes with ethylenediamintetraacetic acid (EDTA) and related complexometric agents [8–10]. Excellent separations were obtained recently by Jones *et al.* [11], who successfully separated all rare earth elements as oxalate complexes by RP-IIC. After a minor modification, this procedure was used to determine the light rare earth elements in ceria-based polishing powders [12].

The aim of this work was to verify the applicability method of Jones *et al.* [11] to the separation of other metal cations, especially divalent metal cations. Factors that influence the analyte retention (eluting ion concentration in the mobile phase, pH, addition of organic modifiers) were studied.

EXPERIMENTAL

Apparatus

The liquid chromatograph consisted of an HPP 5001 high-pressure pump, an LCI 30 injection valve with a 20-μl sampling loop, a TZ 4261 chart recorder (all from Laboratorní Přístroje, Prague, Czechoslovakia) and a Model 732 870 UV–Vis spectrophotometric detector (Knauer, Berlin, Germany) operating at 254 nm. In some instances postcolumn derivatization was used for

0021-9673/93/$06.00

detection, in which event the apparatus was supplement with another HPP 5001 pump and an RE-2M postcolumn reactor (Laboratorní Přístroje). Detection was carried out at 520 nm. A glass column (150 × 3 mm I.D.) packed with an octadecyl-bonded silica gel, Separon SGX RPS (5 μm), was used for the separation. A saturation column (30 × 3 mm I.D.) packed with silica gel Separon SGX (7 μm) (all columns from Tessek, Prague, Czechoslovakia) was connected between the pump and the injection valve to presaturate the mobile phase with dissolved silica and to prolong the lifetime of the analytical column. Before measurements the columns were washed with methanol and water and then with the mobile phase at a flow-rate of 0.1 ml min^{-1} overnight.

The mobile phase was deareated in an ultrasonic bath before measurement. Measurements were carried out at laboratory temperature (22 ± 2°C).

Chemicals

Stock solutions of 0.1 mol l^{-1} tetrabutylammonium hydroxide (TBA-OH) (Fluka, Buchs, Switzerland), oxalic acid and sodium perchlorate were prepared. Mobile phases were prepared by mixing these stock solutions in the required proportions, with additions of organic modifier (methanol, propanol, butanol) and with pH adjustment using dilute NaOH solution. In addition, stock solutions of 0.1 mol l^{-1} $MnCl_2$, $CuCl_2$, $NiCl_2$, $CoCl_2$ and $Ce(NO_3)_3$ were prepared; these solutions were subsequently diluted to concentrations of 1 mmol l^{-1} ($MnCl_2$, $NiCl_2$ and $CoCl_2$), 0.2 mmol l^{-1} [$Ce(NO_3)_3$] or 0.02 mmol l^{-1} ($CuCl_2$) before measurement. A solution of 0.2 mmol l^{-1} 4-(2-pyridylazo)resorcinol (PAR) in 1 mol l^{-1} acetic acid–3 mol l^{-1} ammonia solution was used as the postcolumn derivatization agent [5,13].

All chemicals were of analytical-reagent grade from Lachema (Brno, Czechoslovakia), except TBA-OH. The solutions were prepared in redistilled water.

RESULTS AND DISCUSSION

Metal cations are separated on a C_{18} column using a mobile phase containing the quaternary ammonium cation (Q^+), oxalate ions and, as the case may be, another eluting cation (perchlorate, E^-). It is assumed that metal ions are retained on the stationary phase surface by an ion-interaction mechanism in the form of anionic complexes. Such a system, however, is comparatively complex and, depending on the conditions of the respective measurement (concentration, pH, metal-to-ligand ratio), a number of side-reactions may take place:

dissociation of oxalic acid:

$$H_2L \rightleftharpoons H^+ + HL^- \quad (1)$$

$$HL^- \rightleftharpoons H^+ + L^{2-} \quad (2)$$

complex-forming equilibria of metal cations with oxalate anions (HL^- or L^{2-}, depending on the degree of dissociation):

$$M^{2+} + HL^- \overset{K_1}{\rightleftharpoons} MHL^+ \quad (3a)$$

$$MHL^+ + HL^- \overset{K_2}{\rightleftharpoons} M(HL)_2 \quad (3b)$$

$$M(HL)_2 + HL^- \overset{K_3}{\rightleftharpoons} M(HL)_3^- \quad (3c)$$

etc., or

$$M^{2+} + L^{2-} \overset{K_1'}{\rightleftharpoons} ML \quad (3a')$$

$$ML + L^{2-} \overset{K_2'}{\rightleftharpoons} ML_2^{2-} \quad (3b')$$

etc. For the total concentrations of the metal (c_M) and oxalate (c_L) in the mobile phase, we have

$$c_M = [M^{2+}] + [MHL^+] + [M(HL)_2] + \cdots + [M(HL)_n^{2-n}] + [ML] + [ML_2^{2-}] + \cdots + [ML_n^{2-2n}] \quad (4)$$

$$c_L = [L^{2-}] + [HL^-] + [H_2L] + [MHL^+] + 2[M(HL)_2] + \cdots + n[M(HL)_n^{2-n}] + [ML] + 2[ML_2^{2-}] + \cdots + n[ML_n^{2-2n}] \quad (5)$$

In the presence of the quaternary ammonium cation, negative charge-bearing complexes can be retained by the mechanism under consideration. A purely general solution of the retention model is difficult. For simplicity, we shall assume that, under certain conditions (at constant pH), only one type of ligand and of the anionic

complex prevail in the mobile phase. Let us assume first that in an acidic medium, where oxalic acid is not fully dissociated, HL^- is the prevailing oxalate anion, and the metal ions are retained in the form of an anionic complex $M(HL)_3^-$ (hereafter referred to as X^-). In the course of the retention of analytes by an ion-interaction mechanism, particularly two types of equilibria [14–16] are effective: sorption of the ion-interaction agent on the stationary phase surface and ion exchange among ions of the analyte and eluting ions. The processes that occur can be expressed by the following equations (the dynamic ion-exchange model):

$$A_s + Q_m^+ \overset{K_4}{\rightleftharpoons} (Q^+)_s \quad (6)$$

$$(Q^+)_s + E_m^- \overset{K_5}{\rightleftharpoons} (QE)_s \quad (7)$$

$$(Q^+)_s + HL_m^- \overset{K_6}{\rightleftharpoons} (QHL)_2 \quad (8)$$

$$(Q^+)_s - X_m^- \overset{K_7}{\rightleftharpoons} (QX)_s \quad (9)$$

where the subscripts m and s refer to the mobile and stationary phases, respectively, and A_s represents the free adsorption sites on the stationary phase.

The capacity K_0 of the column is given by the sum

$$K_0 = [A_s] + [(QE)_s] + [(QX)_s] \quad (10)$$

Further, it holds for the capacity factor that

$$k' = q \cdot \frac{[(QX)_s]}{c_M} \quad (11)$$

where q is the phase ratio.

After the above simplification and using eqn. 4 as a basis, the total concentration of a metal can be expressed by means of the respective stability constants:

$$c_M = [X^-]\left(\frac{1}{K_1K_2K_3[HL^-]^3} + \frac{1}{K_2K_3[HL^-]^2} + \frac{1}{K_3[HL^-]} + 1\right) \quad (12)$$

Combining eqns. 10–12 and rearranging, we obtain a relationship describing the dependence of the reciprocal of the capacity factor on the mobile phase composition:

$$\frac{1}{k'} = \frac{\frac{1}{K_1K_2K_3[HL^-]^3} + \frac{1}{K_2K_3[HL^-]^2} + \frac{1}{K_3[HL^-]} + 1}{qK_0} \times \left(\frac{1}{K_4K_7[Q^+]} + \frac{K_5[E^-]}{K_7} + \frac{K_6[HL^-]}{K_7} + [X^-]\right) \quad (13)$$

Eqn. 13 expresses a comparatively complex dependence of the capacity factor on the concentration of oxalate ion that acts simultaneously as both a complexing agent and eluting ion. Fortunately, under normal conditions where the oxalate concentration is markedly higher than that of the metal ions, lower complexes may be neglected and eqn. 13 acquires the following form:

$$\frac{1}{k'} = \frac{1}{qK_0}\left(\frac{1}{K_4K_7[Q^+]} + \frac{K_5[E^-]}{K_7} + \frac{K_6[HL^-]}{K_7} + [X^-]\right) \quad (14)$$

According to eqn. 14, the reciprocal of the capacity factor is directly proportional to the concentration of the eluting ions E^- and HL^- and to the reciprocal of the concentration of the quaternaly ammonium cation Q^+ in the mobile phase. Eqns. 13 and 14 express also the dependence of the capacity factor on the analyte concentration. This dependence applies, however, only in those cases when the analyte concentration is very high. This dependence may be neglected under the common conditions of HPLC analysis, which is obvious directly from eqn. 10 if the last term on the right-hand side is neglected. Eqn. 14 is analogous to a relationship derived by Xianren and Baeyens [16] for the separation of monovalent anions.

When the measurement is carried out at higher pH, it is necessary to assume that the oxalic acid is fully dissociated and the formation of complexes proceeds in accordance with eqns. (3a′), (3b′), etc. Now, let us assume that the prevailing anionic complex is ML_2^{2-} (henceforth denoted X^{2-}). Equations describing the processes taking

place on the column have to be modified as follows:

$$2(Q^+)_s + L_m^{2-} \overset{K'_6}{\rightleftharpoons} (Q_2L)_s \qquad (8')$$

$$2(Q^+)_s + X_m^{2-} \overset{K'_7}{\rightleftharpoons} (Q_2X)_2 \qquad (9')$$

In this case eqns. 6 and 7 also hold true. Solving the system of equations yields

$$k' = \frac{q}{4\left(\frac{1}{K'_1K'_2[L^{2-}]^2} + \frac{1}{K'_2[L^{2-}]} + 1\right)} \times \left\{\left[\frac{K'_7(1 + K_4K_5[Q^+][E^-])^2}{4K_4^2[Q^+]^2(K'_6[L^{2-}] + K'_7[X^{2-}])^2} + \frac{2K_0K'_7}{K'_6[L^{2-}] + K'_7[X^{2-}]}\right]^{0.5} - \frac{(K'_7)^{0.5}(1 + K_5K'_7[Q^+][E^-])}{2K_4[Q^+](K'_6[L^{2-}]P + K'_7[X^{2-}])}\right\}^2 \qquad (15)$$

indicating that if polyvalent ions participate in processes taking place on a column, the dependences of analyte retention on the composition of the mobile phase may be complicated.

The dependences of the capacity factor on mobile phase parameters were studied experimentally with the divalent cations Mn^{2+}, Co^{2+}, Ni^{2+} and Cu^{2+} and, for comparison, also with the Ce^{3+} cation.

In Fig. 1 are shown the dependences of $1/k'$ on the concentration of perchlorate in the mobile phase at constant concentrations of oxalate, TBA^+ and pH. The dependences are linear, consistent with observations acquired with analogicous systems when separating monovalent inorganic anions [16,17]. Fig. 2 illustrates the dependences of $1/k'$ on oxalate concentration at constant pH and TBA^+ concentration; perchlorate ions were not present. These dependences are also linear over a fairly wide range. Hence the dependences in Figs. 1 and 2 satisfy the eqn. 14 well in spite of the fact that the conditions on which the derivation of this equation was based (*e.g.*, degree of dissociation as given by the pH value) were not fully satisfied during the measurements. It is also worth noting that no significant difference was observed between the behaviour of di- and trivalent cations (see also ref. 12).

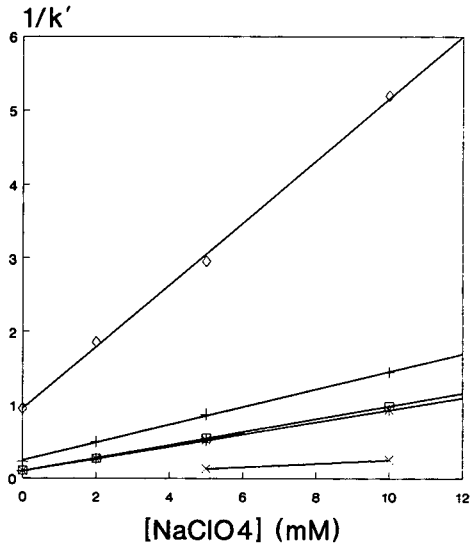

Fig. 1. Effect of perchlorate concentration on analyte retention. Mobile phase: 2 mmol l^{-1} TBA-OH–2 mmol l^{-1} oxalic acid–$NaClO_4$ (pH 4.5). ◇ = Mn^{2+}; + = Co^{2+}; ∗ = Ni^{2+}; × = Cu^{2+}; □ = Ce^{3+}.

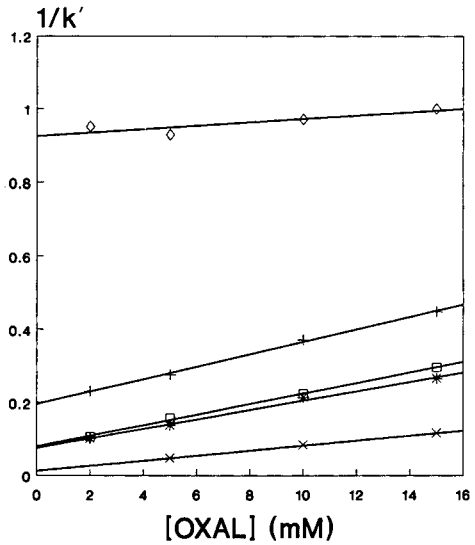

Fig. 2. Effect of oxalate concentration on analyte retention. Mobile phase: 2 mmol l^{-1} TBA-OH–oxalic acid (pH 4.5). Symbols as in Fig. 1.

The $1/k'$ *vs.* $1/[TBA^+]$ dependences at constant pH and eluting ion concentration are demonstrated in Fig. 3. It can be seen that the

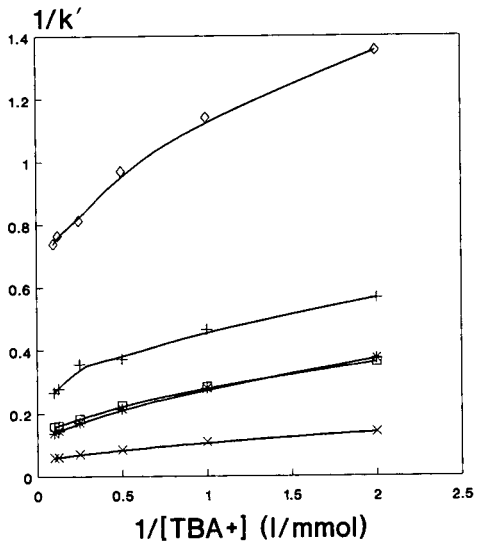

Fig. 3. Effect of ion-interaction agent (TBA^+) on analyte retention. Mobile phase: TBA-OH–2 mmol l^{-1} oxalic acid (pH 4.5). Symbols as in Fig. 1.

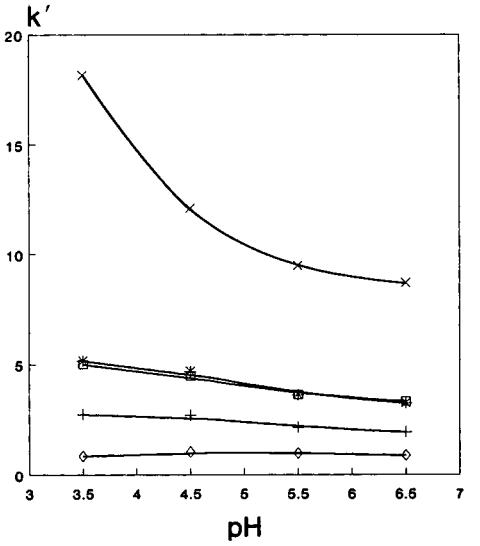

Fig. 4. Effect of mobile phase pH on analyte retention. Mobile phase: 2 mmol l^{-1} TBA-OH–10 mmol l^{-1} oxalic acid, pH adjusted with NaOH. Symbols as in Fig. 1.

experimental dependences deviate from the linearity predicted by eqn. 14 at higher concentrations of the ion-interaction agent. Similar deviations were observed in the separation of inorganic anions and are connected with the limited capacity of the stationary phase (for a more detailed discussion, see ref. 16).

The pH of the mobile phase significantly affects the retention of analytes in the systems examined. The effect of pH can manifest itself particularly in two ways: the degree of dissociation of the mobile phase (oxalic acid) and hence also its eluting capacity increase with increase in pH; and the pH influences the course of complex-forming reactions, the composition of complexes and thus also the capability of the complexes to be retained on the column.

The first of the above effects can be interpreted best with the aid of the dual species approach [18–20]. A mathematical description, however, is complicated in this instance. The experimental dependences shown in Fig. 4 are at least in qualitative agreement with this model.

Analyte retention in the RP-IIC may be affected by the addition of an organic modifier to the mobile phase. Organic modifiers influence especially the sorption of the ion-interaction agent on the non-polar stationary phase. Jandera *et al.* [21] expressed the relationship between the capacity factor and the organic modifier concentration c as

$$\log k' = A - Bc \qquad (16)$$

Both the constants A and B were discussed by Zou *et al.* [22] and the equation was verified for separations of various phenylamine- and naphthylaminesulphonic acids on a C_{18} column in the presence of the TBA^+ cation.

It can be seen from Fig. 5 that the dependences of the capacity factor on methanol concentration satisfy eqn. 16 comparatively well. An addition of higher alcohols affects the retention of analytes more strongly than the addition of methanol. Whereas adding 10% of methanol permits a very good separation within a reasonable time, addition of 5% of propanol or butanol renders the separation almost impossible. An example of separation is shown in Fig. 6; negative peaks belong to anions injected with the sample and separated by the conventional IIC mechanism.

Direct spectrophotometric detection as adopted in the present study is hardly universal. It can be used advantageously for the detection

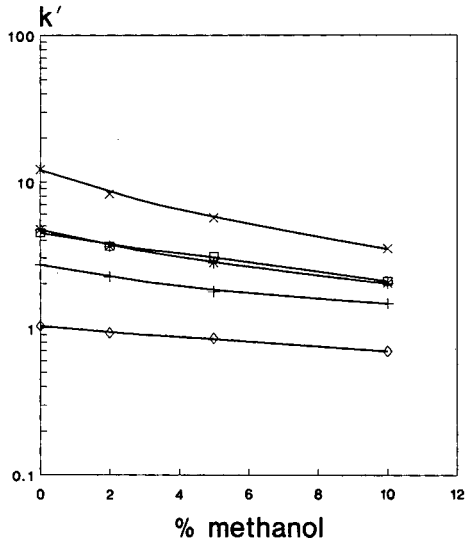

Fig. 5. Effect of methanol concentration on analyte retention. Mobile phase: 2 mmol l^{-1} TBA-OH–10 mmol l^{-1} oxalic acid–methanol (pH 4.5). Symbols as in Fig. 1.

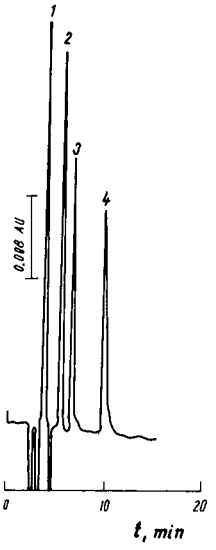

Fig. 6. Separation of the ions (1) Mn^{2+}, (2) Co^{2+}, (3) Ni^{2+} and (4) Cu^{2+}. Mobile phase: 2 mmol l^{-1} TBA-OH–2 mmol l^{-1} oxalic acid–10% (v/v) methanol (pH 4.5). Detection at 254 nm.

of Mn^{2+}, Co^{2+}, Ni^{2+}, and particularly for Cu^{2+} (the detection limits are 3–5 ng for the former three ions and about 0.1 ng for Cu^{2+}). When a more universal method of detection, postcolumn derivatization with PAR, is used, other metal cations can also be determined in the given system. In this instance the sensitivity of detection (slope of the calibration line) is higher, but at the same time the noise of the baseline becomes greater, so that the detection limits are at the ng level. The retention characteristics of some cations are presented in Table I. Of the elements detectable with PAR, Fe^{2+}, Fe^{3+}, Hg^{2+} and Bi^{3+} ions do not form any peaks within a reasonable time. The alkaline earth elements and some other cations (Al^{3+}, Cr^{3+}) cannot be detected using PAR [23], so they do not interfere with the determination. An example of the separation is given in Fig. 7.

TABLE I

CAPACITY FACTORS (k') OF SOME METAL CATIONS WITH MOBILE PHASE CONTAINING 2 mmol l^{-1} TBA-OH, 2 mmol l^{-1} OXALIC ACID AND 5% (v/v) METHANOL (pH 4.5)

Cation	k'	Cation	k'
Mn^{2+}	0.86	Cd^{2+}	0.87
Co^{2+}	3.14	Pb^{2+}	2.00
Ni^{2+}	6.57	Zn^{2+}	4.86
Cu^{2+}	28.00		

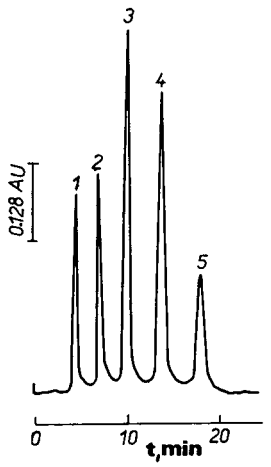

Fig. 7. Separation of the ions (1) Cd^{2+}, (2) Pb^{2+}, (3) Co^{2+}, (4) Zn^{2+} and (5) Ni^{2+}. Mobile phase: 2 mmol l^{-1} TBA-OH–2 mmol l^{-1} oxalic acid–5% (v/v) methanol (pH 4.5). Detection at 520 nm following postcolumn derivatization with PAR.

REFERENCES

1 K. Robards, P. Starr and E. Patsalides, *Analyst*, 116 (1991) 1247.
2 F.C. Smith and R.C. Chang, *The Practice of Ion Chromatography*, Wiley, New York, 1983.
3 D.T. Gjerde, *J. Chromatogr.*, 439 (1988) 49.
4 D. Yan and G. Schwedt, *Fresenius' J. Anal. Chem.*, 338 (1990) 149.
5 R.M. Cassidy and S. Elchuk, *Anal. Chem.*, 54 (1982) 1558.
6 D.F. Hilton and P.R. Haddad, *J. Chromatogr.*, 361 (1986) 141.
7 P. Jones and G. Schwedt, *Anal. Chim. Acta*, 220 (1989) 195.
8 O.N. Obrezkov, V.I. Slyamin and O.A. Shpigun, *Anal. Sci.*, 6 (1990) 617.
9 D. Yan and G. Schwedt, *J. Chromatogr.*, 516 (1990) 383.
10 A. Nitsch, K. Kalcher and U. Posch, *Fresenius' J. Anal. Chem.*, 338 (1990) 618.
11 E.A. Jones, H.S. Bezuidenhout and J.F. van Staden, *J. Chromatogr.*, 537 (1991) 277.
12 P. Janoš and M. Broul, *Chem. Listy*, 86 (1992) 139.
13 *Dionex Application Update, AU 101*, Dionex, Sunnyvale, CA, 1987.
14 R.L. Smith, Z. Iskandarani and D.J. Pietrzyk, *J. Liq. Chromatogr.*, 7 (1984) 1935.
15 R.L. Smith and D.J. Pietrzyk, *Anal. Chem.*, 56 (1984) 1572.
16 Q. Xianren and W. Baeyens, *J. Chromatogr.*, 456 (1988) 267.
17 P. Janoš, I. Vošická and J. Jandlová, *Chem. Listy*, 85 (1991) 752.
18 D.R. Jenke and G.K. Pagenkopf, *Anal. Chem.*, 56 (1984) 85.
19 D.R. Jenke and G.K. Pagenkopf, *Anal. Chem.*, 56 (1984) 88.
20 P.R. Haddad and P.E. Jackson, *Ion Chromatography. Principles and Applications*, Elsevier, Amsterdam, 1990, pp. 142–149.
21 P. Jandera, J. Churáček and B. Taraba, *J. Chromatogr.*, 262 (1983) 121.
22 H. Zou, Y. Zhang and P. Lu, *J. Chromatogr.*, 545 (1991) 59.
23 J. Vialle, M.C. Bertrand, M. Kolosky, O. Paisse and G. Raffin, *Analusis*, 17 (1988) 376.

Journal of Chromatography, 635 (1993) 265–270
Elsevier Science Publishers B.V., Amsterdam

CHROM. 24 865

Simultaneous analysis of carbon oxides and hydrocarbons by gas chromatography–mass spectrometry

R.T. Talasek* and K.E. Daugherty

Department of Chemistry, University of North Texas, Denton, TX (USA)

(First received June 26th, 1992; revised manuscript received December 29, 1992)

ABSTRACT

The simultaneous determination of carbon monoxide, carbon oxide, and C_1–C_4 hydrocarbons is demonstrated by gas chromatography–mass spectrometry. The analysis utilizes room temperature trapping of carbon monoxide on a Molesieve PLOT column, while determination of other species is performed on a PoraPLOT Q column. Carbon monoxide is then eluted at an elevated temperature. Detection limits in the low $\mu g\ m^{-3}$ regime are reported with a linear dynamic range that permits analysis in the mg m^{-3} range. No interferences between analytes or with air components are reported.

INTRODUCTION

Concern over a variety of airborne pollutants has increased from the standpoint of social awareness as well as government regulations. Among the concerns are those pollutants that contain carbon, including the oxides of carbon and light hydrocarbons. To understand the total contribution of these impurities to the environment, it is important to be capable of determining the high (mg m^{-3}) concentration associated with combustion emissions as well as the lower ($\mu g\ m^{-3}$) concentration associated with ambient or indoor measurements. Often it is necessary to determine instantaneous pollutant concentration to correlate with specific events, as well as measurements that represent some time span.

Air sampling using traps for hydrocarbons such as Tenax, porous polymers, or other trapping material [1–5] is very common. However, the trapping efficiency for these materials is poor for hydrocarbons that are gases at room temperature, necessitating cryogenic cooling for this type of sampling [6]. Methane is not trapped at all, even at liquid oxygen temperature. These materials are also ineffective for sampling carbon monoxide and dioxide. Direct analysis of air using bombs or bags is therefore necessary. Gas chromatography has been used in many instances to determine individual components of interest [7–10], but the most universal stationary phase for this type of application is porous polymer material such as the Porapak series (Waters) and the Chromosorb "Century Series" (Johns-Manville) [11]. However, even this separation has severe drawbacks. First, at ambient temperature, carbon monoxide co-elutes with air, making quantitation with a universal detector extremely difficult even at subambient GC temperatures. While carbon monoxide and light hydrocarbons can be separated from air on molecular sieves, carbon dioxide is strongly adsorbed on this stationary phase, making it impractical for use in this determination. Furthermore, the most common universal detector, the thermal conductivity

* Corresponding author. Present address: Texas Instruments, Inc., P.O. Box 655012, M/S 301, Dallas, TX 75265, USA.

0021-9673/93/$06.00

detector, lacks sufficient sensitivity to perform ambient air analysis where some components of interest may be present below 1 mg m^{-3} levels. A flame ionization detector in conjunction with a methanizer is capable of detecting hydrocarbons and carbon oxides at low levels. Unfortunately, the metal catalysts used in methanizers are poisoned by exposure to large quantities of oxygen, making them impractical for repeated air analysis. Also, percent level quantities of oxygen have been shown to produce positive responses with an FID [12], making quantitation of a co-eluting carbon monoxide impossible. Dynamic range may also be a problem, since carbon dioxide is usually present at considerably higher levels than the other components in most air samples.

Detection by mass spectrometry offers a possible solution to co-elution problems mentioned above. Operation of a mass spectrometer in the selective ion monitoring (SIM) mode may offer sufficient sensitivity for ambient air analysis. However, most gas analysis applications require relatively high carrier flow-rates necessary for packed columns and gas sampling valves. Typically, the pressure reduction required for the high vacuum of the mass spectrometer source is achieved by one of several interface types [13–27]. Unfortunately, none of these interfaces provide the desired sensitivity with low-molecular-mass compounds ($m/z < 50$), either due to poor discrimination or dilution in the interface. Direct interfacing of capillary columns to the ion source [28,29] was one of the first methods developed for sample introduction into the mass spectrometer, however smaller diameter columns are incompatible with typical sample volumes (> 0.1 ml) and flow-rates (*ca.* 10–30 ml min^{-1}) associated with the use of gas sampling valves, requiring sample splitting [30] and severely limiting sensitivity. Also the loss of column efficiency due to the so-called vacuum effect is well documented [31,32].

The advent of fused-silica porous layer open tubular (PLOT) columns [33] with the porous polymer and molecular sieve stationary phases typically used in the analysis of low-molecular-mass gases (including hydrocarbons) [34–37] offers a possible compromise to a number of these problems. Wide-bore (0.53-mm) PLOT columns operate well at carrier flows compatible with gas sampling valves. By using a deactivated fused-silica interface of sufficiently small internal diameter (0.2 mm) and sufficient length, the analytical column can be maintained at near atmospheric pressure, thereby preventing the loss of column efficiency mentioned above. This approach requires a differentially pumped mass spectrometer with sufficient pumping capacity to prevent high-pressure ionization effects such as chemical ionization. Two approaches that provide an appropriate combination of chromatography with mass selective detection to achieve this determination are described here.

EXPERIMENTAL

A Hewlett-Packard (Avondale, CA, USA) 5988A quadrupole mass spectrometer equipped with a 5890A gas chromatograph was used for this study. This mass spectrometer is differentially pumped with an electron impact (EI) ion source. While pumping capacity in this configuration is more than adequate for typical narrow-bore capillary carrier flows, it is marginal for a minimum carrier flow of *ca.* 10 ml min^{-1} necessary for flushing a sample loop of sufficient volume in a short enough time to prevent severe band broadening. By separating the forelines of the two diffusion pumps, and using a separate 400 l min^{-1} foreline pump (Fisher Scientific, Pittsburgh, PA, USA) for the source diffusion pump, pumping capacity was increased significantly. This modified vacuum system is capable of maintaining a nominal source vacuum pressure of $2 \cdot 10^{-5}$ Torr (1 Torr = 133.322 Pa) at carrier flows of 10–15 ml min^{-1}. Carrier flows were calculated from averaged linear velocity measurements and column volume, since actual flow-rates are expected to be significantly different with the column end at atmospheric pressure and high vacuum. Average linear velocity was determined from the retention time of neon, which is virtually unretained on these column materials.

Both PoraPLOT Q and Molesieve PLOT 5A (Chrompack, Raritan, NJ, USA) columns 25 m × 0.53 mm I.D. were utilized for this applica-

tion. Timing of valve switching was controlled by a digital valve sequence programmer combined with digital valve interfaces for each valve (Valco, Houston, TX, USA). The programmer also controlled the start of the mass spectrometer and chromatograph programs. A 5 m × 0.2 mm I.D. deactivated fused-silica capillary was used to directly interface the PLOT column to the mass spectrometer source and maintain the PLOT column at atmospheric pressure or above throughout the column, thereby avoiding loss of column efficiency. The direct connection was achieved with a zero dead volume union using special fused-silica adapter fittings (Valco). This configuration allows the use of up to a 0.2-ml sample loop. Sample loops with larger volumes were not used because of the resulting peak broadening, probably due to the limited capacity of the fused-silica restrictor or the sample loop not being flushed in a sufficiently short period of time. For the application using parallel columns, a 1:1 splitter (SGE, Austin, TX, USA) was used to divide the sample injections between the two columns. Carrier gas purified with a rare earth metal getter (SAES Getters, Colorado Springs, CO, USA) was used to lower the $m/z = 28$ background to improve detection limits for the molecular carbon monoxide ion.

Detection limit and linearity evaluations were conducted using a single-stage dynamic blender using mass flow controllers to dilute NIST (National Institute of Standards and Technology) traceable standards [15 ppm (v/v) methane, ethane, ethene, ethyne, propane, propene, propyne, and butane in nitrogen, 10 ppm carbon monoxide in nitrogen and 10 ppm carbon dioxide in nitrogen] (Scott Specialty Gas, Houston, TX, USA). The dilution gas was also nitrogen. Standards were also diluted in air without the carbon dioxide to compare response factors for the two balance gases, as well as identify any interferences or problems with dynamic range in the simultaneous determination of carbon dioxide and other components.

Mass tuning and signal optimization for the most common GC–EI-MS applications (organic mixture analysis) are typically performed with a compound such as perfluorotri-*n*-butylamine (PFTBA) [38], often utilizing a computerized optimization routine. These routines are typically designed to optimize performance at m/z values significantly larger than those of interest for this application. While mass calibration is usually still adequate, a significant gain in sensitivity was obtained by manually optimizing lens voltages using air components (m/z 18, 28, 32) to provide tuning masses. This is only possible with a system in which extreme care has been taken to maintain the air background at a sufficiently low level by minimizing leaks and maintaining sufficient carrier purity. A decrease in electron energy from 70 to 60 eV served to increase the molecular ion with respect to other fragments in all cases. Filament current was also increased from 300 to 400 μA to produce the maximum number of ions. Lens voltages were adjusted to attain maximum responses at these masses.

RESULTS AND DISCUSSION

The properties of molecular sieves when used as chromatographic stationary phases can be modified significantly by varying the water content of the media [39,40]. By modifying the conditioning temperature, carrier gas, and moisture content of the carrier gas, retention properties of the media can be drastically modified. It was determined empirically that 24 hours of conditioning at 200°C utilizing helium carrier gas with less than 1 ppb (v/v) moisture would result in a column that was capable of reversibly trapping carbon monoxide at room temperature. The carbon monoxide can then be eluted by raising the column temperature above 100°C.

Fig. 1 illustrates the first chromatographic approach utilizing the trapping of carbon monoxide on Molesieve PLOT. This configuration allows the Molesieve PLOT column to be removed from the flow path leading to the mass spectrometer. Fig. 2 illustrates SIM chromatograms for m/z 15, 26, 27, 28, and 44 representing carbon monoxide and carbon dioxide molecular ions and prominent ions for C_1–C_2 hydrocarbons using this approach. The $m/z = 27$ ion chromatogram is used to determine ethane and ethene to remove interference from the large nitrogen peak at $m/z = 28$. This chromatogram was gen-

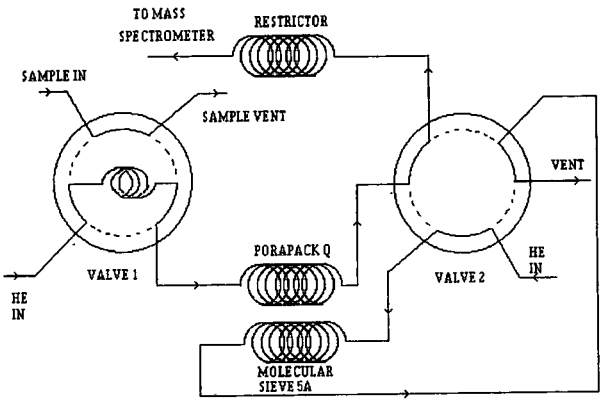

Fig. 1. Plumbing configuration allowing molecular sieve column to be inserted and removed from main chromatographic path. Path represented by solid line for each valve corresponds with position described as Inj in Table I. Dotted line represents Load position.

erated by the valve timing and GC oven temperature scheme shown in Table I. The analysis is begun with both the PoraPLOT and Molesieve PLOT columns in line with the mass spectrometer. After initial injection (valve 1 at $t = 0$) nitrogen, oxygen, carbon monoxide, and methane are allowed to pass through the PoraPLOT to the Molesieve PLOT column. At this low operating temperature, carbon monoxide is virtually immobilized and methane moves very slowly on the conditioned Molesieve PLOT column. Valve 2 is then switched and hydrocarbons and carbon dioxide are eluted to the mass spectrometer. The Molesieve PLOT

TABLE I

VALVE AND TEMPERATURE SEQUENCING

Time (min)	Valve 1	Valve 2	Temperature (°C)	Rate (°C/min)
Initial	Load	Load	30	0
0	Inj	Load	30	0
1.8	Inj	Inj	30	0
6.0	Inj	Load	30	25
10	Inj	Load	130	0
20			End run	

column is placed back in series with the mass spectrometer, the GC oven temperature elevated, and carbon monoxide is eluted. Using this scheme, all components can be separated by a combination of chromatography and mass selection. Nitrogen and carbon monoxide cannot be determined by molecular ions on the PoraPLOT alone because of inadequate mass or chromatographic resolution. Carbon monoxide could be determined at significantly higher (mg m^{-3}) concentrations using m/z 12, which may be of some benefit in evaluation of emission sources, but is inadequate for ambient samples. By separating carbon monoxide from nitrogen, the higher abundance molecular ion can be used, providing much greater sensitivity for carbon monoxide. This configuration prevents high levels of carbon dioxide and water from entering the Molesieve PLOT column, minimizing the

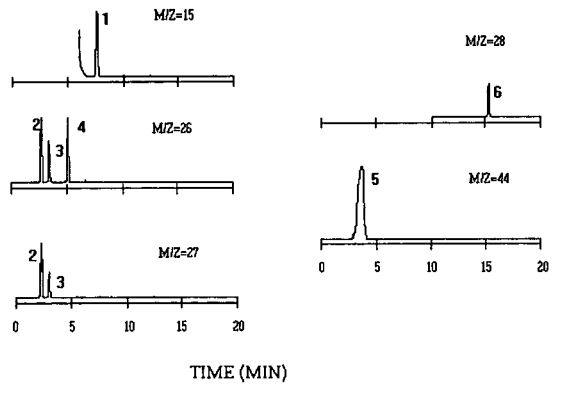

Fig. 2. Selected ion chromatograms of 0.2-ml injection for configuration in Fig. 1 for masses indicated. Components: 1 = methane, 2 = ethene, 3 = ethane, 4 = ethyne, 5 = carbon dioxide, 6 = carbon monoxide at approximately 1 mg ml^{-1}.

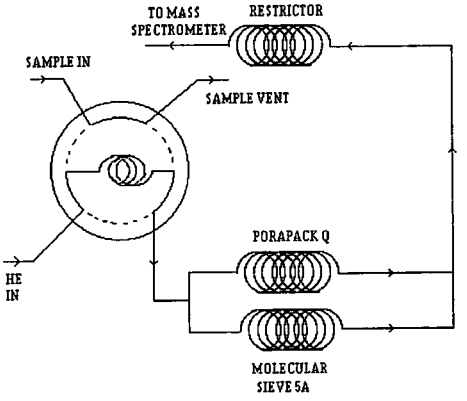

Fig. 3. Plumbing configuration with sample splitting between PoraPlot and molecular sieve columns. Path represented by solid line in injection valve represents sample injection position. Dashed line represents sample load position.

need for thermal reconditioning. However, hydrocarbons with more than two hydrocarbons require temperatures higher than ambient to elute them from the porous polymer column, preventing their determination with this configuration, if carbon monoxide is also to be determined. The possibility of extraneous peaks in future chromatograms also exists, as these hydrocarbons are eventually eluted from the Molesieve PLOT.

Fig. 3 illustrates the second chromatographic approach. This configuration allows samples to be split between the Molesieve PLOT column and the PoraPLOT column. Fig. 4 illustrates SIM chromatograms for m/z 15, 26, 27, 28, 29, 40, 41, and 44 representing carbon monoxide and carbon dioxide molecular ions and prominent ions for a number of C_1–C_4 hydrocarbons. This chromatogram was generated by a single valve event (injection) and GC oven temperature scheme similar to the one used in the two valve configuration used above. The analysis is begun with the sample being split between the PoraPLOT and Molesieve PLOT columns from the initial injection. Once again, carbon monoxide is virtually immobilized on the Molesieve PLOT column while hydrocarbons and carbon dioxide are detected by the mass spectrometer.

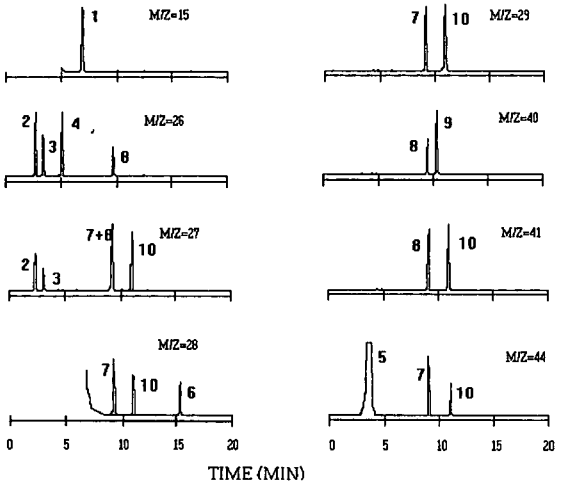

Fig. 4. Selected ion chromatograms of 0.2-ml injection for configuration in Fig. 3 for masses indicated. Components: 1 = methane, 2 = ethene, 3 = ethane, 4 = ethyne, 5 = carbon dioxide, 6 = carbon monoxide, 7 = propene, 8 = propane, 9 = propyne, 10 = butane at approximately 1 mg ml^{-1}.

The temperature is then elevated, and carbon monoxide is eluted to the mass spectrometer. While this configuration suffers from slightly poorer detection limits because of sample splitting, it is much simpler to operate. Unfortunately, it also requires the Molesieve PLOT column to be reconditioned after only a few injections of air. It does allow the direct determination of hydrocarbons with as many as four carbons as well as the carbon oxides in a single run.

Because of the trapping mechanism used in the determination of carbon monoxide, there was some concern about quantitation, especially at lower levels. A calibration curve generated over four orders of magnitude of concentration using the first configuration demonstrated linear response, indicating the trapping process is quantitative under these conditions. Similar results were obtained for carbon dioxide and the hydrocarbons considered here. From the calibration curves, it was possible to determine approximate detection limits for these analytes for this configuration using a response factor that would result in a signal-to-noise level of three to one. These approximate detection limits are listed in Table II. While frequent calibration is always a good practice, low variability in response factors is desirable as a confirmation of proper instrument operation. To evaluate the day-to-day

TABLE II

ANALYTE DETECTION LIMITS AND REPRODUCIBILITY

Analyte	m/z	Lower detection limit ($\mu g\ m^{-3}$)	R.S.D. (at 1 mg m^{-3}) (%) ($n = 5$)
Methane	15	33	4.1
Ethane	27	31	3.9
Ethene	27	28	3.6
Ethyne	26	16	2.7
Propane	29	43	4.0
Propene	41	26	3.1
Propyne	40	24	2.9
Butane	29	59	4.5
Carbon monoxide	28	23	5.6
Carbon dioxide	44	1.8	2.0

variability of this method, response factors were measured daily for blends of all the components mentioned above at approximately 1 mg m^{-3} for seven days. The relative change of response factors as a percentage of the initial measurement demonstrated similar performance to those reported previously for nitrogen and sulfur oxides as determined by GC–MS [41], with relative variation over this period less than 10% for each component.

CONCLUSIONS

The results summarized here demonstrate that GC–MS offers a viable alternative technique to those presently used to determine carbon oxides and low-molecular-mass hydrocarbons. GC–MS offers the possibility of determining species simultaneously from a single whole air sample, often at sensitivities not available with other techniques. While cost and size may prevent replacing many analyzers presently used with this technique, GC–MS offers a new alternative where the characteristics mentioned above are important.

REFERENCES

1 R. Sydor and D.J. Pietrzk, *Anal. Chem.*, 50 (1978) 1842.
2 J.S. Parsons and S. Mitzner, *Environ. Sci. Technol.*, 9 (1975) 1053.
3 J.W. Russel, *Environ. Sci. Technol.*, 9 (1975) 1175.
4 E.D. Pellizzari, J.E. Carpenter, J.E. Bunch and E. Sawicki, *Environ. Sci. Technol.*, 9 (1975) 556.
5 E.D. Pellizzari, J.E. Bunch, J.E. Carpenter and E. Sawicki, *Environ. Sci. Technol.*, 9 (1975) 552.
6 R.D. Cox, M.A. McDevitt, K.W. Lee and G.K. Tannahill, *Environ. Sci. Technol.*, 16 (1982) 57–61.
7 R.N. Dietz, *Anal. Chem.*, 40 (1968) 1576–1578.
8 A. Fish, N.H. Franklin and R.T. Pollard, *J. Appl. Chem.*, 13 (1963) 506–508.
9 A. Lawson and H.G. McAdie, *J. Chromatogr. Sci.*, 8 (1970) 731–734.
10 W.L. Thornsbury, *Anal. Chem.*, 43 (1971) 452–453
11 O.L. Hollis, *Anal. Chem.*, 38 (1966) 309–316.
12 R.T. Talasek, unpublished results.
13 E.J. Bonelli, M.S. Story and J.B. Knight, *Dyn. Mass Spectrom.*, 2 (1971) 177–180.
14 R. Rhyage, *Anal. Chem.*, 36 (1964) 759–764.
15 M. Blumer, *Anal. Chem.*, 40 (1968) 1590–1592.
16 C. Brunee, H.J. Bultemann and G. Kappus, presented at the *17th Ann. Conference on Mass Spectrometry and Allied Topics*, Dallas, TX, 1969, paper No. 46.
17 J. Copet and J. Evans, *Org. Mass. Spectr.*, 3 (1970) 1457–1461.
18 M.A. Grayson and R.L. Levey, *J. Chromatogr. Sci.*, 9 (1971) 687–689.
19 M.A. Grayson and J.J. Bellina, *Anal. Chem.*, 45 (1973) 487–491.
20 P.M. Krueger and J.A. McCloskey, *Anal. Chem.*, 41 (1969) 1930–1935.
21 J.T. Watson and K. Biemann, *Anal. Chem.*, 36 (1964) 1135–1137.
22 M.A. Grayson and C.J. Wolf, *Anal. Chem.*, 42 (1970) 426–430.
23 P.M. Llewellyn and D.P. Littlejohn, presented at the *Pittsburgh Conference on Analytical Chemistry and Spectroscopy, Pittsburgh, PA, 1966.*
24 W.H. McFadden, *J. Chromatogr. Sci.*, 17 (1979) 2–16.
25 R.F. Arrendale, R.F. Severson and D.T. Chortyk, *Anal. Chem.*, 56 (1984) 1533–1537.
26 D. Henneberg, U. Henrichs, H. Husmann and G. Schomburg, *J. Chromatogr.*, 167 (1978) 139–147.
27 J.J. Stern and B. Abraham, *Anal. Chem.*, 50 (1978) 2161–2164.
28 J.C. Holmes and F.A. Morrell, *Appl. Spectr.*, 11 (1957) 86–88.
29 R.S. Golke, *Anal. Chem.*, 31 (1959) 535–541.
30 S. Jacobsson and O. Falk, *J. Chromatogr.*, 497 (1989) 194–199.
31 P.A. Leclercq, G.J. Scherpenzeel, E.A.A. Vermeer and C.A. Cramers, *J. Chromatogr.*, 241 (1982) 61–63.
32 F.W. Hatch and M.E. Parrish, *Anal. Chem.*, 50 (1978) 1164–1168.
33 J. de Zeeuw, R.C.M. de Nijs and L.T. Henrich, *J. Chromatogr. Sci.*, 25 (1987) 71.
34 K. Bachmann and F.J. Reineke, *J. Chromatogr.*, 323 (1985) 323–329.
35 N. Pelz, N.M. Dempster and P.R. Shore, *J. Chromatogr. Sci.*, 28 (1990) 230–235.
36 L.H. Henrich, *J. Chromatogr. Sci.*, 481 (1989) 45–54.
37 L. Do and F. Raulin, *J. Chromatogr.*, 19 (1965) 249–262.
38 L.A. Shadoff and L.B. Westover, *Anal. Chem.*, 39 (1967) 1048–1050.
39 R. Aubeau, J. LeRoy and L. Champeix, *J. Chromatogr.*, 19 (1965) 249–262.
40 B.M. Karlsson, *Anal. Chem.*, 38 (1966) 668–669.
41 R.T. Talasek and K.E. Daugherty, *J. Chromatogr. Sci.*, 30 (1992) 131–135.

Journal of Chromatography, 635 (1993) 271–281
Elsevier Science Publishers B.V., Amsterdam

CHROM. 24 880

Characterization of N-ethoxycarbonyl ethyl esters of amino acids by mass spectrometry

Zhi-Heng Huang, Jian Wang, Douglas A. Gage*, J. Throck Watson and Charles C. Sweeley

Department of Biochemistry, MSU–NIH Mass Spectrometry Facility, Michigan State University, East Lansing, MI 48824-1319 (USA)

Petr Hušek

Institute of Endocrinology, 11694 Prague 1 (Czech Republic)

(First received October 20th, 1992; revised manuscript received January 12th, 1993)

ABSTRACT

Derivatization of amino acids by using ethyl chloroformate–ethanol–pyridine provides volatile products, N-ethoxycarbonyl amino acid ethyl esters (ECEEs), which are easily amenable to GC or GC–MS analysis. MS behavior of these compounds under electron-impact has been studied. The fragments observed in the spectra facilitate recognition of commonly occurring protein amino acids and characterization of unknown analogues.

INTRODUCTION

Analysis of protein hydrolysates for the usual amino acids by GC is now routine (for review articles, see refs. 1–3). The foundation for the most commonly used method was laid by Gehrke *et al.* [4], who developed the procedure for quantitative derivatization to provide N(O,S)-trifluoroacetyl (TFA) amino acid *n*-butyl esters (TAB amino acids). Other variants include some closely related derivatives of analogous perfluoroacyl alkyl esters [1,2].

Procedures for preparation of TAB and related derivatives require two reactions. Although much progress has been made in this respect, a procedure suitable for the quantitative and reproducible derivatization of all protein amino acids in a single reaction remains to be developed. A modified procedure using a mixture of pentafluoropropionic anhydride (PFPA) and hexafluoroisopropanol (HFIP) was introduced to provide N-PFPA amino acid HFIP esters in one step [5,6]. Because these derivatives, contrary to what may be expected, do not form stable anions for all amino acids, their application was mainly restricted to the analysis of certain aromatic amino acids in body fluids. A number of new derivatization methods have been reported in the past decade. These methods include silylation, especially *tert.*-butyldimethylsilylation (TBDMS) [7], an improved procedure superseding the previously employed trimethylsilylation, and the formation of cyclic oxazolidinone derivatives by condensation with 1,3-dichlorotetrafluoroacetone followed by treatment with pentafluoropropionic anhydride [8]. The TBDMS method shows promise in the analysis of protein amino acids, including asparagine, glutamine, and arginine; however, the interpretation of the mass spectra

* Corresponding author.

0021-9673/93/$06.00

of TBDMS derivatives is somewhat more ambiguous than is the interpretation of the mass spectra of N-TFA amino acid alkyl esters. Relatively few non-protein amino acids have been analyzed this way. The oxazolidinone procedure [8], though simple in operation, requires two chromatographic columns for the resolution of all proteic amino acids.

A completely new approach has been reported recently by Hušek and Sweeley [9–11] involving simultaneous N(O,S)-derivatization with ethyl chloroformate (ECF) in water–ethanol–pyridine (Py) (reaction 1). As depicted in Fig. 1, the derivatives, N-ethoxycarbonyl amino acid ethyl esters (ECEE), show excellent resolution on a capillary column and the analysis, including the derivatization is completed within 10 min.

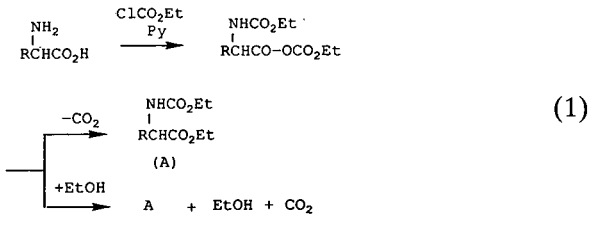

(1)

This paper reports a comprehensive study on the mass spectrometric fragmentation of this interesting family of new derivatives. Interpretation of these spectra may facilitate recognition of individual amino acids and pave the way for the structure elucidation of modified amino acids.

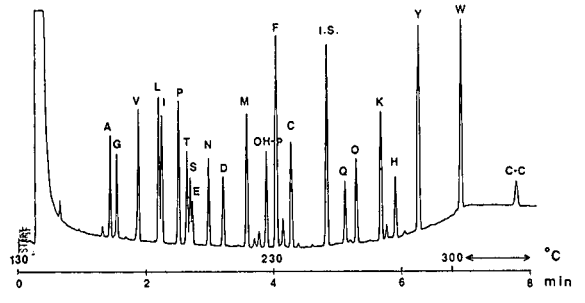

Fig. 1. Gas chromatogram of 22 ECEE amino acids. GC conditions: DB-1701 column, 1 μm, 30 m × 0.53 mm I.D., programmed at 25°C/min between 130 and 300°C, 70 kPa hydrogen. Internal standard (I.S.): *p*-chlorophenylalanine.

EXPERIMENTAL

The amino acids and ethyl chloroformate were purchased from Sigma (St. Louis, MO, USA). The ECEE derivatives were prepared according to the procedure reported previously [9–11]. Analysis by GC–MS was carried out on a JEOL AX-505H double-focusing mass spectrometer coupled to a Hewlett-Packard 5890J gas chromatograph. GC separation employed DB-1701 (30 m length × 0.53 mm I.D. fused-silica capillary column with a 1.0-μm film coating; or 15 m length × 0.25 mm I.D. × 0.25 μm film thickness) available from J. & W. Scientific (Rancho Cordova, CA, USA). Direct (splitless) injection was used. Helium gas flow was approximately 1 ml/min. MS conditions were as follows: interface temperature 280°C, ion source temperature *ca.* 150–200°C, electron energy was 70 eV, scan rate of the mass spectrometer was 1 s/scan over the m/z range 50–500.

RESULTS AND DISCUSSION

In general, the interpretation of the described electron-impact (EI) mass spectra and the assignment of various ions were based on the knowledge on the fragmentation behaviors of some other types of amino acid derivatives [3]. The assignment of molecular ions was experimentally confirmed using gas chromatography–chemical ionization (methane) mass spectrometry, GC–CI(CH_4)-MS, when the expected peak was very weak or absent. Table I lists the mass values of the characteristic peaks in the spectra of individual amino acid derivatives.

Aliphatic amino acids

Fig. 2 shows the mass spectrum of the valine ECEE derivative as a representative of this group (glycine, alanine, valine, leucine, and isoleucine). As shown in Scheme 1, two fragmentation routes (a and b) are possible through the rupture of a carbon-carbon bond α to the amine group. Generally, path b is preferred over a because $^{\cdot}CO_2Et$, the fragment having higher ionization energy compared to that of the alkyl chain, is favored energetically to retain the unpaired electron and to become the neutral prod-

TABLE I

CHARACTERISTIC ION PEAKS IN EI SPECTRA OF ECEE DERIVATIVES OF AMINO ACIDS

Amino acid	M_r	Derivative [$M^{+\cdot}$]	Base peak m/z	M − 73	M − 145	Other important ions, m/z
Gly	75	175	102	102		
Ala	89	189	116	116		
Val	117	217	144	144	72	116
Leu	131	231	158	158	86	102
Ile	131	231	158	158	86	102
Pro	115	215	142	142	70	98
HPr	131	231	158	158	86	68
Ser	105	(205)[a]	132	132	60	175, 129, 101, 86
Thr	119	(219)[a]	129	146	74	175, 101
AHBA[b]	119	219	103	146	74	117, 84
		155[d]	128			110, 83
DABA[c]	118	290	155	217		175, 129, 128, 115, 102, 83, 56
		172[d]	83	99		115, 83, 70, 56
Orn	132	304	142			258, 70
		186[d]	141	113		129, 97, 70
Lys	146	318	156			272, 226, 84
Cys	121	293	220	220	148	174, 114, 102, 74
Cys^2	240	440	188	367		220, 174, 102
Met	149	249	175	176		188, 142, 129, 101, 61
Asp	133	261	188	188	116	142, 74, 70
Glu	147	275	202	202		156, 128, 84
p-Glu	129	157	84	84		
Asn	132	214	141	141	69	174, 102
Gln	146	246	84	173		128
Phe	165	265	176	192	120	131, 102, 91, 74
Tyr	181	353	107	280	208	264, 192
Trp	204	304	130	231		215
His	155	327	238	254	182	154, 81

[a] Mass value given in parentheses indicates the absence of a molecular ion peak in the spectrum.
[b] AHBA = γ-Amino-β-hydroxybutyric acid.
[c] DABA = 2,4-Diaminobutyric acid.
[d] Minor derivatization product.

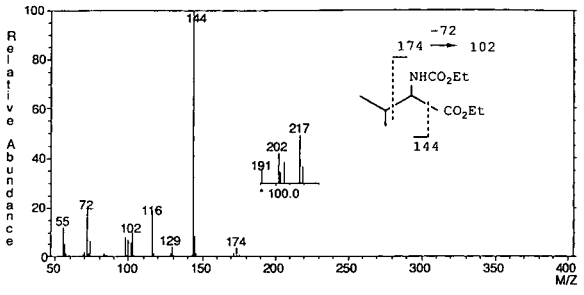

Fig. 2. Mass spectrum of ECEE valine (M_r 217). The asterisk in the inset of the figures throughout the text denotes a multiplication factor.

uct. Subsequent fragmentation of the even-electron ions (EE^+) thus formed is dominated by the loss of 72 u ($^{\cdot}CO_2Et - H^{\cdot}$), giving rise to ions m/z 102 and [M − 145], respectively.

Cyclic amino acids

The mass spectrum of the ECEE derivative of hydroxyproline is shown in Fig. 3 with the corresponding fragmentation pattern depicted in Scheme 2.

Similar to the pattern obtained from the aforementioned simple aliphatic derivatives, the

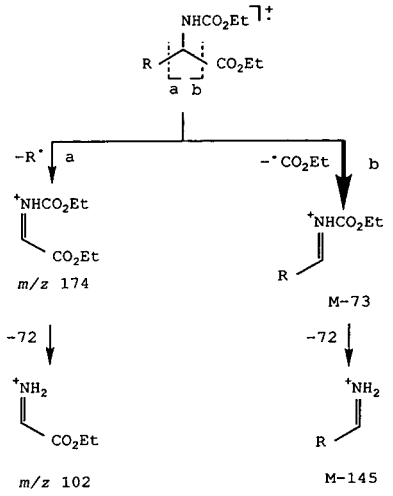

Scheme 1.

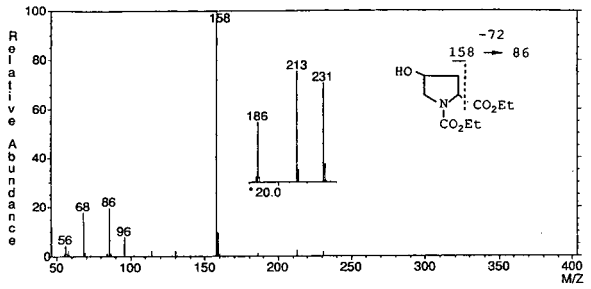

Fig. 3. Mass spectrum of ECEE 4-hydroxyproline (M_r 231).

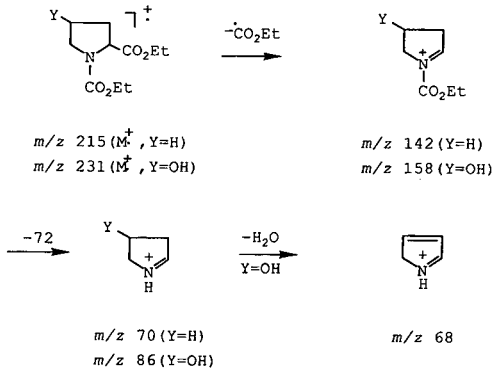

Scheme 2.

highest peak in this spectrum represents the ion formed by a reaction sequence that originates in the splitting of the ester group to yield an ion at m/z 158 (m/z 142 for Pro). This ion loses ($^{\bullet}CO_2Et - H^{\bullet}$) to produce the characteristic even mass ion at m/z 86 (m/z 70 for Pro). Subsequent loss of H_2O from the latter ion results in the formation of an ion of m/z 68.

Another example of the cyclic amino acid series is the ECEE of pyroglutamic acid (Fig. 14), which will be discussed later in a section regarding acidic amino acids.

Hydroxy amino acids

In Fig. 4 the mass spectrum of the serine derivative is given, together with the fragmentation pathways shown in Scheme 3.

As discussed before, the process $[M]^+ \rightarrow [M - 73]^+ \rightarrow [M - 73 - 72]^+$ (m/z 132 and 60 in Fig. 4) remains prominent in the fragmentation of the hydroxy analogues. Two additional fragment peaks, m/z 102 and 86, are formed via rearrangements with concurrent removal of RCHO (R = H for Ser) and EtOH, respectively.

Another sequence of degradation is due to a McLafferty-type rearrangement, which is triggered by a hydrogen migration originating from the β-HO group to produce an abundant ion peak at m/z 175. A subsequent cyclization reaction leads to ions m/z 129 and 101. This sequence is a common feature for all amino acid derivatives having a labile hydrogen atom to permit transition via a six-membered ring.

The ECEE derivative of threonine behaves in a similar way, showing a mass shift of 14 u for ions that retain the side-chain $CH_3CH(OH)$- in the fragment.

Depicted in Fig. 5 is the mass spectrum obtained from a non-protein amino acid, γ-amino-β-hydroxybutyric acid (AHBA), which gives an open-chain derivative with $M^{+\bullet}$ at m/z 219.

Generally, the loss of an ester group is not a

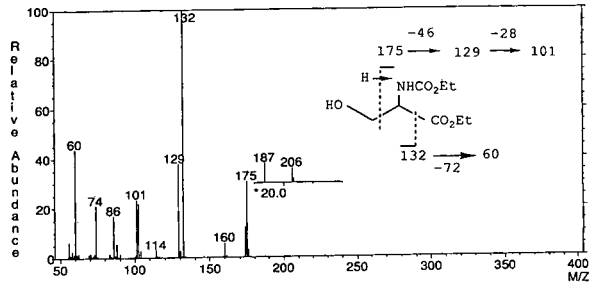

Fig. 4. Mass spectrum of ECEE serine (M_r 205). Fragments arise from $M^{+\bullet}$, although MH^+ (m/z 206) is observed.

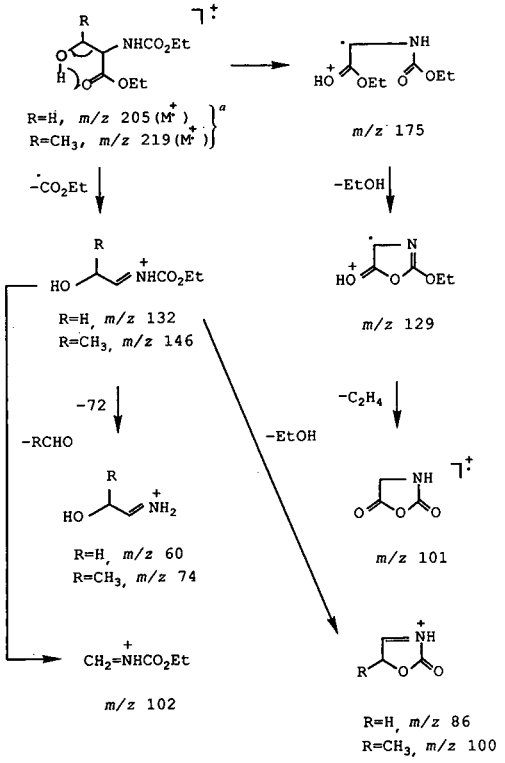

Scheme 3. [a] Derivatives not observed.

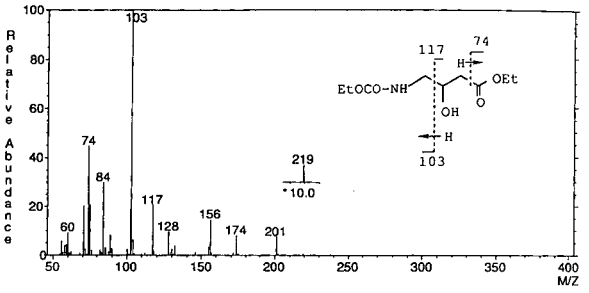

Fig. 5. Mass spectrum of ECEE γ-amino-β-hydroxybutyric acid (M_r 219).

significant process for γ-amino acid derivatives [3]. As indicated in Scheme 4, there are four ions (*m/z* 74, 88, 103 and 117) formed by cleavage along the carbon chain, whereas the terminal immonium ion *m/z* 103, resulting from a rearrangement involving hydrogen-transfer, is the base peak in the spectrum.

Another fragmentation process involves the loss of an EtO• radical from the molecular ion, resulting in the formation of a cyclic ion at *m/z*

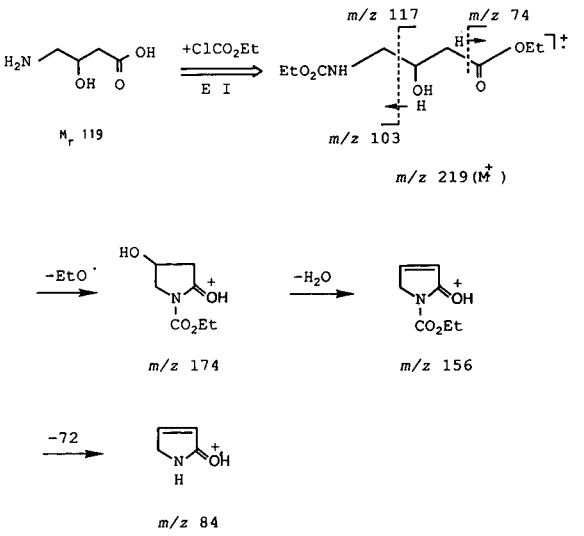

Scheme 4.

174 and its subsequent degradation product ions at *m/z* 156 and 84 (Scheme 4).

Like other γ-amino acids, AHBA undergoes cyclization readily on treatment with ECF–Py to yield N-ethoxycarbonyl dehydropyrrolidone ($M^{+\bullet}$ at 155) as a minor reaction product. Subsequent double hydrogen rearrangement ("McLafferty + 1" rearrangement) is likely responsible for the formation of *m/z* 128 and daughter ions *m/z* 110 and 83 therefrom (Fig. 6; Scheme 5).

Sulfur-containing amino acids

Figs. 7 and 8 present the mass spectra of ECEE cysteine and methionine, respectively.

These amino acids have the same typical fragments as those obtained from aliphatic amino

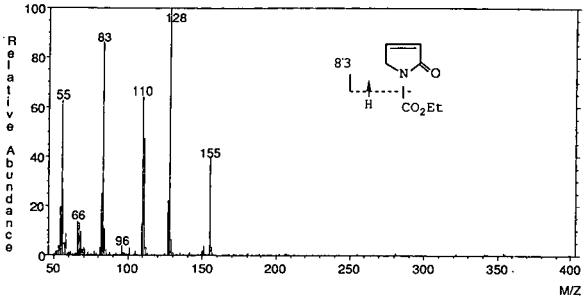

Fig. 6. Mass spectrum of the minor derivatization product of γ-amino-β-hydroxybutyric acid (M_r 155).

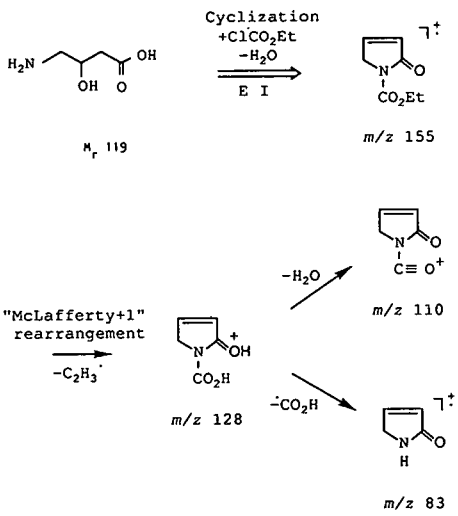

Scheme 5.

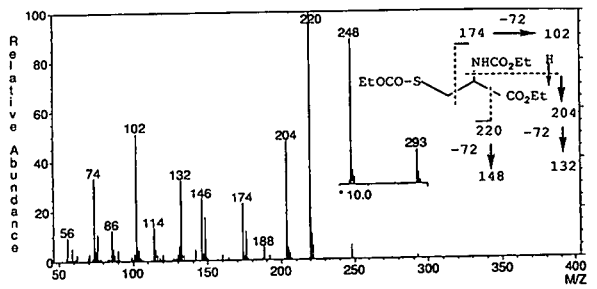

Fig. 7. Mass spectrum of ECEE cysteine (M_r 293).

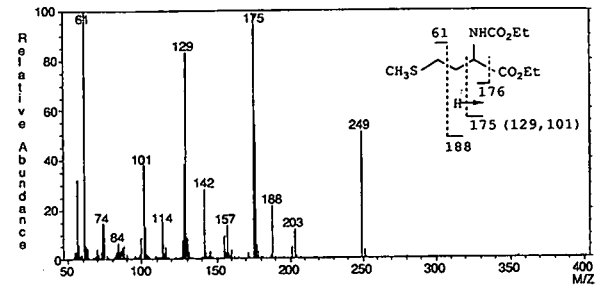

Fig. 8. Mass spectrum of ECEE methionine (M_r 249).

acids. Additional fragments were observed due to the presence of the sulfur atom. Thus, in the spectrum of the cysteine derivative (Fig. 7), a resonance-stabilized ion m/z 204 ($M_r - NH_2CO_2Et$) is formed through the McLafferty rearrangement with charge retention on the fragment that contains sulfur. The consecutive loss of ($^{\cdot}CO_2Et - H^{\cdot}$) and EtOH leads to another two sulfur-containing species m/z 132 and 86 (Scheme 6).

A more prounced influence exerted by the sulfur atom occurs in the spectrum of the methionine derivative (Fig. 8; Scheme 7). An intense ion peak m/z 175 (together with its product ions m/z 129 and 101) due to the McLafferty rearrangement is observed, which is initiated by the transfer of the labile hydrogen, that is activated by α-sulfur. Whereas the low mass end of the spectrum is dominated by the sulfonium ion $CH_3S{=}CH_2^+$ (m/z 61), an ion complementary to m/z 61 is displayed at m/z 188 [61 + 188 = 249 ($M^{+\cdot}$)].

The ECEE derivative of cystine (Fig. 9) is an

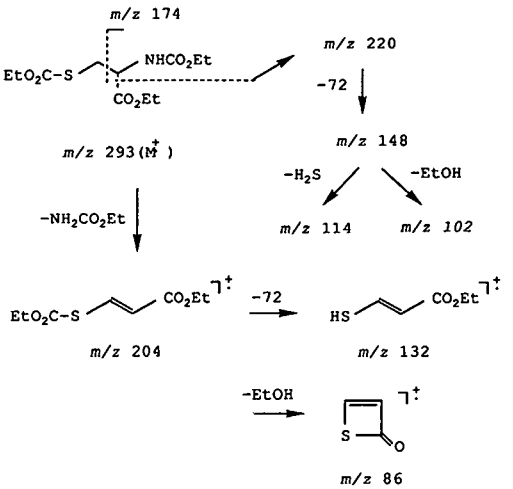

Scheme 6.

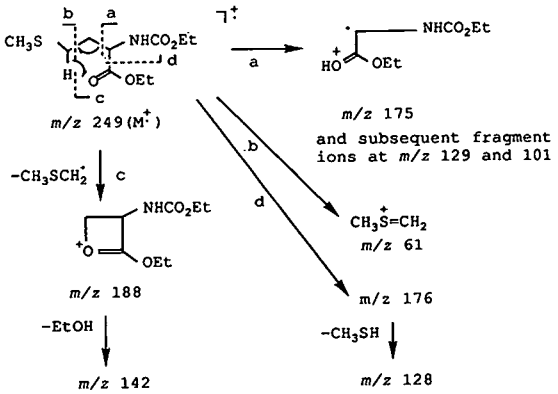

Scheme 7.

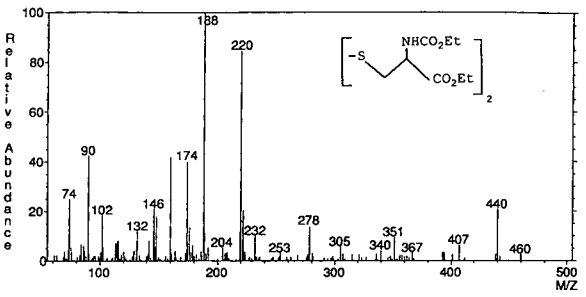

Fig. 9. Mass spectrum of ECEE cystine (M_r 440).

example where fragmentation occurs predominantly due to the influence of the sulfur atom. Two major peaks in the spectrum, m/z 220 and 188, are formed via homolytic fission of the –S–S– linkage and σ-cleavage induced by the electropositive sulfur atom.

Basic amino acids

Because the basic amino acids [2,4-diaminobutyric acid (DABA), ornithine and lysine], after derivatization, demonstrate quite similar degradation patterns, their fragmentations are illustrated by the example of the ECEE derivative of ornithine (Fig. 10).

Generally, the loss of the ester function is not a significant process for these compounds because of the competing reactions due to the remote amino group. Typically, these ECEE amino acids undergo consecutive loss of $^{\cdot}CO_2Et$ and NH_2CO_2Et, which leads to the formation of the stable cyclic immonium ions m/z 128, 142 and 156 (for $n = 2$, 3 and 4), respectively. This synchronic process is rationalized by a S_{Ni} reaction mechanism (see, for example, ref. 12) as presented in Scheme 8.

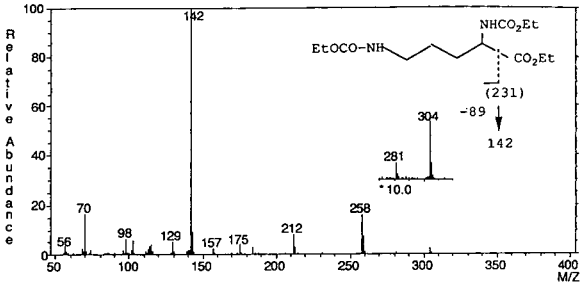

Fig. 10. Mass spectrum of ECEE ornithine (M_r 304).

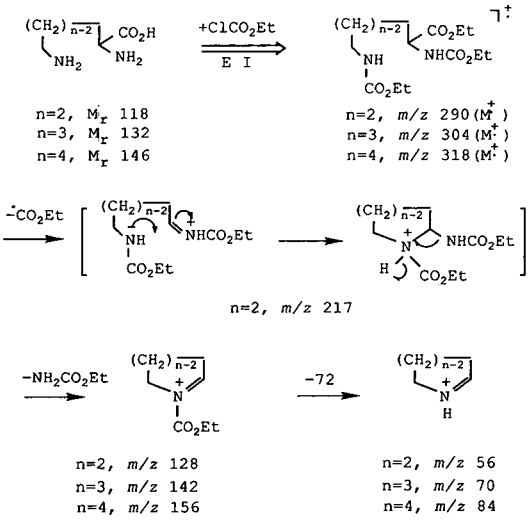

Scheme 8.

Another noteworthy feature of the spectrum depicted in Fig. 10 is the ejection of EtOH from the molecular ion with the formation of the cyclic ions m/z 244, 258 and 272 (for $n = 2$, 3 and 4), respectively (Scheme 9).

Analogous to the methionine derivative, the ECEE DABA undergoes a McLafferty rearrangement to yield product ions at m/z 175, 129 and 101 (Table I).

Two minor by-product peaks are sometimes detected in the gas chromatogram for DABA and ornithine (Fig. 11). These compounds show common peaks $[M-45]^+$, $[M-57]^+$ and $[M-73]^+$ by a mechanism that is not yet clear. The respective ions m/z 83 and 97 are formed as a result of ejecting NH_2CO_2Et from each of the molecular ions (Scheme 10).

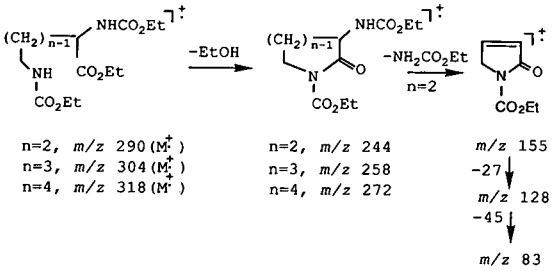

Scheme 9.

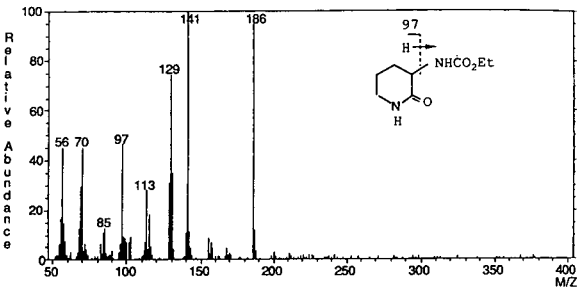

Fig. 11. Mass spectrum of the minor derivatization product of ornithine (M_r 186).

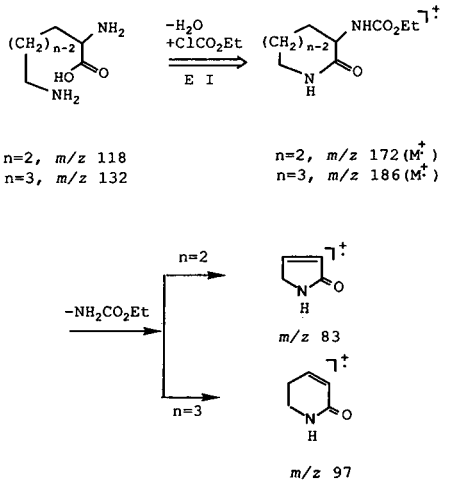

Scheme 10.

Acidic amino acids

The spectrum pattern of the aspartic acid derivative is simple and dominated by the ion at m/z 188 (M_r – $^{\cdot}CO_2Et$) (Fig. 12). This pattern may be explained by the formation of a stabilized cyclic oxonium ion (m/z 188), which facilitates the cleavage of the C–C bond connecting the ester group (Scheme 11).

Shown in Fig. 13 is the mass spectrum of the glutamic acid derivative. The loss of the α-CO_2Et initiates a sequence reaction leading to the pyrrolidinone ions at m/z 156 and 84 (Scheme 12).

Fig. 14 presents the mass spectrum of another derivatization product of glutamic acid, which is produced as a result of dehydration to form pyroglutamic acid followed by esterification by ECF. Because other α-cleavages do not lead to fragmentation, the mass spectrum is comprised almost totally of m/z 84, which is formed by splitting an ester radical from the molecular ion.

Fig. 15 presents the mass spectrum of the

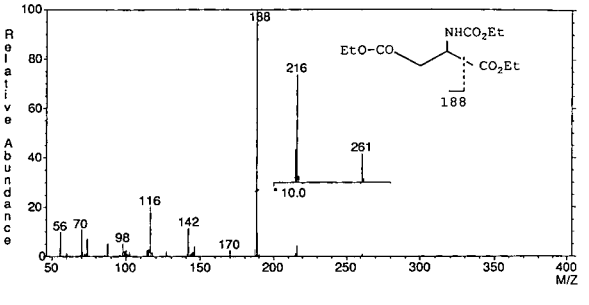

Fig. 12. Mass spectum of ECEE aspartic acid (M_r 261).

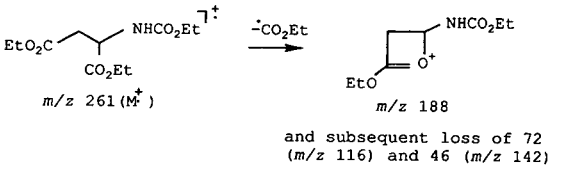

Scheme 11.

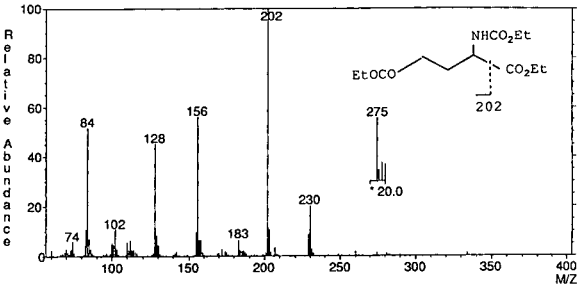

Fig. 13. Mass spectrum of ECEE glutamic acid (M_r 275).

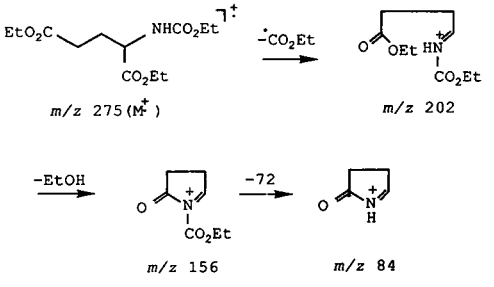

Scheme 12.

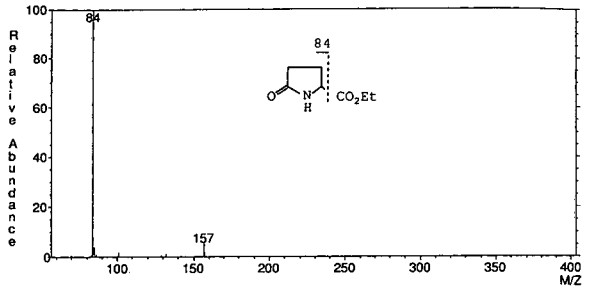

Fig. 14. Mass spectrum of pyroglutamic acid derivative (M_r 157).

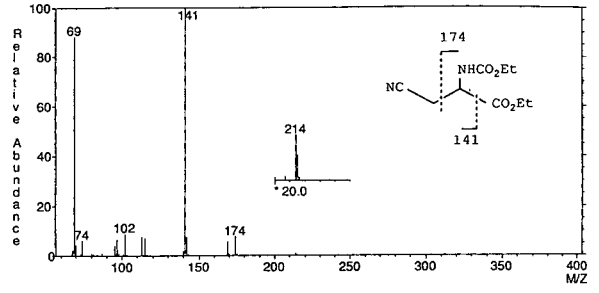

Fig. 15. Mass spectrum of asparagine derivative (M_r 214).

ECEE derivative of asparagine. Instead of the usual N-ethoxycarbonylation-C-esterification, a dehydration of the terminal carboxamide may occur to afford the corresponding nitrile [$M^{+\bullet}$ = m/z 214] (Scheme 13). This pattern is analogous

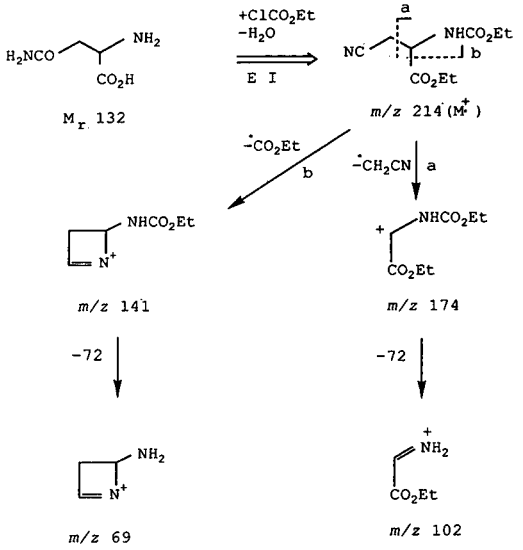

Scheme 13.

to some cases (for example, maleamic and phthalimic acids) documented in the literature [13]. This dehydration product undergoes further fragmentation according to sequences a (loss of $^{\bullet}CH_2CN$) or b (loss of $^{\bullet}CO_2Et$) to give product ions m/z 174 and 102, or m/z 141 and 69, respectively.

The fragmentation of glutamine, a homologue of asparagine with the $^{\bullet}CONH_2$ group one more methylene from the carboxyl, takes place in a different way (Fig. 16, Scheme 14) where the prevailing event is the cyclization induced by functional group interaction between $^{\bullet}CONH_2$ and the amino terminus in the EE^+ species (m/z 173 = $M_r - {}^{\bullet}CO_2Et$).

Aromatic and heterocyclic amino acids

In general, ECEE amino acids with an aromatic (Ar) or heterocyclic group in the side chain afford much more abundant ions due to loss of side chain ($ArCH_2^{\bullet}$). Fig. 17 presents the mass spectrum of the ECEE derivative of phenylalanine. There are essentially two competing primary fragmentation reactions: elimination of

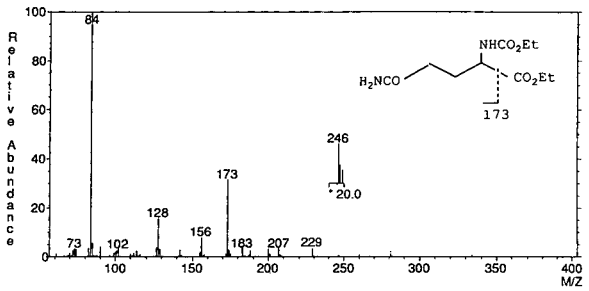

Fig. 16. Mass spectrum of ECEE glutamine (M_r 246).

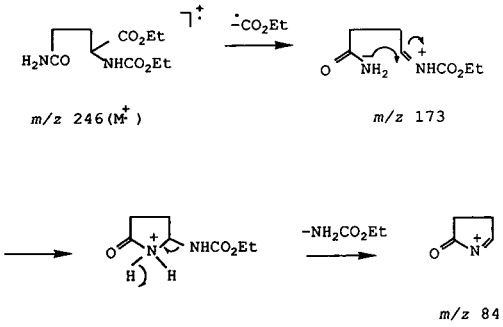

Scheme 14.

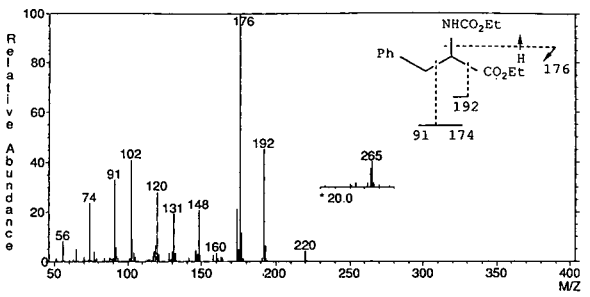

Fig. 17. Mass spectrum of ECEE phenylalanine (M_r 265).

NH_2CO_2Et from $M^{+\cdot}$ to give a conjugated ion m/z 176, and formation of a benzyl-type ion, $ArCH_2^+$ (m/z 91 in Fig. 17) (Scheme 15).

The mass spectra and interpretation for derivatives of tryptophan and histidine are given in Fig. 18 (Scheme 16) and Fig. 19 (Scheme 17), respectively. Different from other amino acid derivatives, ECEE histidine affords not $ArCH_2^+$, but $ArCH_3^{+\cdot}$ by a six-membered ring hydrogen transfer.

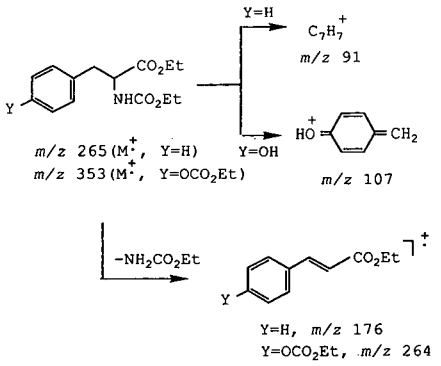

Scheme 15.

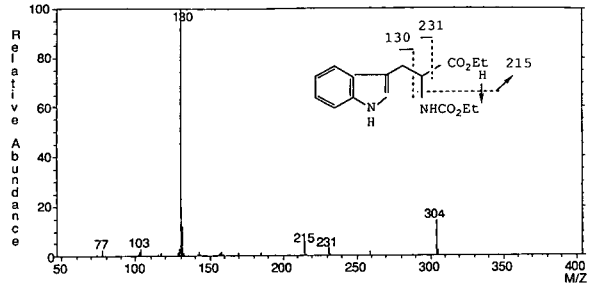

Fig. 18. Mass spectrum of ECEE tryptophan (M_r 304).

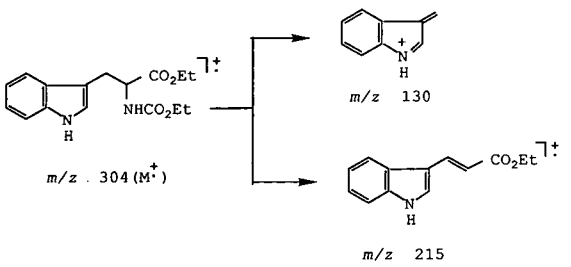

Scheme 16.

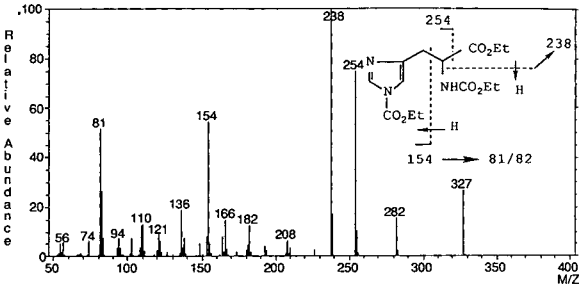

Fig. 19. Mass spectrum of ECEE histidine (M_r 327).

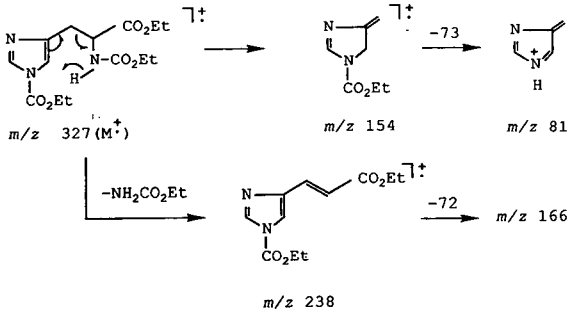

Scheme 17.

ACKNOWLEDGEMENTS

Mass spectral data were acquired at the MSU–NIH Mass Spectrometry Facility which is supported, in part, by a grant (RR00480) to J.T.W. from the National Institutes of Health, National Center for Research Resources.

REFERENCES

1 S.L. MacKenzie, in R.E. Clement (Editor), *Gas Chromatography: Biochemical, Biomedical and Clinical Applications*, Vol. III, Wiley, New York, 1990, Ch. 10, p. 267.
2 W. Vetter, in G.R. Waller and O.C. Dermer (Editors),

Biochemical Applications of Mass Spectrometry, Suppl. Vol., Wiley-Interscience, New York, 1980, p. 439.
3 R.A.W. Johnstone and M.E. Rose, in G.C. Barrett (Editor), *Chemistry and Biochemistry of Amino Acids*, Chapman & Hall, London, New York, 1985, Ch. 17, p. 480.
4 C.W. Gherke, R.W. Zumwalt and L.L. Wall, *J. Chromatogr.*, 37 (1967) 398.
5 P.L. Wood and D.L. Cheney, *Neuromethods*, 3 (1985) 51.
6 R.G. MacFarlane, J.M. Midgley, D.G. Watson and P.D. Owens, *J. Chromatogr.*, 532 (1990) 1.
7 C.J. Biermann, C.M. Kinoshita and R.D. Steele, *J. Chromatogr.*, 357 (1986) 330.
8 P. Hušek, *J. Chromatogr.*, 234 (1982) 381.
9 P. Hušek, *FEBS Lett.*, 280 (1991) 354.
10 P. Hušek and C.C. Sweeley, *J. High Resolut. Chromatogr.*, 14 (1991) 751.
11 P. Hušek, *J. Chromatogr.*, 552 (1991) 289.
12 H. Bosshardt and M. Hesse, *Angew. Chem., Int. Ed. Engl.*, 13 (1974) 252.
13 C.K. Sauers and R.J. Cotter, *J. Org. Chem.*, 26 (1961) 6.

Journal of Chromatography, 635 (1993) 283–289
Elsevier Science Publishers B.V., Amsterdam

CHROM. 24 854

Computer-aided optimization of gradient multiple development thin-layer chromatography

Part II. Multi-stage development

W. Markowski

Department of Inorganic and Analytical Chemistry, Medical Academy, Staszica 6, 20-081 Lublin (Poland)

(First received September 29th, 1992; revised manuscript received January 5th, 1993)

ABSTRACT

A theoretical model of gradient multiple development is presented as a basis for the optimization of separation by planar multi-step development and automated multiple development (AMD). A computer program for the calculation of final R_F values for multi-stage development in the gradient mode for known retention *vs.* eluent composition relationships is reported. The influence of various parameters on the final values of R_F is discussed. The predicted and experimental R_F values were compared and showed satisfactory agreement.

INTRODUCTION

Thin-layer chromatography (TLC) is a very popular method, applied in most analytical laboratories; the increased interest in TLC, despite the advent of HPLC, in recent years is due to its numerous advantages: simplicity, small expenditure of materials, low cost, wide choice of adsorbents [1] and solvents, diversity of techniques and equipment [2,3] and the possibility of analysing several tens of samples in parallel. Modern densitometry has made TLC an accurate and sensitive quantitative method. TLC can also be combined with other physico-chemical methods, *e.g.*, mass spectrometry [4].

One of attractive modes of TLC is the method of multiple development, especially useful in the analysis of complex natural mixtures, e.g., plant extracts composed of numerous solutes with wide differences in polarity. Multiple development (MD) can increase considerably the resolution, R_s, owing to the reconcentration of the spots on each passage of the solvent front so that the spots become more compact, which leads to lower detection limits. It is advantageous that the process can be easily automated [automated multiple development (AMD)], which ensures good repeatability of results. The method has recently become popular in analytical practice [5] and equipment is commercially available (Camag, Muttenz, Switzerland). However, the optimization procedure is frequently carried out by the trial and error method [5] owing to the lack of a theoretical model, which would be helpful in the description of the multiple development process in its various modifications. This paper is an attempt to formulate such a physical model to describe the migration of the solute zones, their dispersion and other phenonema that may distort the development process and which can be included in the model. The model may, it is hoped, form a rational basis of various optimization procedures. The earlier derived equations for mobile phase gradients in TLC [6–8] and for migration in a two-step gradient process [9] have been utilized in the

0021-9673/93/$06.00

present theoretical description of gradient multiple development.

THEORETICAL

General assumptions

We assume that the plate is developed a number of times in the same direction and that the plate is dried after each development and the solvent is completely removed from the adsorbent layer. Further assumptions are as follows: the adsorption layer has identical properties along the whole length (thickness, phase ratio, activity, packing density); the elution strength of the mobile phase is varied according to a programme (isocratic, gradient); the development distance is also varied according to a program (linear, stepwise or in another way); after each development the plate is dried and brought to such a state that the eluent delivered in the next step does not change its properties; the relationships between the retention of solutes and the properties of the eluents (concentration, eluent strength) are known; the solutes are not decomposed and their loss is insignificant; the solvent demixing process in the case of mixed eluents is negligible to a first approximation or can be taken into account in the equation; and the whole elution process can be divided into cycles within which steps are discerned (Fig.1). As a cycle we understand a number of steps in which the same eluent type is used, differing only in the concentration of the modifier; the eluent is the solvent (containing one or more components) and the modifier is the more polar (stronger) component of the eluent.

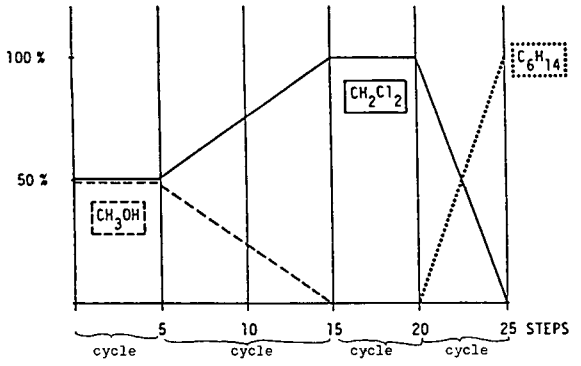

Fig. 1. Principle of partitioning of the programme into cycles and steps.

In the practical realization of the multiple development process, some deviations from these simplifying assumptions may be observed. The security of identical activity of the adsorbent layer is possible only for full automation (AMD). In the case of "manual" developments, the variations in activity may cause changes in R_F values in an unpredictable manner (although for eluents that contain larger proportions of the polar modifier the effects are limited). Also, solvent demixing effects (frontal chromatography of the eluent), which tend to decrease the R_F values, are pronounced only for low contents of modifier. In each evaporation cycle some loss of more volatile sample components may occur, which may reduce the detectability, especially of trace components.

These are very general assumptions of the process of multiple development. Its variations can be classified as follows. If we assume a constant (full) development distance and a mobile phase of constant composition is used, we have the unidimensional chromatographic (UMC) technique [10]. If the distance of development in each step is longer than the previous one, we have incremental multiple development.

The model does not include the programmed multiple development (PMD) introduced by Perry *et al.* [11] when the plate is in contact with the eluent container all the time.

The following notation is used: the subscript i denotes step number; the subscript j denotes substance; y_i denotes distance travelled in step i; $s_{(h,j)}$ denotes the sum of distances travelled by solute j in h steps; $R_{F(i,j)}$ denotes the R_F value of solute j in the ith step; and $v_{e,(i,j)}$ denotes the elution volume corresponding to step i and solute j.

If we assume a programme of qualitative and quantitative composition of the eluents used in the consecutive steps, then for the purposes of computer simulation we must know the relationships between the retention of the sample components and the properties (composition) of the eluents used. For pure solvents it is simplest to give the R_F values of the solutes. On the other

hand, when binary eluents are used, it is convenient to give the parameters of the retention *vs.* modifier concentration plots from which the R_F values can be calculated. For normal-phase systems the equation that follows from the Snyder–Soczewinski competitive adsorption model [12] is most frequently used:

$$\log k_{(i,j)} = \log k_{0(j)} - m_{(j)} \log c_{(i)} \quad (1)$$

If the retention *vs.* eluent composition relationship cannot be described by equations following from the model, a polynomial of a suitable degree can be used (usually a quadratic equation is sufficient) [13]:

$$\log k_{(i,j)} = A_{(0)} + A_{(1)} \log c_{(i)} + A_{(2)}[\log c_{(i)}]^2 \quad (2)$$

$$R_{F(i,j)} = \frac{1}{1 + k_{(i,j)}} \quad (3)$$

In simulation procedures, the R_F values are introduced into the programme or are calculated by suitable subprogrammes.

When planning a multiple development programme, we introduce the number of cycles and steps. Then the development distances for the consecutive steps are to be given and then the eluent compositions used in the consecutive cycles and steps are also to be given. For the programme thus planned, the subprogramme is chosen which calculates the R_F values of solutes in the consecutive steps. Let us consider the process of multiple development for a single n-step cycle. The migration of the solutes is given by the following equations.

For the first step for which the development distance is $z_{(1)}$, the elution volume for all solutes is the same and is equal to $v_{e,(i,j)}$. This follows from the fact that all solutes are applied on the starting line at an equal distance from the lower edge of the adsorbent layer. The migration distances (from the start line) of solutes are

$$y_{(1,y)} = v_{e,1} R_{F(1,j)} \quad (4)$$

After development, the chromatogram is dried so that the spots retain their positions attained after elution. Therefore, we can write that the sum of the paths of a given solute is equal to the distance travelled in the first step. For $h = 1$ we have

$$s_{(h,j)} = \sum_{i=1}^{h=1} y_{(i,j)} = y_{(1,j)} \quad (5)$$

We carry out the next step according to the programme adopted. The development distance is now equal to $z_{(2)}$. We can have two cases: (a) the distance in the second step is greater than that in the first step (the usual case) or (b) it is smaller $[z_{(2)} < z_{(1)}]$.

(a) For the first case, $z_{(2)} > z_{(1)}$. As after the first development the solutes have various positions (distance from the start), then the elution volume in the second step is different for each solute, depending on the distance travelled in the first step. Therefore,

$$v_{e,(2,j)} = z_{(2)} - s_{(1,j)} \quad (6)$$

The migration path in the second step is

$$y_{(2,j)} = v_{e,(2,j)} R_{F(2,j)} \quad (7)$$

and the total path after two steps is

$$s_{(h,j)} = \sum_{i=1}^{h=2} y_{(i,j)} \quad (8)$$

Introducing eqns. 6, 7 and 5 into eqn. 8, we obtain an equation for the sum of migration paths after two developments:

$$s_{(2,j)} = s_{(1,j)} + [z_{(2)} - s_{(1,j)}] R_{F(2,j)} \quad (9)$$

(b) In the second case $[z_{(2)} < z_{(1)}]$, only those solutes are taken into account for which the sum of total paths is smaller than the development distance $z_{(2)}$ for the second step. For solutes which remain at their positions in the second step, we can write the following: if

$$s_{(1,j)} > z_{(2)} \quad (10)$$

then

$$v_{e,(2,j)} = 0; \quad y_{(2,j)} = 0 \quad (11)$$

and

$$s_{(2,j)} = s_{(1,j)} \quad (12)$$

For these solutes the total migration distance after the second step is the same as that after the first step. On the other hand, for solutes for

which $s_{(1,j)} < z_{(2)}$, eqns. 6 and 7 and eqns. 8 and 9 are applied. Similar considerations are applied to further steps until the kth step. For solutes j that fulfil the condition $z_{(k)} > s_{(k-1,j)}$ the following equations are applied:

$$v_{e,(k,j)} = z_{(k)} - s_{(k-1,j)} \quad (13)$$

$$y_{(k,j)} = v_{e,(k,j)} R_{F(k,j)} \quad (14)$$

$$y_{(k,j)} = [z_{(k)} - s_{(k-1,j)}] R_{F(k,j)} \quad (15)$$

$$s_{(h,j)} = \sum_{i=1}^{h=k} y_{(k,j)} \quad (16)$$

and for solutes fulfilling the condition $z_{(k)} < s_{(k-1,j)}$ we apply the equations

$$v_{e,(k,j)} = 0; \quad y_{(k,j)} = 0 \quad (17)$$

and

$$s_{(k,j)} = s_{(k-1,j)} \quad (18)$$

Analogous equations are obtained for n-step development:

$$v_{e,(n,j)} = z_{(n)} - s_{(n-1,j)} \quad (19)$$

$$y_{(n,j)} = v_{e,(n,j)} R_{F(n,j)} \quad (20)$$

$$y_{(n,j)} = [z_{(n)} - s_{(n-1,j)}] R_{F(n,j)} \quad (21)$$

because $h = n$, then

$$s_{(h,j)} = \sum_{i=1}^{h=n} y_{(i,j)} = s_{(n-1,j)} + y_{(n,j)}$$

$$= s_{(n-1,j)} + [z_{(n)} - s_{(n-1,j)}] R_{F(n,j)} \quad (22)$$

For solutes which do not participate in the nth step we have

$$s_{(n,j)} = s_{(n-1,j)} \quad (24)$$

Analysing eqns. 22 and 24, we see that these are typical recurrent equations, in which the $(k-1)$th value is necessary to calculate the kth value. As the programme corresponds to n-step development, the sum of the distances travelled by a solute after n-step development is equal to the final R_F value. Taking into account the two cases , the final equations for the R_F value (R_{FG}; G = gradient) are

$$R_{FG(j)} = s_{(n-1,j)} + [z_{(n)} - s_{(n-1,j)}] R_F(n,j) \quad (25)$$

or

$$R_{FG(j)} = s_{(n-1,j)} \quad (26)$$

These equations form the basis to elaborate a computer program that simulates the multiple development process. The program, written in Pascal, is represented in Fig. 2. It allows not only for the calculation of the final R_F values but also for the graphical representation of the positions of the spots on the chromatogram. The knowledge of the R_F *vs.* i relationships for a chosen program permits the investigation by computer simulations of the effect of the number of steps, their distances and variation of eluent composition. In combination with an equation that determines the final widths of the zones [2], it permits the calculation of R_S values or other parameters that characterize the resolution and its determination [13].

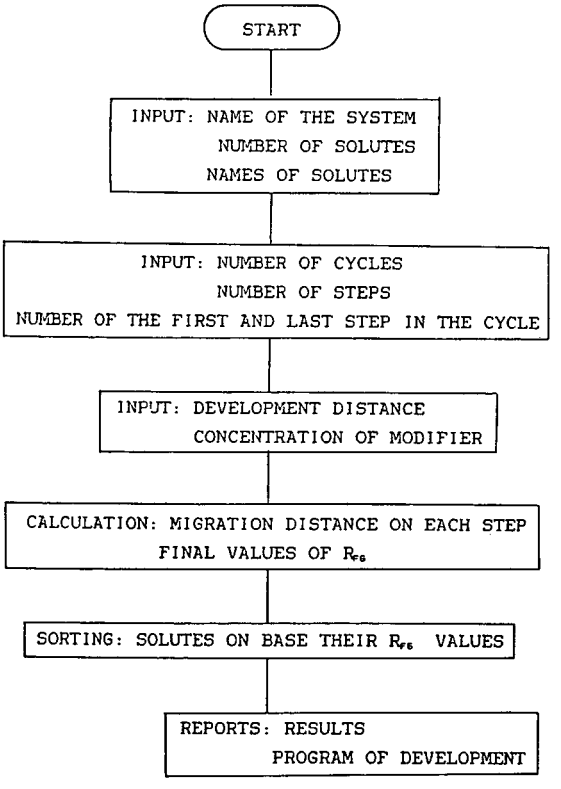

Fig. 2. Flow diagram of the computer programme for calculation of the final values of R_{FG} in multi-stage development.

EXPERIMENTAL

A horizontal sandwich chamber of the DS type [14,15] (Chromdes, Lublin, Poland) was used. Precoated plates (silica gel Si 60; Merck, Darmstadt, Germany) were activated at 100°C for 1 h and cooled in a desiccator. As eluents, solutions of diisopropyl ether in *n*-heptane or toluene were used; the solvents were dried over a molecular sieve (A5). The solutes were spotted on dry plates as 0.1% solutions in the eluent. When the solutes were spotted behind the solvent front, azulene was used as a marker of the mobile phase. After each development (multiple development) the plates were dried for 15 min in a stream of air. When the sample was applied from the edge of the layer, the solution of the test mixture was pipetted in a known volume into the eluent container, introduced into the adsorbent layer to the last drop and a portion of the eluent was introduced. The solutes were visible in daylight.

RESULTS AND DISCUSSION

The equation for the final R_{FG} value was verified experimentally for five-step gradient development with toluene. In the first series of experiments, the R_F values of the solutes were determined for isocratic conditions. The second experiment consisted in multiple development, applying a gradual constant increase of the development distance. The third experiment was similar to the second, except that the distance of the last step was considerably elongated. The results are presented in Tables I and II. Comparison of the simulated and experimentally determined R_F values showed satisfactory agreement. Especially in the third experiment, when the development distance of the fifth step was considerably longer, very good agreement was achieved.

In the next experiment binary eluents were used, the Snyder–Soczewinski two-parameter equation (eqn. 1) being used for the description of retention *vs.* eluent composition relationships. For this purpose a series of isocratic runs were carried out and the R_F values used to determine the constants of the equation, *i.e.*, the slope *m* and the k_0 value (corresponding to pure modifier) (Table III). The computer program was then applied to simulate the multiple development process and to compare the data with the experimental results.

TABLE I

R_{FG} VALUES OBTAINED IN FIVE-STEP DEVELOPMENT

Programme: $z_{(1)} = 20$ mm, toluene; $z_{(2)} = 40$ mm, toluene; $z_{(3)} = 60$ mm, toluene; $z_{(4)} = 80$ mm, toluene; $z_{(5)} = 100$ mm, toluene.

Solute	$R_{FG(calc)}$	$R_{FG(exp)}$	ΔR_{FG}
4-Dimethylaminoazobenzene	0.82	0.68	0.14
Indophenol Blue	0.14	0.13	0.01
Sudan Red G	0.38	0.34	0.04
Fat Green	0.82	0.77	0.05
Fat Orange	0.74	0.78	0.04
Blue Dark	0.76	0.71	0.05
Red	0.61	0.56	0.05

TABLE II

R_{FG} VALUES OBTAINED IN FIVE-STEP DEVELOPMENT

Programme: $z_{(1)} = 20$ mm, toluene; $z_{(2)} = 40$ mm, toluene; $z_{(3)} = 60$ mm, toluene; $z_{(4)} = 80$ mm, toluene; $z_{(5)} = 150$ mm, toluene.

Solute	$R_{FG(calc)}$	$R_{FG(exp)}$	ΔR_{FG}
4-Dimethylaminoazobenzene	0.95	0.98	0.03
Sudan Red G	0.29	0.32	0.03
Fat Green	0.73	0.73	0.00
Fat Orange	0.63	0.64	0.01
Blue Dark	0.66	0.68	0.02
Red	0.52	0.53	0.01

In the first experiment a single-cycle gradient programme was applied, the eluents being composed of diisopropyl ether and *n*-heptane. The results are given in Table IV. The experimental R_F values are lower than the calculated values. The cause of these discrepancies is presumably solvent demixing: as the solvent system contains two components that differ in polarity, a demixing effect is to be expected in steps 3 and 4, tending to decrease the final R_F values.

In the next experiment, a gradient programme composed of three cycles was applied; the results

TABLE III

THE PARAMETERS k_0 AND m OF THE SNYDER–SOCZEWINSKI EQUATION LOG $k_{(i,j)}$ = LOG $k_{0(j)}$ – $m_{(j)}$ LOG $c_{(i)}$, CALCULATED FROM A SERIES OF ISOCRATIC DATA FOR THE SYSTEM *n*-HEPTANE–DIISOPROPYL ETHER WITH SILICA

Solute	k_0	m	r
4-Dimethylaminoazobenzene	0.051	2.27	0.9194
Indophenol Blue	0.093	2.62	0.9512
Sudan Red G	0.144	2.40	0.9589
Fat Green	0.012	3.03	0.9460
Fat Orange	0.037	2.38	0.9364
Blue Dark	0.034	2.69	0.9515

TABLE IV

MULTIPLE DEVELOPMENT IN THE SYSTEM *n*-HEPTANE–DIISOPROPYL ETHER WITH SILICA

Programme: $z_{(1)} = 10$ mm, volume fraction of diisopropyl ether $c_{(1)} = 0.9$; $z_{(2)} = 20$ mm, $c_{(2)} = 0.7$; $z_{(3)} = 30$ mm, $c_{(3)} = 0.4$; $z_{(4)} = 40$ mm, $c_{(4)} = 0.3$.

Solute	$R_{FG(calc)}$	$R_{FG(exp)}$	ΔR_{FG}
4-Dimethylaminoazobenzene	0.78	0.65	0.13
Indophenol Blue	0.63	0.53	0.10
Fat Green	0.82	0.65	0.17
Fat Orange	0.80	0.70	0.10
Sudan Red G	0.59	0.50	0.09

are presented in Table V. Also in this instance the final R_F values are lower than the calculated values, the main presumable cause being solvent demixing [12]; for solutes of lower R_F values ($R_F < 0.6$) the discrepancies are less pronounced owing to weaker demixing effects in the lower part of the plate.

The advantages of multiple development, consisting in a better distribution of the spots along the plate and zone compression, are well known [5]. They can be utilized for micropreparative zonal separations. The use of eqns. 25 and 26, corrected for the point of sample application and shifting of the start line to the edge of the layer, was investigated using Fat Green as the solute (Table VI). The application of the sample solution from the edge (possible with the TLC chamber used [14,15]) allowed a wide starting zone to be produced. By several developments

TABLE V

MULTIPLE DEVELOPMENT WITH THREE DIFFERENT ELUENTS

Programme: cycle 1, $z_{(1)} = 10$ mm, $c_{(1)} = 0.9$ (diisopropyl ether in heptane); $z_{(2)} = 20$ mm, $c_{(2)} = 0.7$; $z_{(3)} = 30$ mm, $c_{(3)} = 0.4$; $z_{(4)} = 40$ mm, $c_{(4)} = 0.2$; cycle 2, $z_{(5)} = 50$ mm, $c_{(5)} = 1.0$ (heptane); cycle 3, $z_{(6)} = 60$ mm, $c_{(6)} = 1.0$ (toluene).

Solute	$R_{FG(calc)}$	$R_{FG(exp)}$	ΔR_{FG}
4-Dimethylaminoazobenzene	0.77	0.78	0.01
Indophenol Blue	0.45	0.44	0.01
Sudan Red G	0.49	0.50	0.01
Fat Green	0.80	0.67	0.13
Fat Orange	0.75	0.72	0.03
Blue Dark	0.74	0.63	0.11

the zone was compressed to a minimum width, which shows that the compression effects are stronger than dispersion spreading of the edges of the zone.

The results obtained indicate that the computer program for simulation in multiple development can be used for the preliminary optimization of separation conditions.

SYMBOLS

$c_{(i)}$ concentration of modifier for the ith step;

$k_{0(j)}$ capacity factor of solute j for unit concentration of modifier (pure modifier) for normal-phase systems and for $c_{(i)} = 0$ (pure water) for reversed-phase systems;

$k_{(i,j)}$ capacity factor of solute j for the ith step;

$m_{(j)}$ slope of the log–log plot for solute j;

$R_{F(i,j)}$ R_F value for solute j corresponding to the ith concentration of modifier;

$R_{FG(j)}$ final R_F value of solute j in gradient development;

v_0 void volume (see comment on v_e);

v_e elution volume [all values of v_0 and v_e are expressed as dimensionless magnitudes related to the void volume, v_e ($v_e = v_e'/v_0'$; $v_0 = v_0'/v_0' = 1$)];

TABLE VI

COMPARISON OF SIMULATED AND EXPERIMENTAL ZONE WIDTHS FOR MULTIPLE DEVELOPMENT

Solute: Fat Green. Distance of development: 50 mm.

Data	Parameter	Lower edge	Upper edge
Experimental	Starting position	0 mm	6 mm
	End position	43 mm	44 mm
	R_F (initial)	0.00	0.60
	R_F (final)	0.86	0.88
Calculated	Starting position	0 mm	6 mm
	End position	43.04 mm	43.41 mm

$y_{(i,j)}$ migration distance of solute j in the ith step;

$s_{(i,j)}$ total migration distance of solute j after i steps;

$z_{(i)}$ development distance of the ith step.

REFERENCES

1 C.F. Poole and S.K. Poole, *Chromatography Today*, Elsevier, Amsterdam, 1991.
2 F. Geiss, *Fundamentals of Thin Layer Chromatography (Planar Chromatography)*, Hüthig, Heidelberg, 1980.
3 D.E. Janchen and H.H. Issaq, *J. Liq. Chromatogr.*, 11 (1988) 1941.
4 H.J. Cortes (Editor), *Multidimensional Chromatography —Techniques and Applications*, Marcel Dekker, New York, 1990.
5 C.F. Poole and M.T. Belay, *J. Planar Chromatogr.*, 4 (1991) 345.
6 E. Soczewinski and W. Markowski, *J. Chromatogr.*, 370 (1986) 63.
7 W. Markowski, *J. Chromatogr.*, 485 (1989) 517.
8 W. Markowski, E. Soczewinski and G. Matysik, *J. Liq. Chromatogr.*, 10 (1987) 1261.
9 W. Markowski and E. Soczewinski, *J. Chromatogr.*, 623 (1992) 139.
10 J.A. Thoma, *Anal. Chem.*, 35 (1963) 214.
11 J.A. Perry, T.H. Jupille and L.J. Glunz, *Anal. Chem.*, 47 (1975) 65A.
12 L.R. Snyder and H. Poppe, *J. Chromatogr.*, 184 (1980) 363.
13 P.J. Schoenmakers, *Optimization of Chromatographic Selectivity*, Elsevier, Amsferdam, 1986, pp. 59–63.
14 T.H. Dzido and E. Soczewinski, *J. Liq. Chromatogr.*, 516 (1990) 461.
15 T.H. Dzido, *J. Planar Chromatogr.*, 3 (1990) 199.

Journal of Chromatography, 635 (1993) 291–306
Elsevier Science Publishers B.V., Amsterdam

CHROMSYMP. 2655

Capillary electrophoretic chiral separations with cyclodextrin additives

I. Acids: chiral selectivity as a function of pH and the concentration of β-cyclodextrin for fenoprofen and ibuprofen☆

Yasir Y. Rawjee, Daniel U. Staerk and Gyula Vigh*

Chemistry Department, Texas A&M University, MS-3255, College Station, TX 77843-3255 (USA)

(First received July 10th, 1992; revised manuscript received November 15th, 1992)

ABSTRACT

An equilibrium model has been developed to describe the pH and cyclodextrin concentration dependence of the electrophoretic mobilities as well as the chiral selectivities observed during the capillary electrophoretic separation of the enantiomers of weak acids. The parameters of the model can be readily derived from three specific sets of capillary electrophoretic experiments: cyclodextrin-free background electrolytes of varying pH values are used in the first set of experiments, background electrolytes with the same high pH but varying concentrations of cyclodextrin are used in the second set, and background electrolytes of the same low pH but with varying concentrations of cyclodextrin are used in the third set of experiments. The model has been tested with fenoprofen and ibuprofen as model substances and β-cyclodextrin as resolving agent, and an excellent agreement has been found between the calculated and the measured values. Baseline separations have been achieved for the enantiomers of both fenoprofen and ibuprofen in less than thirty minutes.

INTRODUCTION

Cyclodextrins (CDs) have been used extensively as chiral resolving agents in thin-layer chromatography [1], HPLC [2], GC [3], and recently, in electrophoretic separations [4–22], including micellar electrokinetic chromatography [4–6], isotachophoresis [7–17], free solution capillary electrophoresis (CE) [18–20], and capillary gel electrophoresis [21,22]. Though elegant chiral CE separations have been achieved with both native α-, β- and γ-cyclodextrins, as well as with peralkylated cyclodextrins, mostly heptakis(2,6-dimethyl-) and heptakis-(2,3,6-trimethyl)-β-cyclodextrins, the operational parameters and background electrolyte compositions which determine the success or failure of a particular separation have not been studied in great detail. Two reports [18,19] indicate that the migration time of a solute increases in a non-linear fashion while peak resolution passes through a maximum as the concentration of the native or derivatized cyclodextrin is increased in the background electrolyte. Another paper [21] used a modified

* Corresponding author.

☆ Presented at the *16th International Symposium on Column Liquid Chromatography, Baltimore, MD, June 14–19, 1992*. The majority of the papers presented at this symposium were published in *J. Chromatogr.*, Vols. 631 + 632 (1993).

0021-9673/93/$06.00

affinity electrophoresis model to describe chiral selectivity as a function of the cyclodextrin concentration in a capillary gel electrophoretic system that contained β- and γ-cyclodextrins incorporated into a polyacrylamide gel matrix. This particular model predicts that the solute migration times increase linearly, while the chiral selectivities increase non-linearly as the cyclodextrin concentration in the gel is increased. However, the effects of other operating parameters, most notably pH, were not studied.

The objective of this series of papers is to examine in detail the effects of the primary CE variables upon the selectivity and the efficiency of chiral CE separations. In this part, the effects of the pH and the concentration of cyclodextrin in the background electrolyte will be studied experimentally using non-steroidal antiinflammatory drugs, ibuprofen and fenoprofen, as model substances. A theoretical model, based on simultaneous multiple equilibria will be presented to account for the observed solute migration times, apparent and true solute mobilities, and chiral selectivities. It will be shown that for the substances studied, the chiral selectivities are at their highest values in low pH background electrolytes (where the acids are hardly dissociated at all), an entirely *non-intuitive* conclusion considering the coulombic nature of the CE separation process and our knowledge of the chiral separation of profens by HPLC on native β-cyclodextrin silica stationary phases [23].

THEORY

The model

In order to account for the effects of both the pH and the CD concentration of the background electrolyte on the mobility of the individual enantiomers and the resulting chiral separation selectivity, both protonation equilibria and complexation equilibria must be considered simultaneously.

Let us consider a background electrolyte which contains a weak acid, HB, and its conjugate base, B^-, as the buffer components and cyclodextrin, CD, as the chiral resolving agent. The enantiomers of the chiral weak acid analyte to be separated from each other are HR and HS. Let us assume that the analytical concentration of the buffer is much higher than that of either the CD or the enantiomers of the analyte, HR and HS. Cyclodextrin will form complexes with both components of the buffer and the analyte. When the concentration of the buffer is much higher than that of the CD and the concentration of the CD is much higher than that of the analyte, then practically all the CD will be tied up in the CD · buffer complex, unless the complex formation constants are uncharacteristically small. Because the analyte concentration is low with respect to that of the CD, and also, because there is a sufficiently high excess of uncomplexed buffer, the analytical concentration of CD is practically the same as the analytical concentration of the CD · buffer complexes, and remains more or less constant whether the analyte is present or not. Therefore, in a first approximation, the CD–buffer equilibria can be omitted from our considerations. For the sake of simplicity, the terms CD and [CD] will be used *in lieu of* the more proper, but cumbersome terms of CD · buffer complex and its concentration [CD · buffer].

Once in solution, both solute enantiomers, HR and HS, undergo acid dissociation according to eqns. 1 and 2:

$$HR + H_2O \rightleftarrows H_3O^+ + R^- \quad (1)$$

$$HS + H_2O \rightleftarrows H_3O^+ + S^- \quad (2)$$

Cyclodextrin will complex with both the protonated and the deprotonated forms of the analyte enantiomers:

$$HR + CD \rightleftarrows HRCD \quad (3)$$

$$HS + CD \rightleftarrows HSCD \quad (4)$$

$$R^- + CD \rightleftarrows RCD^- \quad (5)$$

$$S^- + CD \rightleftarrows SCD^- \quad (6)$$

The equilibrium expressions which describe these reactions are as follows:

$$K_{HR} = [R^-][H_3O^+]/[HR] \quad (7)$$

$$K_{HS} = [S^-][H_3O^+]/[HS] \quad (8)$$

$$K_{HRCD} = [HRCD]/[HR][CD] \quad (9)$$

$$K_{HSCD} = [HSCD]/[HS][CD] \quad (10)$$

$$K_{RCD^-} = [RCD^-]/[R^-][CD] \quad (11)$$

$$K_{SCD^-} = [SCD^-]/[S^-][CD] \quad (12)$$

The mass balance equations of the HR and the HS related species are, in terms of their analytical concentrations, c_{HR} and c_{HS}:

$$c_{HR} = [HR] + [R^-] + [HRCD] + [RCD^-] \quad (13)$$

$$c_{HS} = [HS] + [S^-] + [HSCD] + [SCD^-] \quad (14)$$

The respective mole fractions of the negatively charged species R^-, RCD^-, S^-, SCD^- are:

$$\alpha_{R^-} = [R^-]/c_{HR} \quad (15)$$

$$\alpha_{S^-} = [S^-]/c_{HS} \quad (16)$$

$$\alpha_{RCD^-} = [RCD^-]/c_{HR} \quad (17)$$

$$\alpha_{SCD^-} = [SCD^-]/c_{HS} \quad (18)$$

An analytical expression can be obtained from eqns. 7–12 for the species concentrations $[R^-]$, $[S^-]$, $[RCD^-]$, and $[SCD^-]$, as well as [HR], [HS], [HRCD], and [HSCD]. Substitution of these expressions into eqns. 13–18 yields:

$$\alpha_{R^-} = \frac{1}{1 + K_{RCD}\text{-}[CD] + \frac{[H_3O^+]}{K_{HR}}(1 + K_{HRCD}[CD])} \quad (19)$$

$$\alpha_{S^-} = \frac{1}{1 + K_{SCD}\text{-}[CD] + \frac{[H_3O^+]}{K_{HS}}(1 + K_{HSCD}[CD])} \quad (20)$$

$$\alpha_{RCD^-} = \frac{K_{RCD}\text{-}[CD]}{1 + K_{RCD}\text{-}[CD] + \frac{[H_3O^+]}{K_{HR}}(1 + K_{HRCD}[CD])} \quad (21)$$

$$\alpha_{SCD^-} = \frac{K_{SCD}\text{-}[CD]}{1 + K_{SCD}\text{-}[CD] + \frac{[H_3O^+]}{K_{HS}}(1 + K_{HSCD}[CD])} \quad (22)$$

The effective mobilities of the two enantiomers can be expressed as the sums of the mole fraction-weighted ionic mobilities of the respective species [24]:

$$\mu_R^{eff} = \mu_R^0\text{-}\alpha_{R^-} + \mu_{RCD}^0\text{-}\alpha_{RCD^-} \quad (23)$$

$$\mu_S^{eff} = \mu_S^0\text{-}\alpha_{S^-} + \mu_{SCD}^0\text{-}\alpha_{SCD^-} \quad (24)$$

Combining eqns. 19–22 with eqns. 23–24 we obtain:

$$\mu_R^{eff} = \frac{\mu_{R^-}^0 + \mu_{RCD}^0\text{-}K_{RCD}\text{-}[CD]}{1 + K_{RCD}\text{-}[CD] + \frac{[H_3O^+]}{K_{HR}}(1 + K_{HRCD}[CD])} \quad (25)$$

$$\mu_S^{eff} = \frac{\mu_{S^-}^0 + \mu_{SCD}^0\text{-}K_{SCD}\text{-}[CD]}{1 + K_{SCD}\text{-}[CD] + \frac{[H_3O^+]}{K_{HS}}(1 + K_{HSCD}[CD])} \quad (26)$$

or, after factoring out the ionic mobilities of the uncomplexed species, $\mu_{R^-}^0$ and $\mu_{S^-}^0$:

$$\mu_R^{eff} = \mu_{R^-}^0 \frac{1 + \frac{\mu_{RCD^-}^0}{\mu_{R^-}^0} K_{RCD}\text{-}[CD]}{1 + K_{RCD}\text{-}[CD] + \frac{[H_3O^+]}{K_{HR}}(1 + K_{HRCD}[CD])} \quad (27)$$

$$\mu_S^{eff} = \mu_{S^-}^0 \frac{1 + \frac{\mu_{SCD^-}^0}{\mu_{S^-}^0} K_{SCD}\text{-}[CD]}{1 + K_{SCD}\text{-}[CD] + \frac{[H_3O^+]}{K_{HS}}(1 + K_{HSCD}[CD])} \quad (28)$$

It can be seen that the effective solute mobility is a function of the ionic solute mobilities of both the free and the CD complexed species, the acid dissociation constants, the complex formation constants of both the ionic and the non-dissociated forms of the enantiomers, as well as the

pH and the CD concentration of the background electrolyte.

Separation selectivity (chiral selectivity, $A_{R/S}$, in this case) in CE can be expressed as the ratio of the effective mobilities [23]:

$$A_{R/S} = \frac{\mu_R^{eff}}{\mu_S^{eff}} \tag{29}$$

Substitution of eqns. 27–28 into eqn. 29 yields:

$$A_{R/S} = \frac{\mu^0_{R^-}}{\mu^0_{S^-}} \frac{1 + \frac{\mu^0_{RCD^-}}{\mu^0_{R^-}} K_{RCD^-}[CD]}{1 + \frac{\mu^0_{SCD^-}}{\mu^0_{S^-}} K_{SCD^-}[CD]} \cdot \frac{1 + K_{SCD^-}[CD] + \frac{[H_3O^+]}{K_{HS}}(1 + K_{HSCD}[CD])}{1 + K_{RCD^-}[CD] + \frac{[H_3O^+]}{K_{HR}}(1 + K_{HRCD}[CD])} \tag{30}$$

As long as the base background electrolyte (*sans* CD) behaves as an isotropic medium, the ionic mobilities of the two enantiomers are identical: $\mu^0_{R^-} = \mu^0_{S^-} = \mu^0_-$. The acid dissociation constants of the two enantiomers are also identical: $K_{HR} = K_{HS} = K_H$. Thus, eqn. 30 is simplified to:

$$A_{R/S} = \frac{1 + \frac{\mu^0_{RCD^-}}{\mu^0_-} K_{RCD^-}[CD]}{1 + \frac{\mu^0_{SCD^-}}{\mu^0_-} K_{SCD^-}[CD]} \frac{1 + K_{SCD^-}[CD] + \frac{[H_3O^+]}{K_H}(1 + K_{HSCD}[CD])}{1 + K_{RCD^-}[CD] + \frac{[H_3O^+]}{K_H}(1 + K_{HRCD}[CD])} \tag{31}$$

Eqn. 31 indicates that the chiral selectivity in a CD-based CE system depends on a combination of both thermodynamic parameters (solute specific parameters) and extensive parameters (operator-dependent parameters). The solute specific parameters include the ionic mobilities of the free and the complexed enantiomers (μ^0_-, $\mu^0_{RCD^-}$ and $\mu^0_{SCD^-}$), the acid dissociation constant of the analyte (K_H), the complex formation constants of the ionic enantiomers (K_{RCD^-} and K_{SCD^-}), and the complex formation constants of the protonated enantiomers (K_{HRCD} and K_{HSCD^-}). The operator-dependent extensive parameters are the CD concentration and the pH of the background electrolyte.

Discussion of the model

It can be seen from eqn. 31 that in CD-based chiral CE separations chiral selectivity varies according to three fundamentally different situations depending on whether (i) only the non-ionic forms of the two enantiomers, (ii) only the ionic forms of the two enantiomers, or (iii) both forms of the two enantiomers interact differently with CD.

Type I enantiomers. The separation of Type I enantiomers is the easiest to achieve. Because only the non-ionic forms of the enantiomers interact differently with CD, K_{RCD^-} and K_{SCD^-} are identical. In all probability, $\mu^0_{RCD^-}$ and $\mu^0_{SCD^-}$ are also identical:

$$K_{RCD^-} = K_{SCD^-} = K_{ACD^-} \tag{32}$$

$$\mu^0_{RCD^-} = \mu^0_{SCD^-} = \mu^0_{ACD^-} \tag{33}$$

Thus, the first term of eqn. 31 is reduced to unity, and the $A_{R/S}$ expression is simplified to:

$$A_{R/S} = \frac{1 + K_{ACD^-}[CD] + \frac{[H_3O^+]}{K_H}(1 + K_{HSCD}[CD])}{1 + K_{ACD^-}[CD] + \frac{[H_3O^+]}{K_H}(1 + K_{HRCD}[CD])} \tag{34}$$

It can be seen that the value of the chiral selectivity factor will be different from unity and its magnitude will depend on the values of K_{HRCD}, K_{HSCD}, K_{ACD^-}, K_H, [CD] and pH. If [CD] = 0, $A_{R/S}$ is reduced to unity: there is no chiral separation because the resolving agent, CD, is not present. $A_{R/S}$ changes monotonously as the hydronium ion and the cyclodextrin concentrations are increased. The migration order of the enantiomers cannot be changed by varying either the concentration of CD or the pH. The theoretical chiral selectivity maximum, $A_{R/S} = K_{HSCD}/K_{HRCD}$ can be realized when the "selective complexation" terms (the third term in both

the numerator and the denominator) become much larger than the "parasitic complexation" terms (second term in both the numerator and the denominator) as the concentrations of CD and H_3O^+ are increased *ad infinitum*. This limiting value can be approximated reasonably closely as soon as

$$\frac{[H_3O^+]}{K_H}(1 + K_{HSCD}[CD]) \geq 100(1 + K_{ACD^-}[CD]) \quad (35)$$

i.e.

$$K_{HSCD} \geq \frac{100K_H - [H_3O^+]}{[H_3O^+][CD]} + \frac{100K_H}{[H_3O^+]} K_{ACD^-} \quad (36)$$

If the hydronium concentration is expressed as a multiple of the acid dissociation constant value,

$$[H_3O^+] = nK_H \quad (37)$$

(*i.e.*, $pH = pK_H - \log n$), then eqn. 36 becomes

$$K_{HSCD} \geq \frac{100 - n}{n[CD]} + \frac{100}{n} K_{ACD^-} \quad (38)$$

By taking [CD] = 15 m*M*, a conservative value that can be safely maintained yet one that is close to the solubility limit of β-CD, the highest pH values that lead to maximized chiral selectivities at the fastest migration rates can be calculated from eqn. 38. A few representative K_{HSCD}, K_{ACD^-} and pH combinations are listed in Table I. The minimum K_{HSCD} requirement outlined in rows 1 and 2 of Table I is often fulfilled for Type I chiral acids (*vide infra*) resulting in a simple expression for chiral selectivity:

$$A_{R/S} = \frac{1 + K_{HSCD}[CD]}{1 + K_{HRCD}[CD]} \quad (39)$$

These considerations explain the surprising, non-intuitive, but valid observation that in certain CE separations of chiral weak acids, chiral selectivity increases with decreasing pH, because the parasitic non-selective complexation of the ionic enantiomers is reduced as the ionic species is gradually turned into the selectively complexing nonionic species. In the case of Type I enantiomers there is no reversal in the migration order, *i.e.* $A_{R/S}$ only varies between unity and its maximum value. This makes optimization of the separation simple: the pH of the background electrolyte must be decreased until the selectivity becomes sufficiently high so that the desired peak resolution is realized with the available separation efficiency resulting, automatically, in the shortest possible separation time. Any pH lower than that will result in very rapidly increasing separation time.

TABLE I

REPRESENTATIVE COMPLEXATION CONSTANT AND MAXIMUM pH VALUE PAIRS LEADING TO MAXIMUM CHIRAL SELECTIVITY FOR TYPE I AND TYPE II WEAK ACIDS

n	pH	Type I acid, minimum K_{HSCD} at [CD] = 15 m*M*	Type II acid, minimum K_{HACD} at [CD] = 15 m*M*
1000	$pK_H - 3$	$0.1K_{ACD^-} - 60$	$0.1K_{SCD^-} - 60$
100	$pK_H - 2$	K_{ACD^-}	K_{SCD^-}
10	$pK_H - 1$	$600 + 10K_{ACD^-}$	$600 + 10K_{SCD^-}$
1	pK_H	$6600 + 100K_{ACD^-}$	$6600 + 100K_{SCD^-}$

Type II enantiomers. The separation of Type II enantiomers is more difficult to achieve. Because only the dissociated forms of the enantiomers interact differently with CD, K_{HRCD} and K_{HSCD} are identical:

$$K_{HRCD} = K_{HSCD} = K_{HACD} \quad (40)$$

$\mu^0_{RCD^-}$ and $\mu^0_{SCD^-}$ may be equal or different, depending on the volume of the respective ionic enantiomer · CD complex. Thus, eqn. 35 is simplified only slightly:

$$A_{R/S} = \frac{1 + \frac{\mu^0_{RCD^-}}{\mu^0_-} K_{RCD^-}[CD]}{1 + \frac{\mu^0_{SCD^-}}{\mu^0_-} K_{SCD^-}[CD]} \cdot \frac{1 + K_{SCD^-}[CD] + \frac{[H_3O^+]}{K_H}(1 + K_{HACD}[CD])}{1 + K_{RCD^-}[CD] + \frac{[H_3O^+]}{K_H}(1 + K_{HACD}[CD])} \quad (41)$$

Note that the R enantiomer related values are in the numerator in the first term and in the denominator in the second term of eqn. 41. Therefore, $A_{R/S} < 1$, $A_{R/S} = 1$, and $A_{R/S} > 1$ are possible depending on the relative values of the equilibrium constants and the ionic mobilities, as well as the hydronium and the cyclodextrin concentrations. This also means that the migration order of the enantiomers can be reversed by varying the concentrations of the CD and the hydronium ion.

For Type II enantiomers chiral selectivity can be maximized by forcing the entire second term in eqn. 41 to assume a value of unity. This can be achieved by increasing the value of the non-selective complexation term relative to the selective complexation term by increasing the concentration of the hydronium ion, *i.e.*:

$$\frac{[H_3O^+]}{K_H}(1 + K_{HACD}[CD]) \geq 100(1 + K_{SCD^-}[CD]) \quad (42)$$

or

$$K_{HACD} \geq \frac{100K_H - [H_3O^+]}{[H_3O^+][CD]} + \frac{100K_H}{[H_3O^+]} K_{SCD^-} \quad (43)$$

If the hydronium concentration is once again expressed as a multiple of the acid dissociation constant value as in eqn. 37 (*i.e.* $pH = pK_H - \log n$), eqn. 43 becomes:

$$K_{HACD} \geq \frac{100 - n}{n[CD]} + \frac{100}{n} K_{SCD^-} \quad (44)$$

Except for the different subscripts, this relation is formally analogous to the one in eqn. 38. By taking once again [CD] = 15 mM, the highest pH values that lead to maximized chiral selectivities for Type II acids can be calculated from eqn. 44. A few representative K_{HACD}, K_{SCD^-} and pH combinations are listed in Table I. Once again, the minimum K_{HACD} requirement shown in rows 1 and 2 of the last column of Table I is easily fulfilled for Type II chiral acids (see below) resulting in a reasonably simple expression for chiral selectivity:

$$A_{R/S} = \frac{1 + \frac{\mu^0_{RCD^-}}{\mu^0_-} K_{RCD^-}[CD]}{1 + \frac{\mu^0_{SCD^-}}{\mu^0_-} K_{SCD^-}[CD]} \quad (45)$$

Again, these considerations explain the surprising, non-intuitive, but valid observation that in certain CE separations of chiral weak acids, chiral selectivity increases with decreasing pH. However, chiral selectivities are generally lower than those seen for Type I acids, because unlike in eqn. 39, the selective complexation terms ($K_{RCD^-}[CD]$ and $K_{SCD^-}[CD]$) are now multiplied by the mobility ratios ($\mu^0_{RCD^-}/\mu^0_-$ and $\mu^0_{SCD^-}/\mu^0_-$), which are generally around 0.1 or lower due to the larger size of the cyclodextrin-complexed enantiomer. This decreases the effect of the selective complexation terms with respect to 1 both in the numerator and the denominator. Optimization of the separation is still simple: the pH of the background electrolyte must be decreased until the selectivity becomes sufficiently high so that the desired peak resolution is realized with the available separation efficiency.

However, in the case of Type II acids, there is another alternative that could lead to chiral resolution, namely one could suppress the pH dependent part of second term in eqn. 41. This would occur when

$$1 + K_{SCD^-}[CD] \geq 100\frac{[H_3O^+]}{K_H}(1 + K_{HACD}[CD]) \quad (46)$$

that is, when

$$K_{SCD^-} \geq \frac{100[H_3O^+] - K_H}{K_H[CD]} + \frac{100[H_3O^+]}{K_H} K_{HACD} \quad (47)$$

Using the same $[H_3O^+] = nK_H$ approach as before, eqn. 47 becomes:

$$K_{SCD^-} \geq \frac{100n - 1}{[CD]} + 100nK_{HACD} \quad (48)$$

By taking [CD] = 15 mM, the lowest pH values that also lead to alternative maximized chiral selectivities, albeit possibly at altered migration orders, can be calculated from eqn. 48. A few

TABLE II

REPRESENTATIVE COMPLEXATION CONSTANT AND MINIMUM pH VALUE PAIRS LEADING TO ALTERNATIVE MAXIMUM CHIRAL SELECTIVITIES FOR TYPE II WEAK ACIDS

n	pH	Minimum K_{SCD^-} at [CD] = 15 mM
1	pK_H	$6600 + 100K_{HACD}$
0.1	$pK_H + 1$	$600 + 10K_{HACD}$
0.01	$pK_H + 2$	K_{HACD}
0.001	$pK_H + 3$	$0.1K_{HACD} - 60$

representative K_{HACD}, K_{SCD^-} and pH combinations are listed in Table II. Only the minimum K_{SCD^-} requirement shown in the last row of Table II is likely to occur in practice. In this case the expression for chiral selectivity becomes:

$$A_{R/S} = \frac{1 + \frac{\mu^0_{RCD^-}}{\mu^0_-} K_{RCD^-}[CD]}{1 + \frac{\mu^0_{SCD^-}}{\mu^0_-} K_{SCD^-}[CD]} \frac{1 + K_{SCD^-}[CD]}{1 + K_{RCD^-}[CD]} \quad (49)$$

Because the less-than-unity mobility ratio multipliers ($\mu^0_{RCD^-}/\mu^0_-$ and $\mu^0_{SCD^-}/\mu^0_-$) are absent in the second term of eqn. 49, chances are that the $A_{R/S}$ value will be dominated by the second term meaning that in the high pH background electrolyte the migration order of the enantiomers will be reversed with respect to the one observed at low pH. However, unless this reversal is very important for a particular analysis, the use of the high pH background electrolyte is disadvantageous, because the two terms in eqn. 49 counteract each other resulting in a chiral selectivity that is lower than what could have been achieved in the low pH electrolyte (eqn. 45).

Type III enantiomers. The separation of Type III enantiomers is the most difficult of all to predict. Because both the dissociated and non-dissociated forms of the enantiomers interact differently with CD, eqn. 31 cannot be simplified and an *a priori* selection of the "best" background electrolyte pH is not possible. The migration order may change as either the pH or the CD concentration is varied. These reversals, as well as the actual selectivities, depend on the particular set of complex formation constants and ionic mobilities. A detailed study of the pH is essential if the optimum separation conditions are to be determined. However, from a practical point of view, the use of a low-pH electrolyte seems the most promising approach, because this would maximize the value of the second term in eqn. 31.

Determination of the model parameters

Generally, only μ^0_- and K_H are available of the model parameters, if at all. However, reasonable parameter estimates can be obtained from specifically designed sets of experiments and a few simple assumptions, as follows.

If there is no cyclodextrin in the background electrolyte, then the effective ionic mobilities and the acid dissociation constants of the two enantiomers are identical and both can be determined from electropherograms taken at different pH values. Specifically, when [CD] = 0, eqns. 27 and 28 are simplified to eqn. 50:

$$\frac{\mu^{eff}_-}{\mu^0_-} = \frac{\mu^{eff}_R}{\mu^0_{R^-}} = \frac{\mu^{eff}_S}{\mu^0_{S^-}} = \frac{1}{1 + \frac{[H_3O^+]}{K_{HR}}} = \frac{1}{1 + \frac{[H_3O^+]}{K_{HS}}} = \frac{K_H}{K_H + [H_3O^+]} \quad (50)$$

or:

$$\frac{1}{\mu^{eff}_-} = \frac{1}{\mu^0_-} + \frac{[H_3O^+]}{\mu^0_- K_H} \quad (51)$$

from which the μ^0_- and the K_H values can be determined by plotting $1/\mu^{eff}_-$ as a function of $[H_3O^+]$. Naturally, μ^{eff}_- is calculated by correcting the observed mobilities with the electroosmotic mobilities.

When $pH = pK_H + 3$, $[HR] \ll [R^-]$ and $[HS] \ll [S^-]$, then eqns. 13 and 14 become:

$$c_R = [R^-] + [RCD^-] \quad (52)$$

$$c_S = [S^-] + [SCD^-] \quad (53)$$

and with these, eqns. 19–22 simplify to:

$$\alpha^*_{R^-} = \frac{[R^-]}{[R^-]+[RCD^-]} = \frac{1}{1+K_{RCD^-}[CD]} \quad (54)$$

$$\alpha^*_{S^-} = \frac{[S^-]}{[S^-]+[SCD^-]} = \frac{1}{1+K_{SCD^-}[CD]} \quad (55)$$

$$\alpha^*_{RCD^-} = \frac{[RCD^-]}{[R^-]+[RCD^-]} = \frac{K_{RCD^-}[CD]}{1+K_{RCD^-}[CD]} \quad (56)$$

$$\alpha^*_{SCD^-} = \frac{[SCD^-]}{[S^-]+[SCD^-]} = \frac{K_{SCD^-}[CD]}{1+K_{SCD^-}[CD]} \quad (57)$$

Substitution into eqns. 23–24 yields:

$$\mu_R^{eff} = \mu^0_{R^-}\alpha^*_{R^-} + \mu^0_{RCD^-}\alpha^*_{RCD^-} = \frac{\mu^0_{R^-} + \mu^0_{RCD^-}K_{RCD^-}[CD]}{1+K_{RCD^-}[CD]} \quad (58)$$

$$\mu_S^{eff} = \mu^0_{S^-}\alpha^*_{S^-} + \mu^0_{SCD^-}\alpha^*_{SCD^-} = \frac{\mu^0_{S^-} + \mu^0_{SCD^-}K_{SCD^-}[CD]}{1+K_{SCD^-}[CD]} \quad (59)$$

If $K_{RCD^-}[CD] \gg 1$ and $K_{SCD^-}[CD] \gg 1$, and the CD concentration is close to saturation (18 mM), that is, the enantiomer anions are sufficiently strongly complexed by CD ($K_{RCD^-} \geq 500$), then eqns. 58 and 59 can be rearranged to yield:

$$\mu_R^{eff} = \frac{\mu^0_{R^-}}{K_{RCD^-}} \cdot \frac{1}{[CD]} + \mu^0_{RCD^-} \quad (60)$$

$$\mu_S^{eff} = \frac{\mu^0_{S^-}}{K_{SCD^-}} \cdot \frac{1}{[CD]} + \mu^0_{SCD^-} \quad (61)$$

Both $\mu^0_{RCD^-}$ and K_{RCD^-} can be determined by plotting μ_R^{eff} and μ_S^{eff} as a function of 1/[CD], because μ^0_- is known from the previous calculations. With these values K_{HRCD} and K_{HSCD} can be obtained explicitly from eqns. 27 and 28 as:

$$K_{HRCD} = \frac{K_H}{[H_3O^+][CD]\mu_R^{eff}} \left((\mu^0_- - \mu_R^{eff}) + K_{RCD^-}[CD](\mu^0_{RCD^-} - \mu_R^{eff}) - \frac{[H_3O^+]}{K_H}\mu_R^{eff} \right) \quad (62)$$

$$K_{HSCD} = \frac{K_H}{[H_3O^+][CD]\mu_S^{eff}} \left((\mu^0_- - \mu_S^{eff}) + K_{SCD^-}[CD](\mu^0_{SCD^-} - \mu_S^{eff}) - \frac{[H_3O^+]}{K_H}\mu_S^{eff} \right) \quad (63)$$

If, on the other hand, $K_{RCD^-}[CD] \ll 1$ and $K_{SCD^-}[CD] \ll 1$, while the CD concentration is close to saturation (18 mM), that is, the enantiomer anions are very weakly complexed by CD ($K_{RCD^-} \leq 5$), then eqns. 58 and 59 can be rearranged to yield:

$$\mu_R^{eff} = \mu^0_{R^-} + \mu^0_{RCD^-}K_{RCD^-}[CD] \quad (64)$$

$$\mu_S^{eff} = \mu^0_{S^-} + \mu^0_{SCD^-}K_{SCD^-}[CD] \quad (65)$$

from which the multiples $\mu^0_{RCD^-}K_{RCD^-}$ and $\mu^0_{SCD^-}K_{SCD^-}$ can be determined. Assuming that $[H_3O^+] \geq 100K_H$, and that $K_{HRCD}[CD] \gg 1$, substitution of these multiples into eqns. 27 and 28 results in eqns. 66 and 67,

$$\frac{\mu_R^{eff}[H_3O^+]}{K_H} = \frac{\mu^0_-}{K_{HRCD}} \cdot \frac{1}{[CD]} + \frac{\mu^0_{RCD^-}K_{RCD^-}}{K_{HRCD}} \quad (66)$$

$$\frac{\mu_S^{eff}[H_3O^+]}{K_H} = \frac{\mu^0_-}{K_{HSCD}} \cdot \frac{1}{[CD]} + \frac{\mu^0_{SCD^-}K_{SCD^-}}{K_{HSCD}} \quad (67)$$

which permit the determination of K_{HRCD} and K_{HSCD} from plots of the effective mobilities observed at low pH as a function of 1/[CD].

Once the ionic mobilities, the acid dissociation constants, and the complex formation constants are known, the effective mobilities of the individual enantiomers and the chiral selectivity of the given system can be calculated using eqns. 27 and 28 and 31. The calculated values then can be compared with the measured values to test the validity of the model proposed here. Also, the trends observed in these calculations can be used to predict the directions in which the background electrolyte parameters should be changed in order to achieve (or improve) a particular chiral CE separation.

EXPERIMENTAL

Two electrophoretic systems were used for these experiments. The first unit was built in our laboratory according to Jorgenson *et al.* [25] using a Model 200 variable UV detector (Linear Instruments, Reno, NV, USA), a Model PS/EH30R03.0 high-voltage power supply (Glassman, Whitehouse Station, NJ, USA), a custom-designed dual-loop liquid thermostatting system, a Perspex-glass safety box, a 1-kΩ resistor and an Omniscribe strip chart recorder (Industrial Scientific, Austin, TX, USA) to monitor the current during the separation, a Chrom-1 AT data acquisition board (Keithley-Metrabyte, Tauton, MA, USA) installed in a 386SX-20 NEC personal computer, and our ChromPlot1 data acquisition–data analysis software [26]. The second unit was a commercial electrophoretic instrument, a P/ACE 2100 system, equipped with a variable wavelength UV detector (Beckman Instruments, Fullerton, CA, USA). The electrode at the injection end of the capillary was kept at negative potential; the electrode at the detector end of the capillary was at ground potential.

Untreated, 25 μm I.D., 150 μm O.D. fused-silica capillaries (Polymicro Technologies, Phoenix, AZ, USA) were used in both systems (35 cm from injector to detector, 40 cm total length in the custom-built unit, 39 cm from injector to detector, 45.8 cm total length in the P/ACE unit). Before each and every series of measurements the capillaries were washed with 1 *M* NaOH, rinsed by deionized water and equilibrated by the background electrolyte (5 min, 5 min and 15 min, respectively).

The samples were injected electrokinetically; the injection and separation potentials were identical. The sample concentrations were kept at minimum (generally less than 0.1 m*M*) and the injection time was varied to insure similar sample loadings. In each run, a non-charged electroosmotic flow marker (a dilute solution of nitromethane) was injected at the detector end of the capillary at the same time that the sample was injected at the injection end, providing us with the accurate corrected mobilities. All separations were completed at a thermostatting liquid bath temperature of 37 °C. The UV detectors were set at 209 nm in the home-built unit and 214 nm in the P/ACE unit.

The field strength used for the separations was varied between 150 V/cm and 750 V/cm, depending on the actual conductivity of the background electrolyte. Power dissipation was kept in the 80 to 100 mW range to insure linear potential *vs.* current plots (Ohm-plots).

Native β-cyclodextrin was obtained from American Maize Products Corporation (Hammond, IN, USA). Reagent-grade morpholinoethanesulfonic acid monohydrate (MES), sodium hydroxide, racemic and *S*(+)-ibuprofen (IBU) were obtained from Aldrich (Milwaukee, WI, USA), racemic fenoprofen (FEN) from Sigma (St. Louis, MO, USA), 250MHR PA hydroxyethyl cellulose (HEC) from Aqualon Company (Wilmington, DE, USA). All chemicals were used as received without further purification. All solutions were freshly prepared using deionized water from a Millipore Q unit (Millipore, Milford, MA, USA). The background electrolytes were prepared by weighing the required amount of MES, CD and HEC into a volumetric flask. The flask was first filled with deionized water to 90% of its final capacity, stirred until all the components were dissolved, degassed, and made up almost to mark. Then the pH was adjusted to the desired value by adding a few μl of a 10 *M* NaOH solution and the flask was made up to mark with deionized water. The background electrolyte was degassed again prior to loading into the electrolyte reservoirs.

RESULTS AND DISCUSSION

In order to learn how chiral selectivity depends on the composition of the complex background electrolyte, and to test the validity of the model presented in the Theory section, the parameters were varied individually in small increments, over relatively broad ranges, while all the other parameters were kept constant providing a very precise description of both mobility and chiral selectivity.

The acid dissociation constants, K_H of fenoprofen and ibuprofen were determined using background electrolytes which contained 0.2%

(w/w) HEC and 200 m*M* MES. The pH of the background electrolyte was varied in the 4.1 to 7.1 range by adding NaOH. The effective mobilities of ibuprofen and fenoprofen, corrected for the electroosmotic flow, μ_-^{eff}, were determined in triplicate. The reciprocal effective mobilities are plotted in Figs. 1 and 2 as a function of the hydronium ion concentration according to eqn. 51, for a power load of 95 mW and thermostatting liquid temperature of 37°C.

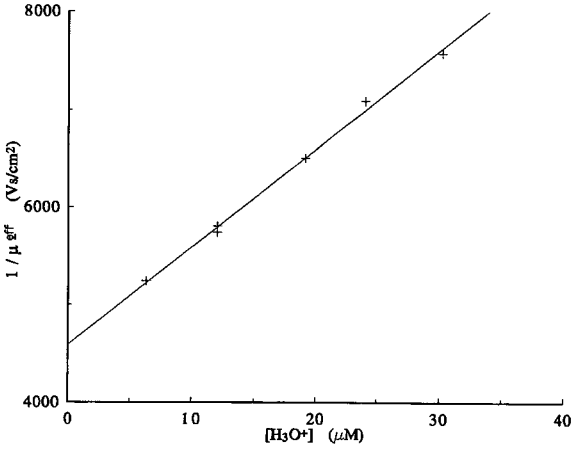

Fig. 1. Reciprocal effective mobility *vs.* hydronium ion concentration plot for fenoprofen in 200 m*M* MES, 0.2% HEC background electrolyte at a thermostatting liquid temperature of 37°C and power load of 95 mW. + = Measured values; solid line = least-square best fit line.

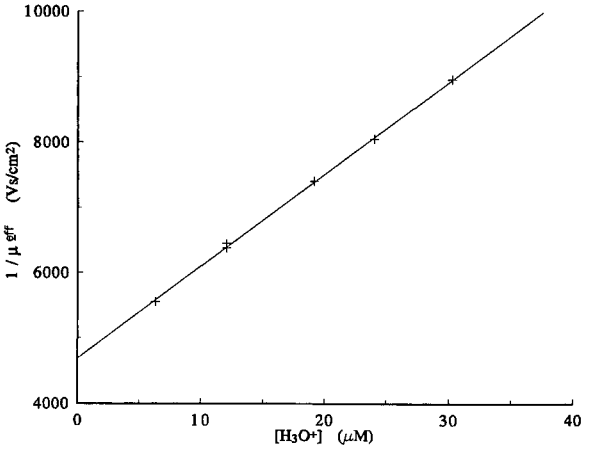

Fig. 2. Reciprocal effective mobility *vs.* hydronium ion concentration plot for ibuprofen. Conditions as in Fig. 1. + = Measured values; solid line = least-square best fit line.

The solid lines represent the least-square best fit lines. The ionic mobilities, μ_-^0, and acid dissociation constant values, K_H, are listed in the first four lines of Table III, along with the literature values of K_H determined at 25°C in pure aqueous solutions [27].

Because the background electrolytes used in these studies have a high concentration (in excess of 100 m*M*), accurate activity coefficient values cannot be calculated using the simple Debye–Hückel approach suggested by Beckers *et al.* [28]. In addition, ibuprofen was reported to adsorb on hydroxyalkylated cellulose [29] dissolved in an electrolyte. Therefore, the acid dissociation constants determined in our measurements are concentration-based apparent dissociation constants, rather than thermodynamic, infinite dilution values. No ionic mobility values were found in the literature for fenoprofen and ibuprofen. However, the measured mobilities compare favorably with the ionic mobility of the structurally similar 4-*tert.*-butylbenzoic acid, $\mu_-^0 = 23.2 \cdot 10^{-5}$ cm^2/Vs, as reported by Hirokawa *et al.* [30].

Next, the effects of cyclodextrin concentration were tested in a high-pH (pH = 7.1) background electrolyte in which both fenoprofen and ibuprofen were almost completely dissociated. When the effective mobilities were plotted against the reciprocal CD concentration accord-

TABLE III

IONIC MOBILITY AND APPARENT EQUILIBRIUM CONSTANT DATA FOR FENOPROFEN AND IBUPROFEN

Conditions as in Figs. 1 to 4.

Parameter	Fenoprofen	Ibuprofen
μ_-^0 (10^{-5} cm^2/Vs)	21.77 ± 0.03	21.32 ± 0.05
K_H	$(4.57 \pm 0.14) \cdot 10^{-5}$	$(3.31 \pm 0.05) \cdot 10^{-5}$
pK_H	4.34	4.48
pK_H [27]	4.50	5.10
$\mu^0_{RCD^-} = \mu^0_{SCD^-}$ (10^{-5} cm^2/Vs)	6.54 ± 0.05	6.60 ± 0.04
$K^0_{RCD^-} = K^0_{SCD^-}$	325 ± 7	1280 ± 5
K_{HRCD}	608 ± 18	1869 ± 48
K_{HSCD}	636 ± 20	1954 ± 49

ing to eqns. 60 and 61, estimates could be obtained for $\mu^0_{RCD^-}$, $\mu^0_{SCD^-}$, $K^0_{RCD^-}$ and $K^0_{SCD^-}$ from the limiting slopes and the intercepts. These estimates were then used to find the best fit between the measured values and the values calculated by eqns. 58 and 59. The $\mu^0_{RCD^-}$, $\mu^0_{SCD^-}$, $K^0_{RCD^-}$ and $K^0_{SCD^-}$ parameters obtained for both fenoprofen and ibuprofen are listed in Table III. The effective mobilities calculated by eqns. 58 and 59 and the best-fit parameters are shown in Figs. 3 and 4 as solid lines. The agreement between the measured and calculated values is very good.

Table III shows that the limiting ionic mobilities of the CD-complexed fenoprofen and ibuprofen are almost identical, in agreement with the observation that at high pH these complexed ions co-migrate. The complex formation constant for fenoprofen is almost four times lower than that of the ibuprofen. This relationship is reminiscent of the retention trend that were observed on β-cyclodextrin silica columns (Cyclobond I, ASTEC, Whippany, NJ, USA), when these columns were operated with high-pH eluents in the reversed-phase mode [23,31,32].

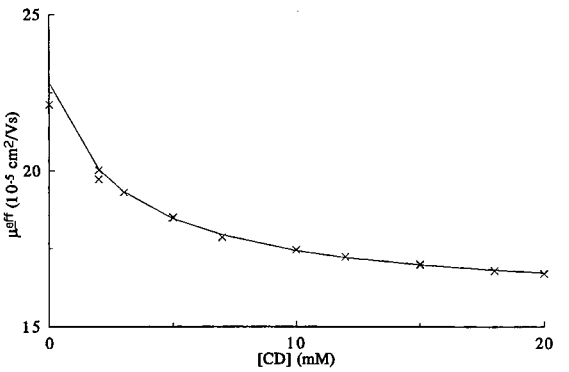

Fig. 3. Effective ionic mobility of fenoprofen as a function of the β-cyclodextrin concentration in a pH = 7.1 background electrolyte. Conditions as in Fig. 1. + = Measured values; solid line = calculated values using the parameters in Table III.

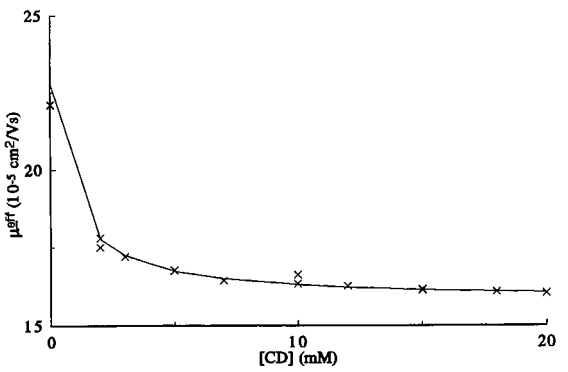

Fig. 4. Effective ionic mobilities of ibuprofen as a function of the β-cyclodextrin concentration in a pH = 7.1 background electrolyte. Conditions as in Fig. 1. + = Measured values; solid line = calculated values using the parameters in Table III.

Finally, a series of mobility measurements were carried out in a pH 4.52 background electrolyte in which both fenoprofen and ibuprofen are only partially dissociated. The CD concentration was varied between 0 and 18 m*M* while all other conditions were kept the same as in Figs. 3 and 4. In another series of measurements the CD concentration was kept constant at 15 m*M*, while the pH of the background electrolyte was varied between 4.0 and 5.6. The complex formation constants of the non-dissociated profen enantiomers (K_{HRCD}, K_{HSCD}) were calculated using the effective mobility values, eqns. 62 and 63, the respective parameters from the first six lines of Table III, and the actual [CD] and [H_3O^+] values. The results are listed in the last two lines of Table III. Interestingly, the complex formation constants of both protonated profens (K_{HRCD}, K_{HSCD}) are about two times larger than the respective complexation constants of the anions ($K^0_{RCD^-}$, $K^0_{SCD^-}$). This behavior is once again similar to what has been observed recently in the HPLC separation of profens on various cyclodextrin silica stationary phases, namely that in organic modifier-free eluents the protonated profens are retained more strongly than the respective anions [31,32].

In order to test the validity of the electrophoretic migration and chiral selectivity model presented here, the effective mobility and chiral selectivity values were calculated using eqns. 27, 28 and 31, the ionic mobilities, the acid dissociation constants, and the complex formation constants listed in Table III. The mobility data for fenoprofen and ibuprofen are compared with the measured values in Figs. 5 to 8, while the three-dimensional electrophoretic mobility surfaces are shown in Figs. 9 and 10. The chiral selectivity data for fenoprofen and ibuprofen are compared

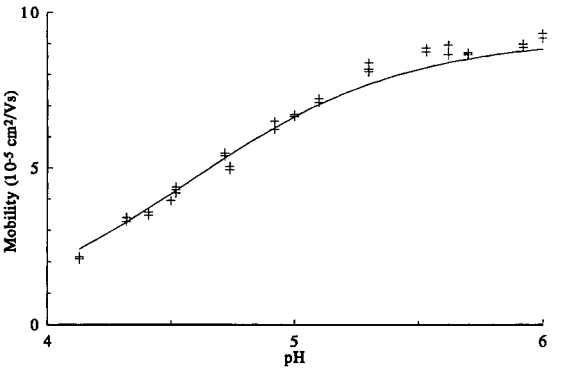

Fig. 5. Comparison of the measured and calculated effective mobilities for the more mobile enantiomer of fenoprofen as a function of the pH. Conditions as in Fig. 3, except [CD] = 15 m*M*. + = Measured values; solid line = calculated values using eqn. 27 and the parameters in Table III.

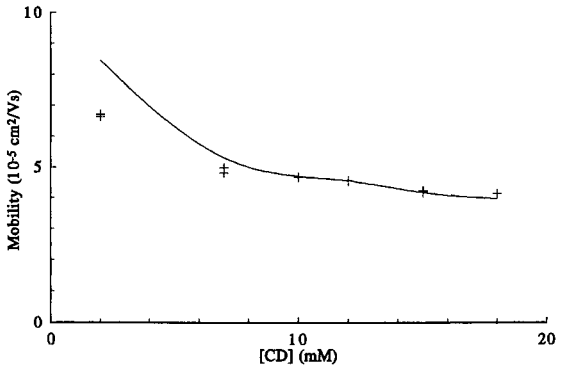

Fig. 6. Comparison of the measured and calculated effective mobilities for the more mobile enantiomer of fenoprofen as a function of the CD concentration. Conditions as in Fig. 3, except $4.50 < pH < 4.53$. + = Measured values; solid line = calculated values using eqn. 27 and the parameters in Table III.

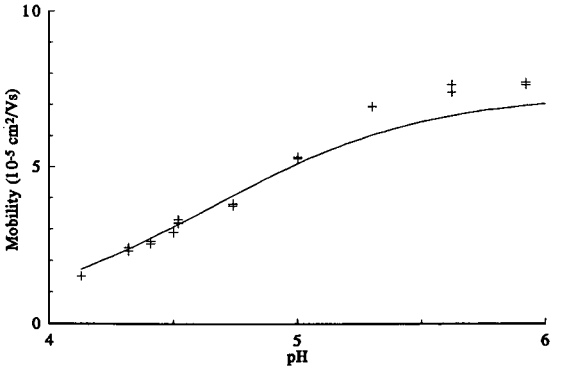

Fig. 7. Comparison of the measured and calculated effective mobilities for the more mobile enantiomer of ibuprofen as a function of the pH. Conditions as in Fig. 3, except [CD] = 15 m*M*. + = Measured values; solid line = calculated values using eqn. 27 and the parameters in Table III.

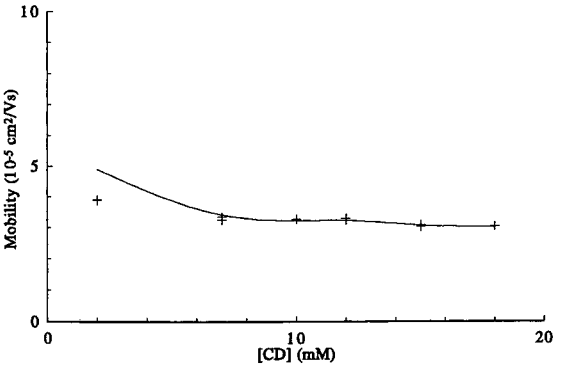

Fig. 8. Comparison of the measured and calculated effective mobilities for the more mobile enantiomer of ibuprofen as a function of the CD concentration. Conditions as in Fig. 3, except $4.50 < pH < 4.53$. + = Measured values; solid line = calculated values using eqn. 27 and the parameters in Table III.

with the measured values in Figs. 11 to 14, while the three-dimensional selectivity surfaces are shown in Figs. 15 and 16.

In all the plots the symbol + stands for the measured values while the continuous line represents the calculated values. It can be seen from Figs. 5–8 and 11–14 that the agreement between the measured and the calculated values is indeed excellent.

The electrophoretic mobility surface is shown from two different viewpoints for fenoprofen (Fig. 9) and ibuprofen (Fig. 10). It can be seen that the surface is strongly curved for both solutes: the mobility decreases rapidly as CD is added to the background electrolyte, but then it levels off above [CD] = 10 m*M*. On the pH axis, most of the mobility change occurs in the $pK_H - 1 < pH < pK_H + 1$ range (where the mobility surface is shaped like a regular mole fraction function).

In the $pH > 5.5$ range, the calculated selectivity values seem to be slightly higher than the measured values (Figs. 11 and 13). This is due to the fact that in the actual electropherograms the peaks of the enantiomers are no longer resolved when the chiral selectivity decreases below

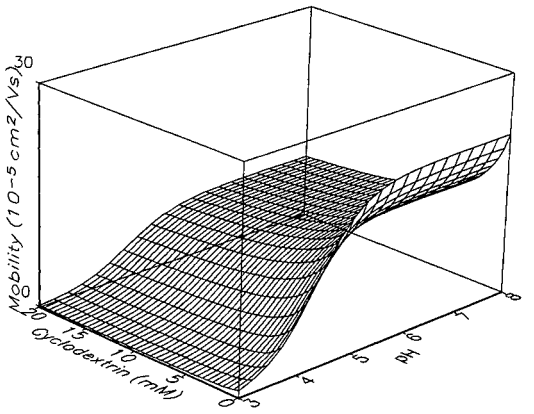

Fig. 9. Three-dimensional effective mobility surface for the more mobile enantiomer of fenoprofen as a function of the CD concentration and the pH, calculated using eqn. 27 and the parameters in Table III.

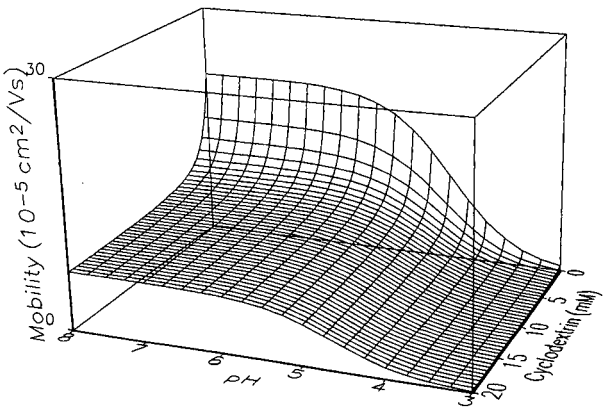

Fig. 10. Three-dimensional effective mobility surface for the more mobile enantiomer of ibuprofen as a function of the CD concentration and the pH, calculated using eqn. 27 and the parameters in Table III.

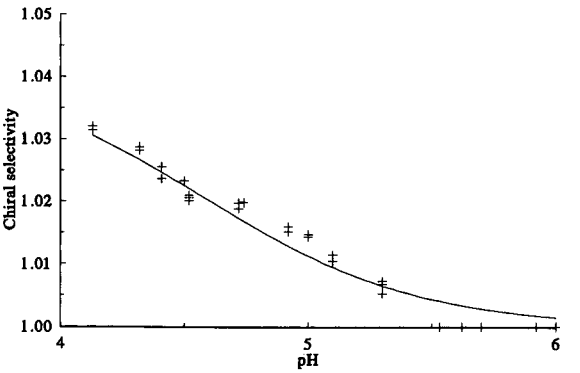

Fig. 11. Comparison of the measured and calculated chiral selectivities for fenoprofen as a function of the pH. Conditions as in Fig. 5. + = Measured values; solid line = calculated values using eqn. 31 and the parameters in Table III.

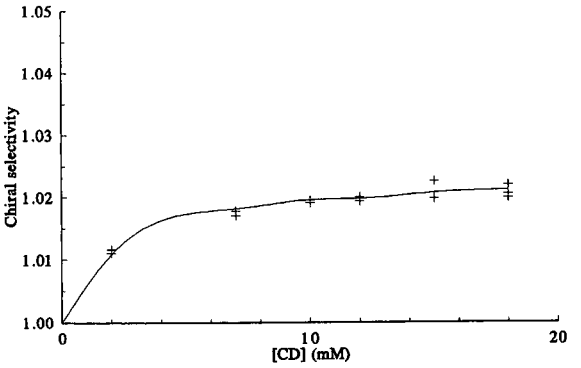

Fig. 12. Comparison of the measured and calculated chiral selectivities for fenoprofen as a function of the CD concentration. Conditions as in Fig. 6. + = Measured values; solid line = calculated values using eqn. 31 and the parameters in Table III.

1.005, resulting in an assigned selectivity of unity. It can be seen from the selectivity surfaces of both fenoprofen (Fig. 15) and ibuprofen (Fig. 16), shown again from two different viewpoints, that both profens belong to the family of Type I enantiomers: chiral selectivities vary monotonously between their pH and CD concentration dependent high values and unity, and the migration order of the enantiomers cannot be reversed by varying either the CD concentration or the pH, or both.

It can be also seen that chiral selectivity increases more rapidly with the CD concentration for ibuprofen than for fenoprofen. The limiting chiral selectivity that can be achieved at pH = 3 and [CD] = 20 m*M* is slightly higher for ibuprofen than for fenoprofen. Both of these trends are due to the fact that the complexation constants of both the ionic and the protonated forms of fenoprofen are about three times smaller than those of the ibuprofen.

By considering the shapes of both the mobility and the selectivity surfaces of the profens, one may conclude that the best strategy to optimize the separation would call for CD concentrations that are close to the solubility limit (15 m*M* is safe) and background electrolyte pH values that

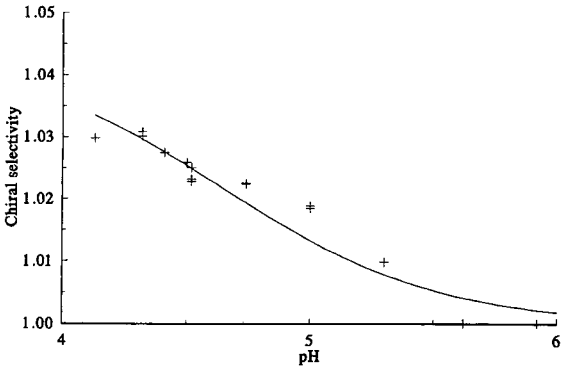

Fig. 13. Comparison of the measured and calculated chiral selectivities for ibuprofen as a function of the pH. Conditions as in Fig. 5. + = Measured values; solid line = calculated values using eqn. 31 and the parameters in Table III.

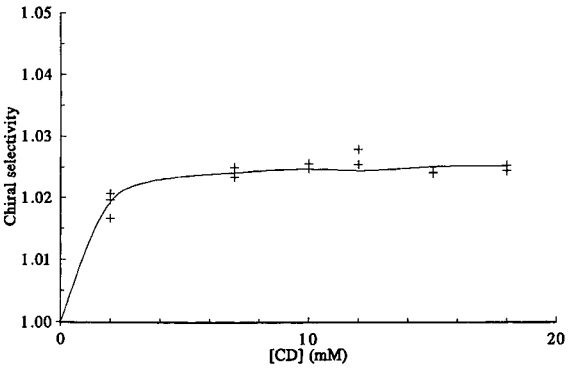

Fig. 14. Comparison of the measured and calculated chiral selectivities for ibuprofen as a function of the CD concentration. Conditions as in Fig. 6. + = Measured values; solid line = calculated values using eqn. 31 and the parameters in Table III.

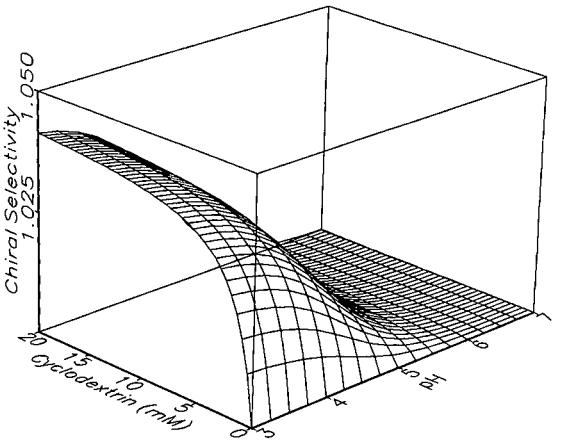

Fig. 15. Three-dimensional chiral selectivity surface for fenoprofen as a function of the CD concentration and the pH, calculated using eqn. 31 and the parameters in Table III.

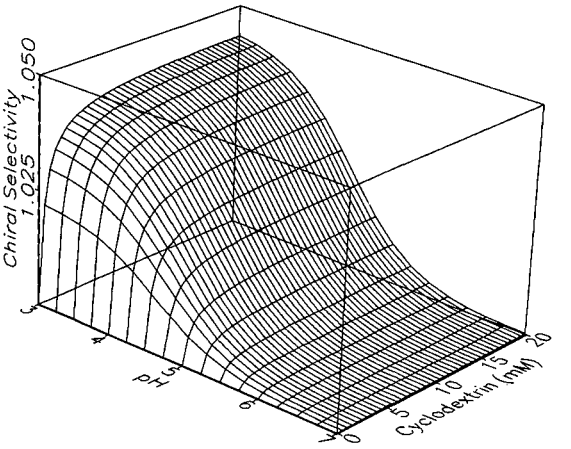

Fig. 16. Three-dimensional chiral selectivity surface for ibuprofen as a function of the CD concentration and the pH, calculated using eqn. 31 and the parameters in Table III.

are not any lower than necessary to achieve the desired minimum selectivity (minimum resolution), and pay as little a migration time penalty as possible.

The electropherogram of a mixture of racemic fenoprofen and ibuprofen is shown in Fig. 17. Baseline separations of the enantiomers can be achieved with 15 m*M* CD at pH 4.5 in about half an hour.

CONCLUSIONS

An equilibrium model has been developed to describe the electrophoretic mobilities of the enantiomers of chiral weak acids and the resulting chiral separation selectivities, as a function of the pH and the cyclodextrin concentration of the background electrolyte. The parameters of the model can be readily derived from three sets of specifically designed separation experiments: one at varying pH values without cyclodextrin in the background electrolyte, one at high pH with varying concentrations of cyclodextrin, and one at low pH with varying concentrations of

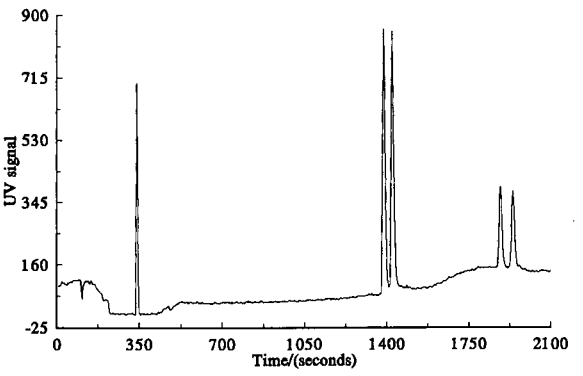

Fig. 17. CE separation of the enantiomers of fenoprofen and ibuprofen. Conditions: 0.2% HEC, 200 m*M* MES, pH = 4.50, [CD] = 15 m*M*.

cyclodextrin in the background electrolyte. The validity of the model has been demonstrated by comparing the measured and the calculated values for two test probes, fenoprofen and ibuprofen.

Fenoprofen and ibuprofen behave with β-cyclodextrin as Type I solutes defined in the Theory, because their chiral selectivity varies monotonously with both the pH and the CD concentration, the migration order of the enantiomers cannot be reversed by varying either the pH or the CD concentration of the background electrolyte, or both, and chiral resolution is absent in high pH electrolytes.

Further work is under way in our laboratory to extend the migration and chiral selectivity model proposed here to other solute types as well.

ACKNOWLEDGEMENTS

Partial financial support of this project by the National Science Foundation (CHE-8919151), the Dow Chemical Company (Midland, MI, USA), Genentech (South San Francisco, CA, USA) and Beckmann Instruments (Fullerton, CA, USA) is gratefully acknowledged. The authors are also indebted to Beckman Instruments for the loan of the P/ACE 2100 instrument. American Maize Products Corporation (Hammond, IN, USA) and the Aqualon Corporation (Wilmington, DE, USA), respectively, are acknowledged for the donation of the cyclodextrin and hydroxyethyl cellulose samples used in this project.

REFERENCES

1 W.L. Hinze, *Sep. Purif. Meth.*, 10 (1981) 159.
2 G. Gubitz, *Chromatographia*, 30 (1990) 555.
3 V. Schurig and H.P. Nowotny, *J. Chromatogr.*, 441 (1988) 155.
4 S. Terabe, H. Ozaki and T. Ando, *J. Chromatogr.*, 348 (1985) 39.
5 J. Liu, K.A. Cobb and M. Novotny, *J. Chromatogr.*, 519 (1990) 189.
6 H. Nishi, T. Fukuyama and S. Terabe, *J. Chromatogr.*, 553 (1991) 503.
7 I. Jelínek, J. Snopek and E. Smolková-Keulemansová, *J. Chromatogr.*, 405 (1987) 379.
8 J. Snopek, I. Jelínek and E. Smolková-Keulemansová, *J. Chromatogr.*, 411 (1987) 153.
9 I. Jelínek, J. Dohnal, J. Snopek and E. Smolková-Keulemansová, *J. Chromatogr.*, 435 (1988) 496.
10 J. Snopek, I. Jelínek and E. Smolková-Keulemansová, *J. Chromatogr.*, 438 (1988) 211.
11 I. Jelínek, J. Snopek and E. Smolková-Keulemansová, *J. Chromatogr.*, 439 (1988) 386.
12 S. Fanali and M. Sinibaldi, *J. Chromatogr.*, 442 (1988) 371.
13 J. Snopek, E. Smolková-Keulemansová, I. Jelínek, J. Dohnal, J. Klinot and E. Klinotová, *J. Chromatogr.*, 450 (1988) 373.
14 I. Jelínek, J. Dohnal, J. Snopek and E. Smolková-Keulemansová, *J. Chromatogr.*, 464 (1989) 139.
15 J. Snopek, I. Jelínek and E. Smolková-Keulemansová, *J. Chromatogr.*, 472 (1989) 308.
16 I. Jelínek, J. Snopek, J. Dian and E. Smolková-Keulemansová, *J. Chromatogr.*, 470 (1989) 113.
17 I. Jelínek, J. Snopek and E. Smolková-Keulemansová, *J. Chromatogr.*, 557 (1991) 215.
18 S. Fanali, *J. Chromatogr.*, 474 (1989) 441.
19 S. Fanali, *J. Chromatogr.*, 545 (1991) 437.
20 J. Snopek, H. Soini, M. Novotny, E. Smolková-Keulemansová and I. Jelínek, *J. Chromatogr.*, 559 (1991) 215.
21 A. Guttman, A. Paulus, A.S. Cohen, N. Grinberg and B.L. Karger, *J. Chromatogr.*, 448 (1988) 41.
22 I. Cruzado and Gy. Vigh, *J. Chromatogr.*, 608 (1992) 421.
23 Gy. Vigh, G. Quintero, Gy. Farkas, in Cs. Horváth and J. Nikely (Editors), *Analytical Biotechnology*, American Chemical Society, Washington, DC, 1990, p. 181.
24 J.W. Jorgenson and K.D. Lukacs, *Anal. Chem.*, 53 (1981) 1298.
25 J.W. Jorgenson and K.D. Lukacs, *Science (Washington, DC)*, 222 (1983) 266.
26 Gy. Vigh, Gy. Farkas and G. Quintero, *J. Chromatogr.*, 495 (1990) 219.

27 C.D. Herzfeldt and R. Kummel, *Drug Dev. Ind. Pharm.*, 9 (1983) 767.
28 J.L. Beckers, F.M. Everaerts and M.T. Ackermans, *J. Chromatogr.*, 537 (1991) 407.
29 S.L. Law, *T'ai-wan Yao Hsueh Tsa Chih*, 36 (1984) 173.
30 T. Hirokawa, M. Nishino, N. Aoki, Y. Kiso, I. Sawamoto, T. Yagi and J.-I. Akiyama, *J. Chromatogr.*, 271 (1983) D1–D106.
31 M.D. Beeson and Gy. Vigh, *J. Chromatogr.*, 634 (1993) 197.
32 Gy. Farkas, G. Quintero, L.H. Irgens and Gy. Vigh, *J. Chromatogr.*, (1993) submitted.

Journal of Chromatography, 635 (1993) 307–312
Elsevier Science Publishers B.V., Amsterdam

CHROM. 24 956

Speciation of aluminum using capillary zone electrophoresis with indirect UV detection

Nian Wu, William J. Horvath, Peng Sun and Carmen W. Huie*

Department of Chemistry, State University of New York at Binghamton, P.O. Box 6000, Binghamton, NY 13902-6000 (USA)

(First received December 14th, 1992; revised manuscript received February 5th, 1993)

ABSTRACT

Capillary zone electrophoresis was evaluated as a method for the speciation of aluminum in aqueous solution using indirect UV absorption detection. Fluoro- and oxalatoaluminum complexes appeared as sharp and well-defined peaks within the electropherogram of aluminum standard solutions when the appropriate ligand was added. Simultaneous separation of these inorganic and organic aluminum species was achieved with good resolution in a single analytical run within 5 min. Indirect UV detection was achieved at 214 nm with a background electrolyte buffer containing 5 m*M* imidazole. The average limit of detection was about 10 n*M* for uncomplexed and complexed aluminum species. Excellent agreement between experimental and theoretical species concentrations (via the thermodynamic speciation model SOILCHEM) was obtained for solutions with varying ligand/aluminum mol ratios and pH values.

INTRODUCTION

The role of aluminum (Al) as a toxic agent in neurodegenerative disorders such as Alzheimer's disease (AD) is a controversial but important topic. In recent years there is growing evidence which suggests that some chemical form(s) of Al could play an important role in governing the absorption and transport of Al in humans [1–5]. Unfortunately, very little is known about the concentrations and identities of Al species present in the environment and in biological systems. This problem is in large part due to the lack of analytical techniques capable of rapid and accurate determination of Al species present in various sample matrices.

Recently a controversial study which statistically links the ingestion of Al through drinking water and the increase frequency of AD has been reported [6]. Although in this study no evidence of direct relationship between Al and AD has been established, it points out the possibility that Al in drinking water may be present in some unique chemical form(s) that makes it more bioavailable than Al found in food stuffs or medications. In this regard it is interesting to note that among the potential inorganic ligands normally present in water, equilibrium calculations suggested that only the fluoride ion will significantly affect Al speciation [7]. The distribution of mononuclear fluoroaluminum species, *e.g.*, AlF^{2+}, AlF_2^+, AlF_3 and AlF_4^-, in water is of particular interest since some of these monomeric Al species have been postulated to facilitate the transport of hydrolyzable Al species through hydrophobic membranes and/or demonstrated to possess properties which alter biochemical pathways [8].

Early analytical methods employed for Al speciation mainly involved some type of indirect method [9]. The key step in all these methods was the use of cation-exchange columns to separate the labile monomeric (inorganic) from the non-labile monomeric (organic) fractions. Based on the concentration of the total monomeric Al,

* Corresponding author.

0021-9673/93/$06.00

corrected 27 Aug. 93/AP In Abstract, line 5 from bottom "The average limit of detection was about 10 nM" should read "The average limit of detection was about 10 μM"

the labile monomeric concentration can then be calculated using thermodynamic-based speciation models. Recently direct determination of inorganic as well as organic Al species have been shown to be possible using ion chromatography (IC). For example, Bertsch and Anderson [10] have demonstrated that fluoro- oxalato-, and citratoaluminum complexes can be separated and quantitated by IC, and that excellent quantitative agreement between predicted species concentrations (calculated from thermodynamic speciation model) and those determined by IC were obtained under various experimental conditions. More recently, Jones [11] has applied an IC technique for the speciation of Al in reservoir and drinking water samples. In these studies major disadvantages of the use of IC methods for Al speciation included their inabilities to separate various inorganic or organic Al species with good efficiency and to resolve mixtures of inorganic and organic Al species into discrete chromatographic peaks under isocratic conditions.

In recent years capillary zone electrophoresis (CZE) has been shown to be a highly efficient technique for the separation of small inorganic as well as organic cations and anions. For example, simultaneous separation of *ca.* ten alkali, alkaline earth and lanthanide metal cations within a single run has been demonstrated using CZE [12]; also, the simultaneous analysis of weak organic acid anions (oxalate and citrate) and inorganic anions (chloride, sulfate, phosphate and carbonate) in diluted urine has been achieved within the same analytical run in a simple and rapid manner [13]. On the other hand, the use of CZE for the efficient separation of metal species with good resolution has also been shown to be feasible. For example, the determination of the oxyanionic species of arsenic, *i.e.*, arsenite and arsenate, in urine was demonstrated [13] and the separation of a mixture of metal complexes present in electroplating solutions, *i.e.*, $Fe(CN)_6^{4-}$, $Fe(CN)_6^{3-}$, $Cu(CN)_4^{3-}$ and $Zn(OH)_4^{2-}$ were also reported [14].

In this communication the separation performance of CZE for the speciation of fluoro- and oxalatoaluminum complexes present in aqueous solutions was evaluated. Detection was performed using indirect absorption method with a background electrolyte containing imidazole as the UV absorber, which was first used by Beck and Engelhardt [15] for the rapid CZE determination inorganic cations and aliphatic amines with excellent detection limits and separation efficiencies. Furthermore, the stability of Al species during CZE separation was examined by comparing measured and predicted concentration values (via the thermodynamic speciation model: SOILCHEM) obtained for the various fluoro- and oxalatoaluminum complexes and the uncomplexed Al under various experimental conditions.

EXPERIMENTAL

Chemicals and materials

Aluminum nitrate, sodium fluoride, sodium oxalate and imidazole were analytical grade and purchased from Baker (Phillipsburg, NJ, USA) or Sigma (St. Louis, MO, USA). Doubly distilled deionized water obtained from a Barnstead Nanopure System (Dubuque, IA, USA) was used for the preparation of all buffer and sample solutions. Polyimide-coated fused-silica capillary with 75 μm I.D. and 360 μm O.D. was obtained from Polymicro Technologies (Phoenix, AZ, USA).

Buffer and sample solutions

All buffer solutions were prepared with a background electrolyte containing 5 m*M* of imidazole. Sample solutions were prepared by adding solution containing the ligand of interest to an appropriate volume of $Al(NO_3)_3$ standard solution in a 100-ml polyethylene (PE) volumetric flask such that the final Al concentration was 0.25 m*M*. The pH of the buffer and sample solutions were adjusted with small amounts of 1 *M* sulfuric acid. Prior to use all solutions were filtered through a 0.45-μm membrane filter and stored in the PE bottles to age for a minimum period of 24 h.

Instrumentation

A home-built CZE instrument was used for all separations. An acrylic box with a safety-interlocked door designed to prevent operator con-

tact with high voltage contained the Speelman voltage source (Model CZE 1000/30 PN, Plainview, NY, USA) and a Linear Instrument UV/Vis absorbance detector (Model 204, Reno, NV, USA) which has been modified for on-line detection at 214 nm. Contact with solution was made via platinum electrodes. All CZE separations were carried out using 350 V/cm field strength. Samples were injected hydrodynamically at the anode (positive polarity) by raising the sample solution reservoir to a height of 10 cm for 10 s. Data were recorded using a Chromjet integrator (Spectra Physics, San Jose, CA, USA).

Capillary preparation

Capillary length was 45 cm with a detection window made by burning off 2 mm of the polyimide coating at approximately 35 cm from the anode end of the capillary. Capillaries were washed with 1 *M* NaOH for 30 min, followed by rinsing with the buffer solution for 1 h and equilibration with the buffer solution overnight.

Speciation calculations

The theoretical species concentration of Al in the sample solutions was calculated by utilizing the SOILCHEM program: an improved version of the thermodynamic geochemical speciation model-GEOCHEM [16].

RESULTS AND DISCUSSION

Fig. 1a shows the CZE separation of a standard solution of $Al(NO_3)_3$ using a background electrolyte buffer containing 5 m*M* imidizole at pH 3.5, and two sharp and well-defined peaks can be observed in the electropherogram. The early peak which appears at a migration time of *ca.* 3.5 min can be assigned to the "free" Al ion (Al^{3+}) since this species predominates in aqueous solution at pH less than 5. This positively charged species would be expected to migrate faster toward the cathode (or detector) when compared to the predominant negatively charged solute present in the sample solution: NO_3^-, which appears as an "inverted" peak at a migration time of *ca.* 6.5 min. Appropriate amount of nitric, hydrochloric and sulfuric acids were added to the buffer and sample solutions for pH adjustments and it was found that separation performance was dependent on the type of acid used. Sulfuric acid was found to provide the best resolution for the CZE separation of various Al species, *vide infra*, but it is not clear at this time why this is the case. It should be noted that based on thermodynamic calculations, the SO_4^{2-} ion could interact with the Al ion to form sulfatoaluminum complexes in the sample solutions. However, by adding a relatively large amount of SO_4^{2-} to the Al standard solutions (mol ratio SO_4: Al = 20:1), we found no significant difference in the retention time or peak area of the free Al ion peak as shown in Fig. 1a. This observation suggests that any sulfatoaluminum complexes formed in the sample solution are likely to exist as weak, electrostatic outer-sphere complexes and are apparently readily dissociated during CZE separation. Similar observations have also been reported for the separation of sulfatoaluminum complexes using IC [10].

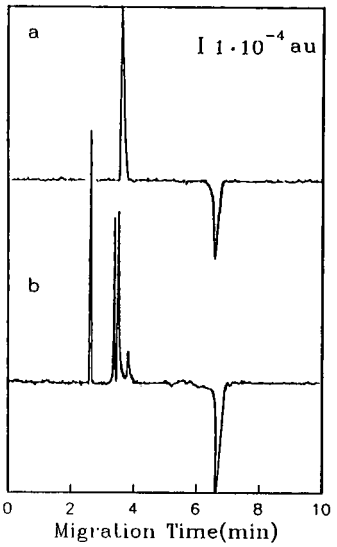

Fig. 1. CZE electropherogram of a 0.25 m*M* $Al(NO_3)_3$ solution with (a) no F and (b) the addition of 0.12 m*M* of NaF. The pH of buffer and sample solutions was matched at 3.5.

Fig. 1b shows that with the addition of F (as NaF) into the Al standard solutions, the peak area of the free Al ion peak was reduced significantly and additional peaks were produced in the CZE electropherogram. The major peak which appears at *ca.* 2.4 min can be assigned to

Na^+ [confirmed by the injection of NaF without the presence of $Al(NO_3)_3$]. On the other hand, assignments of the two smaller peaks which appear at *ca.* 3.2 and 3.8 min, respectively, are not as straightforward. Table I compares experimental data and theoretical values generated by the SOILCHEM program. At a F/Al ratio of 0.5:1 and sample and buffer pH = 3.5 (experimental conditions of Fig. 1b), the predicted concentration values of Al^{3+}, AlF^{2+} and AlF_2^+ are shown to be in good agreement with experimental measurements, which suggests the formation of AlF^{2+} and AlF_2^+ species upon the addition of NaF into the Al standard solution. Furthermore, it was found that the total integrated areas of the free Al ion as shown in Fig. 1a and the cluster of three adjacent peaks (between 3.0 and 4.0 min) as shown in Fig. 1b are similar. These results, along with the fact that no interference peaks were obtained from the CZE separation of NaF alone, suggest that the two smaller peaks which center at *ca.* 3.2 and 3.8 min in Fig. 1b are probably a result of a redistribution of Al between species of differing positive charges upon the addition of NaF and assignments of AlF^{2+} and AlF_2^+ could be made for these two additional peaks. In this case, it would be reasonable to assign AlF^{2+} as the early peak which appears at *ca.* 3.2 min since it possesses a higher positive charge and would be expected to migrate faster toward the detector when compared to AlF_2^+, which was assigned as the latter peak appearing at *ca.* 3.8 min. However, using the same argument, it would be unreasonable to expect the Na^+ to migrate faster than AlF^{2+} as shown in Fig. 1b and, similarly, the early appearance of AlF^{2+} when compared to the free Al ion (a positively triple charge species which appears at *ca.* 3.5 min) is not expected.

In an attempt to understand the migration order of the assigned peaks as shown in Fig. 1b, it is important to note that the mobility (or migration time) of a particular ion in CZE separation is dependent not only on the charge but also the size of the ion [17]. For electrolytes dissolved in aqueous solutions the number of water molecules associated with the ions during their movement through the solution is likely to influence their overall size and mobility. Many experiments have been devised in attempts to determine the hydration of ions in aqueous solutions [18,19]. Unfortunately, the solvation (or hydration) number of many ions is not known with certainty. However, it is interesting to note that under the influence of intense electrical forces, the hydration numbers of NaCl and $AlCl_3$ have been reported to be 7 and 31, respectively [18]. It is possible that under the experimental conditions described in Fig. 1b, the mobilities of

TABLE I

MEASURED (CZE) AND PREDICTED (SOILCHEM) CONCENTRATIONS OF UNCOMPLEXED Al AND COMPLEX FLUOROALUMINUM SPECIES IN SOLUTIONS OF VARYING F:Al MOL RATIOS AND pH VALUES

F/Al[a]	pH	Al^{3+} (m*M*)			AlF^{2+} (m*M*)			AlF_2^+ (m*M*)		
		CZE[b]	CZE[c]	SOILCHEM	CZE[b]	CZE[c]	SOILCHEM	CZE[b]	CZE[c]	SOILCHEM
0.5:1	3.2	0.143	0.141	0.127	0.104	0.101	0.115	0.003	0.008	0.005
	3.5	0.129	0.134	0.132	0.115	0.111	0.113	0.006	0.005	0.005
	4.0	0.135	0.130	0.122	0.112	0.114	0.124	0.003	0.006	0.004
	4.2	0.132	0.137	0.130	0.113	0.108	0.114	0.005	0.005	0.006
1:1	3.2	0.075	0.073	0.058	0.138	0.148	0.144	0.037	0.029	0.048
	3.5	0.068	0.069	0.059	0.150	0.149	0.145	0.031	0.032	0.046
	4.0	0.066	0.069	0.060	0.155	0.156	0.148	0.029	0.025	0.042
	4.2	0.075	0.069	0.059	0.139	0.139	0.147	0.036	0.041	0.044

[a] Total Al concentration = 0.25 m*M*.
[b] pH of the sample and buffer solutions was matched in the range of 3.2 to 4.2.
[c] pH of the buffer was fixed at 3.5 and pH of the sample solutions was adjusted from 3.2 to 4.2.

corrected 27 Aug. 93 In second column, line 2 " 10 to 300 nM " should read " 10 to 500 μM "

the various ions are influenced by the degrees of hydration. The hydration number of the uncomplexed Al ions may be higher than that of Na^+ and AlF^{2+}, thus leading to an increase in the size and/or decrease of the charge of the free Al ion and resulting in a longer migration time.

Table I and Fig. 2 show that good agreement between measured and predicted values extend over a range of pH and mole ratio values when the pH of the sample and background electrolyte buffer were matched. On the other hand, when the pH of the sample and buffer was unmatched, the experimental values of uncomplexed Al and complexed fluoroaluminum species showed minimal changes and also exhibit good agreement with thermodynamic calculated values over a pH range of about one order of magnitude. These results suggest that these fluoroaluminum species exhibited good kinetic stability and maintained their integrity, *i.e.*, minimal redistribution during CZE separation, under the present experimental conditions. The average limits of detection (LOD) for uncomplexed Al and complexed fluoroaluminum species was found to be about 10 n*M* ($S/N = 3$) and the average relative standard deviations ($n = 8$) for mobilities and peak areas were <0.5% and 4%, respectively. The relationship between peak area and concentration was linear in the range 10 to 500 n*M* with the regression equation: A (peak area) = $1.04 \cdot 10^4 C$ (concentration) + $1.09 \cdot 10^3$. The correlation coefficient (r) was 0.998 ($n = 8$).

Fig. 3 shows the CZE separation of a sample solution containing mixed F and oxalate ligands (mole ratio Al:F:oxalate = 1:0.5:1). When compared to Fig. 1b, an additional peak which appears at *ca.* 4.0 min was produced with the presence of oxalate anion. Similarly, a peak which appears at *ca.* 4.0 min was also produced upon the addition of oxalate into Al standard solutions without the present of F. Fig. 4 compares the experimental and thermodynamic calculated values of uncomplexed Al and monooxalatoaluminum species at varying mole ratio of oxalate and Al (in the absence of F) and indicates good agreement for these particular species, suggesting that that additional peak at *ca.* 4.0 min probably arose from the formation of monooxalatoaluminum species. The relatively long migration time obtained for this organic Al species is reasonable since it would have the smallest charge density due to its single positive charge and relatively large size (neglecting hydrating number), thus leading to lower mobility relative to the other positively charged species

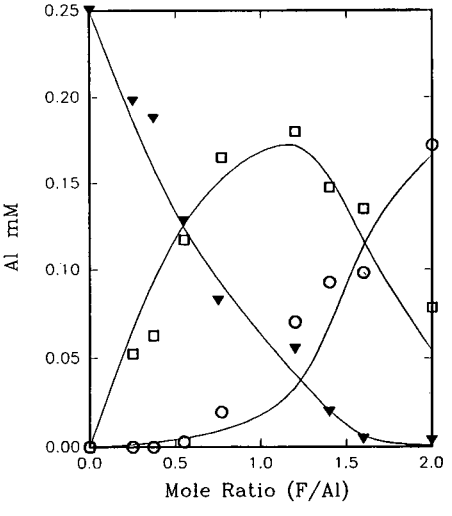

Fig. 2. Measured (symbols) and predicted (solid lines) concentrations of the uncomplexed and fluoro-complexed Al species at varying F:Al mol ratios with total Al concentration equal to 0.25 m*M* and pH of buffer and sample solutions equal to 3.5. ▼ = Al^{3+}, □ = AlF^{2+} and ○ = AlF_2^+.

Fig. 3. CZE electropherogram of a 0.25 m*M* $Al(NO_3)_3$ solution with the presence of 0.13 m*M* F and 0.25 m*M* oxalate. The pH of buffer and sample solutions was matched at 3.5.

corrected 27 Aug. 93/AP In first column, line 24 and 25 " 10 nM (S/N = 3)" should read " 10 μM (S/N = 3)"

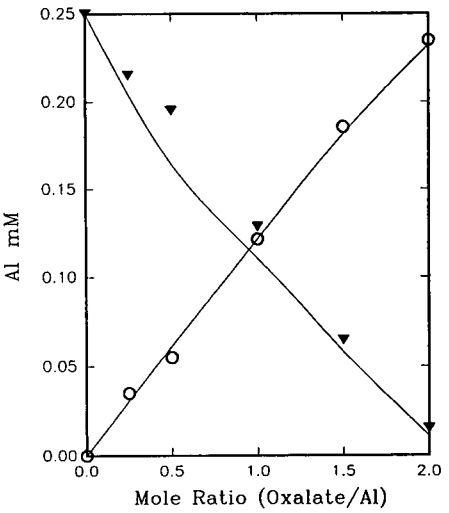

Fig. 4. Measured (symbols) and predicted (solid lines) concentrations of the uncomplexed and monooxalato-complexed Al species at varying oxalate: Al ratios with total Al concentration equal to 0.25 m*M* and pH of buffer and sample solutions equal to 3.5. ▼ = Al^{3+}, ○ = Al-oxalate^{+}.

present in the sample solution. Fig. 3 shows that good resolution can be obtained for the simultaneous separation of inorganic and organic Al complexes within a single CZE run during a period of less than 5 min. This capability demonstrates that CZE possesses a distinct advantage over IC for the separation of sample solutions containing these particular mixed inorganic and organic ligands. Using IC only the uncomplexed Al and AlF^{2+} produced discrete chromatographic peaks while AlF_2^+ and monooxalatoaluminum species were observed to co-elute as a single peak under isocratic conditions [10].

In summary, this work demonstrates that CZE can be used as a powerful technique for the rapid and efficient separation of fluoro- and oxalatoaluminum species present in aqueous solutions. More research is needed to examine the feasibility of using CZE for the separation of other small inorganic and organic Al complexes, as well as protein-bound and macromolecular Al species. In particular, experimental factors which affect the stability or integrity of the Al species during CZE separation and the effects of potential interference ions present in real samples which might form complexes with aluminum should be investigated in detail by comparing experimental and theoretical values.

ACKNOWLEDGEMENT

We thank Mr. Steven G. Santiago, software publication assistant at the University of California-Berkeley for supplying us the SOILCHEM program.

REFERENCES

1 C.T. Driscoll, J.D. Barker, Jr. and C.L. Schofield, *Nature*, 284 (1980) 161.
2 R.B. Martin, *Clin. Chem.*, 32 (1986) 1797.
3 M.A. Akeson and D.N. Munns, *Biochim. Biophys. Acta*, 984 (1989) 200.
4 G.S. Zubenko and I. Hanin, *Brain Res.*, 498 (1989) 381.
5 R.A. Yokel, V. Lidums, P.J. McNamara and U. Ungersted, *Toxic. Appl. Pharm.*, 107 (1991) 153.
6 C.N. Martyn, C. Osmond, J.A. Edwardson, D.J.P. Barker, E.C. Harris and R.F. Lacey, *Lancet*, 1 (1989) 59.
7 J. Johansson, *Acta Chim. Scand.*, 14 (1980) 771.
8 T.L. Macdonald and R. Bruce Martin, *Trends in Biochem. Sci.*, 13 (1988) 15.
9 T.J. Sullivan, H.M. Seip and I.P. Muniz, *Int. J. Environ. Anal. Chem.*, 26 (1986) 61.
10 P.M. Bertsch and M.A. Anderson, *Anal. Chem.*, 61 (1989) 535.
11 P. Jones, *Int. J. Environ. Anal. Chem.*, 44 (1991) 1.
12 A. Westen, P.R. Brown, P. Jandik, W. K. Jones and A. L. Heckenberg, *J. Chromatogr.*, 593 (1992) 289.
13 B.J. Wildman, P.E. Jackson, W.R. Jones and P.G. Alden, *J. Chromatogr.*, 546 (1991) 459.
14 M. Aquilar, X. Huang and R.N. Zare, *J. Chromatogr.*, 480 (1989) 427.
15 W. Beck and H. Engelhardt, *Chromatographia*, 33 (1992) 313.
16 D.R. Parker, L.W. Zelazny and T.B. Kinraide, *Soil Sci. Soc. Am. J.*, 51 (1987) 488.
17 B.L. Karger, A.S. Cohen and A. Guttman, *J. Chromatogr.*, 492 (1989) 585.
18 R.A. Robinson and R.H. Stokes, *Electrolyte Solutions*, Butterworths, London, 2nd ed., 1965, pp. 49–73.
19 A.L. Horvath, *Handbook of Aqueous Electrolyte Solutions: Physical Properties, Estimation and Correlation Methods*, Ellis Horwood, Chichester, 1985, pp. 19–34.

Journal of Chromatography, 635 (1993) 313–318
Elsevier Science Publishers B.V., Amsterdam

CHROM. 24 904

Capillary micellar electrokinetic, sequential multiwavelength chromatographic characterization of a chimeric monoclonal antibody–cytotoxin conjugate

David Emlyn Hughes* and Priscilla Richberg

Bristol–Myers Squibb Company, Pharamaceutical Research Institute, P.O. Box 4755, Syracuse, NY 13221-4755 (USA)

(First received November 17th, 1992; revised manuscript received January 25th, 1993)

ABSTRACT

An analysis of a doxorubicin-conjugated chimeric antibody has been developed by micellar electrokinetic capillary chromatography. The procedure separates the conjugated antibody, the antibody light and heavy chains, antibody fragments, and unconjugated doxorubicin. The protein-derived species are monitored at 280 nm and the doxorubicin bearing species are monitored at 500 nm. Consistency with the proposed *in vivo* mechanism of action of the antibody conjugate in acid media is demonstrated.

INTRODUCTION

The origin of interest in antitumor agents of the anthracycline class (which doxorubicin is a member) began at least as early as the 1950s. Liquid extraction of soil samples collected in India yielded a red solid which was shown to exhibit antitumor activity [1] and was traced to a strain of *Streptomyces*. Later work indicated that the microbial metabolite of interest was rhodomycin B which did not improve survival times *in vitro* testing but did generate interest in anthracycline anticancer agents [2]. Further studies yielded other anthracycline compounds from *Streptomyces peucetius* colonies; in particular, *S. peucetius* var. *caesius* was found to produce doxorubicin, an antibiotic with potent antitumor activity [3].

While chemotherapy with compounds such as doxorubicin continues to be a major therapeutic approach, there are important limitations. Antineoplastic agents are usually toxic to normal cells which reproduce rapidly; in particular, cells contained in the gastrointestinal tract and bone marrow are susceptible. Chemotherapeutic agents, when traditionally administered, are limited by their systemic toxicity.

Delivery of a cytotoxic agent to the site of the cancerous cells allows high local concentrations of the drug while minimizing toxicity to normal cells. One approach is to synthesize "immunotoxins," *i.e.*, IgG antibodies (conjugated with a cytotoxic agent) with a preference or specificity towards tumor cells. Antibodies conjugated with doxorubicin have previously been synthesized via dextran hydrazide–glutaraldehyde derivatization and periodate-oxidized dextran bridges. Although these conjugates were somewhat effective using *in vivo* and *in vitro* targeting models and yielded locally high doxorubicin concentrations, the cytotoxic activity was modest [4,5].

Other antibody–doxorubicin linkers that have been investigated include N-succinimidyl-3-(2-pyridyldithio) propionate [6] and more recently an acid-labile, 13-acylhydrazone [7]. Although

* Corresponding author.

0021-9673/93/$06.00

the overall mechanism of action for 13-acylhydrazone is unclear, it has been postulated that internalization of conjugates into intracellular acidic compartments (such as lysosomes) may release doxorubicin and hence explain the observed cytolytic activity. The structure of doxorubicin and the antibody complex appear in Fig. 1.

The examination of an IgG antibody or antibody–drug conjugate represents a substantial analytical challenge. With an average molecular mass of 150 000 and the likelihood of several forms varying only slightly in amino acid and carbohydrate content, examinations based on molecular mass differences alone would not be expected to be useful. Relatively new separatory procedures, principally size-exclusion, ion-exchange, affinity, hydrophobic interaction and hydroxyapatite chromatography, have proven useful for antibodies [8]. Of these liquid chromatographic techniques, ion-exchange chromatography is possibly the most selective procedure for large proteins (such as antibodies), perhaps implying that charge-dependent separations show substantial promise. Although capillary electrophoresis (CE) (which separates species on the basis of molecular mass and net charge) has been more consistently used for analysis of peptides, proteins such as adrenocorticotropin, transferrin, ribonuclease, insulin and growth hormone [9,10] have also been examined. Importantly, protein studies performed by CE have been shown to be able to separate the major species from species arising from degradative deamidation and amino acid and glycan microheterogeneity [11]. Although CE studies on antibodies are not abundant, one combined theoretical and empirical study [12] demonstrated that a single amino acid difference in a chimeric IgG antibody was detectable. Analysis of conjugated antibodies is substantially more complex. An ideal separating procedure for an antibody conjugate would allow examination of the unconjugated antibody, the agent which is to be complexed with the antibody, and the conjugated antibody. In one study [13], a CE procedure was developed that was capable of separating IgG monoclonal antibody (from mouse ascites), alkaline phosphatase (M_r 140 000), and an alkaline phosphatase–IgG conjugate.

The paper presented here describes the CE examination of a chimeric antibody conjugated with the cytotoxic agent doxorubicin. The conjugated forms are monitored at 280 nm to observe the proteinaceous component of the complex and at 500 nm to determine the extent of doxorubicin conjugation. Method development optimization studies are presented for the sodium dodecyl sulfate (SDS) concentration, sodium borate concentration and pH of the carrier. Selectivity with respect to the heavy and light antibody chains and the F_{ab} antibody fragment is demonstrated.

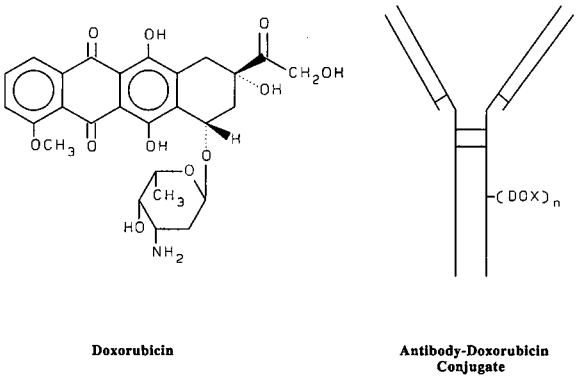

Fig. 1. Chemical structure of doxorubicin and a representation of the structure of the chimeric antibody–doxorubicin conjugate.

EXPERIMENTAL

Materials

Sodium hydroxide 10 *M* solution and sodium borate crystals were obtained from Fisher Chemical (Fair Lawn, NJ, USA). Dodecyl sulfate, sodium salt was purchased from Aldrich (Milwaukee, WI, USA). Pretreated capillary cartridges were purchased from Beckman Instruments (Palo Alto, CA, USA). The samples were chimeric antibody conjugates (Bristol–Myers Squibb, Syracuse, NY, USA). Water from a Milli-Q filtration system (Millipore, Bedford, MA, USA) was used in the preparation of the buffer solutions.

Capillary electrophoresis system

A Beckman P/ACE 2100 capillary electrophoresis system (Palo Alto, CA, USA) using an IBM PS/2 with P/ACE software and Microsoft Windows interface was used throughout this study.

Capillary electrophoresis procedures

The CE separation was performed using a 12 m*M* borate buffer (pH 9.4) containing 25 m*M* sodium dodecyl sulfate. Samples were transferred to P/ACE micro vials contained in sample holders, and applied to the capillary as described below. Upon completion of each sample analysis, the capillary column was cleaned with a high-pressure rinse of 0.1 *M* sodium hydroxide solution for 0.5 min, followed by a high-pressure rinse of the separation buffer solution for 0.5 min.

A fused-silica capillary cartridge (50 cm × 75 μm I.D., Beckman Instruments, catalog number 338467, rinsed by the manufacturer with 0.1 *M* NaOH solution) was used in the separation. Samples were injected by a positive nitrogen pressure of $6.2 \cdot 10^5$ Pa (90 p.s.i.) for 5 s when 214-nm and 280-nm detection were employed and 10 s for 500-nm detection. The samples were then separated by a voltage of 30 kV at 25°C. The samples were monitored at 214, 280 and 500 nm.

The light and heavy chains were formed in excess of 95% purity by heating the antibody conjugate in 1% SDS at 90°C for 2 min. The F_{ab} fragment was produced by a standard papain digestion [14].

RESULTS AND DISCUSSION

When examined by procedures which rely at least in part on the total charge of the species of interest, IgG antibodies may be separated into several forms. Antibodies show variability due to heterogeneity in the amino acid sequence or carbohydrate (oligosaccharide) content or type, as well as forms due to degradation, such as deamidation. For drug-labelled antibodies, further variation is possible due to different drug–antibody conjugation ratios and conformations.

All of the major species described so far would have molecular masses (*ca.* 150 000) very nearly equal to that of an unconjugated, undegraded antibody. Hence, as was mentioned previously, mass-based methods of analysis (such as size-exclusion chromatography) would not be expected to distinguish between the various antibody-derived species. The proteinaceous species would, however, be expected to vary in net charge and hydrophobicity, hence providing a basis for separation.

Initial CE optimization studies with the chimeric antibody studied here suggested that an additional separatory mechanism was required since net charge differences (and hence, temporal separation) between species was insufficient when the ionic strength and pH of the carrier were varied. The addition of SDS to the carrier in concentrations above the critical micellar concentration has been shown to aid separation of neutral or a similar net charge species with smaller molecules. The precise mechanism of separation when analytes of similar mass to SDS micelles such as the IgG antibody are electrophoresed is unclear. Whether separatory enhancement is due to SDS ion-pairing with hydrophobic protein regions or simply differential migration of negatively charged analyte through a zone of negatively charged micelles is not easily determined empirically. Independent of the precise mechanism, the conjugated antibody was found to separate into several species as the SDS concentration increased above the critical micellar concentration (*ca.* 8 m*M*). As in most CE applications, the pH and buffer concentration of the carrier were also found to be critical to the efficient separation of the various species. Method development studies were performed in which the SDS concentration, pH and sodium borate concentration were varied (Figs. 2–4). For these studies, the resolution equation $R_s = 16(t/w)^2$ was employed where R_s is the resolution, t is the migration time of the peak and w is the peak width measured at the baseline. The critical separation was determined to be between three early-migrating species (Fig. 5, peaks 1, 2 and 3) which were present in all samples of antibody conjugate examined and a thermally-induced peak (produced between peaks 2 and 3, Fig. 5). The optimized conditions were 12 m*M*

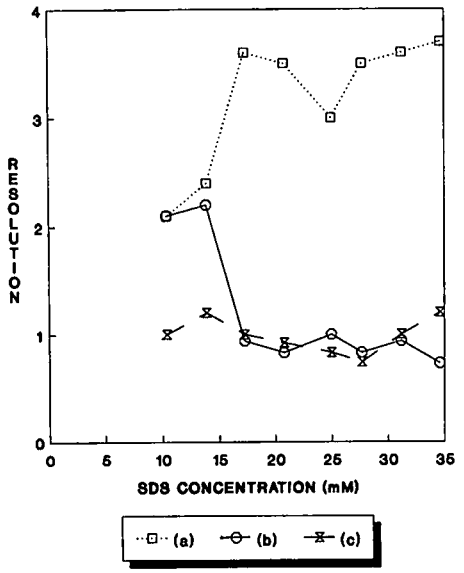

Fig. 2. Resolution of electrophoretic species as a function of SDS concentration at a concentration of 12 m*M* sodium borate and pH 9.4: (a) resolution between peaks 1 and 2, (b) resolution between peaks 2 and a thermally-induced species, and (c) resolution between peaks 2 and 3. Refer to Fig. 5 for peak identification. The thermally-induced peak, appearing between peaks 2 and 3 is not represented.

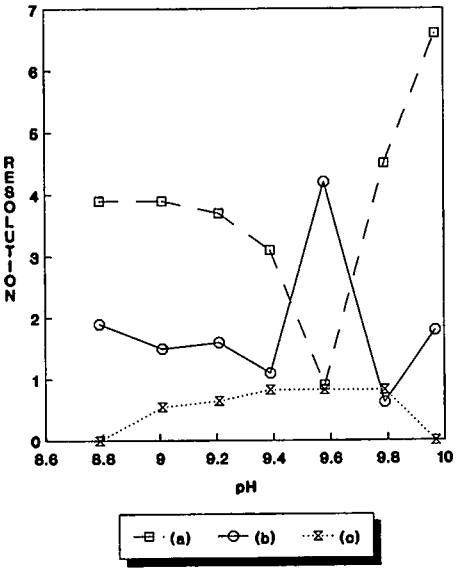

Fig. 3. Resolution of electrophoretic species as a function of pH at an SDS concentration of 25 m*M* and a borate concentration of 12 m*M*: (a) resolution between peaks 1 and 2, (b) resolution between peaks 2 and a thermally-induced species, and (c) resolution between peaks 2 and 3. Refer to Fig. 5 for peak identification. The thermally-induced peak, appearing between peaks 2 and 3 is not represented.

sodium borate, 25 m*M* SDS at a pH of 9.40. Although Figs. 2–4 would suggest that a higher borate concentration would produce a better separation, the antibody is not stable under these conditions and forms measurable amounts of light and heavy chains and antibody fragments.

The final separation appears in Fig. 5 with 280- and 500-nm detection. Detection at 280 nm would be expected to visualize all proteinaceous species whereas 500-nm detection would detect only those species containing doxorubicin. Referring to Fig. 5, the electropherogram represents three antibody conjugate species (1, 2, 3) and doxorubicin (7). Standard techniques for generating the light and heavy chains and the F_{ab} fragment were employed. The resulting species migrated in a third temporal zone, *i.e.*, F_{ab} (4), heavy chain (5) and light chain (6). Hence the separation appears to be capable of detecting degradation of the antibody conjugate to heavy and light chains and the F_{ab} fragment.

To determine whether the electrophoretic separation would be capable of demonstrating

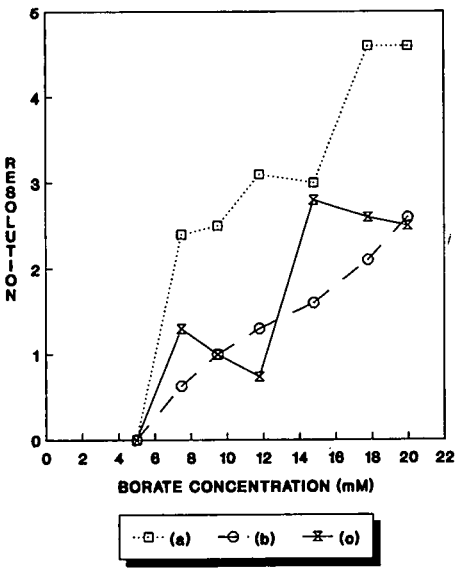

Fig. 4. Resolution of electrophoretic species as a function of sodium borate concentration at an SDS concentration of 25 m*M* and pH 9.4: (a) resolution between peaks 1 and 2, (b) resolution between peaks 2 and a thermally-induced species, and (c) resolution between peaks 2 and 3. Refer to Fig. 5 for peak identification. The thermally-induced peak, appearing between peaks 2 and 3 is not represented.

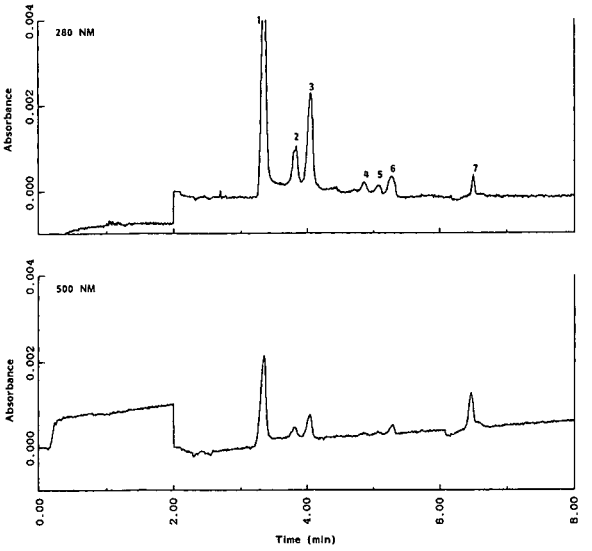

Fig. 5. Electropherogram of the final separation (12 m*M* sodium borate, 25 m*M* SDS, pH 9.4) with detection at 280 nm and 500 nm. Peaks: 1, 2, 3 = antibody conjugate; 4 = F_{ab}; 5, 6 = heavy and light chains; 7 = doxorubicin.

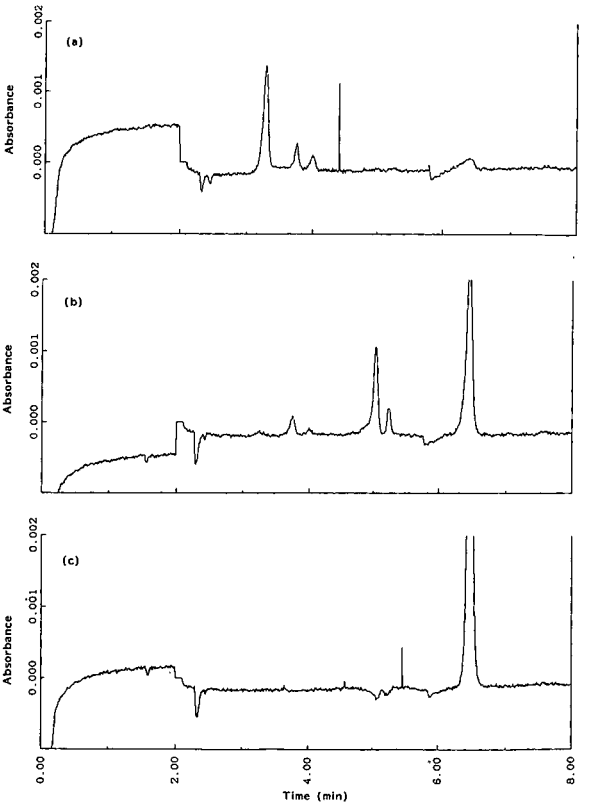

Fig. 6. Acid hydrolysis at pH 1.5 monitored at 500 nm. (a) Initial sample; (b) after 3 min; (c) after 15 min.

the mechanism of action which has been proposed *in vitro*, an acid-degradation study was performed. According to the proposed [7] mechanism, the chimeric antibody–doxorubicin conjugate releases unconjugated doxorubicin in the presence of acid media. If this transformation is monitored at 500 nm, which is selective for doxorubicin and doxorubicin-conjugated species, we would expect a decrease in absorbance of proteinaceous doxorubicin species and an increase in unconjugated doxorubicin. As Fig. 6 illustrates, CE examination of acid hydrolysis at a pH 1.5 is consistent with this model. The electropherogram of the initial sample (a) contains peaks for the conjugate and a low level of unconjugated doxorubicin whereas intermediate exposure to an acidic medium (b) yields predominately conjugated heavy and light chains and doxorubicin. After sufficient time, the antibody is no longer conjugated and substantial doxorubicin is observed (c). Studies were also performed at more biologically-assessable conditions (*ca.* pH 5) with similar but predictably less dramatic results.

In summary, a CE procedure has been developed which allows examination of a doxorubicin-linked chimeric antibody. The proteinaceous species are monitored at 280 nm and the doxorubicin-related species are monitored at 500 nm. The method separates three forms of the antibody, the light and heavy antibody chains, the F_{ab} fragment, and unconjugated doxorubicin. Monitoring of acid hydrolysis of the antibody conjugate revealed the formation of unbound doxorubicin and simultaneous loss of protein-bound doxorubicin in agreement with the proposed *in vivo* mechanism of action.

ACKNOWLEDGEMENTS

The authors acknowledge technical assistance in the antibody fragment selectivity studies by Lt. (jg) Christopher Kolanko, National Naval Medical Center, Bethesda, MD, USA. The authors also acknowledge valuable technical discussions with Barbara Root, David Kirkley, John

Woolever, and Kirk Leister, Bristol–Myers Squibb Company, Analytical Research and Development, Syracuse, NY, USA.

REFERENCES

1 F. Arcamone, A. DiMarco, M. Gaetani and T. Scotti, *G. Microbiol.*, 9 (1961) 83.
2 F. Arcamone, *Doxorubicin Anticancer Antibiotics*, Academic Press, New York, 1981, p. 17.
3 A. DiMarco, M. Gaetani and B.M. Scarpinato, *Cancer Chemother. Rep.*, 53 (1969) 33.
4 R.A. Reisfeld and S. Sell, *Monoclonal Antibodies and Cancer Therapy*, Alan R. Liss, New York, 1985, pp. 244–246, 254.
5 S. Sell and R.A. Reisfeld, *Monoclonal Antibodies in Cancer*, Humana Press, Clifton, NJ, 1985, p. 11.
6 G.L. Wright, Jr., *Monoclonal Antibodies and Cancer*, Marcel Dekker, New York, 1984, p. 197.
7 G.R. Braslawsky, K. Kadow, J. Knipe, K. McGoff, M. Edson, T. Kaneko and R.S. Greenfield, *Cancer Immunol. Immunother.*, 33 (1991) 367.
8 K.M. Gooding and F.E. Regnier, *HPLC of Biological Macromolecules*, Marcel Dekker, New York, 1990, pp. 487–528.
9 A. Guttman, A. Paulus, A.S. Cohen, B.L. Karger, H. Rodrigues and W.S. Hancock, *Electrophoresis 88*, VCH Publishers, New York, 1988, pp. 151–160.
10 P.D. Grossman, J.C. Colburn, H.H. Lauer, R.G. Nielson, R.M. Riggin, G.S. Sittampalam and E.C. Rickard, *Anal. Chem.*, 61 (1989) 1186.
11 S.-L. Wu, G. Teshima, J. Cacia and W.S. Hancock, *J. Chromatogr.*, 516 (1990) 115.
12 B.J. Compton, *J. Chromatogr.*, 559 (1991) 357.
13 S.J. Harrington, R. Varro and T.M. Li, *J. Chromatogr.*, 559 (1991) 385.
14 E. Harlow and D. Lane, *Antibodies*, Cold Spring Harbor Laboratory, Cold Spring Harbor, NY, 1988, p. 628.

Journal of Chromatography, 635 (1993) 319–327
Elsevier Science Publishers B.V., Amsterdam

CHROM. 26 834

Separation of cardiac glycosides by micellar electrokinetic capillary electrophoresis

Hans-Joachim Gaus

Institut für Organische Chemie, Universität Tübingen, Auf der Morgenstelle 18, W-7400 Tübingen (Germany)

Achim Treumann[☆] and Wolfgang Kreis

Pharmazeutisches Institut, Universität Tübingen, Auf der Morgenstelle 8, W-7400 Tübingen (Germany)

Ernst Bayer*

Institut für Organische Chemie, Universität Tübingen, Auf der Morgenstelle 18, W-7400 Tübingen (Germany)

(First received November 3rd, 1992; revised manuscript received December 24th, 1992)

ABSTRACT

The separation of mixtures of primary and secondary cardiac glycosides by micellar electrokinetic capillary electrophoresis modified by cyclodextrins, urea and sodium cholate proved to be suitable for the determination of these hydrophobic compounds. It was possible to distinguish the two anomeric cardenolides glucodigifucoside and glucodigiglucomethyloside with all three buffer systems. Electropherograms of crude plant cell extracts from *Digitalis lanata* were obtained with this method.

INTRODUCTION

Cardiac glycosides isolated from *Digitalis* species constitute a group of pharmaceutically very important natural substances that are used for the treatment of certain cardiac diseases. Very powerful RP-HPLC methods for the determination of cardenolides have been developed and optimized [1,2]. Nonetheless, some compounds with identical polarity co-elute in HPLC even if very sophisticated solvent gradients are applied. They can only be resolved by chemical or enzymatic derivatization and subsequent HPLC or TLC analysis, a very time-consuming procedure that is prone to artefacts and errors. For this reason we have investigated micellar electrokinetic capillary electrophoresis (MECC) [3] for the separation and determination of cardiac glycosides.

Most cardiac glycosides are very hydrophobic compounds as judged by their partition coefficients with *n*-octanol [4]. This can be a handicap in MECC as they tend to migrate very close to the micellar front. Several strategies have been used with other hydrophobic compounds to overcome this problem and to shift the partition equilibrium between aqueous and micellar phase towards the former. Addition of cyclodextrins [5], urea [6], bile salts [7] and organic modifiers such as 2-propanol [8] or acetonitrile [9] to the electrophoresis buffer have proved successful.

To develop a system that is applicable to analyse for digitalis glycosides, we first investi-

* Corresponding author.
☆ Present address: Carbohydrate Research Centre, Department of Biochemistry, The University, Dundee, UK.

0021-9673/93/$06.00

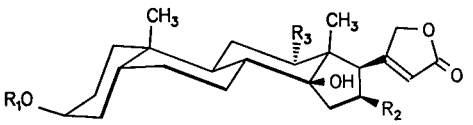

Fig. 1. Structure of the investigated cardiac glycosides. The residues are explained in Table I.

gated the migration behaviour of mixtures of primary and secondary cardiac glycosides with different electrophoresis buffers and then the resolution of a pair of cardenolides differing only in the anomeric form of their carbohydrate side-chain (Fig. 1, Table I). Finally we checked the suitability of MECC for the analysis of complex mixtures (*e.g.*, plant extracts) containing cardenolides.

EXPERIMENTAL

Apparatus

A modular capillary electrophoresis instrument (Grom, Herrenberg, Germany) and a Chromatopac C-R6A (Shimadzu, Kyoto, Japan) for data processing were used. Polyimide-clad fused-silica capillary material of 50 μm I.D. and 360 μm O.D. was obtained from Polymicro Technology (Phoenix, AZ, USA).

Electrophoresis

Capillaries were prepared by flushing the columns for 10 min each with 1 *M* sodium hydroxide solution, water and buffer. All buffers were prepared with doubly distilled water and were degassed by evaporation in an ultrasonic bath. Sample solutions were injected by hydrostatic loading: the injection block was raised by 0.1 m for 30–60 s. Electropherograms of standard solutions were obtained by injection of 5 μl into the block. After hydrostatic loading, excess of sample solution was removed by flushing the injection block. For the injection of small amounts of sample solutions (cell extracts) we used a micro-vial with a 2-μl sample volume. Connection and disconnection of the capillary to the injection block and the micro-vial were done manually. Sample injection with the micro-vial was also done by hydrostatic loading. Between the electrophoretic runs with standard mixtures the capillary was flushed with 50 μl of buffer. Between the analyses of crude cell extracts the

TABLE I

INVESTIGATED CARDIAC GLYCOSIDES

Compound[a]	Abbreviation	R_1 [b]	R_2	R_3
Primary glycosides				
Lanatoside A	LA	Glc-β1–4-α-AcDox-β1–4-Dox-β1–4-Dox-β1–	H	H
Purpureaglycoside A	PA	Glc-β1–4-Dox-β1–4-Dox-β1–4-Dox-β1–	H	H
Lanatoside C	LC	Glc-β1–4-α-AcDox-β1–4-Dox-β1–4-Dox-β1–	H	OH
Desacetyllanatoside C	DC	Glc-β1–4-Dox-β1–4-Dox-β1–4-Dox-β1–	H	OH
Glucoevatromonoside	Gev	Glc-β1–4-Dox-β1–	H	H
Glucogitoroside	Ggr	Glc-β1–4-Dox-β1–	OH	H
Anomeric primary glycosides				
Glucodigifucoside	Gdf	Glc-β1–4-Fuc-β1–	H	H
Glucodigiglucomethyloside	Gdm	Glc-β1–4-Glm-β1–	H	H
Secondary glycosides				
Evatromonoside	Ev	Dox-β1–	H	H
Digitoxin	Dt	Dox-β1–4-Dox-β1–4-Dox-β1–	H	H
α-Methyldigitoxin	α-MDt	α-H_3C-Dox-β1–4-Dox-β1–4-Dox-β1–	H	H
Digoxin	Dg	Dox-β1–4-Dox-β1–4-Dox-β1–	H	OH
α-Acetyldigoxin	α-AcDg	α-AcDox-β1–4-Dox-β1–4-Dox-β1–	H	OH
β-Methyldiginatin	β-MDn	β-H_3C-Dox-β1–4-Dox-β1–4-Dox-β1–	OH	OH

[a] See Fig. 1 for general structure.

[b] Glc = Glucose; α-AcDox = α-acetyldigitoxose; Dox = digitoxose; Fuc = fucose; Glm = glucomethylose.

capillary was rinsed subsequently with 50 μl each of 0.1 *M* sodium hydroxide solution, water and buffer. Sample mixtures containing 80 μ*M* of each glycoside were prepared by mixing standard solutions in water–dimethyl sulphoxide (DMSO).

Pseudo-effective mobilities, $m_{eff,S}$, according to Ackermans *et al.* [10] were determined:

$$m_{eff,S} = m_{app,S} - m_{EOF} = \frac{l_c l_d}{V t_s} - \frac{l_c l_d}{V t_{EOF}}$$

where l_c and l_d are the total length of the capillary and the length from injection to detection, respectively, V is the applied voltage and t_s and t_{EOF} are the observed migration times of the sample and an unretarded neutral molecule, respectively.

Chemicals

Sodium cholate (NaC) for biochemical use was obtained from Merck (Darmstadt, Germany) and analytical-reagent grade sodium dodecyl sulphate (SDS) and α-, β- and γ-cyclodextrins (CDs) from Serva (Heidelberg, Germany). All other chemicals for buffer preparation were of research grade (Merck).

Digitoxin (Dt), evatromonoside (Ev) and lanatoside C (LC) were obtained from Roth (Karsruhe, Germany), lanatoside A (LA) from Arzneimittelherstellung (Dresden, Germany) and α-acetyldigoxin (α-AcDg) and α-methyldigitoxin (α-MDt) from Boehringer (Mannheim, Germany). Desacetyllanatoside C (DC), glucoevatromonoside (Gev), purpureaglycoside A (PA) and β-methyldiginatin (β-MDn) were isolated in our laboratories. The purity (>95%) of these cardiac glycosides were confirmed by HPLC. Glucogitoroside (Ggr) was a gift from Professor M. Wichtl (Marburg, Germany).

RESULTS

As electrically neutral compounds, cardiac glycosides migrated with the electroosmotic flow in capillary zone electrophoresis (CZE) with an alkaline phosphate buffer (data not shown). Interestingly, when CZE is carried out with a borate buffer, electrophoretic mobility and a slight separation can be observed. The electrophoretic mobilities of all cardiac glycosides were about $(-2.75 \pm 0.3) \cdot 10^{-9}$ m^2/V·s in 150 m*M* borate buffer (pH 9.3) at an electric field strength of 18 500 V/m. This is probably due to the formation of borate complexes with the carbohydrate side-chains of the cardenolides [11]. It seems that these borate complexes are not only formed with *cis*-diol [12], as both primary and secondary glycosides without a *cis*-diol structure also show slight electrophoretic mobility (data not shown). Because of the formation of the complexes and the better solubility of the hydrophobic compounds, we decided to prepare the buffers for all the subsequent experiments with borate. Cyclodextrins have been successfully used to increase the solubility of cardiac glycosides in aqueous systems [13]. It therefore appeared reasonable that they could also be suitable for MECC analysis of these compounds.

α-Cyclodextrin had no effect on the migration behaviour of cardenolides compared with the electropherogram with SDS alone. The pseudo-effective mobilities, $m_{eff,S}$, were nearly identical [$(4.275 \pm 0.025) \cdot 10^{-8}$ m^2/V·s in 30 m*M* borate buffer (pH 9.3)–50 m*M* SDS–10 m*M* α-CD; all other conditions as in Fig. 2] for all the investigated cardiac glycosides. β-CD, however, significantly increased the resolution power (Fig. 2). It is interesting that primary glycosides of the C-series (DC, LC) did not yield peaks that could be evaluated but eluted as broad bands. Secondary glycosides of the C-series (Dg, α-AcDg, β-MDg) showed normal peaks although the separation efficiency in general was lower than for the primary glycosides (except of DC and LC).

With γ-CD a very good separation could be achieved for both primary and secondary glycosides (Fig. 3, Tables II and III). The separation efficiency was higher than with β-CD, although again lower theoretical plate numbers for the secondary glycosides were observed. Increasing concentrations of γ-CD induced a reduction in the pseudo-effective mobility, $m_{eff,S}$, as they increased the partitioning of the cardenolides in the aqueous buffer phase (Fig. 4). It was not possible to find an optimum concentration of γ-CD. Ggr and Gev were better separated at low

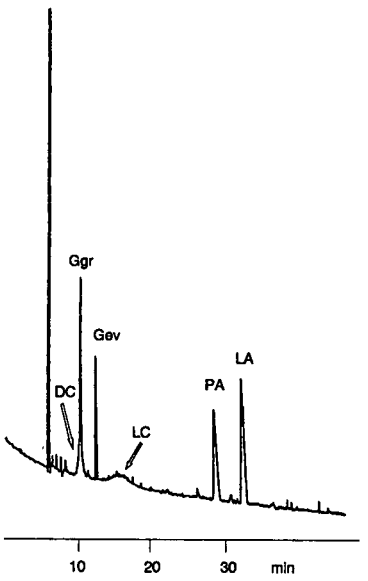

Fig. 2. Electropherogram of six primary cardiac glycosides. Buffer, 30 m*M* $Na_2B_4O_7$–50 m*M* SDS–10 m*M* β-CD (pH 9.3); capillary length, 0.8 m (0.5 m to the detector); detection at 225 nm, range 0.005 (attenuation 4); voltage, 20 kV; current, 33 μA; 30-s hydrostatic injection (0.1 m high).

γ-CD-concentrations whereas the resolution of the secondary cardiac glycosides increased with increasing CD concentration.

With 7 *M* urea–SDS–borate electrophoresis buffer, good separation of the cardenolides investigated could also be achieved (Fig. 5, Tables II and III). Because of the high viscosity of the 7 *M* urea buffer, the time required for hydrostatic injection was longer than with γ-CD–buffer. The borate and SDS concentrations were decreased and the voltage was increased in order to reduce the analysis times, which would otherwise have been unacceptably long (more than 50 min, data not shown). The separation efficiency of primary and secondary glycosides was comparable to that of the γ-CD system.

Sodium cholate (NaC)–borate buffers have been successfully employed for the separation and determination of lipophilic corticosteroids and benzothiazepine analogues by MECC [7]. Test runs with 50 m*M* NaC–30 m*M* borate and 100 m*M* NaC–30 m*M* borate buffers yielded only partial separation of the cardenolide mixtures (data not shown). With an NaC–SDS–borate buffer, however, a good separation of the

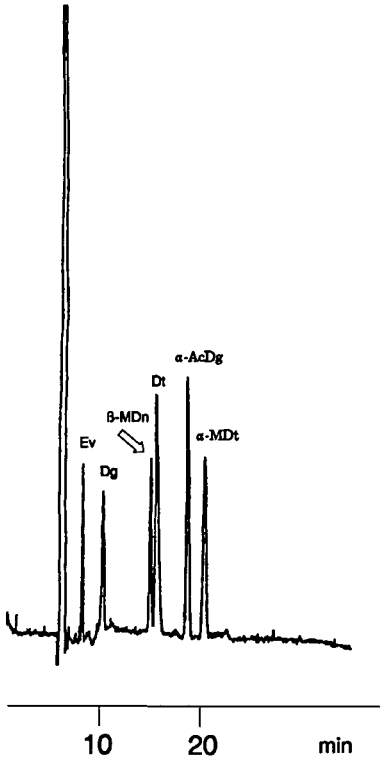

Fig. 3. Electropherogram of six secondary cardiac glycosides. Buffer, 30 m*M* $Na_2B_4O_7$–50 m*M* SDS–10 m*M* γ-CD (pH 9.3); other conditions as in Fig. 2 except attenuation 2.

cardenolides was obtained (Tables II and III). Increasing the NaC concentration resulted in a decrease in the pseudo-effective mobilities, $m_{eff,S}$, of the cardiac glycosides (Fig. 6). This effect seemed to be qualitatively similar to that of the concentration of γ-CD on the migration behaviour of the sample compounds (Fig. 4). The concentration of NaC had virtually no influence on the resolution.

Gdf and Gdgm are two cardiac glycosides that are anomeric at C4′ and they cannot be distinguished by conventional HPLC. A sample isolated from *Digitalis lanata* showed one main peak in the HPLC trace that was diminished by *ca.* 30% after treatment with glucosidase. It was difficult to explain this phenomenon using HPLC. MECC analysis with the three different buffers revealed that the sample contained two main components and that one of them was degraded completely by glucosidase (Table IV). By admixture of a Gdgm standard it could be

TABLE II

SEPARATION OF PRIMARY GLYCOSIDES

Pseudo-effective mobilities, $m_{eff,S}$ ($\times 10^8$ $m^2/V \cdot s$), and electroosmotic flow, m_{EOF} ($\times 10^8$ $m^2/V \cdot s$) (first line), elution number (second line) and number of plates (third line).

Buffer	Conditions	m_{EOF}	DC	LC	Gev	Ggr	PA	LA
30 m*M* borate–50 m*M* SDS–10 m*M* β-CD (pH 9.3)	25 000 kV/m	5.58	−2.37 1 26 500	−3.62 3 –	−2.91 2 38 400	−2.37 1 –	−4.43 4 33 100	−4.56 5 38 000
30 m*M* borate–50 m*M* SDS–10 m*M* γ-CD (pH 9.3)	25 000 kV/m	5.76	−3.12 3 88 400	−3.88 4 68 250	−2.24 2 134 650	−2.19 1 160 000	−4.09 5 68 600	−4.28 6 97 350
22.5 m*M* borate–37.5 m*M* SDS–7 *M* urea (pH 9.3)	32 050 kV/m	5.41	−4.09 1 119 230	−4.4 4 147 550	−4.38 3 192 420	−4.13 2 85 950	−4.53 5 157 500	−4.56 6 150 900
30 m*M* borate–25 m*M* SDS–25 m*M* NaC (pH 9.3)	21 430 kV/m	5.65	−3.15 1 85 500	−3.54 2 99 200	−4.2 4 129 000	−3.85 3 114 000	−4.39 5 25 700	−4.44 6 35 300

TABLE III

SEPARATION OF SECONDARY GLYCOSIDES

Pseudo-effective mobilities, $m_{eff,S}$ ($\times 10^8$ $m^2/V \cdot s$), and electroosmotic flow, m_{EOF} ($\times 10^8$ $m^2/V \cdot s$) (first line), elution number (second line) and number of plates (third line).

Buffer	Conditions	m_{EOF}	Dg	β-Ddn	α-AcDg	Ev	Dt	α-MDt
30 m*M* borate–50 m*M* SDS–10 m*M* β-CD (pH 9.3)	28 570 kV/m	4.9	−2.64 1 5450	−3.11 3 5600	−3.45 4 9200	−3.06 2 15 900	−3.5 5 13 400	−3.57 6 14 900
30 m*M* borate–50 m*M* SDS–10 m*M* γ-CD (pH 9.3)	25 000 kV/m	5.49	−2.74 2 10 000	−3.62 3 31 200	−3.99 5 25 800	−2.03 1 23 300	−3.69 4 11 000	−4.12 6 19 100
22.5 m*M* borate–37.5 m*M* SDS–7 *M* urea (pH 9.3)	32 050 kV/m	5.44	−3.78 1 3450	−4.17 2 10 500	−4.44 4 6000	−5.22 3 7500	−4.46 5 14 300	−4.52 6 17 800
30 m*M* borate–25 m*M* SDS–25 m*M* NaC (pH 9.3)	21 430 kV/m	5.88	−2.25 1 15 800	−2.87 2 10 250	−3.51 3 20 700	−3.83 4 31 900	−4.15 5 9300	−4.31 6 8000

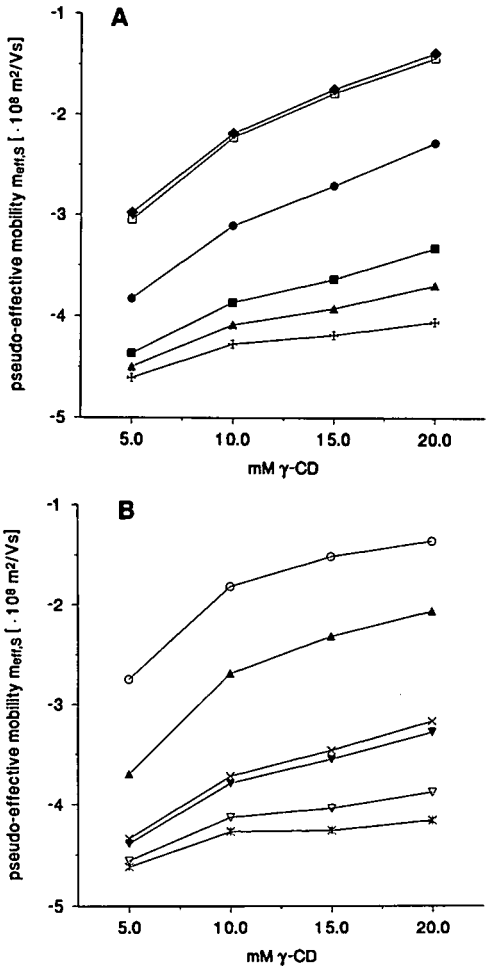

Fig. 4. Influence of γ-CD concentration on $m_{eff,S}$ of (A) primary and (B) secondary cardiac glycosides. (A) ◆ = Ggr; □ = Gev; ● = DC; ■ = LC; ▲ = PA; + = LA. (B) ○ = Ev; ▲ = Dg; × = β-mDn; ▼ = Dt; ▽ = α-AcDg; * = α-MDt. Conditions as in Tables II and III.

shown that the Gdgm is deglucosylated to digitoxigeninglucomethyloside (Dtgm) whereas Gdf is resistant to the glucosidase treatment (Fig. 7).

The capability of analysing complex mixtures such as plant-leaf extracts with the MECC systems would be of great interest. In order to decide whether a main constituent of *Digitalis lanata* leaf extracts was Gdf, Gdgm or a mixture of the two, 50% methanolic extracts were analysed.

With γ-CD the two cardenolides of interest migrated too close to the electroosmotic flow

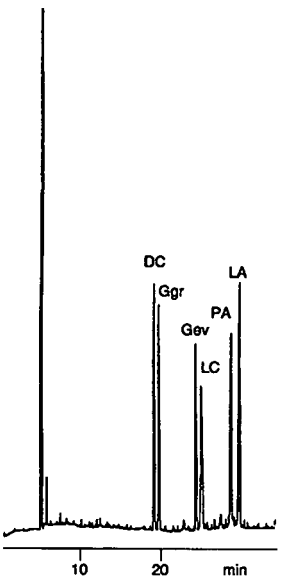

Fig. 5. Electropherogram of six primary cardiac glycosides. Buffer, 22.5 m*M* $Na_2B_4O_7$–37.5 m*M* SDS–7 *M* urea (pH 9.3); capillary length, 0.8 m (0.5 m to the detector); detection at 225 nm, range 0.005 (attenuation 3); voltage, 25 kV; current, 26 μA; 60-s hydrostatic injection (0.1 m high).

(EOF) whereas other cardiac glycosides migrate very close to the micellar front. For this reason electropherograms of crude cell extracts could hardly be evaluated. With NaC–SDS–borate and 7 *M* urea–SDS–borate buffers, cardiac glyco-

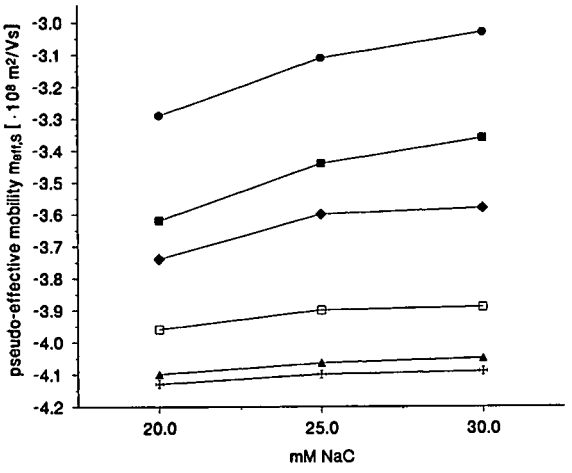

Fig. 6. Influencé of NaC concentration on $m_{eff,S}$ of primary cardiac glycosides. ● = DC; ■ = LC; ◆ = Ggr; □ = Gev; ▲ = PA; + = LA. Conditions as in Table II.

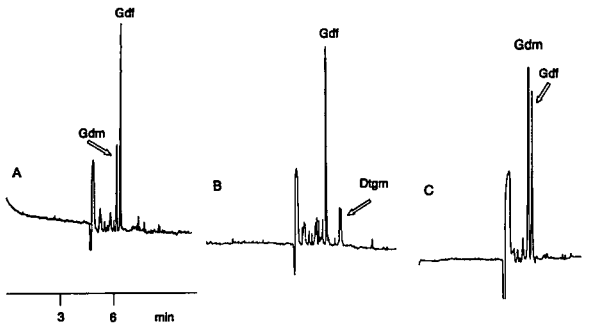

Fig. 7. Electropherograms of cardiac glycosides from *Digitalis lanata*. Buffer, 30 m*M* $Na_2B_4O_7$–50 m*M* SDS–20 m*M* γ-CD (pH 9.3); capillary length, 0.75 m (0.45 m to the detector); detection at 225 nm, range 0.002 (attenuation 4); voltage, 20 kV; current, 38 μA; 30-s hydrostatic injection (0.1 m high). (A) Before glycosidase treatment; (B) after glycosidase treatment; (C) with Gdm standard.

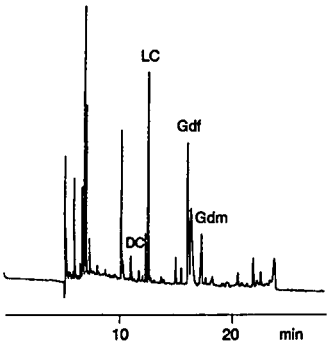

Fig. 8. Electropherogram of a crude cell extract from *Digitalis lanata*. Buffer, 30 m*M* $Na_2B_4O_7$–25 m*M* SDS–25 m*M* NaC (pH 9.3); capillary length, 0.7 m (0.4 m to the detector); voltage, 20 kV; current, 40 μA; methanolic cell extract diluted with electrophoresis buffer; other conditions as in Fig. 2.

sides are sufficiently separated from both the EOF and the micellar front (Table IV). We obtained good and reproducible electropherograms with these systems. However, the migration times differed considerably from those of the standard samples. This difficulty could be overcome by diluting the samples two-fold with the electrophoresis buffer prior to the analysis (Fig. 8). Nevertheless, it will remain necessary to add internal standards for an exact identification until more experience with this method is gained.

An alternative to the analysis of crude extracts would be to carry out a preseparation by HPLC and to separate further the fractions known to contain two or more substances by MECC. This would make identification of single compounds easier and more reliable. We injected a DC-containing fraction from an HPLC separation of a *Digitalis lanata* leaf extract. In order to allow on-line capillary detection in MECC, the 200-μl fraction had to be concentrated twofold by evaporation. Subsequently we were able to show that the fractions contained no Ggr. This compound is barely separated from DC by HPLC

TABLE IV

SEPARATION OF TWO ANOMERIC GLYCOSIDES (Gdf AND Gdm)

Pseudo-effective mobilities, $m_{eff,S}$ ($\times 10^8$ $m^2/V \cdot s$), and electroosmotic flow m_{EOF} ($\times 10^8$ $m^2/V \cdot s$) (first line), elution number (second line) and number of plates (third line).

Buffer	Conditions	m_{EOF}	Gdf	Gdm	Dtgm
30 m*M* borate–50 m*M* SDS–20 m*M* γ-CD (pH 9.3)	26 666 kV/m	5.6	−1.31	−1.18	−2.12
			2	1	3
			193 800	248 700	61 600
22.5 m*M* borate–37.5 m*M* SDS–7 *M* urea (pH 9.3)	32 050 kV/m	5.4	−4.23	−4.27	−4.98
			1	2	3
			135 100	120 400	57 300
30 m*M* borate–25 m*M* SDS–25 m*M* NaC (pH 9.3)	28 570 kV/m	5.15	−3.5	−3.68	−3.81
			1	2	3
			23 000	38 600	83 700

but has clearly different migration times in γ-CD and in NaC-modified MECC (data not shown).

DISCUSSION

CDs have been successfully applied for the separation of several hydrophobic compounds. They have been especially useful for chiral separations in capillary electrophoresis. Nishi *et al.* [14] suggested that with the addition of cyclodextrins to the electrophoresis buffer a new equilibrium is established between the micellar phase, the aqueous phase and the hydrophobic cavity of the CDs.

Whereas the hydrophobic cavity of α-CD appears to be too small for an interaction with the cardiac glycosides, their migration behaviour is clearly changed by β-CD and γ-CD. We could not find an explanation for the observation that two structurally related compounds (DC and LC) migrated with very broad peaks, an effect that was completely abolished with γ-CD. The separation efficiency with γ-CD is higher than that with β-CD. Separation in these systems is based on a complicated dynamic equilibrium between the borate complex in the aqueous phase, inclusion in the CDs and solubilization by the SDS micelles (Fig. 9).

Urea increases the solubility of hydrophobic compounds in aqueous systems and can therefore also be used as a modifier of very lipophilic molecules in MECC. Terabe *et al.* [6] investigated the separation mechanism of urea-modified MECC and came to the conclusion that it is mainly based on the shift of the partition equilibrium between aqueous and micellar phases. They stressed that urea broadens the migration time window and is therefore very suitable for high resolution MECC.

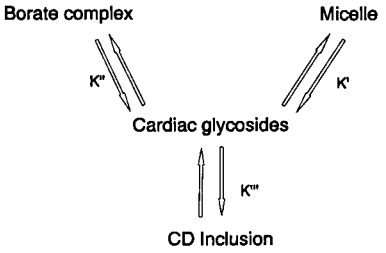

Fig. 9. Separation mechanism of CD-modified MECC.

Bile salts seem to have a smaller solubilizing effect than SDS, which makes them also suitable for analyses of very lipophilic compounds. The similar structure to the aglycones of the cardenolides could make specific solubilization effects possible. Although a good separation with NaC–borate buffers was not possible, the results with the mixed NaC–SDS–borate buffer were very good. It is possible that mixed micelles are formed, the solubilization properties of which are especially suitable for the separation of these compounds [15]. An investigation of the solubilization mechanisms of the different systems would require more comparative analyses. Additional structural analysis of the cardenolides may yield further information on their conformation in different solvents.

All buffer systems investigated show a higher separation efficiency for primary than for secondary cardiac glycosides. A number of explanations for this observation are possible. Borate, which is a constituent of all the buffer systems, can interact better with the hydroxyl groups on the terminal glucosyl residue on primary cardiac glycosides. Additionally, this group of cardenolides shows a greater polarity than secondary cardiac glycosides, which could lead to a better incorporation into the micelles.

We have shown in this paper that MECC can be applied to the separation of Gdf and Gdgm, two cardenolides of identical polarity that comigrate in HPLC. The resolution of these very similar compounds could be readily achieved without prior derivatization or hydrolysis. It is of considerable advantage to have three different MECC methods at hand for the analysis of cardenolides. As there are obvious differences in the solubilization behaviour of the buffers, a sample could be run with different buffers to ensure a reliable identification of a particular compound.

Owing to wall adsorption and perhaps to changes in the formation of micelles, crude tissue extracts have proved to be difficult to analyse by MECC. This is why so far only a few electropherograms of complex mixtures have been published. We were able to achieve a very good resolution with the NaC–SDS–borate and 7 *M* urea–SDS–borate buffers, especially when the

extracts were diluted with the electrophoresis buffer.

CONCLUSIONS

MECC using the three different buffer systems established allows a reliable separation and identification of cardiac glycosides even if they are inseparable by HPLC. It can be used for the analysis of crude cell extracts and for the investigation of HPLC fractions. The possibility of injecting very small sample volumes broadens the range of application of MECC when only limited amounts of sample are available. MECC can be recommended as a method for the routine analysis of cardenolide-containing samples. It is both more economical and less threatening to the environment than HPLC, where large amounts of acetonitrile are used. We conclude that MECC has all the potential to become a valuable tool for the investigation of the biosynthesis, transport and degradation of cardiac glycosides.

ACKNOWLEDGEMENTS

We thank Dr. R. Schubert for helpful discussions. H.-J.G. was supported by the Landesgraduiertenförderung Baden-Württemberg, Germany, and A.T. by the Evangelisches Studienwerk Villigst, Germany.

REFERENCES

1 M. Wichtl, M. Mangkudidjojo and W. Wichtl-Bleier, *J. Chromatogr.*, 234 (1982) 503.
2 W. Kreis, U. May and E. Reinhard, *Plant Cell Rep.*, 5 (1986) 442.
3 J. Vindevogel and P. Sandra, *Introduction to Micellar Electrokinetic Chromatography*, Hüthig, Heidelberg, 1992.
4 N. Dmiri, U. Fricke and W. Klaus, *J. Pharmacol.*, 91 (1987) 31.
5 S. Terabe, Y. Miyasashita, O. Shibata, E.R. Barnhardt, L.R. Alexander, D.G. Patterson, B.L. Karger, K. Hosoya and N. Tanaka, *J. Chromatogr.*, 516 (1990) 23.
6 S. Terabe, Y. Ishihama, H. Nishi, Y. Fukuyama and K. Otsuka, *J. Chromatogr.*, 545 (1991) 359.
7 H. Nishi, T. Fukuyama, M. Matsuo and S. Terabe, *J. Chromatogr.*, 513 (1990) 279.
8 C.P. Ong, C.L. Ng, H.K. Lee and S.F.Y. Li, *J. Chromatogr.*, 547 (1991) 419.
9 J. Vindevogel and P. Sandra, *Anal. Chem.*, 63 (1991) 1530.
10 M.T. Ackermans, F.M. Everaerts and J.L. Beckers, *J. Chromatogr.*, 585 (1991) 123.
11 S. Hoffstetter-Kuhn, A. Paulus, E. Gassmann and H.M. Widmer, *Anal. Chem.*, 63 (1991) 1541.
12 M. van Druin, J.A. Peters, A.P.G. Kieboom and H. van Bekkum, *Tetrahedron*, 41 (1985) 3411.
13 B. Pekić and Z. Lepojević, *Biotechnol. Lett.*, 13 (1991) 399.
14 H. Nishi, T. Fukuyama and S. Terabe, *J. Chromatogr.*, 553 (1991) 503.
15 R. Schubert and K.-H. Schmidt, *Biochemistry*, 27 (1988) 8787.

Journal of Chromatography, 635 (1993) 329–333
Elsevier Science Publishers B.V., Amsterdam

CHROM. 24 844

Simple device for electroelution of proteins from a large number of pieces of polyacrylamide gel

Hege K. Vefring and Arve Osland*

Department of Clinical Chemistry, Central Hospital in Rogaland, Armauer Hansens Vei 20, 4011 Stavanger (Norway)

(First received October 16th, 1992; revised manuscript received December 29th, 1992)

ABSTRACT

A device for electroelution of macromolecules that handles up to 96 different pieces of gel was constructed. The basic unit is the electroelution plate containing the 96 electroelution chambers, which is made from a 96-well tissue culture plate with holes bored in each individual well, both through the base of the plate and through the lid covering the plate. The electroelution plate can be used either with a buffer tank equipped with platinum electrodes or with flat graphite electrodes. Using standard conditions, 60–70% of the proteins with molecular mass less than 70 000 were eluted in 1 h.

INTRODUCTION

Preparative electrophoretic techniques include preparative isoelectric focusing (IEF) in granulated gels and focusing in gels containing immobilized pH gradients. The recovery of proteins using these methods usually involves a second zone electrophoresis into an ion exchanger followed by column chromatography [1]. Although these methods have advantages such as high resolution, even at high protein load, the procedure is cumbersome and time consuming, especially when several samples are to be processed.

One-dimensional [sodium dodecyl sulphate polyacrylamide gel electrophoresis (SDS-PAGE)] [2] and two-dimensional (IEF–SDS-PAGE) [3] gel electrophoresis of proteins are powerful and widely used techniques for the separation of proteins, especially for analytical purposes [4,5]. These high resolution techniques are also used for preparative purposes when the amounts of proteins to be isolated are small.

In order to recover the separated proteins from polyacrylamide gels, electroblotting is usually performed when amino acid sequencing or detection by antibodies is later to be carried out. However, if biological activities such as inhibition of cell growth or antigen stimulation of T-cells are to be tested, it would be favourable to elute the proteins into a buffer solution [6]. Such electroelution of macromolecules from polyacrylamide gels is usually time consuming and needs some care in implementation, *e.g.*, when putting small pieces of gel into dialysis tubes for electroelution [7]. Currently available commercial equipment for electroelution handles only a relatively small number of pieces of gel, and other methods are designed to process several pieces of gel containing the same protein [8] or whole polyacrylamide gels [6]. In this paper, we describe a simple device for the electroelution of proteins that handles a variable number of pieces of gel (1–96) and that can easily be made in any laboratory.

EXPERIMENTAL

Chemicals

Standard protein molecular mass markers (SDS-6H) (Sigma, St. Louis, MO, USA) con-

* Corresponding author.

0021-9673/93/$06.00

taining myosin (M_r 205 000), β-galactosidase (116 000), phosphorylase B (98 000), bovine albumin (66 000), ovalbumin (45 000) and carbonic anhydrase (29 000) were used for quantitative analysis. The standard proteins were dissolved in Laemmli sample buffer [2] giving a protein concentration of 2.0 mg/ml. Prestained molecular mass markers (SDS-7B) (Sigma), used for the preliminary testing of the device, ranged from M_r 26 000 to 180 000.

The electroelution buffer was 190 m*M* glycine–25 m*M* Tris base as described previously for electroblotting [9].

Preparation of pieces of gel

Pieces of polyacrylamide gel were made by polymerizing acrylamide–bisacrylamide (30:0.8) solution containing 0.4 *M* Tris–HCl (pH 8.8) and 0.1% SDS in a glass tube of 5 mm I.D. In the present experiments, 7% polyacrylamide gels containing 1.0 mg/ml of total protein were used. After polymerization, 2 mm pieces of gel were cut from the gel cylinder and placed in the electroelution chambers. Each piece of gel contained *ca.* 45 μg of total protein.

Description of the device

The main part of the device is the electroelution plate containing the electroelution chambers, which is made from a flat-bottomed 96-well tissue culture plate (Costar, Cambridge, MA, USA). The electroelution plate can be used in a buffer tank made of acrylic plastic (Fig. 1B) equipped with platinum electrodes, where the cathode is in the bottom of the tank and the anode in the top lid. When electroelution is carried out, the chambers are separated from the outside buffer by agarose plugs in the bottom and a semipermeable membrane at the top. In order to press the membrane tightly to the wells, the plate lid with the two glued acrylic rods is pressed on to the electroelution plate using rubber bands (Fig. 1A, top view).

The electroelution plate can alternatively be used with flat graphite electrodes (Novablot) (LKB–Pharmacia, Uppsala, Sweden), with the cathode as the lower and the anode as the upper electrode (Fig. 1C). With the semipermeable membrane covering the top of the wells, the

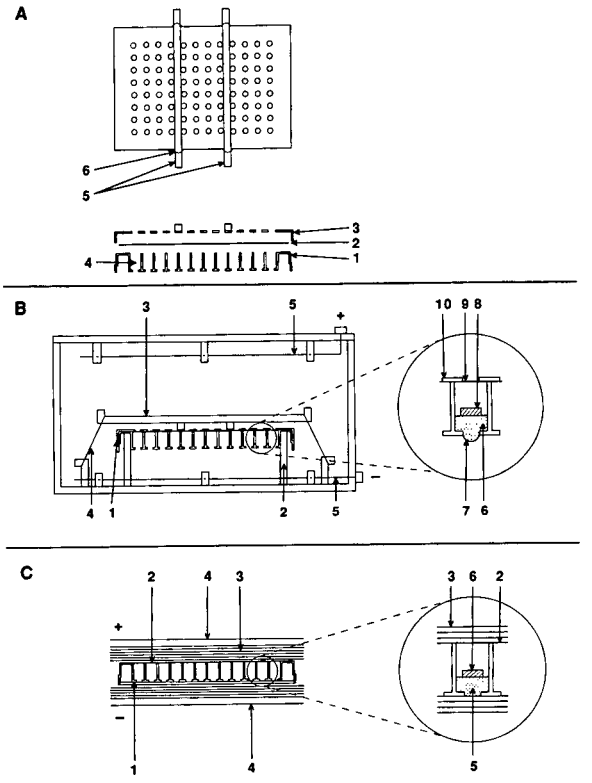

Fig. 1. Description of the electroelution device. (A) Below is a side view of the electroelution plate with the electroelution chambers (wells). The plate (1), membrane (2), lid with holes (3) and electroelution chamber (4) are shown. Above is a top view of the plate lid showing the holes and the acrylic rods (5) used to keep the lid close to the plate with rubber bands (6). (B) Side view of the set-up using the buffer tank. The plate with the membrane and lid (1) is kept in place on the stand (2) by the acrylic rod (3) and rubber bands (4). The electrodes (5) are in the bottom of the tank and on the tank lid. The enlarged diagram of one electroelution chamber shows the agarose plug (6) with an agarose droplet (7), the piece of gel (8), the membrane (9) and the lid (10). (C) Side view of the set-up using the graphite electrodes. The plate (1) with the membrane (2), the wetted filter-papers (3) and the electrodes (4) are shown. The enlarged diagram of one electroelution chamber shows the agarose plug (5), the gel piece (6), the membrane (2) and the wetted filter-papers (3).

electroelution plate is placed between wet filter-papers. The plate lid is not required as the membrane is pressed tightly to the wells by the mass of the graphite electrode (anode).

Set-up for electroelution

In order to prepare the device for use in the buffer tank, the bottom of the electroelution

plate was first sealed with Parafilm (American Can, Greenwich, CT, USA) and molten 1% agarose (in electroelution buffer) was transferred into the wells that were to be used for electroelution. The amount of agarose depends on the desired elution volume, and in the present experiments 100-μl agarose plugs were used. After the agarose had solidified, the plate was turned upside down and the Parafilm removed. Droplets of molten agarose were placed on the plugs to prevent gas bubbles from adhering to the agarose plugs during the electroelution process. After the agarose droplets had solidified, the plate was again turned and the pieces of gel containing the macromolecules to be electroeluted were placed in the wells, which subsequently were filled with electroelution buffer. A semipermeable membrane was placed over the wells, taking care not to introduce any air bubbles, and the lid was pressed on to the membrane and tightened to the plate with rubber bands. The whole plate was immersed in the buffer tank containing buffer just above the plate level, and the plate was anchored to the tank with rubber bands and an acrylic rod as shown in Fig. 1B. Finally, the buffer tank was filled with the electroelution buffer and the top lid with the anode was put in place.

When the electroelution plate was used with flat graphite electrodes, agarose plugs were made as described for the application of the buffer tank. However, to ensure a flat surface of the base of the plate, agarose droplets were not used (Fig. 1C, enlargement). Ten Whatman (Maidstone, UK) 1MM filters were wetted in electroelution buffer and placed on the lower cathode. The electroelution plate, containing the pieces of gel and buffer, was then placed on top of the filters and the semipermeable membrane was carefully fitted on top of the plate, making sure that no air bubbles were trapped inside the chambers. Ten wet filter-papers were laid on the membrane and finally the anode was put on top.

Electroelution and analysis of eluate

To investigate the time course of the process, electroelution was carried out in the buffer tank with a constant current of 200 mA (0.7 mA/cm^2). At time intervals, 25- and 100-μl samples were collected using a Hamilton syringe to penetrate the semipermeable membrane. The polarity of the current was reversed for 30 s prior to sample taking in order to reduce the amount of protein bound to the membrane. The collected samples were mixed with an equal volume of twofold concentrated sample buffer (2xSB) and subjected to analysis by 10% SDS-PAGE [2]. The gel was stained with Coomassie Brilliant Blue and the proteins were determined by videodensitometric scanning (CREAM) (Kem En Tec, Copenhagen, Denmark).

When graphite electrodes were used, electroelution was performed with a current of 0.8 mA/cm^2 as described for electroblotting by the manufacturer. Electroelution was carried out for 1 h, after which the polarity of the current was reversed for 30 s. The anode, the wet filter-papers and the semipermeable membrane were carefully removed and samples of 50 μl of the eluted proteins were collected, mixed with an equal volume of 2xSB and subjected to analysis by SDS-PAGE as described.

RESULTS

In order to follow the electroelution process visually, preliminary experiments were performed in the buffer tank using pieces of gel containing prestained markers. It was observed, as expected, that the eluted proteins concentrated just below the semipermeable membrane. Initially, some leakage between the electroelution chambers and the membrane was observed, but this was avoided by applying a thin layer of silicone grease around the top of each chamber.

When the time course of the electroelution process was investigated, pieces of gel containing standard protein mixture were placed in the wells and electroeluted using the buffer tank. Fig. 2 shows a plot of the amount of the various proteins eluted *versus* electroelution time. The results clearly show that electroelution proceeded more rapidly with low- than with high-molecular-mass proteins. After 60 min, 55–61% of the molecules with $M_r < 70\,000$ were eluted, whereas only 13% of phosphorylase B (98 000) and 11% of β-galactosidase (116 000) were eluted. When electroelution was carried out

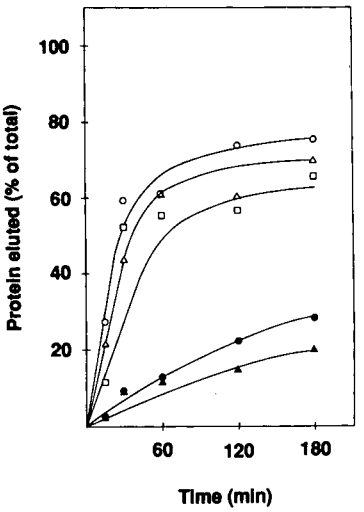

Fig. 2. Time course of the electroelution process using the buffer tank. Standard proteins were electroeluted for the times indicated and determined by SDS-PAGE and densitometric scanning. ○ = carbonic anhydrase (M_r 29 000); △ = ovalbumin (45 000); □ = bovine serum albumin (66 000); ● = phosphorylase *b* (98 000), ▲ = β-galactosidase (116 000).

for an additional 2 h, 65–70% of the proteins with $M_r < 70\,000$ were eluted, hence a relatively small additional yield of these proteins was observed. Regarding the higher molecular mass proteins, 28% of phosphorylase B (98 000) and 20% of β-galactosidase (116 000) were recovered in 3 h whereas no myosin (205 000) was detected.

When electroelution was performed using the graphite electrodes, 60–70% of the proteins with M_r 29 000, 45 000 and 66 000 were eluted in 1 h (Fig. 3). Electroelution of the proteins with M_r 98 000 and 116 000 was not very efficient, releasing only 5–15% of the total protein in 1 h. Myosin (205 000) was not detected. The results obtained with the graphite electrodes were thus similar to those obtained by applying the buffer tank.

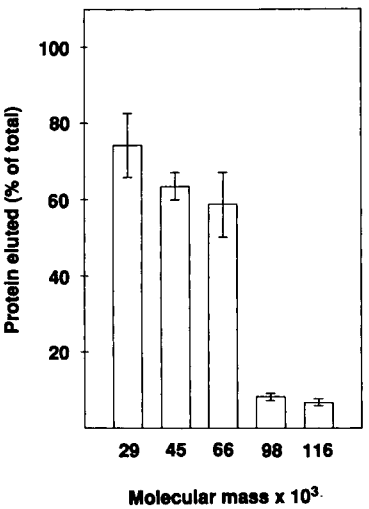

Fig. 3. Electroelution using graphite electrodes. Standard proteins were electroeluted for 1 h and determined by SDS-PAGE and densitometric scanning. The average values (±S.D.) obtained from five different pieces of gel from the same run are shown.

DISCUSSION

We have described a device for the electroelution of macromolecules from a large number of pieces of gel. The device has a simple construction and can easily be made in any laboratory. It is also flexible in use, as any number of pieces of gel between 1 and 96 can be processed. In addition, when electroelution is carried out with the graphite electrodes (Novablot), three electroelution plates can be placed adjacent to each other, allowing up to 288 pieces of gel to be processed simultaneously.

Even though electroelution of molecules with $M_r > 70\,000$ was a slow process, the device has proved to be beneficial for the elution of molecules with $M_r < 70\,000$, especially when total recovery is not important. In 1 h, more than 60% of these molecules were eluted. An improved recovery of the high-molecular-mass proteins might be obtained by prolonging the electroelution time or by modifying the buffer, *e.g.*, by adding SDS.

The format of the electroelution plate is compatible with enzyme immunoassay plates and cell culture plates, hence samples can easily be transferred to these for further testing or processing. We suggest that the device described here can also be used for electroelution of DNA fragments from pieces of agarose gel as well as for rapid buffer exchange of samples containing macromolecules.

REFERENCES

1 P.G. Righetti, M. Faupel and E. Wenisch, in A. Chrambach, M.J. Dunn and B.J. Radola (Editors), *Advances in Electrophoresis*, Vol. 5, VCH, Weinheim, 1992, p. 159.
2 U.K. Laemmli, *Nature*, 227 (1970) 680.
3 P.H. O'Farrell, *J. Biol. Chem.*, 250 (1975) 4007.
4 M. Costas, in A. Chrambach, M.J. Dunn and B.J. Radola (Editors), *Advances in Electrophoresis*, Vol. 5, VCH, Weinheim, 1992, p. 351.
5 N.L. Anderson and N.G. Anderson, *Electrophoresis*, 12 (1991) 883.
6 H. Gulle, B. Schoel and S.H.E. Kaufmann, *J. Immunol. Methods*, 133 (1990) 253.
7 J. Sambrook, E.F. Fritsch and T. Maniatis, *Molecular Cloning: a Laboratory Manual*, Cold Spring Harbor Laboratory Press, Cold Spring Harbor, NY, 1989.
8 B.C. Schultes and N. Dahlmann, *Eur. J. Biochem.*, 192 (1990) 201.
9 H. Towbin, T. Staehlin and J. Gordon, *Proc. Natl. Acad. Sci. U.S.A.*, 76 (1979) 4350.

Journal of Chromatography, 635 (1993) 334–337
Elsevier Science Publishers B.V., Amsterdam

CHROM. 24 888

Short Communication

Size-exclusion chromatography of cellulose and chitin using lithium chloride–N,N-dimethylacetamide as a mobile phase

Makoto Hasegawa*, Akira Isogai and Fumihiko Onabe

Department of Forest Products, Faculty of Agriculture, University of Tokyo, Yayoi, Bunkyo-ku, Tokyo 113 (Japan)

(First received November 23rd, 1992; revised manuscript received January 21st, 1993)

ABSTRACT

Distributions of molecular mass of cellulose and chitin were determined by size-exclusion chromatography (SEC) using 5% (w/w) lithium chloride–N,N-dimethylacetamide as an eluent. The peak positions in SEC patterns of the cellulose samples used corresponded well to their molecular masses, which were measured by a viscometric method using cupriethylenediamine. Thus, the packed gel consisting of styrene–divinylbenzene copolymer was found to be applicable to the SEC analysis of cellulose and chitin, when 5% (w/w) lithium chloride–N,N-dimethylacetamide was used as the solvent for polysaccharides and as the eluent. The elution patterns obtained in this SEC system indicated that the molecular mass of commercial chitins prepared from crab shell is much higher than that of cotton, and that the chitins have two peaks of distribution of molecular mass.

INTRODUCTION

Many kinds of aqueous and non-aqueous solvent systems for cellulose or chitin have been reported so far. Although depolymerization of the polysaccharide molecules occurs to a greater or lesser extent in most systems during and/or after the preparation of cellulose or chitin solutions, some of the solvent systems may be applicable to the media for determining molecular mass and distribution of molecular mass of cellulose or chitin. Cupriethylenediamine (CED, *ca.* 0.5 *M*) is generally used as an aqueous solvent for cellulose samples to determine their molecular mass by the viscosity method, and carbanilation of all hydroxyl groups of cellulose samples followed by size-exclusion chromatography (SEC) using tetrahydrofuran as an eluent is well accepted as the method for obtaining their distribution of molecular mass [1,2]. On the other hand, a few solvent systems have been found for chitin, but only the lithium chloride–N,N-dimethylacetamide (LiCl–DMAc) system is applicable to viscosity measurements of chitin samples. However, so far no papers have reported the measurement of distribution of molecular mass of chitin samples.

Since the LiCl–DMAc system can dissolve cellulose, chitin, and other many polysaccharides with little depolymerization [3–8], this system may be used as the solvent for cellulose and chitin samples for size-exclusion chromatography without any derivatizing steps for the polysac-

* Corresponding author.

0021-9673/93/$06.00

charides. The molecular masses and distributions of molecular mass of some cellulose samples have been estimated by SEC using 0.5% (w/w) LiCl–DMAc as an eluent [9]. In this study, the LiCl–DMAc system was applied to SEC of cellulose and chitin, using an SEC column of copolymer gel consisting of styrene–divinylbenzene.

EXPERIMENTAL

Chemicals and solvents

N,N-Dimethylacetamide and lithium chloride of analytical-reagent grade were purchased from Wako (Osaka, Japan).

The 10% (w/w) LiCl–DMAc solution was prepared by the addition of a predetermined amount of LiCl to DMAc at 80°C with stirring, and the LiCl–DMAc solution thus prepared was kept at 80°C in order to avoid partial precipitation of LiCl.

Cellulose and chitin samples

The cellulose samples used were cotton, regenerated cellulose prepared from ramie [10], microcrystalline cellulose powder (Avicel; Asahi Chemical, Tokyo, Japan) and a low-molecular-mass cellulose prepared by homogeneous hydrolysis of microcrystalline cellulose powder with phosphoric acid [11] (Table I). The viscosity-average degrees of polymerization ($\overline{DP}_v$) of the cellulose samples were evaluated from their intrinsic viscosities, which were measured using 0.5 *M* CED as the cellulose solvent, by the following equation [12]:

TABLE I

VISCOSITY-AVERAGE DEGREES OF POLYMERIZATION ($\overline{DP}_v$) OF CELLULOSE SAMPLES

$\overline{DP}_v$ values were calculated from intrinsic viscosities measured in 0.5 *M* CED, according to $[\eta] = 0.581 \times DP^{1.00}$ [12].

Cellulose sample	$\overline{DP}_v$
Cotton	1690
Regenerated ramie	1190
Microcrystalline cellulose powder	240
Low-molecular-mass cellulose	9

$$[\eta] = 0.571 \times DP^{1.00}$$

Two commercial chitin samples with powder and particle forms prepared from crab shell were used (PSH and CLH, respectively; Yaizu Suisan Kagaku, Shizuoka, Japan).

Preparation of cellulose and chitin solutions

Cellulose solutions in 5% (w/w) LiCl–DMAc were prepared as follows: (1) a dry cellulose sample of 10 mg was suspended in 10 ml of 10% (w/w) LiCl–DMAc; (2) the mixture was heated at 80°C until the cellulose sample was sufficiently swollen (*ca.* 0–24 h, depending on the molecular mass of the cellulose samples); (3) 10 ml of DMAc were added to the mixture to adjust the concentration of the solution to 5% (w/w) LiCl–DMAc; and (4) a clear cellulose solution was obtained after the mixture was kept at room temperature for several days with occasional swirling.

Chitin solutions were prepared by stirring a mixture of a dry chitin sample of 10 mg and 20 ml of 5% (w/w) LiCl–DMAc at room temperature, as described by Terbojevich *et al.* [7].

Apparatus and conditions

A high-pressure pump of the single-plunger type (Milton Ray, New York, USA) with a pressure reservoir and a differential refractometer (R401; Waters, Milford, MA, USA) was used for the SEC system. A packed SEC column consisting of styrene–divinylbenzene copolymer gel (TSK-gel GMHXL; 10 μm particle size, 300 × 7.8 mm I.D.; Tosoh, Tokyo, Japan) was used at room temperature. The column was originally packed with acetone, because it was specially designed for SEC with dimethyl sulphoxide as an eluent. Thus, the solvent in the column was exchanged stepwise from acetone to 5% (w/w) LiCl–DMAc, using DMAc and 0.5%, 1.0% and 3.0% (w/w) LiCl–DMAc, and 5% (w/w) LiCl–DMAc was used as the eluent for the column. The solvents for SEC were degassed using an ultrasonic apparatus. The injection volume and the flow-rate for SEC were 0.26 ml and 0.1 ml/min, respectively. The concentrations of cellulose or chitin in 5% (w/w) LiCl–DMAc for SEC were *ca.* 0.05% (w/w). Before injection, all samples were filtered through a membrane

tec PTFE, average pore diameter of 0.50 μm; Toyo Roshi Kaisha, Tokyo, Japan).

RESULTS AND DISCUSSION

Since standard samples of neither polystyrene nor polyethylene oxide for SEC were soluble in the LICl–DMAc system, a calibration curve for the column with the LiCl–DMAc system could not be obtained by the usual method. Then cellulose samples with various $\overline{DP}_v$ values were subjected to column chromatography in order to obtain the following information: (1) the possibility of using the column system described in this study for SEC analysis of polysaccharides and (2) distribution of molecular mass of cellulose samples.

The size-exclusion chromatograms of cellulose samples dissolved in 5% (w/w) LiCl–DMAc showed that those cellulose samples with higher $\overline{DP}_v$ values (Table I) had SEC patterns with higher molecular mass (Fig. 1). Thus, the elution patterns of celluloses in this system are probably governed by their molecular mass, and therefore this system may be applicable to SEC of polysaccharides without any derivatizing steps. Furthermore, the distribution of molecular mass of cotton was relatively narrow in comparison with that of regenerated ramie, and the low-molecular-mass cellulose also had a sharp distribution pattern. These results are very consistent with those obtained by SEC analysis of carbanilates of cellulose samples [13].

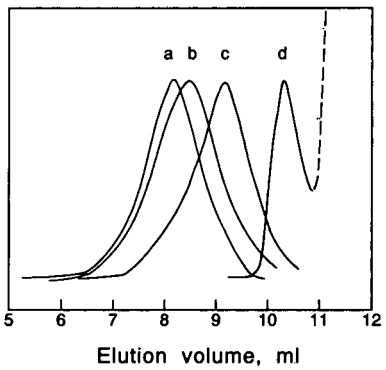

Fig. 1. SEC patterns of celluloses in 5% (w/w) LiCl–DMAc. Cellulose samples; (a) cotton; $\overline{DP}_v = 1690$, (b) regenerated ramie; $\overline{DP}_v = 1190$, (c) microcrystalline cellulose; $\overline{DP}_v = 240$; and (d) low-molecular-mass cellulose; $\overline{DP}_v = 9$. A large peak due to the solvent components of cellulose samples always appears at the end of the SEC patterns, and a part of the elution pattern of low-molecular-mass cellulose is overlapped by the large peak.

As shown in Fig. 2, although two chitin samples had similar elution patterns, the chitin PSH had slightly higher molecular mass than that of the chitin CLH. Since 1 and 2 days were required for complete dissolution of the chitins PSH and CLH, respectively, in LiCl–DMAc at room temperature, the longer dissolution treatment may bring about the slight depolymerization of the chitin CLH.

The void volume and the total volume of the same type of column, which were obtained using tetrahydrofuran as the eluent, were 5.3 and 11.5 ml, respectively. However, the values using 5% (w/w) LiCl–DMAc as the eluent could not be obtained, because the usual standard samples suitable for determining these values were insoluble in the LiCl–DMAc system. The peak positions of the chitin samples indicate that they had DP values much higher than those of the cellulose samples used. Furthermore, the elution patterns of chitins clearly showed two peaks with relatively narrow distributions. Judging from the elution patterns, the peak at the smaller elution volume is not due to the void volume of this column, but is probably due to the original distribution of molecular mass of chitins. Since the expansion parameters must be different to some extent between cellulose and chitin molecules in LiCl–DMAc, DP values of chitins may not be directly comparable with those of cellu-

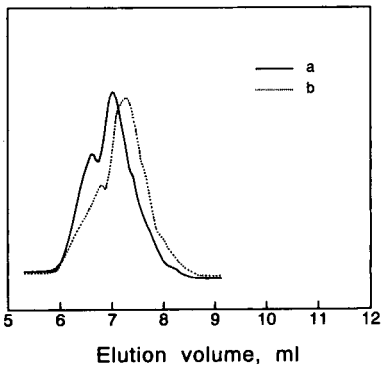

Fig. 2. SEC patterns chitins in 5% (w/w) LiCl–DMAc. Chitin samples: (a) chitin PSH and (b) chitin CLH.

loses on the basis of the elution volumes obtained in this system. Nevertheless, chitin samples seem to have molecular mass much higher than that of cotton ($\overline{DP}_v = 1690$), on the assumption that both chitin and cellulose molecules have similar molecular expansion states, which are probably governed by their β-1,4 glycoside bonds. Since light-scattering analysis of chitins in LiCl–DMAc revealed that they had DP values of *ca.* 2500 [7], the relationship between the molecular masses of chitins and those of celluloses, obtained in the SEC analysis, is consistent with the report. SEC analyses using LiCl–DMAc will be further studied in order to establish the best method for determining the molecular mass and distribution of molecular mass of cellulose, chitin and other polysaccharides.

ACKNOWLEDGEMENTS

The authors wish to thank Mr. N. Matsushita and Mr. H. Yamazaki of Tokyo Research Center, Tosoh Co. (Kanagawa, Japan), for providing the specially packed column for SEC. They also thank Dr. S. Kuga for valuable discussions during this work.

REFERENCES

1 L.R. Schroeder and F.C. Haigh, *Tappi J.*, 62 (1979) 103.
2 H.-U. Körner, D. Gottschalk and J. Puls, *Das Papier*, 38 (1984) 255.
3 P.R. Austin, *US Pat.*, 4 059 457 (1977).
4 A.F. Turbak, A. El-Kafrawy, F.W. Snyder and A.B. Auerbach, *US Pat.*, 4 302 252 (1981).
5 C.L. McCormick, *US Pat.*, 4 278 790 (1981).
6 C.L. McCormick, P.A. Callais and B.H. Hutchinson, Jr., *Macromolecules*, 18 (1985) 2394.
7 M. Terbojevich, C. Carraro and A. Cosani, *Carbohydr. Res.*, 180 (1988) 73.
8 M. Terbojevich, A. Cosani, G. Conio, A. Ciferri and E. Bianchi, *Macromolecules*, 18 (1985) 640.
9 A.L. Kvernheim and E. Lystad, *Acta Chem. Scand.*, 43 (1989) 209.
10 A. Isogai and R.H. Atalla, *J. Polym. Sci., Part A*, 29 (1991) 113.
11 A. Isogai and M. Usuda, *Mokuzai Gakkaishi*, 37 (1991) 339.
12 D.K. Smith, R.F. Bampton and W.J. Alexander, *Ind. Eng. Chem., Process Design Develop.*, 2 (1963) 57.
13 M. Hasegawa, unpublished results.

Journal of Chromatography, 635 (1993) 338–341
Elsevier Science Publishers B.V., Amsterdam

CHROM. 24 945

Short Communication

Determination of the neurolathyrogen β-N-oxalyl-L-α,β-diaminopropionic acid using high-performance liquid chromatography with fluorometric detection

A. Geda

Department of Plant Breeding and Genetics, Indira Gandhi Agricultural University, Raipur 492012 M.P. (India)

C.J. Briggs* and S. Venkataram

Faculty of Pharmacy, University of Manitoba, Winnipeg R3T 2N2 (Canada)

(First received November 17th, 1992; revised manuscript received February 4th, 1993)

ABSTRACT

This paper describes a sensitive spectrofluorometric HPLC method suitable for determining picogram levels of β-N-oxalyl-L-α,β-diaminopropionic acid (ODAP), a neurotoxin. Aqueous extracts of powdered *Lathyrus sativus* seeds were treated with 9-fluorenylmethyl chloroformate (FMOC) and the ODAP–FMOC derivative analyzed by reversed-phase chromatography using a μBondapak C_{18} column. The excitation and emission wavelengths were 254 and 315 nm, respectively. The mobile phase was sodium acetate buffer (0.05 *M*, pH 6.35)–acetonitrile (72:28, v/v) at a flow-rate of 1 ml/min. This method represents a major advance over the standard spectrophotometric assays used currently.

INTRODUCTION

Lathyrism [1,2], a motor-neurone disease in humans, is associated with excess consumption of β-N-oxalyl-L-α,β-diaminopropionic acid (ODAP), also known as BOAA [1] or by the preferred IUPAC name L-2-amino-3-oxalyl-aminopropanoic acid [3–6]. This compound is present in the seed of *Lathyrus sativus* L., the grass pea, a legume cultivated in India, Bangladesh and Ethiopia. It grows in poor soil and is resistant to salt, flood and drought [7–9]. It is a staple food which is rich in protein. Lathyrus constitutes a health hazard when alternative food is in limited supply [4,10–12]. The concentration of ODAP in seed is genetically controlled and modified by environmental factors. It can range from 0.1–0.4% in the dry seed [13].

Several methods have been described for determination of ODAP including electrophoresis, spectroscopy and high-performance liquid chromatography (HPLC) [14–18]. In this paper a simple and precise method for the estimation of ODAP in Lathyrus seed is presented based on a HPLC–spectrofluorometric technique reported earlier [18] which used gradient chromatography. The method reported here is sensitive, reprodu-

* Corresponding author.

cible and utilizes precolumn derivatization with 9-fluorenylmethyl chloroformate (FMOC) [19] followed by reversed-phase HPLC with fluorescence detection. The system is suitable for determination of ODAP in seeds and could be used to assay ODAP in animal tissue at sub-microgram levels.

MATERIALS AND METHODS

The reference standard of ODAP was provided by Dr. P. Nunn, Kings College, London, UK. *Lathyrus sativus* seeds were obtained from Dr. C. Campbell, Agriculture Canada Research Station, Morden, Manitoba, Canada. A standard amino acid mixture was obtained from Sigma (St. Louis, MO, USA). FMOC was purchased from Pierce (Rockford, IL, USA). All other chemicals were analytical grade and solvents were HPLC grade from Fisher Scientific, Canada. Purified water was produced using a Millipore Milli-Q unit. Purified water was produced using a Millipore Milli-Q unit. Aqueous solvents were filtered through a 0.45-μm membrane prior to use.

HPLC analysis

All chromatographic studies utilized a Waters HPLC system with a M45 pump and a U6K injector. A 300 × 3.9 mm stainless steel μBondapak C_{18} column, 10 μm particle size, (Waters Chromatography Division, Millipore) was used. A Shimadzu RF-535 variable-wavelength spectrofluorometer with a CR 501 integrating recorder was used for collection of data and their analysis. The excitation and emission wavelengths were 254 and 315 nm, respectively. The FMOC derivatives of sample and standard were eluted using sodium acetate buffer (0.05 *M*, pH 3.65)–acetonitrile (72:28, v/v) as the mobile phase at a flow-rate of 1 ml/min at ambient temperature of 23°C.

Preparation of derivative

A known amount of ODAP or sample was derivatized by the addition of 1 ml borate buffer (0.025 *M*, pH 9.6), 1 ml acetone and 0.1 ml FMOC (0.1 *M*, freshly prepared in acetone). The tube was vortex mixed for 2 min and derivatization was complete in 30 min at room temperature. A 2-ml volume of hexane–ethyl acetate (1:1) was added, vortex mixed for 30 s and 1.3 ml of aqueous layer was collected. Since the ODAP–FMOC derivative is soluble in acetone and insoluble in hexane, diethyl ether, ethyl acetate and chloroform, the aqueous layer was taken for HPLC injection. To optimize the derivatization conditions, concentrations of FMOC up to 1.0 *M* were studied. Similarly, 2,3-diaminopropanoic acid (DAP) and a standard mixture of 17 amino acids were also derivatized and analyzed.

Preparation of lathyrus seed extract

Aqueous extract of seed material was prepared from 10–100 mg of seed powder. A 2-ml volume of water was added and the sample was placed on a mechanical shaker for 12 h. The aqueous solution was separated after centrifugation (10 min at 3000 *g* in an IEC clinical centrifuge) and subsequently filtered through a 5-μm membrane; 5–10 μl of the extract were used for derivatization and 10 μl of the product were taken for HPLC analysis.

RESULTS AND DISCUSSION

As shown in Fig. 1, the retention time for the ODAP–FMOC derivative was 8.4 min and for unreacted FMOC 48.4 min. Peak areas corresponding to ODAP–FMOC were recorded. The precision of the method was assessed by repeated analyses of samples containing known concentrations of ODAP. The relative standard deviation for within-day precision ranged from 6.3 to 8.7% ($n = 4$). The day-to-day variation observed in peak area was in the range of 8.1 to 11.5%. There was also some variation in the retention time of the ODAP–FMOC peak ranging from 8.1 to 8.6 min. Hence standard samples of known ODAP concentration were required on each day. The ODAP–FMOC derivative eluted before the DAP–FMOC or any of the amino acid–FMOC derivatives from a lathyrus extract or standard plant amino acid mixture. The reason for selecting DAP and the amino acid mixture was to identify any possible interference

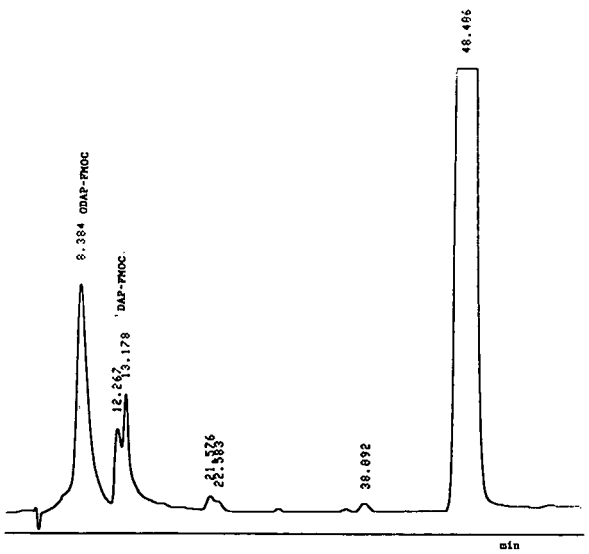

Fig. 1. A typical chromatogram of ODAP-FMOC and DAP-FMOC derivatives using a μBondapak C_{18} column.

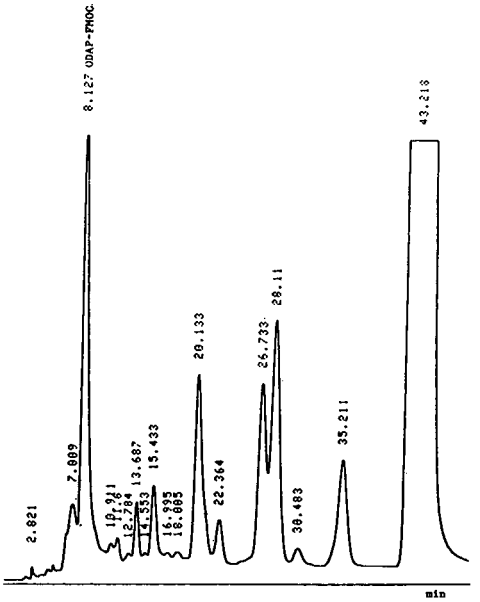

Fig. 2. A typical chromatogram of the FMOC-derivatized seed extract using μBondapak C_{18} column.

from these compounds with the ODAP–FMOC peak. Furthermore, DAP is the hydrolysis product of ODAP and any aqueous plant extract would contain amino acids as normal constituents. DAP exists in two isomeric forms and the doublet peaks at 12.3 and 13.2 min possibly correspond to their FMOC derivatives.

The amount of FMOC selected for derivatization was based on preliminary experiments which showed that the molar concentration of FMOC should be at least 100 times that of ODAP. Hence, 0.1 ml of a 0.1 *M* solution was used and found adequate for the reaction to be complete.

A typical chromatogram of the derivatized seed extract is shown in Fig. 2. It shows the presence of a number of peaks including the FMOC derivatives of amino acids, secondary metabolites and other normal constituents of an aqueous seed extract [20,21]. To reduce the total elution time of these compounds the column was flushed with pure acetonitrile 20 min after injection. The system was then re-equilibrated with 45 ml of the mobile phase before the next injection. Concentrations were determined by estimation of peak areas with reference to calibration curve for derivatized ODAP (correlation coefficient = 0.9745, intercept = −32.191 and the slope = 27543.6, linear up to 14 nmol of ODAP). The detection limit was found to be 15 pmol on column.

This HPLC–spectrofluorometric procedure showed that the average ODAP content of the *Lathyrus sativus* seed samples studied was 0.33 g/100 g of seed material. Breeding programs designed to eliminate ODAP from lathyrus seed may adopt this method for analysis of seed with very low levels of ODAP.

CONCLUSIONS

HPLC combined with spectrofluorometry can be used for the detection and quantitative estimation of pmol amounts of ODAP in Lathyrus seed. This technique is suitable for estimation of neurotoxic content of individual seeds from a single pod which is desirable for selection and breeding Lathyrus varieties with low ODAP content. This represents a major advance over spectrophotometric methods conventionally used to assay this compound in plant material.

ACKNOWLEDGEMENTS

The authors are pleased to acknowledge the financial support of International Development

Research Centre (IDRC) and Agriculture Canada Research Station, Brandon, Manitoba, Canada. A.G. was the recipient of an IDRC international fellowship.

REFERENCES

1 P.S. Spencer, H.H. Schaumburg, D.F. Cohn and P.K. Seth, *Research Progress in Motor Neuron Disease*, Rose FC, Pitman Medical, London, 1984, pp. 312–327.
2 W.H. Sleeman, *Rambles and Recollections of an Indian Official*, Vol. 1, Hatchard & Sons, London, 1844, p. 127.
3 E.A. Bell, *INILSEL Chemistry Committee Meeting Report*, Dhaka, Bangladesh, Dec. 2, 1991.
4 K.T. Ganapathy and M.P. Dwivedi, *Studies on the clinical epidemiology of lathyrism*, Indian Council of Medical Research, New Delhi, 1961, pp. 1–55.
5 D.N. Roy, *Natl. Med. J. Ind.*, 1 (1955) 70–80.
6 P.S. Spencer, D.N. Roy, V.S. Palmer and M.P. Dwivedi, in A.K. Kaul and D. Combes (Editors), *Lathyrus and Lathyrism*, Third World Medical Research Foundation, New York, 1986, pp. 297–305.
7 C.L. Gowda and A.K. Kaul, *Pulses in Bangladesh*, FAO/Bangladesh Agricultural Research Institute, Dhaka, 1982.
8 P. Kumar, *Sci. Today*, (1983) 43.
9 M.S. Lal and I. Swarup, in P.S. Spencer (Editor), *The Grass Pea Threat and Promise*, Third World Medical Research Foundation, New York, 1989, pp. 55–60.
10 S.L.N. Rao, K. Malathy and P.S. Sharma, *World Rev. Nutr. Diet.*, 10 (1969) 214–238.
11 T. Gebre-ab, Z.Q. Gabriel, M. Maffi, Z. Ahmed, T. Ayele and H. Fanta, *Ethiop. Med. J.*, 19 (1978) 1–11.
12 S.L.N. Rao, *Anal. Biochem.*, 86 (1978) 386–395.
13 K.L. Rathod, in P.S. Spencer (Editor), *The Grass Pea Threat and Promise*, Third World Medical Research Foundation, New York, 1989, pp. 168–174.
14 C.J. Briggs, N. Parreno and C.G. Campbell, *Planta Med.*, 47 (1983) 188–190.
15 V. Vega and E.A. Bell, *Phytochemistry*, 6 (1967) 759–761.
16 E.A. Bell, *Nature*, 203 (1964) 378–380.
17 G.E. Kisby, D.N. Roy and P.S. Spencer, *J. Neurosci. Methods*, 26 (1988) 45–54.
18 G.E. Kisby, D.N. Roy and P.S. Spencer, in P.S. Spencer (Editor), *The Grass Pea, Threat and Promise*, Third World Medical Research Foundation, New York, 1989, pp. 133–138.
19 L.A. Carpino and G.Y. Han, *J. Org. Chem.*, 37 (1972) 3404–3409.
20 Y.-H. Kuo and F. Lambein, *Phytochemistry*, 30 (1991) 3241–3244.
21 F. Lambein, J.K. Khan, C. Becu and A. De Bruyn, *Phytochemistry*, 31 (1992) 887–892.

Journal of Chromatography, 635 (1993) 342–345
Elsevier Science Publishers B.V., Amsterdam

CHROM. 24 875

Short Communication

Preparative separation and properties of (*E*)- and (*Z*)-steroidal α,β-unsaturated ketoximes

Qinjian Zhao* and Zhensu Li

Department of Medicinal Chemistry, Beijing Medical University, Beijing 100083 (China)

(Received December 14th, 1992)

ABSTRACT

A procedure for the preparative resolution of (*E*)- and (*Z*)-norgestimate (17β-acetyloxy-13-ethyl-18,19-dinorpregn-4-en-20-yne 3-oxime) using flash chromatography is described. A longer column and less polar solvents were applied to overcome the small $\Delta R_F(0.05)$ for the isomers of norgestimate. The optical rotations of the *E* and *Z* isomers were +4.7° and +94.7° (in $CHCl_3$), respectively. The *E*/*Z* isomer ratio in the mixture was found to be 1.5 both by ^1H NMR spectrometry (4-olefinic H peaks) and by measurement of optical rotations. The validity of the above two methods was confirmed by the calibration graphs obtained with the resolved isomers. The properties of the resolved isomers are discussed with a comparison with those for testosterone oxime.

INTRODUCTION

Since the early 1970s, many α,β-unsaturated ketoximes of steroids have emerged as better drugs than their ketosteroids [1–3]. Some of them, such as norgestimate (17β-acetyloxy-13-ethyl-18,19-dinorpregn-4-en-20-yne 3-oxime) (**1**), are widely in use as oral contraceptives. These compounds are the *E* and *Z* isomers of 3-ketoximes, as two peaks were observed by HPLC with tablets [4] and in pharmacokinetic studies [5]. Norgestimate is used as a contraceptive. However, the physical properties and biological activities of (*E*)- and (*Z*)-norgestimate have never been characterized, so it was considered necessary to study the different properties and to elucidate the different biological effects of these different isomers.

As all the Δ^4-3-one oximes are very similar with respect of the differences in their isomers, the clinically important norgestimate was chosen as an example of α,β-unsaturated 3-ketoximes to study the *E* and *Z* isomers. These isomers have been separated as cyclodextrin inclusion complexes by HPLC on a cyanopropylsilica stationary phase [6]. Subsequently, the same group reported the separation of these isomers by conventional and overpressure TLC [7]. Only a few micrograms of isomers, which is insufficient to characterize their spectral and physical properties, can be obtained by these methods. Flash chromatography [8] was employed tentatively to separate the *E* and *Z* isomers of **1** on a preparative scale.

* Corresponding author. Present address: Department of Chemistry, Catholic University of America, Washington, DC 20064, USA.

0021-9673/93/$06.00

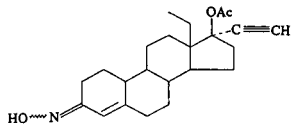

1

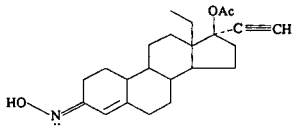

(E)-1, 1a

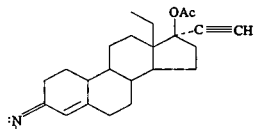

(Z)-1, 1b

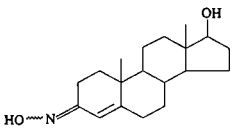

2

EXPERIMENTAL

Melting points were determined with the capillary method and are uncorrected. ^{1}H NMR spectra were recorded on a JEOL FX-90Q or Variant VXR-300 Fourier transform NMR spectrometer. C^2HCl_3 was used as the solvent, while and tetramethylsilane (TMS) served as the internal standard. Optical rotations were measured in a 1-dm cell on a Perkin-Elmer Model 271 polarimeter at 589 nm (Na D line). UV spectra were obtained with a Shimazu UV-260 spectrophotometer. Mass spectra (electron impact mode, 100 eV) were measured on a VG-25-255 spectrometer. Microanalyses were carried out using a Perkin-Elmer Model 240-C elemental analyser. Microspherical silica gel [40–63 μm (230–400 mesh)] (similar to Merck silica gel 60, according to the manufacturer) used for flash chromatography and silica gel GF_{254} for TLC were purchased from Shandong Jime Chemical Factory.

17β-Acetyloxy-13-ethyl-18,19-dinorpregn-4-en-20-yne 3-oxime (1)

One-pot synthesis of **1** from 17β-hydroxy-13-ethyl-18,19-dinorpregn-4-en-20-yn 3-one gave a total yield of 80% [9]. Compound **1** (white solid): m.p. 214–216°C (lit. [10] m.p. 214–218°C); $[\alpha]_D^{15}(CHCl_3) = +40°$ (lit. [10] +41°); ^{1}H NMR (300 and 90 MHz), δ 8.35 (s, broad, disappeared/^2H_2O, 1 H, =NOH), 6.58 [s, 0.4 H, (*Z*)-4-olefinic H], 5.92 [s, 0.6 H, (*E*)-4-olefinic H], 2.60 (s, 1 H, –C≡CH), 2.04 (s, 3 H, $-OCOCH_3$), 1.00 (t, 3 H, 18-CH_3).

*Separation of **1a** and **1b***

A column with an I.D. of 2.5 cm was used and 50–100-meshs and was added to cover the bottom of the column (*ca.* 1 cm depth). A slurry of silica gel in light petroleum (b.p. 30–60°C) was poured into the column, giving a height of silica in the column of 25 cm. The column was washed with light petroleum (b.p. 30–60°C)–diethyl ether (2:1) (less polar than the developing solvent used for TLC; see Table I) for 20 min at atmospheric pressure. A 300-mg amount of **1** was dissolved in CH_2Cl_2 and mixed with 1 g of silica gel. After the mixtures had dried completely, they were placed on the top of the column. Eluent [light petroleum (b.p. 30–60°C)–diethyl ether (2:1)] was added to the column and the pressure of nitrogen applied to the column was adjusted so as to make the surface of the solvent in the column fall at *ca.* 5 cm/min [8]. The eluate was collected in 10-ml fractions using an automatic fraction collector. TLC was used to monitor the appearance of the compounds. The elution was terminated after all the isomers in the mixture had been washed off the column according to the TLC examination. Fractions with the same components were combined and concentrated by rotary evaporation under vacuum at ambient temperature. Concentration nearly to dryness afforded **1a**, **1b** or a **1a–1b** mixture as while solids.

*Fraction 1: (E)-**1**, -**1a**.* Yield 120 mg (40%), m.p. 214–216°C, $[\alpha]_D^{15} = +4.7°$; ^{1}H NMR (90 MHz), δ 8.20 (s, broad, disappeared/^2H_2O, 1 H, =NOH), 5.88 (s, 1 H, 4-olefinic H), 2.59 (s, 1 H, –C≡CH), 2.04 (s, 3 H, $-OCOCH_3$), 1.00 (t, 3 H, 18-CH_3); MS, *m/z* (relative intensity, %) 369 (M^+, 23), 340 ($M^+ + 1 - NO$, 100), 310 ($M^+ - OCOCH_3$, 42). Analysis: calculated for $C_{23}H_{31}NO_3$, C 74.70, H 8.46, N 3.79; found C 75.02, H 8.55, N 3.74%.

*Fraction 2: (Z)-**1**, -**1b**.* Yield 106 mg (35%), m.p. 219–221°C, $[\alpha]_D^{15} = +94.7°$; ^{1}H NMR (90

MHz), δ 7.64 (s, broad, disappeared/^2H_2O, 1 H, =NOH), 6.55 (s, 1 H, 4-olefinic H), 2.59 (s, 1 H, –C≡CH), 2.04 (s, 3 H, $-OCOCH_3$), 1.00 (t, 3 H, 18-CH_3); MS, *m/z* (relative intensity, %) 369 (M^+, 22), 340 ($M^+ + 1 - NO$, 100), 310 ($M^+ - OCOCH_3$, 36). Analysis: calculated for $C_{23}H_{31}NO_3$, C 74.70, H 8.46, N 3.79; found, C 74.66, H 8.72, N 3.78%.

In addition to **1a** and **1b**, 55 mg of **1** were recovered as a mixture of **1a** and **1b** (yield 18%). The total recovery yield of the separation was 93%.

RESULTS

In flash chromatography, eluent(s) giving R_F = 0.35 (in TLC with the same solvent) for the centre of the mixtures and a 17-cm length of the column have been suggested [8]. An R_F value of less than 0.19 was chosen in our work in order to obtain a better resolution for the isomer mixture with small ΔR_F (*ca.* 0.05). When a 25-cm column (length increased from the commonly used 17 cm) and a less polar eluent were used, the isomers of **1** were successfully resolved on a preparative scale with nearly a quantitative recovery of **1**. The purities of the isomers were determined by ^1H NMR spectrometry because studies with some analogues of **1** showed that the 4-H chemical shifts are different for different isomers [11,12]. Some properties of the *E* and *Z* isomers (**1a** and **1b**), together with that of the isomers of testosterone oxime (**2**), are given in Table I.

TABLE I

SOME PROPERTIES OF ISOMERS OF α,β-UNSATURATED 3-KETOXIMES **1** AND **2**

Parameter	Norgestimate (**1**)		Testosterone oxime (**2**)	
	E	*Z*	*E*	*Z*
R_F in TLC	0.22[a] 0.27[7,b]	0.17[a] 0.24[7,b]	0.33[11,c]	0.20[11,c]
M.p. (°C)	214–216	219–221	204–206	228–229
λ_{max} (nm)[d]	241.0	243.0	241.5	243.0
^1H NMR, δ_{4-H} (ppm)	5.88	6.55	5.76	6.49
$[\alpha]_D^{15}(CHCl_3)$	+4.7	+94.7		

[a] Eluent: light petroleum (b.p. 30–60°C)–diethyl ether (3:2).
[b] Eluent: *n*-hexane–methyl ethyl ketone–diethylamine (8:1:1).
[c] Eluent: benzene–ethyl acetate (3:1).
[d] In ethanol.

DISCUSSION

The differences in λ_{max} in the UV spectra and δ_{4-H} in the ^1H NMR spectra are consistent with the results reported for some analogues [11,12], *viz.*, $\lambda_{max}(Z) - \lambda_{max}(E) \approx 2$ nm and $\delta_{4-H}(Z) - \delta_{4-H}(E) \approx 0.7$ ppm. It was also found that the absorption band is broader for the *Z* isomer than the *E* isomer for **1**, which is consistent with the results reported for **2** [11]. This indicates an accuracy in the determination of the *E*/*Z* isomers ratio by HPLC [7,13] with detection at a certain wavelength, as it is very likely that different isomers could have different molar absorptivities at the wavelength used.

The optical rotations of these isomers, which have not previously been reported, were found to differ (see Table I). Derivatization of the keto group into an oxime does not introduce any chiral centre. However, the optical rotations for the *E* and *Z* isomers are different. First, as their parent compound is optically active, it is not surprising that the oximes showed optical activity. Second, the differing values of the optical rotation for the two isomers might be explained by the magnetic dipoles and electric dipoles being different for *E* and *Z* isomers. From the optical rotations of **1**, **1a** and **1b**, we can calculate that the *E*/*Z* isomer ratio (**1a**/**1b**) is 1.5. This value is consistent with the result derived from the ratio of the peak areas for the 4-olefinic-H signals in the ^1H NMR spectra of the different isomers. This *E*/*Z* ratio of 1.5 is similar to the values reported for other analogues [7,11]. The ^1H NMR and optical rotation methods for the determination of the *E*/*Z* ratio are reliable, because the calibration graphs for both methods obtained with the resolved isomers confirmed their validity.

It was found that **1a** and **1b** are stable in the solid state and in non-polar solvents, such as ethyl acetate and chloroform. No isomerization

was detected over at least several weeks. However, rapid isomerization was observed in polar solvents, such as methanol and acetone. The equilibrium point ($E/Z = 1.5$) can be achieved in few days at ambient temperature. This is also the reason why we chose a low polarity and low boiling points of the eluents solvents in flash chromatography for resolution. The E/Z isomer ratio in the mixture or solution might be controlled by the internal energies of the different isomers. This may be understood in the future by calculations of the energies of E and Z isomers using appropriate molecular modelling software.

The binding of **1** to the progesterone and androgen receptors (PR and AR) was found to be different to that of its parent ketosteroid [5,14]. This indicates that the =NOH group plays an important role in the binding of **1** to PR and AR. As the spatial arrangements of (E)- and (Z)-**1** for O and H atoms in the 3-oxime substituent are very different, one can speculate that the binding of **1a** and **1b** to the receptors could not be the same. However, it is not feasible to measure the relative binding affinity to receptors of an individual isomer, as the species would isomerize into each other in aqueous solution, which cannot be avoided in the receptor binding assay. The only way to study the binding to the receptors is through molecular modelling, which is under investigation.

In conclusion, a convenient and preparative resolution of norgestimate (**1**) (or other α,β-steroidal oximes) using flash chromatography has been developed. The studies of the characteristics of the resolved isomers indicated that the E/Z isomer ratio determined by HPLC may be inaccurate owing to the different absorbances of the two isomers at a certain wavelength. An accurate and convenient method for determining the E/Z isomer ratio is to use the ^{1}H NMR signals of the 4-olefinic hydrogen, which are different for the E and Z isomers.

REFERENCES

1 A.P. Shroff, *J. Med. Chem.*, 13 (1970) 748.
2 A.P. Shroff, G.O. Harper and R.P. Blye, *J. Med. Chem.*, 16 (1073) 113.
3 R.W. Rebar and K. Zeserson, *Contraception*, 44 (1991) 1.
4 P.A. Lane, P.O. Mayberry and R.W. Young, *J. Pharm. Sci.*, 76 (1987) 44.
5 J. Killinger, D.W. Hahn, A. Phillips, N.S. Hetyei and J.L. McGuire, *Contraception*, 32 (1985) 311.
6 M. Gazdag, G. Szepesi and L. Huszar, *J. Chromatogr.*, 371 (1986) 227.
7 K. Ferenczi-Fodor, I. Kovacs and G. Szepesi, *J. Chromatogr.*, 392 (1987) 464.
8 W.C. Still, M. Kahn and A. Mitra, *J. Org. Chem.*, 43 (1978) 2923.
9 Q. Zhao, *Master's Dissertation*, Beijing Medical University, Beijing, 1989.
10 A.P. Shroff, *Ger. Offen.*, DE 2 633 210 (1977).
11 S. Hara, K. Oka and Y. Ike, *Chem. Ind. (London)*, (1967) 832.
12 M. Patthy and E. Tomori, *J. Chromatogr.*, 191 (1980) 145.
13 S. Archer, *US Pat.*, 4 507 290 (1985).
14 A. Phillips, K. Demarest, D.W. Hahn, F. Wong and J.L. McGuire, *Contraception*, 41 (1990) 399.

Journal of Chromatography, 635 (1993) 346–348
Elsevier Science Publishers B.V., Amsterdam

CHROM. 24 920

Short Communication

Adsorption chromatography on cellulose

IX. Chiral separations with aqueous solvents and liquid–liquid systems

Huynh Thi Kieu Xuan and M. Lederer*

Institut de Chimie Minérale et Analytique, Université de Lausanne, Boîte Postale 115, Centre Universitaire, CH-1015 Lausanne 15 (Switzerland)

(First received September 15th, 1992; revised manuscript received January 28th, 1993)

ABSTRACT

The enantiomers of substituted tryptophans were examined by thin-layer chromatography on microcrystalline cellulose. Aqueous solvents and liquid–liquid systems yielded essentially the same separations, suggesting that adsorption can play a role in liquid–liquid (partition) systems in some instances.

INTRODUCTION

In previous work [1–3], we had been impressed by the readiness with which tryptophan enantiomers separate with aqueous solvents on microcrystalline cellulose thin layers. The separations and also those of enantiomers of methyl-substituted tryptophans were shown to be insensitive to temperature and to salt concentration in the solvent [1] and also to the salt used [2]. They were, however, sensitive to the type of cellulose used as adsorbent, native cellulose giving poorer separations than microcrystalline cellulose [3].

Enantiomer separations have also been reported with classical partition solvents such as butanol–acetic acid–water by Dalgliesh [4] and with polar solvents such as pyridine–ethanol–water by Yuasa and co-workers [5,6]. In view of the differences in the chiral properties of various celluloses, a comparison of adsorption and partition systems can only be made if the same adsorbent is used in both systems. We report here on comparative results obtained on Merck DC Plastikfolien plates (Art. 5577), which are made of microcrystalline cellulose. We also report on a number of substituted tryptophans that were not available to us in previous work.

EXPERIMENTAL

All chromatograms were prepared by ascending development in glass containers with a tightly closing lid on 20 cm × 20 cm DC Plastikfolien plates (Merck Art. 5577), cellulose layer thickness 0.1 mm. The sample solutions (in water) were applied to the thin layer as fine lines (less

* Corresponding author.

than 1 mm wide) by means of PTFE paint brushes size 00. With capillaries the porosity of the layers produces much larger zones. After a development of about 100 mm the chromatograms were exposed to iodine vapour (in a desiccator), which produced brown spots that copied well on a photocopier. This proved to be a much better means of documentation than reaction with ninhydrin and subsequent photography.

RESULTS AND DISCUSSION

The results obtained with substituted tryptophans are shown in Table I and Figs. 1 and 2.

TABLE I

R_F VALUES OF SUBSTITUTED TRYPTOPHANS ON MERCK DC PLASTIKFOLIEN CELLULOSE PLATES

Compound	Solvent								
	1 *M* NaCl			Pyridine–ethanol–water (1:1:1)			Butanol–acetic acid–water (4:1:5)		
	D-	L-	ΔR_F	D-	L-	ΔR_F	D-	L-	ΔR_F
4-Methyltryptophan	0.33	0.25	0.08	0.52	0.42	0.10	0.50	0.45	0.05
5-Methyltryptophan	0.35	0.27	0.08	0.54	0.48	0.06	0.53	0.49	0.04
6-Methyltryptophan	0.33	0.26	0.07	0.55	0.47	0.08	0.52	0.48	0.04
4-Fluorotryptophan	0.47	0.39	0.08	0.60	0.53	0.07	0.54	0.50	0.04
5-Fluorotryptophan	0.48	0.42	0.06	0.64	0.59	0.05		0.52	>0.03
6-Fluorotryptophan	0.47	0.40	0.07	0.65	0.61	0.04	0.54	0.51	0.04
5-Hydroxytryptophan	0.31	0.25	0.06	0.48	0.41	0.07	0.30	0.28	0.02

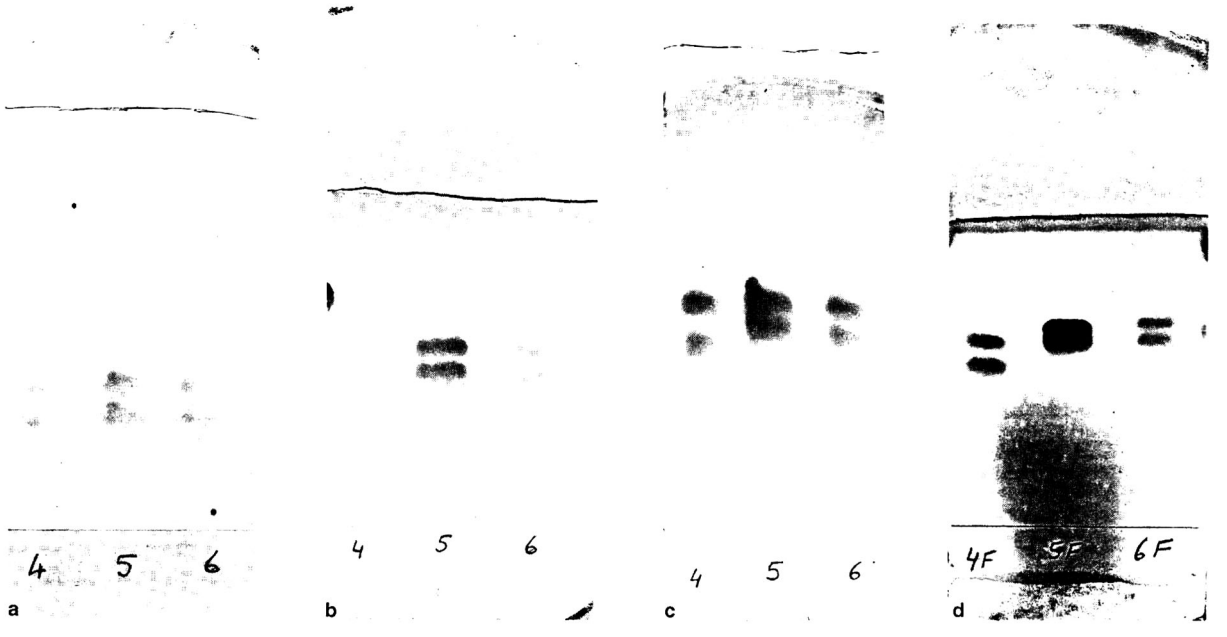

Fig. 1. Thin-layer chromatograms of (a) 4-, 5- and 6-methyltryptophan developed with 1 *M* NaCl; (b) 4-, 5- and 6-methyltryptophan developed with ethanol–pyridine–water (1:1:1); (c) 4-, 5- and 6-fluorotryptophan developed with 1 *M* NaCl; and (d) 4-, 5- and 6-fluorotryptophan developed with ethanol–pyridine–water (1:1:1).

There are a few notable features: (a) there is little difference between "adsorption" and "partition" chromatograms as far as the separation of enantiomers is concerned; (b) a substituent in the 5-position increases the R_F value and decreases the separation factor in most instances; (c) the separation factors do not change much with the various substituents; and (d) Yuasa and co-workers' polar solvent [5,6] separates enantiomers as efficiently as an aqueous solvent, whereas Dalgliesh's less polar mixture [4] gives smaller R_F differences.

TABLE II

R_F VALUES OF D- AND L-KYNURENINE ON MERCK DC PLASTIKFOLIEN CELLULOSE PLATES

Solvent	D-	L-	ΔR_F
1 *M* NaCl	0.61	0.54	0.07
Ethanol–pyridine–water (1:1:1)	0.51	0.43	0.08
Butanol–acetic acid–water (4:1:5)	0.55	0.50	0.05
Ethanol–butanol–water:			
2:1:2	0.46	0.34	0.12
1:1:1	0.50	0.39	0.11
5:3:7	0.57	0.47	0.10
5:1:9	0.65	0.54	0.11

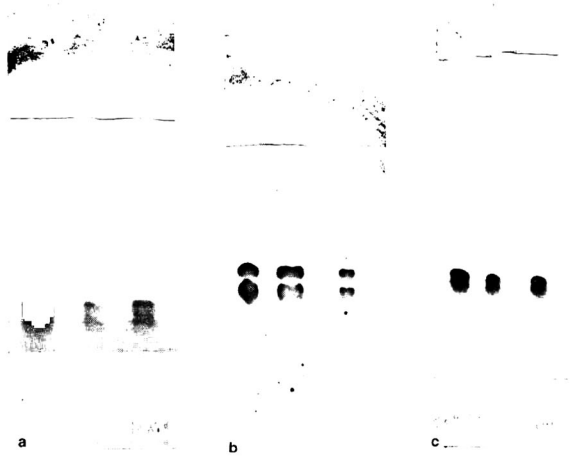

Fig. 2. Thin-layer chromatograms of 5-hydroxytryptophan with different loadings on each layer (most on right, least on left): (a) developed with 1 *M* NaCl; (b) developed with ethanol–pyridine–water (1:1:1); (c) developed with butanol–acetic acid–water (4:1:5).

The results for kynurenine are given in Table II. Several butanol–ethanol–water mixtures were also tried and those rich in ethanol and water gave even larger R_F differences for the enantiomers than an aqueous solvent.

These results pose a problem for the theory of chromatography. It is generally assumed that the cellulose in partition (*i.e.*, liquid–liquid) chromatography plays the role of an inert support. In the treatise by Copius Peereboom [7], comparisons are listed between experimental partition coefficients and those calculated from paper chromatograms by various workers for amino acids, sugars, organic acids and steroids, and in all instances the agreement is excellent. Similar work was also done by Eliseeva [8] with inorganic ions with equally good agreement. Even for water-miscible solvents, Martin [9] postulated a "partition mechanism" if one considers the stationary phase to be like a saturated solution of a sugar.

However, this work clearly presents an exception. For strongly adsorbed compounds, adsorption and hence also chiral discrimination can still be functioning in addition to the liquid–liquid mechanism, which without doubt is the major contributor to most separation effects obtained in solvents such as butanol–acetic acid–water.

REFERENCES

1 A.O. Kuhn, M. Lederer and M. Sinibaldi, *J. Chromatogr.*, 469 (1989) 253.
2 M. Lederer, *J. Chromatogr.*, 501 (1990) 367.
3 M. Lederer, *J. Chromatogr.*, 604 (1992) 55.
4 C.E. Dalgliesh, *Biochem. J.*, 64 (1956) 483.
5 S. Yuasa, A. Shimada, K. Kameyama, M. Yasui and K. Adzuma, *J. Chromatogr. Sci.*, 18 (1980) 311.
6 S. Yuasa and A. Shimada, *Sci. Rep.*, 31 (1982) 13.
7 J.W. Copius Peereboom, in C.L. Wilson and D.W. Wilson (Editors), *Comprehensive Analytical Chemistry*, Vol. IIC, Elsevier, Amsterdam, 1971, p. 11.
8 G.D. Eliseeva, *Tr. Kom. Anal. Khim. Akad. Nauk SSSR*, 6 (1955) 439.
9 A.J.P. Martin, *Annu. Rev. Biochem.*, 19 (1950) 517.

Journal of Chromatography, 635 (1993) 349–350
Elsevier Science Publishers B.V., Amsterdam

CHROM. 24 838

Book Review

Liquid chromatography–mass spectrometry, by W.M.A. Niessen and J. van der Greef, Marcel Dekker, New York, 1992, VI + 479 pp., price US$ 165.00 (USA and Canada), US$ 189.75 (rest of world), ISBN 0-8247-8635-1.

This is a soundly written book from two well known experts in the field who manage to convey a sense of depth and comprehensiveness in the way they approach this timely subject. The topic is really a "hot" item in analytical chemistry and developments and changes in this area are certainly taking place at a surprising pace. In fact, at the time of writing the manuscript the authors themselves acknowledge that owing to the considerable progress to be expected in the field, the text would need updating even by its appearance date. Considering the very recent developments, for instance in high-flow electrospray, this was indeed an accurate prediction.

Nevertheless, the text covers under five main headings with a total of 20 chapters virtually everything there is to know about the coupling of liquid chromatography to mass spectrometry, providing an accurate and thorough perspective of the various hybrid systems existing on the market.

The General Introduction gives both a brief but sufficient overview of the individual techniques of liquid chromatography and mass spectrometry and a summarized but informative account of the interfacing of the two systems. In this regard, general logistic problems and solutions are included with a very good discussion of important practical aspects such as flow splitting and miniaturization of LC systems. This is all covered in the first 80 pages of text and is followed by a very detailed 218-page presentation of interface technology covering, after a general and thorough overview, each and every one of the known interfaces.

This information is addressed in eight chapters containing abundant and clear illustrations on the moving belt interface, direct liquid introduction, thermospray, continuous-flow fast atom bombardment, the particle beam interface, electrospray and ionspray, supercritical fluid chromatography–mass spectrometry and capillary electrophoresis–mass spectrometry. Each of these chapters provides a very detailed account of the technology and physical principles behind the various interfaces and also presents a summary of data on applications, tabulated in a very useful form for rapid reference. Pertinent bibliographic references can be found up to articles that appeared in 1991, which is indeed a major effort for a book appearing early in 1992. Also, the different ionization methods and mechanisms on which these interfaces are based are discussed in five information-rich chapters dealing with electron impact, chemical ionization, ion evaporation, fast atom bombardment and induction of fragmentation by collision techniques.

Although, as indicated by the authors, the book is focused on strategies and principles of operation rather than on a simple revision of applications, there is a chapter illustrating the applicability of LC–MS interfaces, emphasizing the state of the art for qualitative and quantitative analysis and limitations in general. Well documented cases of pharmaceutical, biochemical and environmental applications are reviewed, demonstrating the use of LC–MS in solving real problems that are difficult to approach by CG–MS techniques.

Finally, even though each chapter ends with specific conclusions and perspectives, the book incorporates a final major heading devoted to these considerations. Both final chapters within this heading would by themselves be very useful to those already working or considering future work with LC–MS systems. Accordingly, the

book is destined to become an indispensable source of knowledge and practical information to users approaching the field of LC–MS from either the chromatography or the mass spectrometry end, provided, of course, that they can afford the relatively high price.

Barcelona (Spain) Emilio Gelpí

Journal of Chromatography, 635 (1993) 351–353
Elsevier Science Publishers B.V., Amsterdam

CHROM. 24 864

Book Review

Trace metal analysis and speciation (*Journal of Chromatography Library*, Vol. 47), edited by I.S. Krull, Elsevier, Amsterdam, 1991, XVI + 302 pp., price Dfl. 240.00, US$ 150.00, ISBN 0-444-88209-X.

The book *Trace Metal Analysis and Speciation*, edited by I.S. Krull (Department of Chemistry, Barnett Institute, Northeastern University, Boston), arose from a mini-symposium held in 1987 at the *Eastern Analytical Symposium* in New York. It appeared to the organizers that the material presented was certainly worth collection and presentation in the format of a book. This was an excellent idea and the result presented here is of great value.

The scope of this book has been carefully and well targeted. Total metal determination by various spectroscopic techniques is already a well beaten path and the Editor has evidently well avoided following it. The field of speciation is most often the privilege of expert laboratories. Here, all their very different expertise is gathered, offering to the reader a considerable expansion of analytical possibilities addressing the area of trace metal determinations and speciation. All chapters are written by leading experts in the field. They cover coupled systems between the most recent techniques both with respect to the different types of chromatography (gas or liquid) and the various type of detectors. In all nine chapters, general fundamentals of the separation techniques used are given. Interfaces are described when needed. General good criticisms with regard to the limits and pitfalls of tandem systems are presented. Applications to real samples are discussed whenever possible. The many figures, tables and lists of references will allow the reader to obtain a good start to solving his or her particular speciation problem.

The titles of the chapters are as follows: Chromatography—element-selective detection; interfacing of gas chromatography with microwave-induced plasma emission detection (GC–MIP); Determination of organometallic compounds in environmental samples with element-specific detectors; Chromatographic sample introduction for plasma mass spectrometry; The future of intelligent spectrometers in speciation by atomic emission spectrometry; Inductively coupled plasma mass spectrometry for element-selective detection in liquid chromatography; The use of complexing eluents for high-performance liquid chromatographic determination of metal species; Instrumentation and procedures for the long-term monitoring of metal ions in industrial effluents by liquid chromatography with electrochemical detection; Ion chromatographic speciation of trace metals; and Interfacing of GC–HPLC with direct current plasma (DCP) emission spectroscopic detection for trace metal analysis and speciation.

Chapter 1. This chapter deals with the interfacing of gas chromatography with microwave-induced plasma (MIP) emission detection for the determination of metals. It offers a comprehensive overview of the different approaches of interfacing between both gas (GC) and liquid chromatography (HPLC) with MIP. Application of these techniques to the chromatographic detection of metal is very well described. An excellent discussion on the possible use of metal chelates of sufficient volatility will inform the reader of the wide range of applications and errors associated with the chromatographic detection of metals after derivatization with complexing ligands such as 2,4-pentanedione (acetylacetone) and its fluorinated derivatives.

Chapter 2. A very wide array of technical solutions have been adapted for the determination of organometallic compounds. This chapter has the difficult task of covering all main trends

developed. Here also both gas and liquid chromatography interfaced with various detectors are discussed (mainly atomic absorption or plasma emission detectors). A good perspective is given of hydride generation methods. Many examples referring to arsenic speciation are given and most particularly with HPLC–ICP techniques. It is obvious that the author has mastered these techniques well and can provide useful criticisms with regard to the potential and limitations of each trend.

Chapters 3 and 5. The combination of these two chapters provides a complete overview of the various possibilities of coupling between either gas or liquid chromatography and ICP-MS. Direct practical considerations make these contributions of great interest. These two chapters should have been consecutive in the arrangement of the book. They both give a short statement of the fundamentals of ICP-MS operation. Procedures for interfacing gas and liquid chromatography with the ICP-MS system are well described. Environmental applications of arsenic, tin and mercury speciation are given using HPLC–ICP-MS systems. Gas chromatography coupled to ICP-MS is also well commented upon with a special mention of the combination of GC–MIP-MS and its application to the determination of halogenated compounds. Chromatographic procedures to minimize interferences are discussed and results for trace metal determinations in sea water are mentioned.

Chapter 4. The authors of this chapter provide the reader with a comprehensive overview of the possibilities and problems associated with improved detection systems for plasma emission detection. Multi-channel array and charge-transfer detectors are described and their respective advantages and weaknesses discussed. Special emphasis is placed on the applications of the charge-injection device to the simultaneous multi-element emission analysis of chromatographic eluents.

Chapter 6. This and all the subsequent chapters cover the field of metal speciation applying liquid separation methods prior to detection. The first part of this chapter is an excellent and extensive review of recent metal cation separation techniques involving HPLC coupled with UV or fluorimetric detection. The numerous complexing agents, postcolumn reactions, applications to real samples, detailed descriptions and comments provide the reader with a complete overview of the possibilities of this analytical approach. The second part of the chapter describes the mathematical and fundamental aspects of retention in HPLC separations based on ion-exchange-type mechanisms.

Chapter 7. Here the detection mode considered after metal separation by liquid chromatography is electrochemistry. The author describes the principles and pitfalls of an automated system designed to monitor the effluents of industrial activities or rivers. It is based on chromatography and on-line electrochemistry of metal complexes. Optimization of the formation of dithiocarbamate complexes with regard to full automation is discussed with respect to the type of application. Finally, several real examples are described and discussed adding to the value of the work presented.

Chapter 8. Metal speciation is treated here using ion chromatographic separation techniques interfaced with various detectors including ICP-AES. An extensive review of the various techniques used for ion chromatography, referring more specifically to ion-exchange chromatography or ion-pair chromatography, are described. Most of the emphasis of this chapter is directed towards applications to the speciation of Cr(III,VI), Fe(II,III), As(III,V), Te(IV), Se(IV,VI), V(IV,V), Sn(II,IV), Hg(I,II) and elements such as Al(III), Au(I, III), Cu(I,II) and Mg(II,III) in various samples.

Chapter 9. This last chapter is complementary to Chapters 1, 2, 3 and 5. It focuses on the determination of organometallic compounds of tin or mercury in real samples such as fish. The advantages of GC interfaced to a flame ionization or a direct current plasma (DCP) detector are presented with many practical details. Similarly, the possibilities of HPLC with on-line hydride generation and DCP detection applied to organotin detection in various type of samples are well presented, discussing clearly the possibilities, limits and pitfalls of the technique. A very

detailed conclusion gives good highlights of the future potential coupled systems based on chromatography and DCP detectors.

Speciation is the future of trace metal determination. This book is certainly published at the right time and will contribute to expanding this specific domain of analytical chemistry by providing the reader with an insight into the future and information on the wide range of possibilities available to date. It should be on the shelf of anyone concerned with trace metal determination in general.

Talence (France) Olivier F.X. Donard

Author Index

Vol. 635, No.2

Journal of Chromatography

NEWS SECTION

ANNOUNCEMENTS

10th LC–MS MONTREUX SYMPOSIUM, ITHACA, NY, USA, JULY 21–23, 1993 AND SHORT COURSE ON LC–MS, SFC–MS AND CE–MS, JULY 19–20, 1993

The 10th Montreux Symposium on LC–MS, SFC–MS, CE–MS and MS–MS will deal with all areas of these topics including technical developments with on-line and off-line aspects, theoretical considerations and applications of the techniques in environmental, clinical and pharmaceutical analysis and other fields.

Sub-topics will be introduced by plenary and invited research lectures, followed by oral and poster presentations. A major portion of the symposium will be devoted to panel and group discussions on the state-of-the-art LC–MS, SFC–MS, CE–MS and MS–MS.

Abstracts may be submitted until June 1, 1993.

The registration fee for the symposium is US$ 495.

An introductory course in LC–MS, SFC–MS and CE–MS will be offered on the two days preceding the symposium.

Topics to be covered include:

- Ionization methods;
- LC–MS interfaces: principles, techniques and applications of:
  - Continuous flow FAB
  - Thermospray LC–MS
  - Particle beam interfaces
  - Electrospray/ionspray interfaces
  - APCI
  - Novel interfaces
- LC–MS–MS: principles and applications;
- SFC–MS;
- CE–MS.

Registration fee for the short course will be US$ 525 (US$ 475 for symposium attendees). The deadline for course registration is June 1, 1993.

For further information contact: Dr. Jack Henion, Drug Testing and Toxicology Program, NY State College of Veterinary Medicine, Cornell University, 925 Warren Drive, Ithaca, NY 14850, USA. Fax: (+1-607)

INTERNATIONAL ION CHROMATOGRAPHY SYMPOSIUM 1993, BALTIMORE, MD, USA, SEPTEMBER 12–15, 1993

The scientific program will cover the following general topic areas:

- Environmental applications;
- New instrumentation and phases;
- Applications;
- Fundamental principles; and,
- Industrial applications.

Abstracts are welcomed describing original research in areas including:

- Ion analysis in the electrical generation industry;
- Separation selectivity and column technology;
- Interactions at the capillary–wall interface and ion separations;
- Air and water monitoring;
- Theoretical aspects of IC;
- Special sample treatment procedures;
- Detection techniques;
- Selectivity modification in CE;
- Carbohydrate separations;
- Process monitoring;
- Pharmaceutical applications; and,
- Applications to waste management problems.

The registration fee is US$ 350 for speakers; US$ 250 for full-time university registrants (faculty or student); and US$ 575 for participant registration prior to July 1, 1993. A US$ 50 surcharge will apply to all registrations paid after July 1, 1993.

Paper- and poster presenters are invited to submit a manuscript for inclusion in the proceedings which will be published as a special issue of the *Journal of Chromatography*. Instructions for manuscript preparation will be provided upon acceptance of an abstract.

For further information contact: Century International, P.O. Box 493, Medfield, MA 02052, USA. Tel.: (+1-508) 359-8777; Fax: (+1-508) 359-8778.

8th SYMPOSIUM ON SEPARATION SCIENCE AND TECHNOLOGY FOR ENERGY APPLICATIONS, GATLINBURG, TN, USA, OCTOBER 24–28, 1993

Topics to be emphasized at this symposium are:

- Solvent extraction;
- Adsorption, ion exchange, and chromatography;
- Membrane separations;
- Separation methods for waste management; and,
- Novel or new separation techniques.

Papers on any topic in separation science will be considered for presentation at the symposium. Anyone interested in presenting a paper at one of the sessions should submit a 200-250 word abstract no later than April 1, 1993.

A special poster session is being scheduled for the presentation of selected papers on the session topics indicated, as well as for the description of significant advances in other areas of separation science.

The registration fee for regular attendees is US$ 275.

For further information contact: Dr. J.T. Bell, Oak Ridge National Laboratory, P.O. Box 2008, Oak Ridge, TN 37831-6223, USA. Tel.: (+1-615) 574-4934; or, Dr. J.S. Watson, K-25 Plant, P.O. Box 2003, Oak Ridge, TN 37831-7298, USA. Tel.: (+1-615) 574-6795.

ELECTROPHORESIS '93, CHARLESTON, SC, USA, NOVEMBER 7–10, 1993

The program of this symposium will bring together experts to examine new developments, theories and applications of electrophoretic techniques dealing with all aspects of electrophoresis as it relates to the separation and detection of bioproducts, such as: 2D, capillary, DNA, genetics, PCR, analytical clinical forensics, imaging, preparative, biotechnology, detection, gels, molecular biology, and sequencing.

The comprehensive program will include lectures, poster presentations, stimulating discussion sessions, workshops, new products and instrumentation exhibits, student awards, best poster competition and social events.

Free practical workshops will be presented, beginning Sunday, November 7, to all interested registrants. Registration will be on a first-come, first-serve basis.

The deadline for submission of Abstracts is June 1, 1993.

For further details contact: Mrs. Janet Cunningham, Electrophoresis '93, c/o The Electrophoresis Society, P.O. Box 279, Walkersville, MD 21793, USA. Tel.: (+1-301) 898-3772; Fax: (+1-301) 898-5596.

13th INTERNATIONAL SYMPOSIUM ON HPLC OF PROTEINS, PEPTIDES AND POLYNUCLEOTIDES, SAN FRANCISCO, CA, USA, NOVEMBER 30–DECEMBER 3, 1993

This international meeting will examine new developments and applications in the areas of HPLC and other high resolution techniques for the analysis

of purification of proteins, peptides, and polynucleotides. Sessions will also include advances in biopharmaceutical, carbohydrate and lipid analysis. The program will include invited and contributed lectures, poster presentations and discussion sessions.

You are invited to submit abstracts describing original research in areas including:

- Electrokinetic separations;
- Column technology and support materials;
- Protein conformation and chromatographic behaviour;
- Polypeptide structural studies;
- Protein purity and QC of recombinant proteins;
- Polynucleotides;
- Polysaccharides;
- Membrane proteins;
- Lipids and lipoproteins;
- Affinity chromatography;
- Analytical applications;
- Sample preparation;
- Preparative chromatography of bio-polymers;
- High resolution electrophoresis;
- Integrated purification systems;
- Biospecific detectors;
- Mass spectroscopy;
- Process monitoring;
- Recovery of recombinant proteins;
- Protein–surface interaction;
- Molecular biorecognition;
- Isolation and purification techniques;
- Regulatory issues and quality control;
- Detection and amplification;
- Electrophoresis;
- Separation and protein engineering;
- Membrane technology; and,
- Special topics.

The Scientific Committee welcomes suggestions for additional topics to be covered in the Symposium. Abstracts must be submitted before July 1, 1993. Proceedings will be published as a special symposium volume of the *Journal of Chromatography.*

The registration fee is US$ 400 for advanced registration, US$ 450 for on-site registration, and US$ 100 for students.

For further information contact: Ms. Paddy Batchelder, Conference Manager, 7948 Foothill Knolls Drive, Pleasanton, CA 94588, USA. Tel.: (+1-510) 426-9601; Fax: (+1-510) 846-2242.

INTERNATIONAL SYMPOSIUM ON PURITY DETERMINATION OF DRUGS, STOCKHOLM, SWEDEN, DECEMBER 6–8, 1993

The rapid development of analytical techniques offers new possibilities to control the purity of drug substances. Methods based on TLC, GC, LC, LC–MS, CE and NMR are frequently used by the pharmaceutical industry in order to establish purity. The state of the art of these techniques and their relevance in purity testing will be discussed during the symposium. The symposium is addressed to those who are involved in development, quality control, registration and monitoring of medicinal products as well as those working on pharmacopoieal monographs.

Sessions will include such topics as:

Registration and pharmacopoieal requirements: rational impurity limits – an overview; viewpoints on toxicological testing of impurities; purity of enantiomers – a regulatory point of view; quality requirements on rDNA derived proteins.

Technics: overview on analytical techniques; aspects on selectivity and detection in separation techniques; peak purity and optimization of LC.

Poster session: modern TLC applied to drug analysis; NMR-spectroscopy for structural determination and purity control; the use of thermoanalytical methods in pharmaceutical development; quantitative aspects on CE.

Panel discussion: analytical aspects on packaging and container material; classification of chiral stationary and mobile phases for LC; optimization and validation of chiral LC methods.

Other sessions will include: purity and structural analysis of recombinant derived human insulin-like growth factor I; identification of inorganic impurities in pharmaceutical material; residual solvents; influence of impurities on the physicochemical properties of pharmaceutical materials; and, purity determination of reference substances.

Poster abstracts may be submitted up to October 1, 1993.

For further information contact: The Swedish Academy of Pharmaceutical Sciences, Symposium on "Purity Determination of Drugs", P.O. Box 1136, S-111 81 Stockholm, Sweden. Tel.: (+46-8) 245-085; Fax: (+46-8) 205-511.

24th ANNUAL SYMPOSIUM OF THE INTERNATIONAL ASSOCIATION OF ENVIRONMENTAL ANALYTICAL CHEMISTRY, OTTAWA, CANADA, MAY 16–19, 1994

This symposium will feature recent developments in instrumentation, sample preparation and analytical techniques on all aspects of environmental chemistry (air, water, soil, sediments, food, biological materials, etc.). The program will consist of invited keynote speakers and contributed oral and poster presentations. A special workshop on supercritical fluid extraction for environmental analyses is also planned.

For further information contact: Dr. M. Malaiyandi, CAEC, Chemistry Department, Carleton University, 1255 Colonel By Drive, Ottawa, Canada, K1S 5B6. Fax: (+1-613) 788-3749; or Dr. J.F. Lawrence, Food Research Division, Banting Research Centre, Health Protection Branch, Ottawa, Ontario, Canada, K1A 0L2. Fax: (+1-613) 941-4775.

COURSES

CHROMATOGRAPHIC FUNDAMENTALS COURSE, KENT, OH, USA, JUNE 7–11, 1993

This course will provide a coherent overview of chemical separations via chromatographic methods. It is unique from most other short courses in that material will be included on gas, liquid and thin-layer methods. It will emphasize the three techniques as complementary rather than competing processes. The course will be a blend of fundamental information on theory and instrumentation with emphasis placed on the latest developments and trends. Additional periods will provide time to discuss practical problems related to HPLC, GC, GC–MS, TLC and CE instrumentation.

For further information contact: Dr. Carl J. Knauss, Chemistry Department, Kent State University, Kent, OH 44242, USA. Tel.: (+1-216) 672-2327; Fax: (+1-216) 672-3816.

ADVANCE EUROPEAN TRAINING COURSE IN LIQUID CHROMATOGRAPHY AND CAPILLARY ELECTROPHORESIS, MONTPELLIER, FRANCE, SEPTEMBER 14-17, 1993

The aim of this European training course is to disseminate the latest information and research methodology in HPLC and related techniques to a wide range of pharmaceutical, chemical, medical, cosmetic and food enterprises.

This course will cover the following topics:

- Enantiomeric separations by chromatographic techniques and CZE;
- Optimization in LC and expert systems;
- Capillary electrophoresis; and,
- Method, software and instrument validation in LC.

The course will be given as lectures and workshops by various specialists. Instrument demonstrations will also be a feature of the course.

Simultaneous translation English-French and *vice-versa* is provided.

The course fee is FF 4000.

For further information contact: Professor Fabre or Dr. M.D. Blanchin, Laboratoire de Chimie Analytique, Faculté de Pharmacie, 34060 Montpellier Cedex 1, France. Tel.: (+33-67) 63-5432; Fax: (+33067) 61-1622.

CALL FOR NOMINATIONS

CHIRALITY MEDAL

Nominations are invited for the Chirality Medal to be awarded in 1993 at the 4th International Symposium on Chiral Discrimination in Montreal, Quebec, Canada. The Chirality Medal was instituted by the Italian Chemical Society in connection with the International Symposium on Chiral Discrimination in Rome 1991. This Medal is awarded to recognise distinguished achievement in any aspect of the field of chiral discrimination. Nominations, together with a short supporting statement, should be sent before 30 April 1993 to: Professor A.F. Fell, Secretary, Chirality Medal Honours Committee, Pharmaceutical Chemistry University of Bradford, Bradford BD7 1DP, UK.

CALENDAR OF FORTHCOMING EVENTS

May 3–5, 1993
Veldhoven, Netherlands
EURORESIDUE II – International Conference on Residues of Veterinary Drugs in Food

Contact: Dr. N. Haagsma, Section of Food Chemistry, Department of Food of Animal Origin, Faculty of Veterinary Medicine, University of Utrecht, P.O. Box 80.175, 3508 TD Utrecht, Netherlands. Tel.: (+31-30) 535-365/535-367; Fax: (+31-30) 532-365.

May 3–5, 1993
Szombathely, Hungary
5th Symposium on the Analysis of Steroids

Contact: Professor S. Görög, c/o Chemical Works of Gedeon Richter Ltd., P.O. Box 27, H-1475 Budapest, Hungary. Tel.: (+36-1) 1574-566; Fax: (+36-1) 1571-578; Telex: 22-5067 richt h.

■ **May 4, 1993**
Greenford, UK
Meeting on Capillary Chromatography

Contact: The Secretary, Suite 4, Clarendon Chambers, 32 Clarendon Street, Nottingham NG1 5JD, UK. Tel.: (+44-602) 500-596; Fax: (+44-602) 500-614.

May 9–14, 1993
Hamburg, Germany
17th International Symposium on Column Liquid Chromatography

Contact: Gesellschaft Deutscher Chemiker, Abteilung Tagungen, P.O. Box 900440, Varrentrappstrasse 40-42, W-6000 Frankfurt am Main 90, Germany. Tel: (+49-69) 7917-360; Fax: (+49-69) 7917-475.

May 24–28, 1993
Riva del Garda, Italy
15th International Sympsium on Capillary Chromatography

Contact: Professor Dr. P. Sandra, I.O.P.M.S., Kennedypark 20, B-8500 Kortrijk, Belgium. Tel.: (+32-56) 204-960; Fax: (+32-56) 204-859.

May 25–27, 1993
Ghent, Belgium
5th International Symposium on Quantitative Luminescence Spectrometry in Biomedical Sciences

Contact: Dr. Willy R.G. Baeyens, Symposium Chairman, University of Ghent, Pharmaceutical Institute, Harelbekestraat 72, B-9000 Ghent, Belgium. Tel.: (+32-91) 218-951, ext. 246; Fax: (+32-91) 217-902.

■ **May 25–27, 1993**
San Diego, CA, USA
Pollution Prevention Conference on Low- and No-VOC Coating Technologies

Contact: Coleen Northeim, Research Triangle Institute, P.O. Box 12194, Research Triangle Park, NC 27709-2194, USA. Tel.: (+1-919) 541-5816.

■ **May 27–28, 1993**
Riva del Garda, Italy
2nd European Symposium on Analytical Supercritical Fluid Chromatography and Extraction

Contact: Professor Dr. P. Sandra, I.O.P.M.S., Kennedypark 20, B-8500 Kortrijk, Belgium. Tel.: (+32-56) 204-960; Fax: (+32-56) 204-859.

June 2–4, 1993
Stockholm, Sweden
International Symposium on Analysis of Peptides

Contact: Swedish Academy of Pharmaceutical Sciences, Symposium on "Analysis of Peptides", P.O. Box 1136, S-111 81 Stockholm, Sweden. Tel.: (+46-8) 245-085; Fax: (+46-8) 205-511.

June 2–4, 1993
Sandefjord, Norway
ICES-ELPHO '93, Meeting of the International Council of Electrophoresis Societies

Contact: Professor Nils Olav Solum, Research Institute for Internal Medicine, Rikshopitalet, Pilestredet 32, N-0027 Oslo, Norway. Tel.: (+47-2) 868-226; Fax: (+47-2) 868-303.

■ **June 7–11, 1993**
Kent, OH, USA
Chromatographic Fundamentals Course

Contact: Dr. Carl J. Knauss, Chemistry Department, Kent State University, Kent, OH 44242, USA. Tel.: (+1-216) 672-2327; Fax: (+1-216) 672-3816.

June 14–16, 1993
Arlington, VA, USA
Prep '93, 10th International Symposium on Preparative Chromatography

Contact: Washington Chromatography Discussion Group, c/o Barr Enterprises, P.O. Box 279, Walkersville, MD 21793, USA. Tel.: (+1-301) 898-3772; Fax: (+1-301) 898-5596.

■ **June 20–25, 1993**
Loughborough, UK
Short Course in Radioisotope Techniques

Contact: Miss C.L. Archer, Course Secretary, Loughborough University of Technology, Loughborough, Leicestershire LE11 3TU, UK. Tel.: (+44-509) 222-581.

June 27–July 1, 1993
Santa Barbara, CA, USA
Fullerenes '93, 1st International Interdisciplinary Colloquium on the Science and Technology of the Fullerenes

Contact: (for North America) Kim Cavellero, Pergamon Seminars, 660 White Plains Rd, Tarrytown, NY 10591-5153, USA, or: (for UK and all other countries), Gill Spear, Pergamon Seminars, c/o Elsevier Advanced Technology, Mayfield House, 256 Banbury Road, Oxford OX2 7DH, UK. Tel.: (+44 865) 512242; Fax: (+44 865) 310981

June 29–July 4, 1993
York, UK
XXVIII Colloquium Spectroscopicum Internationale

Contact: XXVIII Colloquium Spectroscopicum Internationale, Department of Chemistry (CSI Secretariat), Loughborough University of Technology, Loughborough, Leicestershire LE11 3TU, UK. Tel.: (+44-509) 222-575; Fax: (+44-509) 233-163; Telex: 34319.

July 11–14, 1993
Crete, Greece
6th International Symposium on Polymer Analysis and Characterization

Contact: Judith A. Sjoberg, Professional Association Management, 815 Don Gaspar, Santa Fe, NM 87501, USA. Tel.: (+1-505) 989-4735; Fax: (+1-505) 989-1073.

July 11–15, 1993
Brno, Czech Republic
Chemometrics III, 3rd Czech Chemometric Conference

Contact: Dr. Josef Havel, Department of Analytical Chemistry, Masaryk University, Kotlarska 2, CS-61137 Brno, Czech Republic. Tel.: (+42-5) 7129-284; Fax: (+42-5) 740-108.

■ **July 19–20, 1993**
Ithaca, NY, USA
Short Course on LC–MS, SFC–MS and CE–MS

Contact: Dr. Jack Henion, Drug Testing and Toxicology Program, NY State College of Veterinary Medicine, Cornell University, 925 Warren Drive, Ithaca, NY 14850, USA. Fax: (+1-607) 255-3235.

■ **July 21–23, 1993**
Ithaca, NY, USA
10th LC–MS Montreux Symposium

Contact: Dr. Jack Henion, Drug Testing and Toxicology Program, NY State College of Veterinary Medicine, Cornell University, 925 Warren Drive, Ithaca, NY 14850, USA. Fax: (+1-607) 255-3235.

July 26–29, 1993
Washington, DC, USA
107th Annual International Meeting and Exposition of the AOAC

Contact: Margaret Ridgell, AOAC, 2200 Wilson Blvd., Suite 400, Arlington, VA 22201-3301, USA. Tel.: (+1-703) 522-3032; Fax: (+1-703) 522-5468.

■ **Aug. 22–27, 1993**
Newport, RI, USA
1993 Gordon Conference on Reactive Polymers, Ion-Exchangers and Adsorbents

Contact: Professor Csaba Horváth, Department of Chemical Engineering, Yale University, P.O. Box 2159 Yale Station, New Haven, CT 06520, USA. Tel.: (+1-203) 432-2217; Fax: (+1-203) 432-4360.

Aug. 23–27, 1993
Budapest, Hungary
9th Danube Symposium on Chromatography

Contact: Symposium Secretariat, Professor László Szepesy, Department of Chemical Technology, Technical University of Budapest, Budafoki út 8., H-1521 Budapest, Hungary. Tel.: (+36-1) 186-9000; Fax: (+36-1) 181-2755; Telex: 225931 muegy h.

Aug. 23–27, 1993
Calgary, Canada
9th International Conference on Fourier Transform Spectroscopy

Contact: Conference Office, The University of Calgary, 2500 University Drive NW, Calgary, Alberta T2N 1N4, Canada. Tel.: (+1-403) 220-5051; Fax: (+1-403) 289-7287.

Aug. 24–27, 1993
Boston, MA, USA
EPRI/EPA/DOE 1993 SO_2 Control Symposium

Contact: Electric Power Research Institute, Attn: Pam Turner, Conference Coordinator P.O. Box 10412, Palo Alto, CA 94303-9743, USA.

Aug. 29–Sept. 3, 1993
Bratislava, Czech Republic
9th International Symposium on Advances and Application of Chromatography in Industry

Contact: Department of Analytical Chemistry, Slovak Technica University, Radinského 9, 812 37 Bratislava, Czech Republic. Tel.: (+42-7) 560-43; Fax: (+42-7) 493-198.

Sept. 5–11, 1993
Edinburgh, UK
EUROANALYSIS VIII, 8th European Conference on Analytical Chemistry

Contact: Miss P.E. Hutchinson, Analytical Division, The Royal Society of Chemistry, Burlington House, Piccadilly, London W1V 0BN, UK. Tel.: (071) 4378656; Fax: (071) 734-1227; Telex: 268001.

■ **Sept. 7–10, 1993**
Guildford, UK
10th International Bioanalytical Forum on Biofluid and Tissue Analysis for Drugs, including Hypolipidaemics

Contact: Guildford Academic Associates, 72 The Chase, Guildford GU2 5UL, UK. Tel. (N/A early June) & Fax: (+44-483) 65324.

Sept. 7–10, 1993
Verona, Italy
12th Internation Symposium on Biomedical Applications of Chromatography and Electrophoresis and 2nd International Symposium on the Applications of HPLC in Enzyme Chemistry

Contact: Dr. Franco Tagliaro, Istituto di Medicina Legale, Università di Verona, Policlinico, I-37134 Verona, Italy. Tel.: (+39-45) 807-4618/807-4246; Fax: (+39-45) 505-259.

Sept. 8–10, 1993
Prague, Czech Republic
4th Workshop on Chemistry and Fate of Modern Pesticides and Related Pollutants

Contact (for Eastern European countries): Dra. J. Hajslova, Department of Food Chemistry and Analysis, Institute of Chemical Technology, Suchbátarova 5, 166 28 Prague 6-Dejvice, Czech Republic. Fax: (+42-2) 311-4769. For all other countries, contact: IAEAC, M. Frei-Häusler, P.O. Box 46, CH-4123 Allschwil 2, Switzerland. Fax: (+41-61) 482-0805.

Sept. 12–15, 1993
Baltimore, MD, USA
1993 International Ion Chromatography Symposium

Contact: J.R. Strimaitis, Century International, P.O. Box 493, Medfield, MA 02052, USA. Tel.: (+1-508) 359-8777; Fax: (+1-508) 359-8778.

■ **Sept. 13–17, 1993**
Loughborough, UK
Workshop in Liquid Scintillation Counting

Contact: Dr. Peter Warwick, Nuclear Chemistry Laboratories, Loughborough University of Technology, Loughborough, Leicestershire LE11 3TU, UK. Tel.: (+44-509) 222-585; Fax: (+44-509) 233-163.

■ **Sept. 14–17, 1993**
Montpellier, France
Advance European Training Course in Liquid Chromatography and Capillary Electrophoresis

Contact: Professor Fabre or Dr. M.D. Blanchin, Laboratoire de Chimie Analytique, Faculté de Pharmacie, 34060 Montpellier Cedex 1, France. Tel.: (+33-67) 63-5432; Fax: (+33067) 61-1622.

Sept. 19–22, 1993
Montreal, Canada
4th International Symposium on Chiral Discrimination

Contact: Chiral Secretariat, Conference Office, McGill University, West Tower, Suite 490, Montreal, Quebec H3A 1B9, Canada. Tel.: (+1-514) 398-3770; Fax: (+1-514) 398-4854.

Sept. 19–22, 1993
Research Triangle Park, NC, USA
2nd National Symposium on Planar Chromatography: Modern Thin-Layer Chromatography

Contact: Mrs. Janet Cunningham, Barr Enterprises, P.O. Box 279, Walkersville, MD 21793, USA. Tel.: (+1-301) 898-3772; Fax: (+1-301) 898-5596.

Sept. 29–Oct. 1, 1993
Lausanne, Switzerland
International Symposium on Phytochemistry of Plants used in Traditional Medicine

Contact: Professor K. Hostettmann, Institut de Pharmacognosie et Phytochimie, Ecole de Pharmacie, Université de Lausanne, BEP, CH-1015 Lausanne, Switzerland. Tel.: (+41-21) 692-2861; Fax: (+41-21) 692-2880.

■ **Oct. 11–13, 1993**
St. Louis, MO, USA
Chiral Separations Short Course and Workshop

Contact: Professor D.W. Armstrong, University of Missouri-Rolla, 142 Schrenk Hall, Rolla, MO 65401, USA. Fax: (+1-314) 341-6033.

■ **Oct. 24–28, 1993**
Gatlinburg, TN, USA
8th Symposium on Separation Science and Technology for Energy Applications

Contact: Dr. J.T. Bell, Oak Ridge National Laboratory, P.O. Box 2008, Oak Ridge, TN 37831-6223, USA. Tel.: (+1-615) 574-4934 or (+1-615) 574-6874. Or, Dr. J.S. Watson, K-25 Plant, P.O. Box 2003, Oak Ridge, TN 37831-7298, USA. Tel.: (+1-615) 574-6795.

■ **Nov. 7–10, 1993**
Charleston, SC, USA
ELECTROPHORESIS '93

Contact: Mrs. Janet Cunningham, ELECTROPHORESIS '93, c/o The Electrophoresis Society, P.O. Box 279, Walkersville, MD 21793, USA. Tel.: (+1-301) 898-3772; Fax: (+1-301) 898-5596.

■ **Nov. 30– Dec. 3, 1993**
San Francisco, CA, USA
13th International Symposium on HPLC of Proteins, Peptides and Polynucleotides

Contact: Ms. Paddy Batchelder, Conference Manager, 7948 Foothill Knolls Drive, Pleasanton, CA 94588, USA. Tel.: (+1-510) 426-9601; Fax: (+1-510) 846-2242.

■ **Dec. 6–8, 1993**
Stockholm, Sweden
International Symposium on Purity Determination of Drugs

Contact: The Swedish Academy of Pharmaceutical Sciences, Symposium on "Purity Determination of Drugs", P.O. Box 1136, S-111 81 Stockholm, Sweden. Tel.: (+46-8) 245-085; Fax: (+46-8) 205-511.

Feb. 22–25, 1994
Antwerp, Belgium
HTC 3 – 3rd International Symposium on Hyphenated Techniques in Chromatography

Contact: Congress Secretariat, Dr. R. Smits, p/a BASF Antwerpen N.V., Central Laboratory, Scheldelaan, B-2040 Antwerp, Belgium. Tel.: (+32-3) 568-2831; Fax: (+32-3) 568-3250.

May 8–13, 1994
Minneapolis, MN, USA
HPLC '94: 18th International Symposium on Column Liquid Chromatography

Contact: Mrs. Janet Cunningham, Barr Enterprises, P.O. Box 279, Walkersville, MD 21793, USA. Tel.: (+1-301) 898-3772; Fax: (+1-301) 898-5596.

■ **May 16–19, 1994**
Ottawa, Canada
24th International Symposium of the International Association of Environmental Analytical Chemistry

Contact: Dr. M. Malaiyandi, CAEC, Chemistry Department, Carleton University, 1255 Colonel By Drive, Ottawa, Canada, K1S 5B6. Fax: (+1-613) 788-3749; or Dr. J.F. Lawrence, Food Research Division, Banting Research Centre, Health Protection Branch, Ottawa, Ontario, Canada, K1A 0L2. Fax: (+1-613) 941-4775.

June 20–24, 1994
Bournemouth, UK
20th International Symposium on Chromatography

Contact: Executive Secretary, The Chromatographic Society, Nottingham Polytechnic, Burton Street, Nottingham, NG1 4BU, UK. Tel.: (+44-602) 500-596; Fax: (+44-602) 500-614.

■ Indicates new or amended entry.

TrAC - Trends in Analytical Chemistry: Reference Edition

Volume 11: 1992

TrAC Compendium Series Volume 11

The Reference Edition of Trends in Analytical Chemistry (TrAC) is a compilation of the archival material reprinted from the regular issues of the journal. TrAC provides a topical digest of current developments and new ideas in the analytical sciences. It does so in the form of broadly-based, easy-to-read scientific reviews, backed up by news and other features of interest to the international analytical chemistry community. For subscribers to the library edition of TrAC, the reference editions form an integral part of the annual subscription, but for others these indispensable sources of information can be purchased individually. They provide informative and stimulating reading for all those who use analytical methods.

This latest volume contains all the archival material published in 1992. It covers a wide range of analytical techniques and applications of interest to academic and research workers in chemistry, biochemistry, clinical chemistry, pharmaceutical chemistry and toxicology.

A selection of the Contents.

Capillary Electrophoresis in Chemical/Pharmaceutical Quality Control *(A. Pluym, W. Van Ael, M. De Smet)*. Image Analysis in Chemistry. I. Properties of Images, Greylevel Operations, the Multivariate Image. II. Multivariate Image Analysis *(P. Geladi et al.)*. Silica Based, Solid Phase Reagents for Derivatizations in Chromatography *(F.-X. Zhou, J.M. Thorne, I.S. Krull)*. Mapping Post-Translational Modifications of Viral Proteins by Mass Spectrometry *(J.J. Gormann)*. Fluorescence Detection in Capillary Electrophoresis *(L.N. Amankwa, M. Albin, W.G. Kuhr)*. Biomolecular Tracing through Accelerator Mass Spectrometry *(J.S. Vogel, K.W. Turteltaub)*. Solid-Phase Reactors in Flow Injection Analysis *(M.D. Luque de Castro)*. Capillary Electrophoresis: A Powerful Tool for Biomedical Analysis and Research? *(D. Perrett, J. Ross)*. Bioanalytical Sample Preparation using Microdialysis and Ultrafiltration Capillaries *(M.C. Linhares, P.T. Kissinger)*. Models of Time-Series Analysis - a Helpful Tool for Evaluation of Noisy Data in Distribution Analysis *(K. Doerffel)*. Bio-Analytical Applications of Fourier Transform Infrared Spectroscopy *(M. Jackson, H.H. Mantsch)*. X-ray Absorption Spectroscopy in Chemistry. I. Extended X-ray Absorption Fine Structure. II. X-ray Absorption near Edge Structure *(P. Behrens)*. Mechanism of the Peroxyoxalate Chemiluminescence Reaction *(P.J.M. Kwakman, G.J. de Jong, U.A.Th. Brinkman)*. Plasma Spectrometric Detection for Supercritical Fluid Chromatography *(J.M. Carey, J.A. Caruso)*. Electrochemistry of Biopolymers *(J.A. Cox, A. Pryzjazny)*. High-Field NMR Spectroscopy as an Analytical Tool for Quantitative Determinations: Pitfalls, Limitations and Possible Solutions *(Cs. Szántay, Jr.)*. Abrasive Stripping Voltammetry - an Electrochemical Solid State Spectroscopy of Wide Applicability *(F. Scholz, B. Lange)*. Polymer Coatings as Stationary Phases in High-Performance Liquid Chromatography *(M. Hanson, K.K. Unger)*. Lasers in Mass Spectrometry *(J. Gorbally)*. Author Index. Subject Index.

1993 viii + 402 pages
Price: US $ 354.25 / Dfl. 620.00
ISBN 0-444-89926-X

ELSEVIER
SCIENCE PUBLISHERS

ORDER INFORMATION

For USA and Canada
ELSEVIER SCIENCE PUBLISHERS
Judy Weislogel
P.O. Box 945
Madison Square Station,
New York, NY 10160-0757
Tel: (212) 989 5800
Fax: (212) 633 3880

In all other countries
ELSEVIER SCIENCE PUBLISHERS
P.O. Box 211
1000 AE Amsterdam
The Netherlands
Tel: (+31-20) 5803 753
Fax: (+31-20) 5803 705

US$ prices are valid only for the USA & Canada and are subject to exchange rate fluctuations; in all other countries the Dutch guilder price (Dfl.) is definitive. Customers in the European Community should add the appropriate VAT rate applicable in their country to the price(s). Books are sent postfree if prepaid.

PUBLICATION SCHEDULE FOR THE 1993 SUBSCRIPTION

Journal of Chromatography and *Journal of Chromatography, Biomedical Applications*

MONTH	O 1992	N 1992	D 1992	J	F	M	A	M	
Journal of Chromatography	623/1 623/2 624/1 + 2	625/1 625/2	626/1 626/2 627/1 + 2	628/1 628/2 629/1 629/2	630/1 + 2 631/1 + 2 632/1 + 2 633/1 + 2	634/1 634/2	635/1 635/2 636/1 636/2	637/1 637/2 638/1 638/2	The publication schedule for further issues will be published later.
Cumulative Indexes, Vols. 601–650									
Bibliography Section						649/1			
Biomedical Applications				612/1	612/2	613/1	613/2 614/1	614/2 615/1	

INFORMATION FOR AUTHORS

(Detailed *Instructions to Authors* were published in Vol. 609, pp. 437–443. A free reprint can be obtained by application to the publisher, Elsevier Science Publishers B.V., P.O. Box 330, 1000 AH Amsterdam, Netherlands.)

Types of Contributions. The following types of papers are published in the *Journal of Chromatography* and the section on *Biomedical Applications:* Regular research papers (Full-length papers), Review articles, Short Communications and Discussions. Short Communications are usually descriptions of short investigations, or they can report minor technical improvements of previously published procedures; they reflect the same quality of research as Full-length papers, but should preferably not exceed five printed pages. Discussions (one or two pages) should explain, amplify, correct or otherwise comment substantively upon an article recently published in the journal. For Review articles, see inside front cover under Submission of Papers.

Submission. Every paper must be accompanied by a letter from the senior author, stating that he/she is submitting the paper for publication in the *Journal of Chromatography.*

Manuscripts. Manuscripts should be typed in **double spacing** on consecutively numbered pages of uniform size. The manuscript should be preceded by a sheet of manuscript paper carrying the title of the paper and the name and full postal address of the person to whom the proofs are to be sent. As a rule, papers should be divided into sections, headed by a caption (*e.g.*, Abstract, Introduction, Experimental, Results, Discussion, etc.) All illustrations, photographs, tables, etc., should be on separate sheets.

Abstract. All articles should have an abstract of 50–100 words which clearly and briefly indicates what is new, different and significant. No references should be given.

Introduction. Every paper must have a concise introduction mentioning what has been done before on the topic described, and stating clearly what is new in the paper now submitted.

Illustrations. The figures should be submitted in a form suitable for reproduction, drawn in Indian ink on drawing or tracing paper. Each illustration should have a legend, all the *legends* being typed (with double spacing) together on a *separate sheet.* If structures are given in the text, the original drawings should be supplied. Coloured illustrations are reproduced at the author's expense, the cost being determined by the number of pages and by the number of colours needed. The written permission of the author and publisher must be obtained for the use of any figure already published. Its source must be indicated in the legend.

References. References should be numbered in the order in which they are cited in the text, and listed in numerical sequence on a separate sheet at the end of the article. Please check a recent issue for the layout of the reference list. Abbreviations for the titles of journals should follow the system used by *Chemical Abstracts.* Articles not yet published should be given as "in press" (journal should be specified), "submitted for publication" (journal should be specified), "in preparation" or "personal communication".

Dispatch. Before sending the manuscript to the Editor please check that the envelope contains four copies of the paper complete with references, legends and figures. One of the sets of figures must be the originals suitable for direct reproduction. Please also ensure that permission to publish has been obtained from your institute.

Proofs. One set of proofs will be sent to the author to be carefully checked for printer's errors. Corrections must be restricted to instances in which the proof is at variance with the manuscript. "Extra corrections" will be inserted at the author's expense.

Reprints. Fifty reprints will be supplied free of charge. Additional reprints can be ordered by the authors. An order form containing price quotations will be sent to the authors together with the proofs of their article.

Ovomucoid Bonded Column for Direct Chiral Separation

ULTRON ES-OVM

Narrow-Bore Column (2.0 I.D. x 150 mm) for Trace Analyses
Analytical Column (4.6 I.D., 6.0 I.D. x 150 mm) for Regular Analyses
Semi-Preparative Column (20.0 I.D. x 250 mm) for Preparative Separation

Analysis of Trace FLURBIPROFEN in Metabolite with NARROW-BORE COLUMN

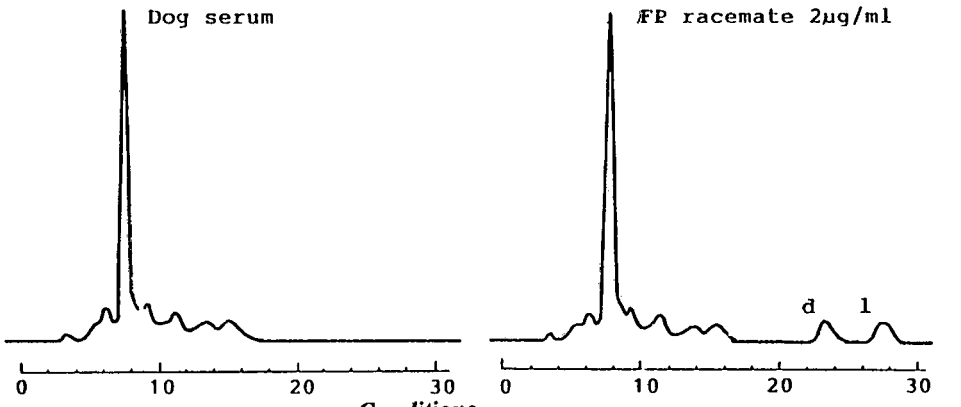

Conditions

Column: ULTRON ES-OVM(2.0I.D. x 150mm)
Mobile Phase: 20mMPhosphate Buffer(pH=3.0)/CH3CN =100/15
Flow Rate: 0.1ml/min
Temperature: 25°C
Injection: 5µl
Detection: UV- 247nm(0.05AUFS)

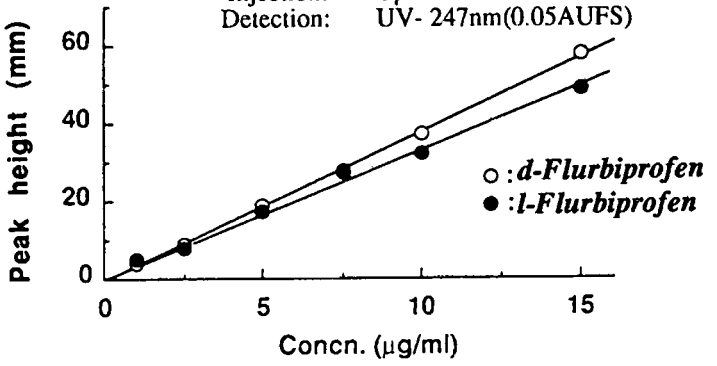

Calibration Curve for Each Enantiomer of Flurbiprofen

SHINWA CHEMICAL INDUSTRIES, LTD.

50 Kagekatsu-cho, Fushimi-ku, Kyoto 612, JAPAN
Phone:+81-75-621-2360 Fax:+81-75-602-2660

In the United States and Europe, please contact:

Rockland Technologies, Inc.

538 First State Boulevard, Newport, DE 19804, U.S.A.
Phone: 302-633-5880 Fax: 302-633-5893

This product is licenced by Eisai Co., Ltd.